9-3-2019

Statistical L-moment and L-moment Ratio Estimation and their Applicability in Network Analysis

Timothy S. Anderson

Statistical L-moment and L-moment Ratio Estimation and their Applicability in Network Analysis

DISSERTATION

Timothy S. Anderson, Major, USAF
AFIT/GAP/ENC/19S

DEPARTMENT OF THE AIR FORCE
AIR UNIVERSITY

AIR FORCE INSTITUTE OF TECHNOLOGY

Wright-Patterson Air Force Base, Ohio

AFIT/GAP/ENC/19S

STATISTICAL L-MOMENT AND L-MOMENT RATIO ESTIMATION AND THEIR APPLICABILITY IN NETWORK ANALYSIS

DISSERTATION

Presented to the Faculty

Graduate School of Engineering and Management

Air Force Institute of Technology

Air University

Air Education and Training Command

in Partial Fulfillment of the Requirements for the

Degree of Doctorate of Statistics

Timothy S. Anderson, M.S.

Major, USAF

23 August 2019

AFIT/GAP/ENC/19S

STATISTICAL L-MOMENT AND L-MOMENT RATIO ESTIMATION AND THEIR APPLICABILITY IN NETWORK ANALYSIS

DISSERTATION

Timothy S. Anderson, M.S.
Major, USAF

Committee Membership:

Dr. Schubert Kabban
Chairman

Dr. Andrew J. Geyer
Member

Dr. Richard F. Deckro
Member

Dr. Fairul Mohd-Zaid
Member

Abstract

This research centers on finding the statistical moments, network measures, and statistical tests that are most sensitive to various node degradations for the Barabási-Albert, Erdös-Rényi, and Watts-Strogratz network models. Thirty-five different graph structures were simulated for each of the random graph generation algorithms, and sensitivity analysis was undertaken on three different network measures: degree, betweenness, and closeness. In an effort to find the statistical moments that are the most sensitive to degradation within each network, four traditional moments: mean, variance, skewness, and kurtosis as well as three non-traditional moments: L-variance, L-skewness, and L-kurtosis were examined. Each of these moments were examined across 18 degrade settings to highlight which moments were able to detect node degradation the quickest. Closeness was the most sensitive network measure, and the mean was the most sensitive moment across all scenarios. The results showed L-moments and L-moment ratios were less sensitive than traditional moments. Subsequently sample size guidance and confidence interval estimation for univariate and joint L-moments were derived across many common statistical distributions for future research with L-moments.

Table of Contents

Page

Abstract iv

List of Figures viii

List of Tables xii

I. Introduction 1

II. Background 4

2.1 Introduction to Graphs 4
Network Measures 7
Random Graph Generating Models 10
Graph Matching 17
Graph Classification 19
Change Point Detection 21
2.2 Statistical Moments: Traditional and L-moments 22

III. Sensitivity of Network Measures, Moments, and Tests to Network Degradation 27

3.1 Research question 1a: What Network Measures and Moments are Sensitive to Network Degradation? 28
Sensitivity Analysis Design and Methods 28
Erdös-Rényi Sensitivity Analysis 34
Erdös-Rényi Concluding Remarks 40
Barabási-Albert Sensitivity Results 41
Barabási-Albert Concluding Remarks 47
Watts-Strogratz Sensitivity Results 48
Watts-Strogratz Conclusions 54
Conclusions 54
3.2 Research Objective 1b: What are Appropriate Statistical Tests to use to Detect Network Degradation 56
Method 1: Empirical Quantile Testing Methods 57
Method 2: Non-Parametric Testing Methods 59
Method 3: Parametric Testing Methods 67
3.3 Research Question 1c: Which Combination of Network Measures and Tests are most Effective at Detecting Network Changes in Data Applications 68
3.4 Statistical Testing Summary 79
3.5 Contributions and Conclusions for Network Sensitivity 80

Page

IV. L-moments and L-moment ratios Sample Size Guidance 82

Calculating Expectations and Variance of Sample L-moments 82
4.1 L-Moments and L-moment Ratios Sample Size Requirements for Common Distributions 90
Inference and Sample Size Guidance Summary 107

V. L-moments and L-moment ratios Confidence Interval Estimation 110

5.1 Methods of Interval Estimations for L-Moments 110
Exact Bootstrap For L-moment estimation 110
Numerical Inversion of Characteristic Generating Function for L-moment Estimation 112
5.2 Wald Based Exact Variance Confidence Intervals for L-moments 113
Summary of Wald Based Exact Variance Interval Estimates of L-moments 125
5.3 Wald Based Approximate Variance Confidence Intervals for L-moment Ratios 126
Summary of Wald Based Approximate Variance Interval Estimates of L-moment Ratios 136
5.4 Interval Estimates of Joint L-moment Ratios 136
Multivariate Wald Based Exact Variance Confidence Intervals for Joint L-moment Ratios 137
Multivariate Wald Based Unbiased Variance Confidence Intervals for Joint L-moment Ratios 142
Exact Bootstrap and Characteristic Generating Function Confidence Intervals for Joint L-moment Ratios 143
Summary of Interval Estimates of Joint L-moment Ratios 148
5.5 Conclusion 149

VI. Conclusions 150

Appendix A. Appendix A: Chapter 3 Algorithm, Tables, and Figures 153

Appendix B. Appendix B: Theoretical Derivations for the Exact Variance and Covariance of Sample L-moments 194

Page

Appendix C. Appendix C: Math Lab and R Code for Generating Coefficients for the Four Joint Intervals Methods from Chapter 5 231

Bibliography 257

List of Figures

Figure		Page
1	Simple undirected graph with 7 nodes and 12 edges (7,12)	5
2	Star and Line Graph (6 nodes)	10
3	Example of Barabási-Albert Graph ($n = 12, m_0 = 3$)	13
4	Example of a circle graph	14
5	Random Graph Watts Strogratz $p = 1$	15
6	Adjacency matrix Barabási-Albert ($n = 32$, $m0 = 2$)	15
7	Adjacency matrix Erdös-Rényi ($n = 32$, $m = 64$	15
8	Adjacency matrix Watts-Strogratz ($n = 32$, $m1 = 2$, $p = 1/2$)	16
9	Example for reading tables	33
10	Least Square Power Estimates by Network Measure and Moment for Erdös-Rényi Model	39
11	Least Square Power Estimates by Network Measure and Moment for Barabási-Albert Model	46
12	Least Square Power Estimates by Network Measure and Moment for Watts-Strogratz Model	53
13	Adjacency Matrix for Immunoglobulin Protein Network	69
14	Distributions of Network Measures for the Immunoglobulin Protein Network	70
15	Adjacency Matrix for High School Network Days 1-4	75
16	Plot of Exact Variance Sample L-moments for the standard normal distribution, Sample Size 4-50	93
17	Plots of Approximate Variance L-moment ratios for the standard normal distribution, Sample Size 4-50	94
18	Plot of Exact Variance Sample L-moments for the standard uniform distribution, Sample Size 4-50	96

Figure Page

19 Plot of Exact Variance Sample L-moments for the exponential(1) distribution, Sample Size 4-50 98

20 Plots of Approximate Variance L-moment ratios for the exponential(1) distribution, Sample Size 4-50 98

21 Plot of Exact Variance Sample L-moments for the gumbel(0,1) distribution, Sample Size 4-50 100

22 Plots of Approximate Variance L-moment ratios for the gumbel(0,1) distribution, Sample Size 4-50 101

23 Plot of Exact Variance Sample L-moments for the pareto($\frac{3}{\sqrt{2}}, 4$) distribution, Sample Size 4-50 106

24 Plots of Approximate Variance L-moment ratios for the pareto($\frac{3}{\sqrt{2}}, 4$) distribution, Sample Size 4-50 107

25 Skewness of Wald Based Exact Variance Confidence Intervals for the normal distribution 120

26 Skewness of Wald Based Exact Variance Confidence Intervals for the uniform distribution 121

27 Skewness of Wald Based Exact Variance Confidence Intervals for the exponential distribution 122

28 Skewness of Wald Based Exact Variance Confidence Intervals for the gumbel distribution 123

29 Skewness of Wald Based Exact Variance Confidence Intervals for the pareto distribution 124

30 Skewness of Wald Based Approximate Variance Confidence Intervals for the normal distribution 131

31 Skewness of Wald Based Approximate Variance Confidence Intervals for the exponential distribution 133

32 Skewness of Wald Based Approximate Variance Confidence Intervals for the gumbel distribution 134

33 Skewness of Wald Based Approximate Variance Confidence Intervals for the pareto distribution 135

Figure Page

34 Joint Confidence Interval L-moment Ratios: sample size 50 for the normal distribution 145

35 Joint Confidence Interval L-moment Ratios: sample size 150 for the exponential distribution 147

A1 Power results for the Erdös-Rényi model for k = 5 and 6 across network measures, moments, degrade setting and proportions according to the key from Figure 9 155

A2 Power results for the Erdös-Rényi model for k = 7 and 8 across network measures, moments, degrade setting and proportions according to the key from Figure 9 156

A3 Power results for the Erdös-Rényi model for k = 9 and 10 across network measures, moments, degrade setting and proportions according to the key from Figure 9 157

A4 Power results for the Erdös-Rényi model for k = 11 across network measures, moments, degrade setting and proportions according to the key from Figure 9 158

A5 Power results for the Barabási-Albert model for k = 5 and 6 across network measures, moments, degrade setting and proportions according to the key from Figure 9 160

A6 Power results for the Barabási-Albert model for k = 7 and 8 across network measures, moments, degrade setting and proportions according to the key from Figure 9 161

A7 Power results for the Barabási-Albert model for k = 9 and 10 across network measures, moments, degrade setting and proportions according to the key from Figure 9 162

A8 Power results for the Barabási-Albert model for k = 11 across network measures, moments, degrade setting and proportions according to the key from Figure 9 163

A9 Power results for the Watts-Strogratz model for k = 5 and 6 across network measures, moments, degrade setting and proportions according to the key from Figure 9 165

Figure Page

A10 Power results for the Watts-Strogratz model for k = 7 and 8 across network measures, moments, degrade setting and proportions according to the key from Figure 9 166

A11 Power results for the Watts-Strogratz model for k = 9 and 10 across network measures, moments, degrade setting and proportions according to the key from Figure 9 167

A12 Power results for the Watts-Strogratz model for k = 11 across network measures, moments, degrade setting and proportions according to the key from Figure 9 168

List of Tables

Table		Page
1	Bounds on Network Measures	9
2	Network Models Parameter Settings	29
3	Network Simulation Settings	29
4	Isolates Created in Simulation of 1,000 graphs with $m = 2$	30
5	Full Factorial at lowest Proportion	34
6	Moments achieving > 0.90 power for degree in the Erdös-Rényi Network Model	35
7	Moments achieving > 0.90 power for betweenness in the Erdös-Rényi Network Model	36
8	Moments achieving > 0.90 power for closeness in the Erdös-Rényi Network Model	37
9	Least Square Power Estimates by Network Measure and Moments for Erdös-Rényi Model	38
10	Least Square Power Estimates based on Interaction of Network Measure and Moments for the Erdös-Rényi Model above 0.80	40
11	Moments achieving > 0.90 power for degree in the Barabási-Albert Network Model	42
12	Moments achieving > 0.90 power for betweenness in the Barabási-Albert Network Model	43
13	Moments achieving > 0.90 power for closeness in the Barabási-Albert Network Model	44
14	Least Square Power Estimates by Network Measure and Moments for Barabási-Albert Model	45
15	Least Square Power Estimates based on Interaction of Network Measure and Moments for the Barabási-Albert Model above 0.80	47

Table Page

16 Moments achieving > 0.90 power for degree in the Watts-Strogratz Network Model 49

17 Moments achieving > 0.90 power for betweenness in the Watts-Strogratz Network Model 50

18 Moments achieving > 0.90 power for closeness in the Watts-Strogratz Network Model 51

19 Least Square Power Estimates by Network Measure and Moments for Watts-Strogratz Model 52

20 Least Square Power Estimates above 0.90 based on Interaction of Network Measure and Moments for Watts-Strogratz Model 54

21 Moment and (proportion of detects out of 35) for the Empirical Quantile Method at a proportion of degrade = 1/10 and power 0.90 58

22 Graph Simulation Settings for Non-parametric test comparisons 60

23 Erdös-Rényi Smallest Proportion of Node Degrade to Achieve 0.80 Power Based on Closeness 62

24 Barabási-Albert Smallest Proportion of Node Degrade to Achieve 0.80 Power Based on Closeness 64

25 Watts-Strogratz Smallest Proportion of Node Degrade to Achieve 0.80 Power Based on Closeness 65

26 Degrade Settings 71

27 Degraded Immunoglobulin Protein Network detection power using $1/10^{th}$ proportion setting by statistical test and network measure 72

28 Degraded Immunoglobulin Protein Network detection power using $1/20^{th}$ proportion setting by statistical test and network measure 73

29 Graph Characteristics of Nodes & Edges 76

Table Page

30 High School Networks Nodes Selected and Number Degraded for Each Degrade Level 76

31 Power to Detect Degraded High School Network for Day 1 at $p = 1/2$ 77

32 Power to Detect Degraded High School Network for Day 2-4 at $p = 1/2$ 78

33 Expected Values of L-moments for Common distributions [18] 91

34 Exact and Approximate Variances for normal(0,1) 92

35 Exact and Approximate Variance for uniform(0,1) 95

36 Exact and Approximate Variance for exponential(1) 97

37 Exact and Approximate Variance for gumbel(0,1) 100

38 Exact and Approximate Variance for pareto($\frac{3}{\sqrt{2}}, 4$) 105

39 Coverage of Wald-based Exact Variance Confidence Interval for L-moments at $\alpha = 0.10$ 116

40 Coverage of Wald-based Exact Variance Confidence Interval for L-moments at $\alpha = 0.05$ 117

41 Coverage of Wald-based Exact Variance Confidence Interval for L-moments at = 0.02 118

42 Coverage of Wald-based Approximate Variance Confidence Interval for L-moment Ratios at = 0.10 127

43 Coverage of Wald-based Approximate Variance Confidence Interval for L-moment Ratios at = 0.05 129

44 Coverage of Wald-based Approximate Variance Confidence Interval for L-moment Ratios at = 0.02 130

45 Covariance l_3 and l_4 for common distributions 137

46 Coverage for Joint Confidence Interval $\alpha = 0.10$ 139

47 Coverage for Joint Confidence Interval $\alpha = 0.05$ 140

Table Page

48 Coverage for Joint Confidence Interval $\alpha = 0.02$ 141

49 Empirical Joint Coverage Comparison at $\alpha = 0.05$ 144

50 Time in Seconds to Calculate Mean and Covariance Estimates for Building Intervals 148

A1 Erdös-Rényi Average Number of Nodes Degraded within Simulation 154

A2 Barabási-Albert Average Number of Nodes Degraded within Simulation 159

A3 Watts-Strogratz Average Number of Nodes Degraded within Simulation 164

A4 Tukey's Pairwise comparison for Erdös-Rényi model 169

A5 Tukey's Pairwise comparison for Barabási-Albert model 169

A6 Tukey's Pairwise comparison for Watts-Strogratz model 170

A7 Erdös-Rényi Power based on Empirical Quantile Degrade Detection Low Degrade 171

A8 Erdös-Rényi Power based on Empirical Quantile Degrade Detection Med Degrade 172

A9 Erdös-Rényi Power based on Empirical Quantile Degrade Detection High Degrade 173

A10 Barabási-Albert Power based on Empirical Quantile Degrade Detection Low Degrade 174

A11 Barabási-Albert Power based on Empirical Quantile Degrade Detection Med Degrade 175

A12 Barabási-Albert Power based on Empirical Quantile Degrade Detection High Degrade 176

A13 Watts-Strogratz Power based on Empirical Quantile Degrade Detection Low Degrade 177

A14 Watts-Strogratz Power based on Empirical Quantile Degrade Detection Med Degrade 178

Table Page

A15 Watts-Strogratz Power based on Empirical Quantile Degrade Detection High Degrade . . . 179

A16 Erdös-Rényi Power Based on Non-parametric Tests with Low Degrade . . . 180

A17 Erdös-Rényi Power Based on Non-parametric Tests with Medium Degrade . . . 181

A18 Erdös-Rényi Power Based on Non-parametric Tests with High Degrade . . . 182

A19 Erdös-Rényi Power Based on Non-parametric Tests with Random Degrade . . . 183

A20 Barabási-Albert Power Based on Non-parametric Tests with Low Degrade . . . 184

A21 Barabási-Albert Power Based on Non-parametric Tests with Medium Degrade . . . 185

A22 Barabási-Albert Power Based on Non-parametric Tests with High Degree Degrade . . . 186

A23 Barabási-Albert Power Based on Non-parametric Tests with Random Degrade . . . 187

A24 Watts-Strogratz Power Based on Non-parametric Tests with Low Degrade . . . 188

A25 Watts-Strogratz Power Based on Non-parametric Tests with Medium Degrade . . . 189

A26 Watts-Strogratz Power Based on Non-parametric Tests with High Degrade . . . 190

A27 Watts-Strogratz Power Based on Non-parametric Tests with Random Degrade . . . 191

A28 Power to Detect degrade High School Network for Day 1 at p = 1/3 . . . 192

A29 Power to Detect degrade High School Network for Day 2 at p = 1/3 . . . 192

Table Page

A30 Power to Detect degrade High School Network for Day 3 at p = 1/3 193

A31 Power to Detect degrade High School Network for Day 4 at p = 1/3 193

STATISTICAL L-MOMENT AND L-MOMENT RATIO ESTIMATION AND THEIR APPLICABILITY IN NETWORK ANALYSIS

I. Introduction

Network analysis is of great interest to the Department of Defense, as it has the ability to model a multitude of different structures and capabilities. For instance, critical cyber infrastructures, logistics networks, terrorist social networks and newly emerged drone swarm networks are of high priority to national security. In January 2018, the United States Air Force conducted its largest ever drone swarm network consisting of 103 drones [25]. As swarm technology grows and the tasks they complete become ever more complex, so will the need for methods that are able to monitor these networks in efficient manners. The networks mentioned are just a small subset of the types of networks that our national security relies heavily upon, and the demand for network research will only increase.

With the increased reliance on network structures comes a need to develop tools to characterize and monitor such networks. Many tools currently in existence rely on mathematical and computational methods to characterize and compare networks of interest via graphical or network models. Recently, a heavier emphasis has been placed on statistical tools, as such tools are thought to be able to both characterize a network well and potentially be more sensitive when comparing networks. This research focuses on one particular type of statistical measure based upon distributional characteristics, called L-moments, as a means to sensitively and robustly detect changes in common network models. As such, this work focuses on two main objectives. First, L-moments are examined with respect to their sensitivity toward

detecting changes in networks. A comparison of the sensitivity of L-moments and traditional distributional moments in detecting change across network models of various size using various network measures is conducted. Secondly, theoretical properties are developed for L-moments with respect to sample size criterion and confidence interval estimation. This is performed in order to inform further use and investigation of L-moments in analyses focused upon sensitive and robust characterizations of statistical distributions. With respect to the definition of detecting "change" in networks, change is defined as a degradation in the network via the loss of nodes from a network.

The document is structured as follows: the second chapter provides background knowledge on network measures, random graph generating models, and statistical moments, both traditional and L-moments, that are utilized within this research. This is followed by a literature review of graph matching, graph classification, and change point detection as it pertains to networks. In Chapter 3, a framework is developed for statistical methods that can monitor changes with a degree of accuracy within real world networks by researching the following three questions: 1) what network measures and moments are sensitive to network changes, 2) what are appropriate statistical tests to use to detect these changes, and 3) which combination of network measures and tests are the most sensitive at detecting network changes in data applications. The last two chapters, Chapter 4 and 5, derive theoretical properties of L-moments and L-moment ratios, in order to provide sample size guidance and accurate interval estimations to inform future research on the use of L-moments for detecting changes in networks and other distributional comparisons using L-moments.

In summary, this research demonstrates the usefulness of various statistical tests to detect changes within some network by utilizing network measures in several network models and two real world data applications. In addition, theoretical results for L-

moments are advanced by providing sample size guidance and interval estimates for L-moments and L-moment ratios that will further their usefulness within network research and other fields.

II. Background

2.1 Introduction to Graphs

In order to create mathematical or statistical tools to characterize and monitor real-world networks, the networks themselves must be characterized well. Often, network characterization is accomplished through graphs and graph properties. The term "graphs" will primarily be used when discussing theoretical representations and "networks" for real world representations. The following sections providing background on properties and random graphs are mainly summarized from Newman's textbook titled *Networks* [33].

A graph is a representation of the relationship or connections of some underlying structure. Typically a graph, G, is defined by its nodes, N, and edges, E.

$$G = (N, E) \text{ where } N = \{n_1, n_2, ...n_m\} \text{ and } E = \{(n_a, n_b) | n_a, n_b \in N\},$$

where N is the set of m nodes, and E is defined by the 2-element subsets (n_a, n_b) of N which describes all the edges that exist between nodes n_a and n_b. Here, nodes are defined as a finite set, and edges are defined as a subset of nodes. This research was centered on the structure and properties of undirected and unweighted simple graphs. Simple graphs have two key properties: 1) no self-edge, meaning no edge originates and ends at the same node; and 2) no multi-edge, which implies there cannot be more than one edge between two nodes. All graphs will initially be assumed to be unweighted, meaning that every edge or node has the same weight across the entire network. Lastly, graphs are initially assumed to be undirected, meaning that there is no fixed direction for an edge from one node to another. Figure 1 is an example of such a graph with no self-edge and no direction indicated between nodes via the

Figure 1. Simple undirected graph with 7 nodes and 12 edges (7,12)

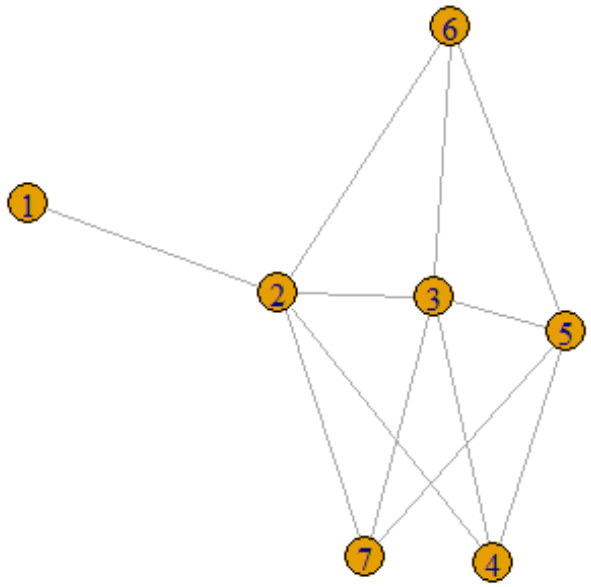

absence of arrows on the edges. For this particular graph, $N = 7$ and $E = 12$.

Graphs may be described through an adjacency matrix which is an m x m matrix, where m denotes the number of nodes. This matrix is created by simply placing a one in the respective i^{th} row and j^{th} column if an edge exists between the i^{th} and j^{th} node and is denoted zero otherwise. Due to the restriction of self-edges, the main diagonal consists of all zeros. The following adjacency matrix corresponds to the graphical representation seen in Figure 1.

Adjacency Matrix for Figure 1:

$$\begin{bmatrix} 0 & 1 & 0 & 0 & 0 & 0 & 0 \\ 1 & 0 & 1 & 1 & 0 & 1 & 1 \\ 0 & 1 & 0 & 1 & 1 & 1 & 1 \\ 0 & 1 & 1 & 0 & 1 & 0 & 0 \\ 0 & 0 & 1 & 1 & 0 & 1 & 1 \\ 0 & 1 & 1 & 0 & 1 & 0 & 0 \\ 0 & 1 & 1 & 0 & 1 & 0 & 0 \end{bmatrix}$$

A common measure used in graph research to characterize relations between nodes is geodesic distance, which is the shortest path between any two nodes. Examining nodes 1 and 4 in Figure 1, the geodesic distance between these two nodes is equal to 2 and is composed of the two edges that connect node 1 to node 2, and then node 2 to node 4. Some pairs of nodes will have multiple paths that achieve the geodesic distance. Considering nodes 1 and 5, the geodesic distance between these nodes contains three edges, but there are four paths that achieve this (nodes: 1-2-3-5, 1-2-4-5, 1-2-6-5, and 1-2-7-5). Geodesic distance was computed for several of the network measures.

In an attempt to characterize the structure of a network, I focused on the following three network measures: degree, betweenness, and closeness which were chosen based on the work of Guzman *et al.* [14]. In their work, graphs were generated using a random graph generation algorithm created by Morris *et al.* [32] in order to identify statistical dependencies among pairs of 24 different, common graph measures. Guzman *et al.*'s research found that all 24 measures fit into one of five groups of graph network measures. Network measures whose measure of dependence, Spearman's correlation coefficient, were greater than 0.84 were grouped together. The first four groups consisted of highly correlated measures which met this condition, and

the last group consisted of uncorrelated group measures; that is, all those remaining measures that failed to meet this criteria. Betweenness, and degree were selected as initial graph network measures since each belonged to a different group of highly correlated network measures. The fourth highly correlated group only had measures that pertained to weighted graphs. As such, the third measure (closeness) was chosen from the remaining uncorrelated group measures. By selecting these three measures from the different groups described by Gutzam *et al.*, I attempted to optimize the information gained from a particular graph through these measures while limiting the number of network measures to investigate. The following section describes each of these three network measures.

Network Measures.

Degree is defined as the number of edges connected to a particular node. The following formula is used for calculating degree in an undirected graph:

$$D_i = \sum_{j}^{n} A_{ij}, \tag{1}$$

where D_i represents the degree of node i, and A_{ij} is the i, j^{th} entry of the adjacency matrix. Degree values for the nodes of Figure 1 are (1,5,5,3,4,3,3) respectively. The degree of a network carries much information about the importance of each node, as degree measures how well connected a node is within the graph. A higher degree node may serve as a bridge to other less connected nodes; degree is among the most commonly used and well-studied measures with respect to networks [33].

Betweenness for a node is measured by the number of times a node lies on the shortest path between two other nodes. The formula for calculating betweenness for

node k, (B_K) is the following:

$$B_k = \sum_{ij} l_{ij}, \text{ for } i \neq j, \tag{2}$$

where l_{ij} is 1 when node k lies on the geodesic path between nodes i and j. When there are multiple geodesic paths between two nodes, the value counted toward each node on the different paths is the average number of geodesic paths. Notice that the summation in Equation 2 is over all the paths, hence why two indices exist in one summation. Betweenness values for the nodes of Figure 1 are (0,6,1.5,.5,1,.5,.5) respectively. In general, betweenness represents a measure of the flow between specific nodes and therefore describes a node in a way degree cannot. For instance, a node with only two edges connecting to two large clusters has degree measure of two (arguably low), but its betweenness score may be magnitudes higher depending on the size of the clusters.

Closeness of a particular node is computed as the average number of edges from that particular node to all the other nodes in a graph. One form of closeness, known as inverse closeness for an undirected graph, is calculated using the following formula:

$$C_i = \frac{1}{\sum_j (gd)_{ij}}, \text{ for } i \neq j, \tag{3}$$

where C_i is the closeness calculated for node i, and $(gd)_{ij}$ is the geodesic distance between node i and j. To calculate this form of closeness for node i, one sums across all the geodesic paths between node i and every other node j. Hence the summation is over j, i is fixed. The inverse as given in Equation 3 is more widely used in literature since its measure matches that of the other network measure discussed. Inverse closeness gives high values for more central nodes, and low values for less central nodes which is analogous to values provided by other network measures. The

range for closeness is quite small when compared to other measures, and as such, small perturbations in the graph can have large effects on this measure. Inverse closeness values for the nodes of Figure 1 are $(\frac{1}{12}, \frac{1}{7}, \frac{1}{7}, \frac{1}{9}, \frac{1}{9}, \frac{1}{9}, \frac{1}{9})$ respectively.

For each of these network measures, several different forms of the measures are available. For instance, betweenness and closeness may be normalized by multiplying by $(n-1)$, where n is the number of nodes in the network or by multiplying by the number of node pairs $\binom{n}{2}$. While this helps when comparing these measures between nodes or graphs, the probability distribution of each measure for the graph remains the same as multiplying by a constant merely shifts the probability distribution values, yet does not alter the probability associated with a specific node. A great example of this can be observed for the network measure closeness, which is sensitive to the size of the graph. Denny shows an example of this within his research utilizing the dataset known as Zachary's Karate Club Network [6] in which he gives the range of closeness as (0.01-0.02). It becomes difficult for a particular node to keep close relationships with all nodes as the number of nodes grow, but this can be corrected by multiplying by the number of nodes. While doing so better highlights relationships for large graphs, it does not alter the associated probability distribution of closeness. Table 1 gives the theoretical bounds for each of the network measures utilized for simple, undirected graphs.

Table 1. Bounds on Network Measures

degree	$[1, n-1]$
betweenness	$[0, \binom{n-1}{2}]$
closeness	$[\frac{1}{n-1}, \frac{1}{\sum_{i=1}^{n-1} i}]$

where n = the number of nodes

Explanation of these bounds are conveyed in the star and line graph which are shown in Figure 2. For degree, the lower bound exists when a node only has one edge

Figure 2. Star and Line Graph (6 nodes)

connecting it to the rest of the graph, which can be seen in the line graph for nodes 1 and 2. The upper bound exists, when a node is connected to every other node as depicted in the star graph. For betweenness, it is possible for a node not to lie on any geodesic path between all pairs of nodes in a particular network, which establishes its lower bound. Node 1 in the line graph is a representation of this, having betweenness values of zero. The upper bound of betweenness exists in the star graph with the center node connected to all other nodes. Thus the center node is on the geodesic path between all pairs and as such, its betweenness value is $\binom{n-1}{2}$ which equals 10. For closeness, the lower bound exists in the line graph for nodes 1 and 2 where the nodes are the least central, (closeness equals $\frac{1}{\sum_{i=1}^{n-1} i}$), but for the node which is the center of the star graph, its closeness value is at its maximum, $\frac{1}{(n-1)}$. While these are bounds for any graph, I was only focused on the structures of three specific graph generating models and are the topic of the next section.

Random Graph Generating Models.

Random graph generating models are useful tools in studying specific network properties found in the real world. A random graph generating model has both fixed and random parameters and is created in such a way so as to model specific network

characteristics. Due to the variation of the random parameters within each model, the set of graphs across all fixed parameters represents an entire family of graphs that could be created. Thus, one specific representation of a random graph created is just one of many graphs that could be represented based on the randomness of the free parameters. Therefore, it is possible to describe the family of all graphs with the same fixed parameters through the probability distributions of network characteristics associated with all the possible graphs that the randomness can create. This research was centered around three specific random graph generating models: the Erdös-Rényi, Barabási-Albert and Watts-Strogatz model, all with certain fixed parameters, and all for which probability distributions were estimated. A description of each of these random graph generating models follows.

The Erdös-Rényi graph model is sometimes referred to as "the" random graph. It was one of the first graph generating models theorized, introduced in the 1950's by Paul Erdös and Alfred Rényi [9]. The graph is known as:

$$G(n, m)$$

with (n) nodes and (m) number of edges. The graph is built on the principle that all edges have the same probability of occurrence and are independent from one another. Figure 1, shown earlier, is an example of a $G(n, m)$ graph, specifically, G(7,12). In the Erdös-Rényi model, the number of nodes and edges are fixed and the randomness comes in the form of the location of the edges. These edges are chosen uniformly and randomly from all possible edge locations. Due to the random placement of edges, two limitations exist when trying to model real world networks with an Erdös-Rényi graph: the degree distribution is mostly not right skewed and the edges are randomly assigned. Some real world networks, and specifically social networks, have degree distributions which are right skewed, and the edges are usually correlated in some

fashion depending on the physical nature of the graph in question [3]. One random graph generating model that seeks to model these traits is the Barabási-Albert model.

The Barabási-Albert model may overcome the limitations of the Erdös-Rényi model because the Barabási-Albert model is structured to create a degree distribution which follows a power-law distribution with highly correlated edges. The Barabási-Albert model is a special case of Price's model which generates scale-free networks through linear preferential attachment [33]. Scale-free networks are defined as those whose degree distributions follow a power law distribution.

Preferential attachment was introduced by Barabási and Albert in 1999 as an explanation for scale-free networks [3]. Preferential attachment is the notion that as new nodes are added, they tend to attach to nodes with higher degree versus those nodes that have lower degree. As such, the preferential attachment characteristic tends to generate a degree distribution for the graph that is right-skewed with edges that are correlated. The fixed variables of the Barabási-Albert model include, n the number of nodes, m_0 the number of edges added on each iteration as the model is built (each node is added), and the linear preferential attachment process. Equation 4 defines the preferential attachment process, which determines the probability that a new node added is connected to an existing node, where i and k represents the connectivity for the particular node, [3]

$$\prod(k_i) = \frac{k_i}{\sum_j (k_j)}, \quad j = 1, ..., n \tag{4}$$

Figure 3 shows a representation of a Barabási-Albert graph that has twelve nodes and three edges which were added with each new node. This graph is built in sequence where a new node is added at each time step and m_0 number of edges connect the new node to some existing node. Those edges are attached with probability calculated in Equation 4 to some existing node. The Barabási-Albert model does not typically

have a large number of well connected nodes, a characteristic seen in some networks. However, the Watts-Strogratz model discussed next has this characteristic.

Figure 3. Example of Barabási-Albert Graph ($n = 12, m_0 = 3$)

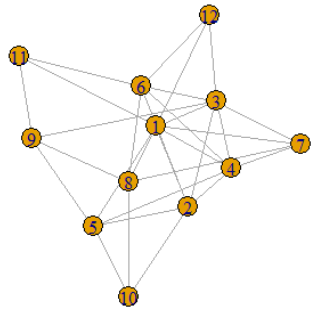

The Watts-Strogatz model is known as the "small-world model" which describes the property that all nodes are connected by a relatively few number of connections. This model was introduced in 1998 by Watts and Strogatz in order to simulate a graph that had both transitivity and short path lengths [39]. Transitivity is the tendency that two nodes which are connected to an identical third node, should be connected to each other as well. Neither the Erdös-Rényi graph nor the Barabási-Albert graph were designed to capture this trait.

A circle graph, shown in Figure 4 with $n = 12$ nodes, has high transitivity while a random graph has short path lengths. The fixed variables of the Watts-Strogratz model are, the number of nodes (n), the connectedness value (m_1), and the probability of rewiring each of the edges (p_1). The Watts-Strogratz model initially starts with a circle graph with n nodes, each with the same degree, D. The connectedness value establishes to how many nodes a particular node is initially connected. The Watts-Strogratz graph in Figure 5 has twelve nodes and a neighborhood connected value

Figure 4. Example of a circle graph

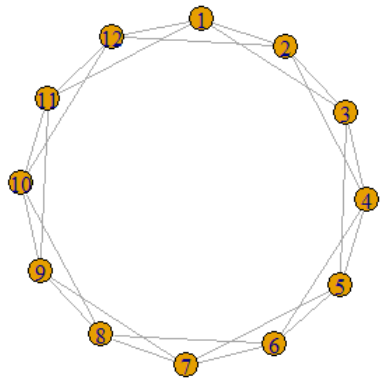

of two. Then, each edge is moved to some new node chosen at random through the process called "rewiring" uniformly with probability, p_1. As p_1 varies between 0 and 1, strikingly different graphs are generated. For instance p_1 equals 0 results in the circle graph as shown in Figure 4, and $p = 1$ results in the completely random graph as shown in Figure 5. By building the graph with rewiring, the Watts-Strogratz model simulates graphs with both properties of transivity and short path lengths [33].

Figures 6-8 are heat plots that compare the potential adjacency matrix of the Erdös-Rényi, Barabási-Albert, and Watts-Strogratz models with 32 nodes and 64 edges for each model. The heat index measures the potential for an edge to exist between two nodes in the adjacency matrix where red represents no edge/potential, and edge potential increases from red, blue, green, orange, yellow and pink.

Figure 5. Random Graph Watts Strogratz $p = 1$

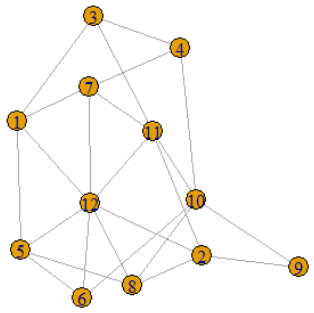

Figure 6. Adjacency matrix Barabási-Albert ($n = 32$, $m0 = 2$)

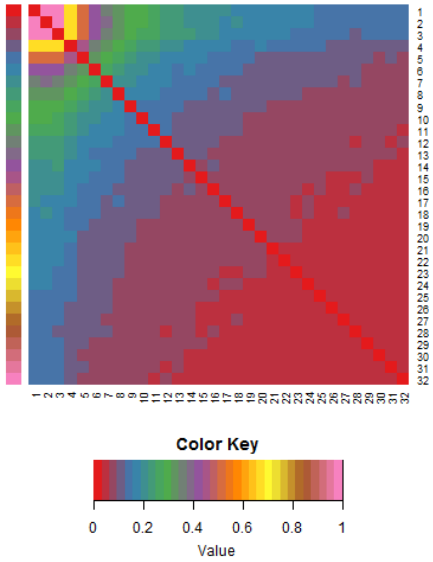

Figure 7. Adjacency matrix Erdös-Rényi ($n = 32$, $m = 64$

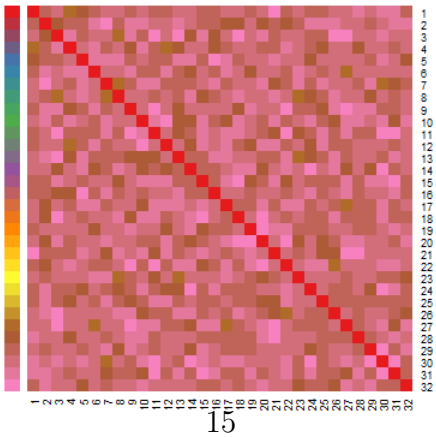

For the Barabási-Albert model, depicted in Figure 6, edges are concentrated among the first nodes since the top left of Figure 6 is mostly pink. However, the Erdös-Rényi model, depicted in Figure 7, demonstrates all edge locations as having an equally high potential for connectivity via a random scattering of edges.

Figure 8. Adjacency matrix Watts-Strogratz ($n = 32$, $m1 = 2$, $p = 1/2$)

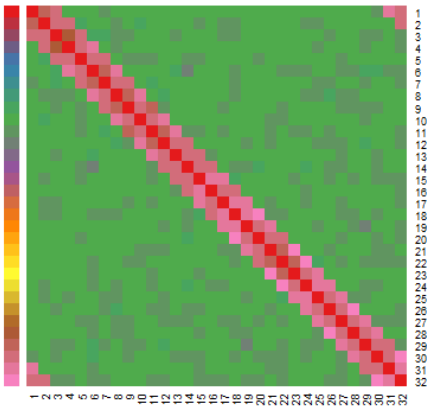

Lastly, the Watts-Strogratz model, depicted in Figure 8, has edges concentrated closest to its neighbors, demonstrated by the greatest potential for edge locations along the diagonal. These examples provide insight into the edge placement that these generating algorithms create. Many real world networks have properties of these three graph generating models, and as such, this research was centered around simulating random graphs from these generation models.

Methods to detect changes within a network are grouped depending on the nature of the network characterization used to identify change. For instance, graph matching techniques seek to compare two networks via their graphs to determine how different one is from the other. Graph classification techniques seek to classify the graph of a network as a particular network or something different. Change point detection seeks to determine the point when a graph is changing. All of these techniques rely primarily on deterministic mathematical tools, which can be computationally intensive.

Graph Matching.

Network monitoring for the intent of detecting a change within a network takes several forms and is closely related to graph matching, which is sometimes referred to as graph comparisons. In 2004, Conte *et al.* provided a thorough examination into graph matching by researching exact and inexact matching algorithms from over 160 graph matching papers [5]. Exact matching is described best by *edge-preserving*, which means if two nodes are connected in one graph, then they must be connected in the other graph. Several forms of exact matching exists: *graph isomorphism*, *subgraph isomorphism*, *monomorphism*, and *homomorphism*. The most restrictive type of graph matching is graph isomorphism which requires a one-to-one correspondence for every node in each graph. Subgraph isomorphism relaxes the requirement of one-to-one correspondence for every node, and seeks to answer whether one graph contains a *subgraph* that is *isomorphic* to the other graph. Monomorphism requires that each node is mapped to a distinct node between each graph and that each edge has a corresponding edge in the comparison graph. The comparison graph is allowed to have additional edges and nodes. Lastly, homomorphism relaxes the constraint on the nodes that each node is mapped to a distinct node, such that only in one graph do nodes have to be mapped to distinct nodes in the comparison graph. There is no efficient way to solve any of these methods at this time as each belongs to the class of NP-complete problems, aside from graph isomorphism which has not been proven to be NP-complete. Inexact matching relaxes the *edge-preserving* constraint by minimizing a function which adds a penalty when the edge-preserving constraint is not met. While inexact methods helps efficiency and solution generation, the trade space is accurate representations between the graphs.

In 2013, Livi and Rizzi compared multiple methods for graph matching based on the similarities or dissimilarities of any two graphs [27]. The methods they examined

utilized graph edit distance, graph kernels, and graph embedding techniques which all can be formulated in terms of similarities and dissimilarities. Graph edit distance methods seek to match graphs directly and are a measure of similarity and dissimilarity between the graphs in questions. In these methods, edit operations are made in order to change one graph into the other and can be held to exact or inexact matching methods. The second method Livi and Rizzi highlight is graph kernel which utilizes the similarity between two graphs with respect to some implicitly defined feature space. Based on kernel selection and the use of an algorithm, typically a support vector machine, a classification result with some probability is generated for the two graphs in question. Lastly, graph embedding is a hybrid of graph edit distance and graph kernels for networks whose common mathematical structure or metrics are not easily defined. Graph embedding methods seek a vector representation of a graph's structure and metrics such that edit distance or graph kernels can be applied directly. Livi and Rizzi give a multitude of examples for each of these methods, but their conclusions and comparisons focus only on computational complexity. Livi and Rizzi conclude that graph matching is a challenging problem due to the graph's complexity and diverse content. In short graph matching, techniques are a compromise between computational cost and accuracy.

Macindoe and Richards use the distribution of certain structural features within subgraphs in order to compare two graphs[28]. Using these features, they define two graph's similarity through the earth mover's distance between the features distributions. Earth mover's distance is a measure of the distance between two probability distributions over some region D. The network measures (features) they selected were: leadership, bonding, and diversity. They researched 15 different graphs across 9 types of networks and calculated their similarity values using the earth mover's distance. Finally, they then performed clustering on the networks based on these values. While

their work covers both graph matching through calculation of a similarity score, and classification based upon clustering, they highlight a mathematical approach built on distributions of network measures for comparing graphs.

The last highlighted research conducted by Mohd-Zaid *et al.* had some success utilizing a statistical method of monitoring networks through a graphical model [30]. Mohd-Zaid *et al.* created a test of hypothesis to monitor a Barabási-Albert graph. Their work utilized L-moments, a statistical extension to classical distribution moments such as mean and variance, and demonstarted the ability to detect changes (based upon graph degradation) with a high degree of power for networks that were characterized as Barabási-Albert.

Graph Classification.

While graph matching techniques seek to compare two graphs, graph classification methods seek to classify (label) graphs based on some characteristic. Graph classification techniques typically use graph matching techniques such as graph edit distance, graph kernels, and graph embedding, as the first step before graph classification, such as the work of Macindoe *et al.* [28]. This section focuses on research that took an approach outside one of the graph matching methods described earlier in order to classify graphs.

Li *el al.* based their classification algorithm, a support vector machine, on topological and attribute features and compared their algorithm to the current state of the art for kernel methods for machine learning [26]. In their research, instead of relying on common kernels such as random walk, shortest path, cyclic pattern, subtree and subgraph, they computed 20 network measures (degree, clustering, number of nodes, and so forth) into a feature vector and utilized this feature vector as an input for support vector machine in order to correctly classify a number of different

datasets. Their research concluded that the feature vector was either on par with or outperformed the kernel methods for classification while overall lowering computational times. This shows that topological graph attributes (network characteristics) are well poised for discriminating the structures within different classes of graphs.

Moonesinghe *et al.* examined graph classification based on the probabilistic substructure of graphs using a maximum entropy algorithm [31]. Binary feature vectors were constructed from subgraphs using a frequent subgraph mining algorithm for all graphs in four databases that they considered. This process was repeated until their maximum entropy algorithm converged. Their classification results for each dataset examined and compared the maximum entropy method with an Adaboost and support vector machine classifier. The probabilistic model outperformed the support vector machine and Adaboost methods in all but one dataset respectively.

Jin *et al.* researched classification using subgraphs, but sought to reduce computational time by only performing data mining once instead of using a repeated approach [22]. The team's pattern exploration algorithm first looked for complementary discriminative patterns within each graph, and it then grouped them into co-occurrence rules. A discrimination score was calculated for each pattern and the algorithm stopped after all patterns had been evaluated, or if one pattern achieved a perfect discrimination score for the dataset. The optimal solution for co-occurrence rules have patterns with high frequency in one graph and low frequency in a differing graph. They reported results comparing their method with two alternative subgraph approaches that did not take co-occurrence into account, and the results showed that their technique achieved similar performance but drastically cut computational time.

Change Point Detection.

Multiple fields, studies, and researchers are interested in detecting anomalies [29] within networks or focused on change point detection [23]. While a lot of research exists in these areas, there is little to no overarching guidance or study that helps practitioners highlight which network measures or statistical moments are more advantageous to detecting changes based on a networks structure. However, there are a few notable studies worth pointing out, and they are highlighted below.

Serin and Balcisoy performed an entropy based sensitivity analysis of several networks extracted from the DBLP [1] dataset for several network measures [36]. They examined degree, betweenness, and closeness, and they scored each node based on the difference in the entropy of the measure between the full network and the network with only that node removed. Based on this sensitivity, they implemented a visualization algorithm to highlight these influential nodes. The bulk of their work rested in the visualization tool with no analysis highlighting the most sensitive network measures. While entropy may describe the uncertainty about each node, comparison of networks based upon node entropy alone is not possible since node entropy is not unique. Hence, traditional and non-traditional moments were utilized by the next researchers in order to detect changes within networks.

Mohd-Zaid *et al.* researched the effect of node and edge degradation of Barabási-Albert networks by examining L-moments and joint L-moments of the networks' degree distribution [30]. After extensive normality testing, they derived a univariate and multivariate normal test for testing L-moments and joint L-moments and found that the joint L-moment $(\lambda_2, \tau_3, \tau_4)$ test had significant power at detecting degradation for the different Barabási-Albert networks simulated. Their work demonstrates that moments based on network measures are useful at detecting changes in a network graph when an underlying assumption is made about the specific type of network

model.

Summary of Previous Research.

The current state of graph matching, classification, and change point detection is mainly concentrated within deterministic mathematical and graphical solutions which come with certain limitations due to trade-offs between computational cost and accuracy. Several statistical based approaches were described. This research was built on the statistical approaches of Mohd-Zaid *et al.* and answers which moments, network measures, and tests are most sensitive to detect change (i.e. node deletion) for different network types. This was accomplished by expanding the work of Mohd-Zaid *et al.* to include the Erdös-Rényi and Watts-Strogratz networks, traditional moments, and the additional network measures of betweenness and closeness. Normality assumptions are not required and examined, with non-parametric testing methods relying on univariate distributions so as to not mis-specify distributions or correlation structures of the moments and measures considered. Robust statistics that properly capture underlying distributions of graph models is needed and as such, both traditional moments and L-moments were considered. Background on these moments are examined next.

2.2 Statistical Moments: Traditional and L-moments

Statistical moments are useful tools to ascertain and summarize an underlying population. Casella-Berger [4] defines for each integer n, the n^{th} *moment* of random variable X, μ_n as:

$$\mu_n = E[X^n]$$

and the n^{th} *central moment* of X, μ_n as:

$$\mu_n = E(X - \mu_1)^n$$

where E refers to the expectation operator. The first moment, u_1, or just μ is known as the mean and the second central moment, $\mu_2 = var(x)$, is known as the variance. Higher order moments are typically scaled by the second moment and known as skewness and kurtosis. These moments can help define a distribution and in some cases, uniquely define a distribution [15]. While traditional moments are commonly used for most statistical research, other types of moments, such as L-moments, exist with some useful properties. By entertaining a wide range of moments, this research investigated the use of the moments that are best suited to the underlying structures. Hence some background on L-moments are discussed next.

L-moments were first introduced by Hosking in 1990 and were shown to be an alternative to estimating distributional parameters through traditional moments [18]. Hosking's approach consisted of linear combinations of the sample order statistics. There are many different uses for L-moments. Specific fields utilize these moments more than traditional moments for several reasons, foremost of which is their property of robustness against outliers [18]. Hosking also showed that sample L-moments are "viable for heavy tailed distributions and even those distributions for which the mean may not exist" [19]. This is a result of the L-moments being a linear combination of the order statistics and as such, they are less affected by outliers. Then, the formal definition of the r^{th} sample L-moment of ordered random variables X is:

$$l_r = \binom{n}{r}^{-1} \sum_{1 \le i_1} \sum_{< i_2 <..} ... \sum_{.i_r \le n} r^{-1} \sum_{k=0}^{r-1} (-1)^k \binom{r-1}{k} X_{i_{r-k:n}} \tag{5}$$

where r is the r^{th} moment, $i_{r-k:n}$ signifies the order statistic from an ordered sample of size n. The sample L-moment is estimated by what is known as a U-statistic and this particular U-statistic is a "function of the sample order statistics averaged over all subsamples of size r from an observed sample of size n" [18]. U-statistics are known for the following mathematical properties: unbiasedness, asymptotic normality, and some modest resistance to outliers which make them suitable for statistical analysis and inference [18]. Further, asymptotic normality may be useful when considering L-moments in large networks. From Equation 5, the first four sample L-moments in a sample of size n are given as the following [18]:

$$\begin{aligned}
l_1 =& n^{-1} \sum_i X_i, \\
l_2 =& \binom{n}{2}^{-1} 2^{-1} \sum \sum_{i>j} (X_{i:n} - X_{j:n}), \\
l_3 =& \binom{n}{3}^{-1} 3^{-1} \sum \sum \sum_{i>j>k} (X_{i:n} - 2X_{j:n} + X_{k:n}), \\
l_4 =& \binom{n}{4}^{-1} 4^{-1} \sum \sum \sum \sum_{i>j>k>l} (X_{i:n} - 3X_{j:n} + 3X_{k:n} - X_{l:n}).
\end{aligned} \tag{6}$$

When $r = n$, the sample L-moment Equation 5 reduces to the formal population L-moment equation given in Hosking's original paper [18]. In his paper, Hosking proves that if the mean of a random variable exists, then all L-moments exist; further, unlike traditional moments, L-moments uniquely characterize the underlying distribution [18]. Hosking also shows that L-moments and traditional central moments are analogous. Finally, Hoskings additionally derived sample L-moments ratios which are calculated as:

$$t_i = \frac{l_i}{l_2}, \forall i > 2 \tag{7}$$

and are analogous to 3^{rd}, 4^{th} and higher order traditional centralized moments. t_3 is known as the sample L-skewness and t_4 as the sample L-kurtosis. Due to the way the sample L-moment ratios, t_3 and t_4, are defined, they are able to achieve the full range of values available from the population L-moment ratios, τ_3 and τ_4, unlike the higher order traditional moment ratios, skewness and kurtosis [18], which cannot always obtain the full range of values from the population skewness and kurtosis. The next section highlights some research that compares traditional moments to L-moments and seeks to answer sample sizes requirements when working with L-moments.

L-moments versus Traditional Moments.

Multiple studies [13][34][35] have conducted comparison analysis between L-moments and traditional moments and highlighted the advantages of L-moments. Perez *et al.* showed a theoretical comparison of properties between moments and L-moments [34]. Their purely theoretical work provided no conclusions as to when which type of moment is better or what sample sizes are sufficient for estimating L-moments. Guttman's research focused on L-moment sample size, but only for his particular set of precipitation data [13]. Guttman estimated mean departure of L-moments from the population L-moment for the entire population for different sample sizes of his specific dataset. This is a useful technique when the entire population is known, yet full knowledge of an entire population is rarely known. Sankarasubramanian and Srinivasan's research focused on sampling properties of L-moments and traditional moments [35]. Their research focused on four distributions: Generalized Normal, Pearson-3, Generalized Extreme Value and Generalized Pareto. They simulated data for the Generalized Normal and Pearson-3 distributions since no closed form solutions for these distributions exist. They estimated L-moments for a fixed number of parameter values in each distribution and estimated sample variance using a regression

model. From this data, they were able to calculate bias and variance for a small range of sample sizes for l_2 and t_3. Those results were then compared to sample size estimates for variance and skewness, which were calculated using traditional moments. While their research concluded bias and variance existed for some sample sizes, L-moment sample variance was based upon statistical models not exact calculations. In conclusion, since L-moments may uniquely characterize a distribution, they may be quite useful in characterizing network measures in graph comparisons. However, a robust study of the required sample size to estimate L-moments, particularly for distributions associated with the network measures of networks, is necessary in order to assure comparisons and tests based upon these measures are appropriately powered for network research.

Summary.

In this chapter, a brief introduction into graphs, network measures, and random graph generating models were presented. Then, an overview on topics as it relates to network degradation detection was presented within the following topics: graph monitoring, graph classification, and change point detection. Lastly, statistical theory, background, and research comparing moments were given for traditional and L-moments. The next chapter addresses the first research objective which is to determine which network measures, moments, and statistical tests are the most sensitive at detecting change via degradation of networks through node elimination for common network generation models.

III. Sensitivity of Network Measures, Moments, and Tests to Network Degradation

When attempting to detect changes within a network, many different deterministic mathematical tools exist, but come with high computational cost and lengthy time requirements. This research examines statistical distributions of various moments from network measures and induces network degradation in the form of node removal to examine the sensitivity of both moment estimators and network measures with respect to network degradation. The findings also highlight which statistical test, network measures, and characteristics (moments) might be leveraged for detecting changes in networks without the high computation cost of other common graphical methods. Here, network changes are examined in the context of network degradation via the elimination of nodes from the network. Network measures and moments were simulated from three random graph models in order to answer the following research objectives: what network measures and moments are sensitive to network degradation, what are appropriate statistical tests to use to detect network degradation, and which combination of network measures and tests are most effective at detecting network changes in data applications. Here, the best and most sensitive methods are determined by which combinations of network measures and moments detect the smallest change (loss of node) within the network at high power. This sensitivity analysis was conducted through a large simulation across three random graph models: the Erdös-Rényi, Barabási-Albert, and Watts-Strogratz models.

In order to answer each of these objectives, the work, theory, or simulation that took place is presented next. In addition, these research objectives are separated into three research questions: 1a) what network measures and moments are sensitive to network degradation, 1b) what are appropriate statistical tests to use to detect network degradation, and 1c) which combination of network measures and tests are

most effective at detecting network changes in data applications. For research question 1a, the sensitivity analysis design is outlined. Then, the simulation and testing methods are described, as well as the results of the simulation. For research question 1b, various statistical testing methods are detailed, changes to the simulation design are described, and the results concerning which statistical tests are most sensitive are presented. In conclusion, for research objective 1c, the results from questions 1a and 1b are applied to two real world data sets.

3.1 Research question 1a: What Network Measures and Moments are Sensitive to Network Degradation?

Sensitivity Analysis Design and Methods.

Simulations were utilized to answer research questions 1a and 1b. A description of this simulation as it pertains to research question 1a follows. In general, three network models of varying size were examined. For each model, network measures and statistical moments were calculated. Then, networks were degraded (nodes removed) and changes in the statistical moments of the network measures were used to determine which could detect this change. Specifically, all simulations were conducted within R studio, utilizing the following packages: *igraph, lmom*, and *moments*. The *igraph* package was utilized to create random graphs according to the Erdös-Rényi (ER), Barabási-Albert (BA), and Watts-Strogratz (WS) models. The *lmom* and *moments* package calculated the traditional moments and L-moments utilized. An initial seed was set when generating data for repeatability. The particular fixed parameter settings for each network model were chosen to have reasonably comparable graphs of a particular size across network models. Table 2 shows the number of nodes for each network model, determined by k, which will be referenced as the size of the network with respect to node count, e.g., the size of the network is 2^k. Next, m, which is

Table 2. Network Models Parameter Settings

Models	Nodes	Edges
Erdös-Rényi	2^k	Total Edges ($2^k m$)
Barabási-Albert	2^k	Edges Added per Node (m)
Watts-Strogratz	2^k	Connectedness (m)

referred to as the edge density parameter, affects how many edges each graph will contain. Each of the graphical models had the same number of nodes across sizes (k) and approximately the same number of edges (E). The first three labeled rows of Table 3 provide the settings for building the initial networks for seven different network sizes considered, each with five different edge density settings.

Table 3. Network Simulation Settings

Row	Network Models	ER, BA, and WS
1	Network Sizes (2ˆk)	k = 5,6,7,8,9,10,11
2	Number of Edges ($\sim 2^k m$)	m = 2,3,4,5,6
3	Total No. of Graphs	105
4	Degrade Level	Low, Medium, High
5	Proportion of Degrade (p)	p = 1/2, 1/3, /1/4, 1/5, 1/7, 1/10
6 7	No. of Degrade Settings per Graph	18
	Total Graphs in All Simulated	1890

BA - Barabási-Albert; ER - Erdös-Rényi; WS - Watts-Strogratz

For each of the 105 initial networks, three network measures (degree, betweenness, and closeness) were calculated, and seven moments were calculated for each of the network measures: m_1 (mean), m_2 (variance), m_3 (skewness), m_4 (kurtosis), l_2 (L-scale), t_3 (L-skewness), and t_4 (L-kurtosis). All networks were verified to be connected, and any isolates created due to the network generation mechanisms were removed. An isolate is any node that is not connected to any other node, and can occur during the

random generation of certain models and simulation of network degradation. Table 4 highlights the number of isolates created within the initial simulation for three notional network sizes, all with edge density of $m = 2$. Approximately two percent of the nodes were removed from the Erdös-Rényi model and less than one percent from the Watts-Strogratz model. No isolates were created for the Barabási-Albert model because this network model begins fully connected. Each of the three random graph

Table 4. Isolates Created in Simulation of 1,000 graphs with $m = 2$

	Erdös-Rényi		
graph size	No. of isolates	avg per graph	% of all nodes
small - 32 nodes	397	< 1	$< 2\%$
medium - 216 nodes	4,549	< 5	$\sim 2\%$
large - 1024 nodes	18,625	< 19	$< 2\%$
	Watts-Strogratz		
graph size	No. of Isolates	avg per graph	% of all nodes
small - 32 nodes	231	< 1	$< 1\%$
medium - 216 nodes	2,121	< 3	$< 1\%$
large - 1024 nodes	8,594	< 9	$< 1\%$

models were simulated 50,000 times and a particular network degradation was executed on the network. The fourth through sixth rows of Table 3 lists the settings for degrading each of the 105 simulated networks based upon three degrade levels (low, medium, and high) and six proportion settings ($p = \frac{1}{2}, \frac{1}{3}, \frac{1}{4}, \frac{1}{5}, \frac{1}{7}, \frac{1}{10}$). The low degrade level represents removing nodes from the set of all nodes whose degree is equal or less than the 20^{th} percentile of node degree for that particular network, and rounded down in the cases where the 20^{th} percentile was not an integer value. The proportion (p) of degrade was used to randomly select which of these nodes were removed. Any resulting isolates were also removed. The medium degrade level represents removing nodes from the set of all nodes whose degree is between the 40^{th} or 60^{th} percentile of node degree for that particular network, and rounded up in the cases where the 40^{th} percentile was not an integer value and rounded down in the case where the 60^{th}

percentile was not an integer value. The high degrade level represents removing nodes from the set of all nodes whose degree is equal or greater than the 80^{th} percentile of node degree for that particular network, and rounded up in the cases where the 80^{th} percentile was not an integer value. Pseudo code for this simulation can be found in Appendix A listed as Algorithm 1.

It is important to make the distinction that the proportion selected is coming from a subset of nodes, represented by the degrade level (low, medium, high), of the entire number of nodes in the network. Hence, at the lowest setting, $p = 1/10$, anywhere from $1 - 3\%$ of the nodes across all network models are being removed across all degrade levels. At most, less than 20% of nodes are ever removed within this study. Tables A1 - A3 within Appendix A highlight the average number of nodes removed for each combination of nodes, edge density, degrade and proportion setting.

Statistical Methods (1a).

To answer the first question concerning which network measures and moments are sensitive to detect degradation within a network via node deletion, each network was degraded based upon the network settings (low, medium, high) and proportion of nodes deleted ($p = 1/10$ to $1/2$). For each of the networks simulated empirical distributions for each of the 21 moments (7 moments for each of the 3 network measures) were derived based on 500 random networks. Each of the 21 empirical distribution functions across all three random graph generated models were compared prior to and after the degrade. The non-parametric Kolmogorov-Smirnov (K-S) test [16] was chosen to detect changes within the empirical distributions of moments since parametric assumptions do not hold or exist across all network measure moments. The K-S Test has two assumptions (A1 and A2) and is described next.

The first (A1) assumption is that the observation from each random sample pop-

ulation (degraded and non-degraded network) are independent and identically distributed. The second (A2) assumption is that the two populations are mutually independent. Based on these assumptions the hypothesis is testing whether or not the empirical cumulative distribution functions (CDF) are equal.

$$H_0 : F(t) = G(t) \quad H_a : F(t) \neq G(t) \text{ for at least one } t \tag{8}$$

$$J = \frac{mn}{d} \underset{(-\infty<t<\infty)}{max} |F_m(t) - G_n(t)|. \tag{9}$$

$F(t)$ is the non-degraded network's empirical distribution function, while $G(t)$ is the degraded network empirical distribution function. J is the test statistic, and m and n are the sample sizes for each of the two random samples, while d is their greatest common divisor. J is tested against any possible difference between the two distributions at a given α level. If the greatest difference between the two CDFs is too large, the null hypothesis is rejected and the distributions are considered different.

Recall, each of these empirical distributions for a particular moment is created by combining 500 random graph moments together. Sensitivity was determined by calculating the empirical power of the K-S Test to detect the change for each network measure, characteristics for each network size, and degrade setting. Empirical power to detect the change was defined as the number of times out of 1,000 (50,000 graphs grouped into 1000 distributions of size 500) the K-S Test detected the change. These empirical results were binned into two categories ranging from red < 0.90 power to green representing 0.90 or higher power. If the network measure and moment achieved at least 0.90 power, it was considered sensitive to detecting the change. Due to the large number of tests, degrade settings, network sizes, measures, and characteristics, results are presented graphically as heatplots. Figure 9 is an example of this plot for the Erdös-Rényi graph with parameter settings $k = 5$, and $m = 2$. In this figure, 9

blocks are formed within the entire matrix. Along the y axis, the blocks correspond to each of the three network measures, degree, betweenness, and closeness. While the x axis blocks correspond to each of the degrade settings, low, medium, high. Within each block, the y-axis has seven settings relating to the test statistics utilized in order, $(m_1, m_2, m_3, m_4, l_2, t_3, t_4)$ and the x-axis has six settings for probability of degrade, $(\frac{1}{2}, \frac{1}{3}, \frac{1}{4}, \frac{1}{5}, \frac{1}{7}, \frac{1}{10})$.

Figure 9. Example for reading tables

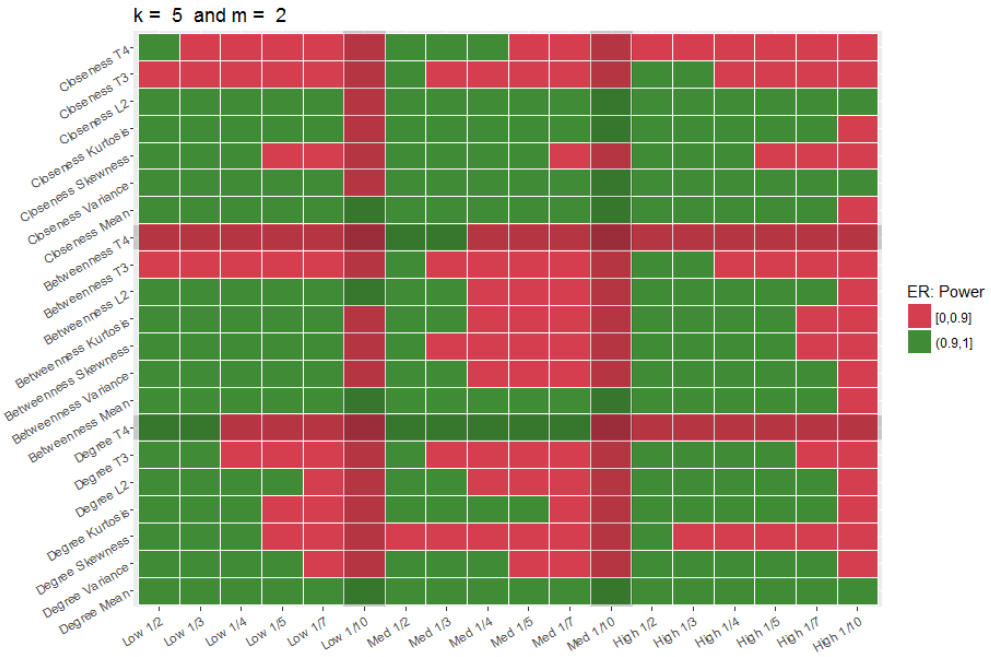

Analysis of this simulation at a proportion (p) of 1/10 follows as this was the smallest proportion of nodes removed. Analysis included 1) identifying which moments and network measures achieved power of at least 0.90 and 2) which measures and moments had statistically significantly higher power as evidenced by utilizing a full factor ANOVA model. Full results can be found in Appendix A, in Figures A1-A9. Table 5 lists the five factors and each of their levels. Inference based on the ANOVA results are reported based on Tukey's pairwise comparison of different levels for of the factors: moments and network measures.

Table 5. Full Factorial at lowest Proportion

Levels	Factors				
	Node Size, k	Edge Density, m	Network Measure	Moment	Degrade
1	5	2	betweenness	mean	low
2	6	3	closeness	variance	medium
3	7	4	degree	skewness	high
4	8	5		krutosis	
5	9	6		L-scale	
6	10			L-skewness	
7	11			L-kurtosis	

Tukey's HSD [24] allows one to make an α-level family of pairwise comparisons among all compared factors levels. Based on this test, one can determine if there is a statistically significant difference between factor levels compared. Tukey's HSD has the following three assumptions for all factor levels: independent, normally distributed and homogeneity of variance. The hypothesis is the following:

$$H_0 : \mu_i = \mu_{i'} \;\; H_a : \mu_i \neq \mu_{i'} \tag{10}$$

where μ_i is the mean of a particular level within a factor, and $\mu_{i'}$ represents another factor level for comparison. The test is built using the studentized range distribution and tests whether or not the corresponding confidence interval contains zero.

Erdös-Rényi Sensitivity Analysis.

Tables 6 - 8 highlight the moments which had power above 0.90 for all three degrade settings for each of the network measures for the Erdös-Rényi network model at a proportion of 1/10. Beginning with the network measure degree (Table 6), the

mean (m_1) detected the degradation at $p = 1/10$ in all 35 different network sizes. As such, it is highlighted in green in the bottom right cell of Table 6. As the graph size increased, there was an increase in the number of traditional moments detecting the degradation, as well as the L-moment, L-kurtosis (t_4). When looking across all graph sizes while holding the density constant, only the mean (m_1) maintained power to detect the degrade. However, across all densities, while holding the number of nodes constant, L-kurtosis (t_4) maintained power for $k = 9, 10, 11$ and kurtosis (m_4) maintained power for $k = 10$ and 11.

Table 6. Moments achieving > 0.90 power for degree in the Erdös-Rényi Network Model

k	m					
	2	3	4	5	6	common $\forall$ m
5	m_1	m_1	m_1	m_1	m_1	m_1
6	m_1	m_1	m_1	m_1	m_1	m_1
7	m_1	m_1	m_1	m_1	m_1	m_1
8	m_1	$m_1\tau_4$	$m_1\tau_4$	$m_1\tau_4$	$m_1\tau_4$	m_1
9	$m_{1,4}\tau_4$	$m_{1,4}\tau_4$	$m_1\tau_4$	$m_1\tau_4$	$m_1\tau_4$	$m_1\tau_4$
10	$m_{1,2,3,4}\tau_4$	$m_{1,4}\tau_4$	$m_{1,4}\tau_4$	$m_{1,4}\tau_4$	$m_{1,4}\tau_4$	$m_{1,4}\tau_4$
11	$m_{1,2,3,4}\tau_4$	$m_{1,4}\tau_4$	$m_{1,4}\tau_4$	$m_{1,4}\tau_4$	$m_{1,4}\tau_4$	$m_{1,4}\tau_4$
common $\forall$ k	m_1	m_1	m_1	m_1	m_1	m_1

m_1 (mean), m_2 (variance), m_3 (skewness), m_4 (kurtosis), l_2 (L-scale), t_3 (L-skewness), and t_4 (L-kurtosis)

For the network measure betweenness (Table 7) the same trends hold as for degree (Table 6) with one exception. For small sparse graphs ($k = 5, m = 2 - 4$ and $k = 6, m = 4$) no moment achieved > 0.90 power to detect the degradation at $p = 1/10$. The mean (m_1) was the only moment consistent in lower sized graphs,

and as the graph increased, additional moments detected the degrade. In looking for consistency, across graph sizes only the mean (m_1) consistently achieved power to detect the degrade with the exception of L-kurtosis (τ_4) for $k = 10$ and 11. When looking across edge density, again, only the mean consistently achieved power.

Table 7. Moments achieving > 0.90 power for betweenness in the Erdös-Rényi Network Model

k	m					
	2	3	4	5	6	common $\forall$ m
5	-	-	-	m_1	m_1	m_1
6	m_1	-	m_1	m_1	m_1	m_1
7	m_1	m_1	m_1	m_1	m_1	m_1
8	$m_{1,2}l_2$	m_1	m_1	m_1	m_1	m_1
9	$m_{1,2,3,4}l_2$	m_1	m_1	m_1	$m_1\tau_4$	m_1
10	$m_{1,2,3,4}l_2$	$m_1\tau_4$	$m_1l_2\tau_4$	$m_1l_2\tau_4$	$m_1l_2\tau_4$	m_1
11	$m_{1,2,3,4}l_2\tau_4$	$m_1\tau_4$	$m_{1,2}l_2\tau_{3,4}$	$m_{1,2}l_2\tau_4$	$m_{1,2}l_2\tau_4$	$m_1\tau_4$
common $\forall$ k	m_1	m_1	m_1	m_1	m_1	m_1

m_1 (mean), m_2 (variance), m_3 (skewness), m_4 (kurtosis), l_2 (L-scale), t_3 (L-skewness), and t_4 (L-kurtosis)

Finally, closeness has an expanded list of moments (all traditional moments and L-variance) that detected the degradation at $p = 1/10$ with high power (Table 8). Starting with the second smallest graph size, where $k = 6$, multiple moments showed sensitivity (power > 0.90). Similar to the network measures of betweenness and degree, across graph size, holding density constant, the mean (m_1) remains sensitive, meaning power remains above 0.90, for closeness. Across density, holding graph size constant, some variations appear. For $k = 5$, the mean was consistently sensitive. However, for $k = 6$ and 7 the variance (m_2) was sensitive. For $k \geq 8$, kurtosis (m_4)

and L-scale (l_2) consistently achieved high power. By removing the smallest edge density ($k = 5$), the mean (m_1) is consistent across all node sizes and edge densities. By excluding the smallest node size, the variance (m_2) becomes consistent across all other combinations. This is noted by the mean (m_1) and variance (m_2) both contained in the bottom right cell, but not highlighted as neither maintains power in all the combinations of graphs and degrade settings examined.

Table 8. Moments achieving > 0.90 power for closeness in the Erdös-Rényi Network Model

k	m					
	2	3	4	5	6	common $\forall$ m
5	-	m_1	m_1	m_1	m_1	-
6	$m_{2,4}l_2$	$m_{1,2,4}$	$m_{1,2,4}l_2$	$m_{1,2,4}l_2$	$m_{1,2}l_2$	m_2
7	$m_{2,4}l_2$	$m_{1,2,4}l_2$	$m_{1,2,4}l_2$	$m_{1,2,4}l_2$	$m_{1,2,4}l_2$	$m_{2,4}l_2$
8	$m_{2,4}l_2$	$m_{1,2,4}l_2$	$m_{1,2,4}l_2$	$m_{1,2,4}l_2$	$m_{1,2,4}l_2$	$m_{2,4}l_2$
9	$m_{1,2,4}l_2$	$m_{1,2,3,4}l_2$	$m_{1,2,3,4}l_2$	$m_{1,2,4}l_2$	$m_{1,2,3,4}l_2$	$m_{1,2,4}l_2$
10	$m_{1,2,4}l_2$	$m_{1,2,3,4}l_2\tau_4$	$m_{1,2,3,4}l_2\tau_3$	$m_{1,2,3,4}l_2\tau_4$	$m_{1,2,4}l_2$	$m_{1,2,4}l_2$
11	$m_{1,2,4}l_2$	$m_{1,2,3,4}l_2$	$m_{1,2,3,4}l_2$	$m_{1,2,3,4}l_2\tau_4$	$m_{1,2,3,4}l_2$	$m_{1,2,4}l_2$
common $\forall$ k	-	m_1	m_1	m_1	m_1	$m^*_{1,2}l^{**}_2$

m_1 (mean), m_2 (variance), m_3 (skewness), m_4 (kurtosis), l_2 (L-scale), t_3 (L-skewness), and t_4 (L-kurtosis)

* $k \geq 6$ and $m \geq 3$ and ** $k \geq 7$ and $m \geq 3$

Recall ANOVA was used to estimate the effects of network measures and moments across a multitude of different node sizes, edge densities, and degrade settings based on the empirical power to detect the degrade. The Least Square estimates for resulting power from the Erdös-Rényi simulation are shown in Table 9 and graphed in Figure 10. Closeness was the most sensitive measure based on the simulation run with a

mean power of 0.71 across all factors (95% CI: 0.70 - 0.72). The mean was the most sensitive moment with a mean power of 0.98 across all factors (95% CI: 0.96 - 1.00).

Table 9. Least Square Power Estimates by Network Measure and Moments for Erdös-Rényi Model

	Power Estimate	95% CI
Network Measure		
closeness	0.7107	(0.6976, 0.7239)
betweenness	0.5822	(0.5691, 0.5954)
degree	0.5530	(0.5399, 0.5662)
Moments		
Mean (m_1)	0.9811	(0.9610, 1.000)
Variance (m_2)	0.6909	(0.6708, 0.7110)
Skewness (m_3)	0.4358	(0.4157, 0.4558)
Kurtosis (m_4)	0.6901	(0.6700, 0.7102)
L-scale (l_2)	0.6904	(0.6703, 0.7105)
L-skewness (t_3)	0.2599	(0.2398, 0.2800)
L-kurtosis (t_4)	0.5592	(0.5391, 0.5793)

CI - Confidence Interval

Figure 10 shows the 95% confidence interval for each measure and moment based on the simulation that was studied. The y-axis reflects estimated power, while the x-axis lists the varying effects, both measures and moments. Graphically, it is easy to tell that closeness has the greatest power estimate across all network measures, while the mean has significantly more power than any other moment for the Erdös-Rényi model.

Figure 10. Least Square Power Estimates by Network Measure and Moment for Erdös-Rényi Model

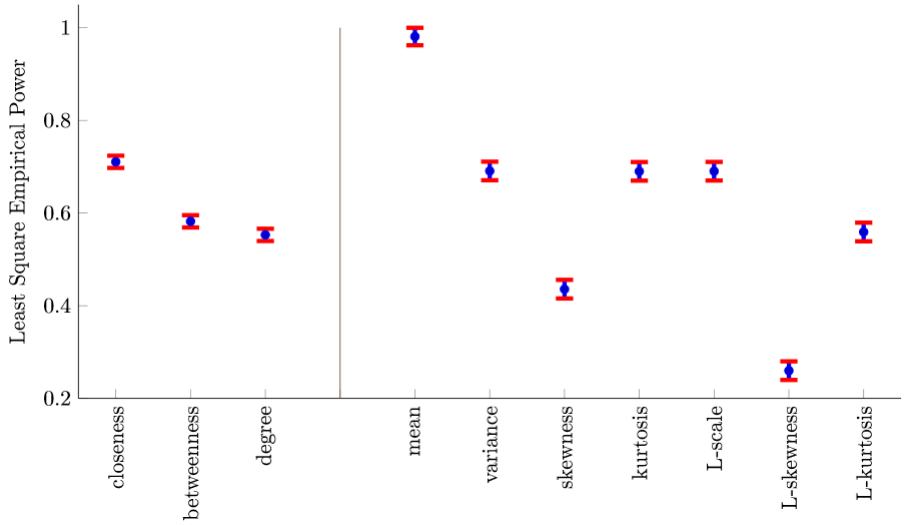

There were significant differences in the resulting power between all network measures (all p-values < 0.0001), the mean versus all other moments (all p-values < 0.001) and higher moments (skewness and kurtosis) versus their L-moment counterpart (L-skewness and L-kurtosis) (both p-values < 0.0001). Within network measures, closeness had the highest power to detect the degrade followed by betweenness and degree. Closeness resulted in significantly more power to detect the degrade than either betweenness or degree. On average, closeness had 12% more power than betweenness (95% CI: 10 - 15%) and 15% more power than degree (95% CI: 13 - 18%). When comparing the mean to all other moments, the mean averaged between 29% to 72% more power than any other moment or L-moment considered. Lastly, when comparing traditional moments and L-moments, there was no significant difference in power to detect the degradation between variance and L-scale (p-value 1.00). However, skewness had 17% significantly more power than L-skewness, and kurtosis had 13% significantly more power than L-kurtosis on average. All power results for the Erdös-Rényi network can be found in Appendix A Figures A1-A4 and ANOVA results in

Table A4.

Erdös-Rényi Concluding Remarks.

Table 10. Least Square Power Estimates based on Interaction of Network Measure and Moments for the Erdös-Rényi Model above 0.80

Network Measure	Moment	Power Estimate	95% CI
closeness	mean	0.9741	(0.9274, 1.0)
closeness	variance	0.9200	(0.8733, 0.9668)
closeness	kurtosis	0.9117	(0.8649, 0.9584)
closeness	L-scale	0.9209	(0.8742, 0.9676)
betweenness	mean	0.9692	(0.9225, 1.0)
degree	mean	1.000	(0.9532, 1.0)

CI - Confidence Interval

A concise way to portray the sensitivity analysis for the Erdös-Rényi simulation exist when looking at the ANOVA model estimates for the interaction of network measures and moments. Table 10 highlights the moments for each network measure that achieved a power estimate above 0.80. Closeness in all traditional moments except skewness, and L-scale achieved high power estimates. In addition, the mean was the only moment for the network measures betweenness and degree that achieved a power estimate above 0.80. Both of these findings confirm the results in Tables 6 - 8 when looking for consistent sensitivity across all graph combinations. Due to the construction of the Erdös-Rényi model, the random placement of edges, closeness is more sensitive to node degrade than between and degree. Closeness not only detected the location shift in the mean, but also in higher order moments based on dispersion (both traditional and L-moment) and kurtosis. The location shift alone was detected in all network measures, while the mean received the highest power estimate, of 1.0

(a perfect score which matches results in Table 6 where the mean detected the change in every graph combination.

Barabási-Albert Sensitivity Results.

Specific moments which had power above 0.90 at a proportion of 1/10 across all degrade settings and network measures for the Barabási-Albert network model are shown in Tables 11 - 13. Beginning with the network measure degree (Table 11), the mean (m_1) detected the degradation in 31 different network sizes, failing to detect the change in size $k = 5$, except when m was 2. As the graph size increased, variance (m_2) and L-scale (l_2) detected the change as well. Even L-skewness (τ_3) detected the change in large sparse graphs. Across all graph sizes $k >5$, while holding the density constant, only the mean (m_1) maintained power > 0.90 to detect the degrade. In addition, while holding the number of nodes constant, excluding $k = 5$, the mean (m_1) maintained power for $k = 6 - 11$, whereas variance (m_2) and L-scale (l_2) maintained power for $k = 10$ and 11.

Table 11. Moments achieving > 0.90 power for degree in the Barabási-Albert Network Model

k	m					
	2	3	4	5	6	common $\forall$ m
5	m_1	-	-	-	-	m_1
6	m_1	m_1	m_1	m_1	m_1	m_1
7	m_1	m_1	m_1	m_1	m_1	m_1
8	$m_{1,2}l_2\tau_3$	m_1l_2	m_1	m_1	m_1	m_1
9	$m_{1,2}l_2\tau_3$	$m_1l_2\tau_3$	$m_{1,2}l_2$	$m_{1,2}$	$m_{1,2}$	m_1
10	$m_{1,2}l_2\tau_3$	$m_{1,2}l_2\tau_3$	$m_{1,2}l_2$	$m_{1,2}l_2$	$m_{1,2}l_2$	$m_{1,2}l_2$
11	$m_{1,2}l_2\tau_3$	$m_{1,2}l_2\tau_3$	$m_{1,2}l_2$	$m_{1,2}l_2$	$m_{1,2}l_2$	$m_{1,2}l_2$
common $\forall$ k	m_1	m_1	m_1	m_1	m_1	m_1

m_1 (mean), m_2 (variance), m_3 (skewness), m_4 (kurtosis), l_2 (L-scale), t_3 (L-skewness), and t_4 (L-kurtosis)

The results based on the network measure betweenness (Table 12) differed slightly from degree (Table 11). All node densities for $k = 5$ failed to achieve 0.90 power at the degrade proportion of $1/10^{th}$. It appears that betweenness is the least sensitive of the network measures to the node degradation that is being simulated. The mean of closeness and degree were both able to detect the degradation within these graph combinations. The mean (m_1) was the only moment consistent in lower sized graphs, and as the graph size increased, all other moments detected the degrade in some graph combination. In looking for consistency, across graph sizes only the mean (m_1) consistently achieved power > 0.90 to detect the degrade, although variance (m_2) detected the change for $k = 8$ and 9. L-scale (l_2) also detected the change for $k = 8, 9$, and 11. Across edge density, only the mean (m_1) consistently achieved power > 0.90, with variance (m_2) detecting the change when $m = 2$. In addition, L-scale

(l_2) detected the change for $m = 2, 3$, and 4.

Table 12. Moments achieving > 0.90 power for betweenness in the Barabási-Albert Network Model

k	m					
	2	3	4	5	6	common $\forall$ m
5	-	-	-	-	-	
6	$m_{1,2}l_2$	m_1l_2	m_1l_2	m_1	m_1	m_1
7	$m_{1,2}l_2$	$m_{1,2}l_2$	m_1l_2	m_1l_2	m_1	m_1
8	$m_{1,2}l_2\tau_3$	$m_{1,2}l_2\tau_3$	$m_{1,2}l_2$	$m_{1,2}l_2$	$m_{1,2,3,4}$	$m_{1,2}l_2$
9	$m_{1,2}l_2\tau_3$	$m_{1,2}l_2$	$m_{1,2}l_2$	$m_{1,2,3}l_2$	$m_{1,3,4}$	m_1
10	$m_{1,2}l_2\tau_{3,4}$	$m_{1,2}l_2\tau_3$	$m_{1,2}l_2$	$m_{1,2,3,4}l_2$	$m_{1,2,3,4}l_2$	$m_{1,2}l_2$
11	$m_{1,2}l_2\tau_{3,4}$	$m_{1,2}l_2\tau_3$	$m_1l_2\tau_3$	$m_{1,2,3,4}l_2$	$m_{1,2,3,4}l_2$	m_1l_2
common $\forall$ k	$m_{1,2}l_2$	m_1l_2	m_1l_2	m_1	m_1	m_1

m_1 (mean), m_2 (variance), m_3 (skewness), m_4 (kurtosis), l_2 (L-scale), t_3 (L-skewness), and t_4 (L-kurtosis)

As seen in the Erdös-Rényi model, multiple moments (all traditional moments and L-variance) based on closeness detected the change with high power (Table 13). As seen with betweenness, closeness failed to meet the 0.90 power in the smallest graph size where $k = 5$. Starting with the second smallest graph size, where $k = 6$, multiple moments showed sensitivity. Specifically, all traditional moments and L-scale (l_2) achieved power > 0.90 for all edge densities except for skewness (m_3), when $k = 3$. This trend of all traditional moments and L-scale (l_2) remained sensitive across all graph combinations. Across graph sizes greater than $k = 5$ holding density constant, the mean (m_1), variance (m_2), and kurtosis (m_4) remained sensitive for closeness. Skewness (m_3) was also sensitive except when $m = 3$, and L-scale (l_2) was sensitive when $m = 2$. Across edge density and holding graph size constant for $k > 5$,

the mean (m_1), variance (m_2), and kurtosis (m_4) were consistently sensitive as well. Again, skewness (m_3) was sensitive except when $k = 6$ and 7, and L-scale (l_2) was sensitive except when $k = 7$.

Table 13. Moments achieving > 0.90 power for closeness in the Barabási-Albert Network Model

k	m					
	2	3	4	5	6	common $\forall$ m
5	-	-	-	-	-	
6	$m_{1,2,3,4}l_2$	$m_{1,2,4}l_2$	$m_{1,2,3,4}l_2$	$m_{1,2,3,4}l_2$	$m_{1,2,3,4}l_2$	$m_{1,2,4}l_2$
7	$m_{1,2,3,4}$	$m_{1,2,4}l_2$	$m_{1,2,4}l_2$	$m_{1,2,3,4}l_2$	$m_{1,2,3,4}l_2$	$m_{1,2,4}$
8	$m_{1,2,3,4}l_2$	$m_{1,2,3,4}l_2$	$m_{1,2,3,4}l_2$	$m_{1,2,3,4}l_2$	$m_{1,2,3,4}l_2$	$m_{1,2,3,4}l_2$
9	$m_{1,2,3,4}l_2$	$m_{1,2,3,4}l_2$	$m_{1,2,3,4}l_2$	$m_{1,2,3,4}l_2$	$m_{1,2,3,4}l_2$	$m_{1,2,3,4}l_2$
10	$m_{1,2,3,4}l_2$	$m_{1,2,3,4}l_2$	$m_{1,2,3,4}l_2$	$m_{1,2,3,4}l_2$	$m_{1,2,3,4}l_2\tau_3$	$m_{1,2,3,4}l_2$
11	$m_{1,2,3,4}l_2$	$m_{1,2,3,4}l_2$	$m_{1,2,3,4}l_2$	$m_{1,2,3,4}l_2$	$m_{1,2,3,4}l_2$	$m_{1,2,3,4}l_2$
common $\forall$ k	$m_{1,2,3,4}$	$m_{1,2,4}l_2$	$m_{1,2,3,4}l_2$	$m_{1,2,3,4}l_2$	$m_{1,2,3,4}l_2$	$m_{1,2,4}l_2^*$

m_1 (mean), m_2 (variance), m_3 (skewness), m_4 (kurtosis), l_2 (L-scale), t_3 (L-skewness), and t_4 (L-kurtosis)

* $k \geq 8, m \geq 3$

The Least Square estimates for resulting power shown in Table 14 are based on the Barabási-Albert simulation. Closeness was the most sensitive measure with a mean power of 0.79 across all factors (95% CI: 0.77 - 0.80). The mean was the most sensitive moment with a mean power across all factors of 0.95 (95% CI: 0.93 - 0.97). In addition, estimated power for L-scale and variance across all factors was 0.86, which were the second most sensitive moments. These results match well with what was shown in Tables 11 - 13, which showcased the mean (m_2) and L-scale (l_2) as common across m and k for several sizes across all network measures.

Table 14. Least Square Power Estimates by Network Measure and Moments for Barabási-Albert Model

	Power Estimate	95% CI
Network Measure		
closeness	0.7905	(0.7777, 0.8033)
betweenness	0.7275	(0.7147, 0.7403)
degree	0.6488	(0.6360, 0.6616)
Moments		
Mean (m_1)	0.9518	(0.9323, 0.9713)
Variance (m_2)	0.8644	(0.8449, 0.8839)
Skewness (m_3)	0.7399	(0.7204, 0.7594)
Kurtosis (m_4)	0.7039	(0.6844, 0.7234)
L-scale (l_2)	0.8696	(0.8500, 0.8891)
L-skewness (t_3)	0.5802	(0.5607, 0.5997)
L-kurtosis (t_4)	0.3460	(0.3265, 0.3656)

CI - Confidence Interval

Figure 11 shows the 95% confidence interval for each measure and moment based on the simulation that was studied. Although closeness and the mean have the highest estimated power for the Barabási-Albert model, both variance and L-scale are close behind with estimated power above 0.80.

Figure 11. Least Square Power Estimates by Network Measure and Moment for Barabási-Albert Model

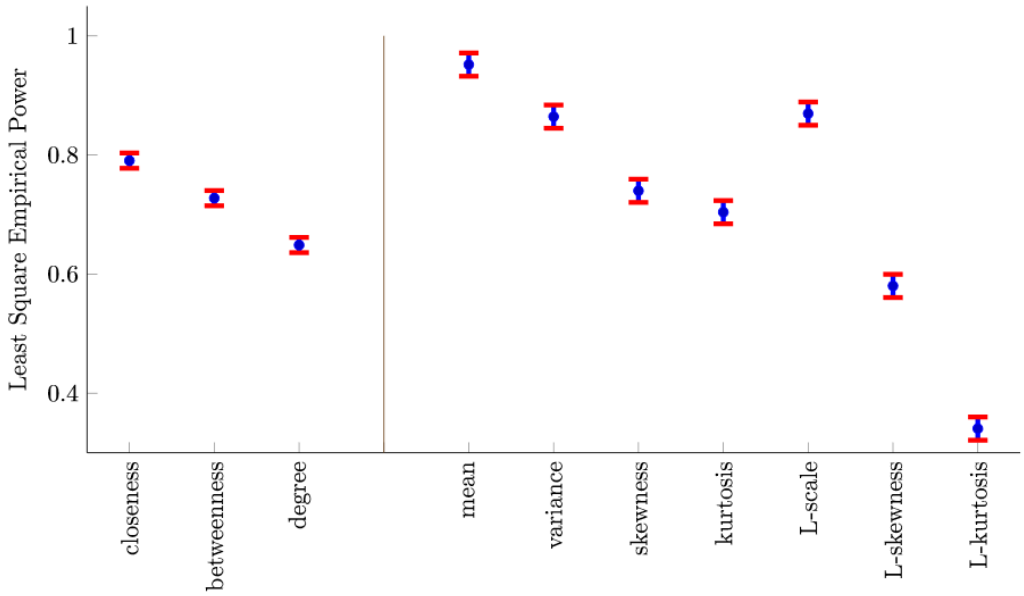

There were significant differences in the resulting power between all network measures (all p-values < 0.0001), the mean versus all other moments (all p-values < 0.001) and higher moments (skewness and kurtosis) versus their L-moment counterpart (L-skewness and L-kurtosis) (both p-values < 0.0001). Within network measures, closeness had the highest power to detect the degrade followed by betweenness and degree. Closeness resulted in significantly more power to detect the degrade than either betweenness or degree. On average, closeness had 7% more power than betweenness (95% CI: 5 - 10%) and 14% more power than degree (95% CI: 12 - 16%). When comparing the mean to all other moments, the mean averaged between $8-60\%$ more power than any other moment or L-moment. The smallest average power across all models came from L-skewness and L-kurtosis. Lastly, when comparing traditional moments and L-moments there was no significant difference in power to detect the degradation between variance and L-scale (p-value 1.00). However, skewness had 15% significantly more power than L-skewness, and kurtosis had 35% significantly more

power than L-kurtosis on average. All power results for the Barabási-Albert network can be found in Appendix A Figures A5-A8 and ANOVA results in Table A5.

Barabási-Albert Concluding Remarks.

Table 15. Least Square Power Estimates based on Interaction of Network Measure and Moments for the Barabási-Albert Model above 0.80

Network Measure	Moment	Power Estimate	95% CI
closeness	mean	0.9483	(0.9053, 0.9914)
closeness	variance	0.9406	(0.8976, 0.9836)
closeness	skewness	0.8833	(0.8403, 0.9263)
closeness	kurtosis	0.9080	(0.8649, 0.9510)
closeness	L-scale	0.9436	(0.9005, 0.9866)
betweenness	mean	0.9466	(0.9036, 0.9896)
betweenness	variance	0.8777	(0.8346, 0.9207)
betweenness	L-scale	0.8973	(0.8543, 0.9403)
degree	mean	0.9604	(0.9174, 1.0)

CI - Confidence Interval

Concluding remarks for the Barabási-Albert simulation can also be rolled up based on the interaction of network measures and moments. The moments for each network measure that achieved a power estimate above 0.80 are highlighted in Table 15. Closeness in all traditional moments and L-scale achieved power estimates above 0.80, with skewness achieving the lowest at 0.8833. Utilizing the network measure betweenness: the mean, variance, and L-scale, all achieved estimates above 0.80, with variance having the lowest estimated power at 0.8777. Once again, the mean was the only moment for the network measures degree that achieved high power, with an estimate of 0.9604. These results also reflect the findings in Tables 6 - 8 for the

Barabási-Albert model. The Barabási-Albert model is constructed quite different from the Erdös-Rényi model, the preferential attachment process that creates a right skewed degree distribution also appears to increase the sensitivity of betweenness and closeness. In addition to the network measure moments sensitive for the Erdös-Rényi model, closeness is now sensitive to skewness and betweenness is sensitive to dispersion (both traditional and L-moment). Degree still only detected the location shift in the mean, yet received the highest power estimate of all (0.9604).

It's worth pointing out that once again no higher order L-moment ratio (L-skewness and L-kurtosis) achieved a power estimate above 0.80. The highest estimate based on the interaction of degree with L-moment ratios was L-skewness, at 0.5664. As the same graph combinations that Mohd-Zaid *et al.* simulated were examined, this stands in contrast to his multivariate test that appeared sensitive based on the joint moments of L-scale, L-skewness, and L-kurtosis. The results in Table 11 do highlight L-skewness being sensitive in higher graph sizes with lower edge densities, but across all graph combinations the power estimate remained low and L-kurtosis performed even lower.

Watts-Strogratz Sensitivity Results.

Once again, Tables 16 - 18 highlight the moments which had power above 0.90 at proportion of 1/10 for all three degrade settings for each of the network measures for the Watts-Strogratz network model. The mean (m_1) detected the degradation in all 35 different network sizes based on the network measure degree (Table 16) and is highlighted in green in the bottom right cell. As the graph size increased to $k = 8$, L-kurtosis (τ_4) was sensitive to detect the change, and when $k > 8$, kurtosis (m_4), L-scale (l_2) and L-skewness (τ_3) became sensitive in certain combinations of graph size and density. Across all graph sizes while holding the density constant, only the

mean (m_1) maintained power > 0.90 to detect the degrade. In addition, L-kurtosis (τ_4) was sensitive for $k = 10$ and 11, while L-scale (l_2) was sensitive for $k = 11$. Across all densities, while holding the number of nodes constant, only the mean (m_1) remained sensitive to detect the degradation at p = 1/10.

Table 16. Moments achieving > 0.90 power for degree in the Watts-Strogratz Network Model

k	m					
	2	3	4	5	6	common $\forall$ m
5	m_1	m_1	m_1	m_1	m_1	m_1
6	m_1	m_1	m_1	m_1	m_1	m_1
7	m_1	m_1	m_1	m_1	m_1	m_1
8	m_1	$m_1\tau_4$	$m_1\tau_4$	$m_1\tau_4$	$m_1\tau_4$	m_1
9	m_1	$m_1\tau_4$	$m_1\tau_4$	$m_1\tau_4$	$m_1\tau_4$	m_1
10	$m_{1,4}\tau_4$	$m_1 l_2\tau_4$	$m_1 l_2\tau_4$	$m_1\tau_4$	$m_1\tau_4$	$m_1\tau_4$
11	$m_{1,4}l_2\tau_4$	$m_{1,2,4}l_2\tau_{3,4}$	$m_1 l_2\tau_4$	$m_1 l_2\tau_4$	$m_1 l_2\tau_4$	$m_1 l_2\tau_4$
common $\forall$ k	m_1	m_1	m_1	m_1	m_1	m_1

m_1 (mean), m_2 (variance), m_3 (skewness), m_4 (kurtosis), l_2 (L-scale), t_3 (L-skewness), and t_4 (L-kurtosis)

Utilizing the network measure betweenness at a proportion of 1/10, (Table 17) no moment achieved > 0.90 power to detect the change in a handful of sparse graphs ($k = 5, m = 2 - 4$ and $k = 6, m = 4$). The mean (m_1) was the only moment sensitive in lower sized graphs, and as the graph increased, additional moments (variance and all L-moments) detected the degrade for $k > 8$ in different graph size combinations with power > 0.90. Across graph sizes and graph densities, only the mean (m_1) consistently achieved power > 0.90 to detect the degrade.

Table 17. Moments achieving > 0.90 power for betweenness in the Watts-Strogratz Network Model

k	m					
	2	3	4	5	6	common $\forall$ m
5	-	-	-	m_1	m_1	m_1
6	m_1	-	m_1	m_1	m_1	m_1
7	m_1	m_1	m_1	m_1	m_1	m_1
8	m_1	m_1	m_1	m_1	m_1	m_1
9	m_1	$m_1 l_2$	$m_{1,2} l_2 \tau_4$	$m_{1,2} l_2 \tau_4$	$m_{1,2} l_2 \tau_4$	m_1
10	m_1	$m_1 l_2 \tau_4$	$m_{1,2} l_2 \tau_4$	$m_{1,2} l_2 \tau_4$	$m_{1,2} l_2 \tau_4$	m_1
11	m_1	$m_1 l_2 \tau_4$	$m_{1,2} l_2 \tau_{3,4}$	$m_{1,2} l_2 \tau_{3,4}$	$m_{1,2} l_2 \tau_4$	m_1
common $\forall$ k	m_1	m_1	m_1	m_1	m_1	m_1

m_1 (mean), m_2 (variance), m_3 (skewness), m_4 (kurtosis), l_2 (L-scale), t_3 (L-skewness), and t_4 (L-kurtosis)

On par with the results from the Erdös-Rényi and Barabási-Albert simulation, the network measure closeness had multiple moments (all traditional moments and L-variance) that detected the node degradation with high power (Table 18). Starting with the smallest graph size, multiple moments showed sensitivity. Similar to betweenness and degree, across graph size holding density constant, the mean (m_1) remained sensitive for closeness. Across density while holding graph size constant, variation existed in smaller sizes. For $k = 5$, the mean (m_1) was consistently sensitive to the degradation. However, for $k = 6$ and 8 kurtosis (m_4) and L-scale (l_2) were also sensitive. For $k > 9$, all traditional moments and L-scale (l_2) consistently achieved power > 0.90 to detect the degrade. By removing the smallest edge density ($m = 2$), the mean (m_1) was sensitive across all graph sizes and edge densities. By removing the smallest graph size ($k = 5$), the variance (m_2) was sensitive across all other com-

binations. This was noted in Table 18 as mean (m_1) and variance (m_2) were both contained in the bottom right cell, but not highlighted as neither maintained power > 0.90 in all combinations of graphs and degrade settings examined.

Table 18. Moments achieving > 0.90 power for closeness in the Watts-Strogratz Network Model

k	m					
	2	3	4	5	6	common $\forall$ m
5	$m_{1,2,4}l_2$	m_1	m_1	m_1	m_1	m_1
6	$m_{2,4}l_2$	$m_{1,2,4}l_2$	$m_{1,2,4}l_2$	$m_{1,2,4}l_2$	$m_{1,2,4}l_2$	$m_{2,4}l_2$
7	$m_{2,4}l_2$	$m_{1,2,4}l_2$	$m_{1,2,4}l_2$	$m_{1,2,4}l_2$	$m_{1,2,4}l_2$	$m_{2,4}l_2$
8	$m_{2,4}l_2$	$m_{1,2,4}l_2$	$m_{1,2,4}l_2$	$m_{1,2,3,4}l_2$	$m_{1,2,4}l_2$	$m_{2,4}l_2$
9	$m_{1,2,3,4}l_2$	$m_{1,2,3,4}l_2$	$m_{1,2,3,4}l_2$	$m_{1,2,4}l_2$	$m_{1,2,3,4}l_2$	$m_{1,2,3,4}l_2$
10	$m_{1,2,3,4}l_2$	$m_{1,2,3,4}l_2\tau_4$	$m_{1,2,3,4}l_2\tau_3$	$m_{1,2,3,4}l_2\tau_4$	$m_{1,2,4}l_2$	$m_{1,2,3,4}l_2$
11	$m_{1,2,3,4}l_2\tau_3$	$m_{1,2,3,4}l_2$	$m_{1,2,3,4}l_2\tau_3$	$m_{1,2,3,4}l_2\tau_{3,4}$	$m_{1,2,3,4}l_2\tau_4$	$m_{1,2,3,4}l_2$
common $\forall$ k	$m_{2,4}l_2$	m_1	m_1	m_1	m_1	m_{12}

m_1 (mean), m_2 (variance), m_3 (skewness), m_4 (kurtosis), l_2 (L-scale), t_3 (L-skewness), and t_4 (L-kurtosis)

The Least Square estimates (Table 19) and resulting graph (12) based on the Watts-Strogratz simulation show that closeness was the most sensitive measure with a mean power of 0.73 across all factors (95% CI: 0.72 - 0.74). The mean was the most sensitive moment with a mean power of 0.98 across all factors (95% CI: 0.97 - 1.00). Once again, these findings reinforce the results from Tables 16 - 18.

Table 19. Least Square Power Estimates by Network Measure and Moments for Watts-Strogratz Model

	Power Estimate	95% CI
Network Measure		
closeness	0.7355	(0.7226 , 0.7484)
betweenness	0.6007	(0.5878 , 0.6136)
degree	0.5542	(0.5413 , 0.5671)
Moments		
Mean (m_1)	0.9872	(0.9677 , 1.00)
Variance (m_1)	0.7110	(0.6915 , 0.7305)
Skewness (m_2)	0.4547	(0.4351 , 0.4742)
Kurtosis (m_3)	0.6511	(0.6316 , 0.6707)
L-scale (m_4)	0.7462	(0.7266 , 0.7657)
L-skewness (t_3)	0.3058	(0.2862 , 0.3253)
L-kurtosis (t_4)	0.5549	(0.5354 , 0.5745)

CI - Confidence Interval

Figure 12 shows the 95% confidence interval for each measure and moment based on the simulation that was studied. Once again, closeness and the mean contribute the most toward estimated power based based on the Watts-Strogratz model. As seen in the Erdös-Rényi model, only the mean has an estimated power above 0.80.

Figure 12. Least Square Power Estimates by Network Measure and Moment for Watts-Strogratz Model

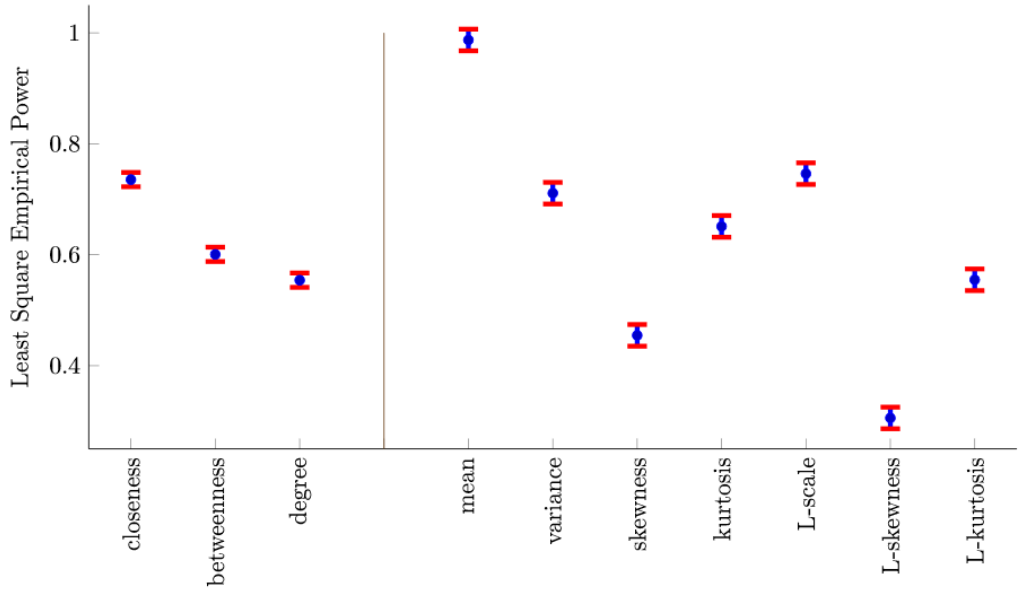

There were significant differences in the resulting power between all network measures (all p-values < 0.0001), the mean versus all other moments (all p-values < 0.001) and higher moments (skewness and kurtosis) versus their L-moment counterpart (L-skewness and L-kurtosis) (both p-values < 0.0001). Within network measures closeness had the highest power to detect the degrade followed by betweenness and degree. Closeness resulted in significantly more power to detect the degrade than either betweenness or degree. On average closeness had 13% more power than betweenness (95% In addition,: 11 - 15%) and 18% more power than degree (95% CI: 15 - 20%). When comparing the mean to all other moments, the mean averaged between 24% more power up to 68% more power than any other moment or L-moment. Lastly, when comparing traditional and L-moments, there was no significant difference in power to detect the degradation between variance and L-scale (p-value 1.00). However, skewness had 14% significantly more power than L-skewness, and kurtosis had 9% significantly more power than L-kurtosis on average. All power results for the

Watts-Strogratz network can be found in Appendix A Figures A9-A12 and ANOVA results in Table A6.

Table 20. Least Square Power Estimates above 0.90 based on Interaction of Network Measure and Moments for Watts-Strogratz Model

Network Measure	Moment	Power Estimate	95% CI
closeness	mean	0.9838	(0.9378, 1.0)
closeness	variance	0.9326	(0.8866, 0.9786)
closeness	kurtosis	0.9263	(0.8804, 0.9723)
closeness	L-scale	0.9344	(0.8885, 0.9804)
betweenness	mean	0.9780	(0.9320, 1.0)
degree	mean	1.000	(0.9540, 1.0)

CI - Confidence Interval

Watts-Strogratz Conclusions.

The last model simulated, the Watts-Strogratz compares closely to the Erdös-Rényi simulation when looking at the interaction of network measures and moments in Table 10. All network measure moments that achieved high power for the Erdös-Rényi model also achieved high power for the Watts-Strogratz . Specifically, all moments had higher estimates as well, except the mean based on degree which remained at 1.0. The additional structure imposed in the Watts-Strogratz model, the initial neighborhood connections formed before random edges are moved, increased the detection of the node degrade across all moments with high power.

Conclusions.

Overall, sensitivity in detecting degradation within the networks with respect to the moments were fairly consistent across each network model. Due to its construction the Barabási-Albert model needs a slightly higher proportion selected before

consistent degrade detection for any single moment occurs, and this holds across all network sizes considered. The mean was the most consistent moment to detect a $1/10^{th}$ degrade, followed by measures of dispersion (variance and L-scale). The lowest performing moments at a 1/10 proportion of degrade were related to skewness. When comparing network measures, closeness had multiple moments test sensitive to the lowest network degrade even in smaller networks. These conclusions were confirmed by the ANOVA results when examining the predicted power across all simulation scenarios. Closeness and the mean had the significantly highest power estimates across all simulations, averaging 0.80-0.90 in power to detect the degrade in a network at a proportion of degrade of 1/10 node removal. L-scale and variance had the next highest power at about 0.70, with measures of kurtosis and skewness resulting in overall low predicted power, at most achieving an unacceptable 55% power.

Although only the results for the smallest proportion change was presented in this chapter, all degrade settings are summarized in Appendix A. As expected, when the network size increased and density was held constant, power increased on average across measures and statistics. In addition, when the edge density of the network increased and size was held constant, power was decreased on average across measures and statistics. This confirms the intuition that the sparser the network is the more node degradation affects the the network measures. The inverse is confirmed as well, the denser a network is the less affected its network measures are to node degrade. As the network is more sparse, holding node count constant and lowering the number of edges, detecting changes due to nodal degradation increased. The inverse also held. As the graph became more dense, meaning the ratio of nodes to edges decreases, power on average was reduced. For the Barabási-Albert graphs the moments detected node degradation across each of the three network measures fairly well, with the notable exception of the higher L-moments and highest probability of degrade. The measures

were not sensitive for degradation on the Erdös-Rényi graph except in the largest graph size, and the most sensitive network measure was closeness. A similar trend was found for the Watt-Strogratz graph where the medium degrade setting was the least detectable along with the smallest graph size.

The network measure closeness performed consistently the best at detecting the degradation with > 0.90 power across all sizes and edge densities. In addition, the mean was the most sensitive of all statistics regardless of graph size, edge density, network measure, degrade setting, or probability, detecting the lowest degrade setting of $1/10^{th}$ of all nodes with > 0.90 power. In general, L-moments were not as sensitive across all settings as the mean to detect changes with > 0.90 power and a $1/10$ proportion degrade. However, L-scale, L-skewness, and L-kurtosis were sensitive especially in larger networks.

Different moments based on the interaction of network measures and moments appear to have high sensitivity across all graph combinations and settings. All three graph models showed the mean for closeness, betweenness, and degree and variance, kurtosis, and L-scale for closeness as sensitive. The Barabási-Albert model the following additional moments of: skewness for closeness, and variance and L-scale for betweenness. The next section will build on these findings to examine which statistical test could be employed to detect the degradation.

3.2 Research Objective 1b: What are Appropriate Statistical Tests to use to Detect Network Degradation

Three different methods of statistical testing become potential candidates for detecting change based on the simulation and the findings. The first method utilizes the empirical distributions created from the 50,000 replicated moments for each of the network measures simulated from research question 1a. The second method examined

is non-parametric based, comparing the degraded and non-degraded networks directly based on both the Kolmogorov-Smirnov and Sign Test. The last method compares degraded and non-degraded networks directly via parametric normality assumptions. These testing methods will be referred to as Empirical Quantile, non-parametric, and parametric tests respectively.

Method 1: Empirical Quantile Testing Methods.

To determine sensitivity utilizing the empirical quantile method from the dataset simulation, empirical distributions for each moment of a particular network measure were created for all graph sizes utilizing 50,000 replications. In general, the following hypothesis is being tested: the empirical distributions of the degraded graph F(t) is equal to the non-degraded graph G(t).

$$\begin{aligned} H_0 &: F(t) = G(t) \\ H_a &: F(t) \neq G(t) \end{aligned} \tag{11}$$

The difference arises in how the test is constructed. For the empirical quantile test, the test statistic utilized is a particular degraded graph's moment calculated from one of the network measures. The rejection region is now based on the *alpha* level rejection region of the empirical distribution for that particular network measure's moment.

The number of times out of the 50,000 replications that the degraded moment fell outside the α level (0.05) acceptance region was reported as empirical power. The full results for the Erdös-Rényi, Barabási-Albert, and Watts-Strogratz network models across all degrade levels are shown in the Appendix A as Table A7-A15. A summary of the number of times a particular moment detected the degrade for each moment and degrade level with 0.90 power or greater, across all network sizes at the

lowest proportion of degrade, p = 1/10, can be seen below in Table 21. Recall 35 network sizes (combinations of m and k) were simulated, and the number of times out of the 35 possible combinations that a moment detects the change with high power is reported next to the moment.

Table 21. Moment and (proportion of detects out of 35) for the Empirical Quantile Method at a proportion of degrade = 1/10 and power 0.90

Degrade	closeness	betweenness	degree
Erdös-Rényi			
Low	$m_1(25)$	$m_1(20)$, $l_2(3)$	$m_1(18)$
Medium	$m_1(24)$, $m_2(2)$, $l_2(3)$	$m_1(19)$	$m_1(29)$
High	$m_1(15)$	$m_1(5)$	$m_1(30)$, $l_2(1)$
Barabási-Albert			
Low	$m_1(24)$	$m_1(17)$, $l_2(19)$	$m_1(31)$
Medium	$m_1(23)$	$m_1(14)$, $l_2(15)$	$m_1(30)$
High	$l_2(2)$, $t_3(2)$	$l_2(6)$	$m_1(30)$, $l_2(7)$, $t_3(4)$
Watts-Strogratz			
Low	$m_1(26)$	$m_1(22)$, $l_2(1)$	$m_1(20)$
Medium	$m_1(26)$, $m_2(3)$, $l_2(3)$	$m_1(20)$	$m_1(31)$
High	$m_1(16)$	$m_1(9)$, $m_2(1)$, $l_2(1)$	$m_1(30)$

m_1 (mean), m_2 (variance), m_3 (skewness), m_4 (kurtosis), l_2 (L-scale), t_3 (L-skewness), and t_4 (L-kurtosis)

Overall, the mean detected the degradation the most consistently with the exception of closeness and betweenness in the high degrade within the Barabási-Albert simulation. No other moment showed consistency in detection with > 0.90 power, although L-scale (l_2) was fairly consistent for betweenness in the Barabási-Albert and Watts-Strogratz network models. L-scale, l_2, was the second most prevalent moment at detecting the degrade using betweenness in the Barabási-Albert simulation. Vari-

ance and L-skewness detected the change in 7 and 5 different graph combinations, and no other moment met the power level of 0.90. Aside from an overall lower proportion of detection (recall the K-S Test achieved > 0.90 power for 31 out of 35 comparisons), a limitation with implementing this empirical quantile test is that the empirical distribution has to be created. This is possible if one can correctly characterize a real world network using a random graph generating model. However, not all networks have such a model from which to build the empirical distributions. Therefore, currently this method is only usable for select networks where such a model exists.

Method 2: Non-Parametric Testing Methods.

Two non-parametric tests, the K-S and Sign Test were also examined. The K-S Test was used in the the analysis of research question 1a, examining the sensitivity of particular measures and moments to degradation in networks. Neither the K-S Test nor the Sign Test rely on distributional forms of the network measures, and unlike the Empirical Quantile method, both the K-S and the Sign Test can be used on the original and degraded networks directly. To compare the performance of these tests, a new simulation was run with a few variations from the original (Table 3). The new settings are given in Table 22 and consist of three main changes.

Table 22. Graph Simulation Settings for Non-parametric test comparisons

Graphical Models	BA, ER, and WS
Graph Sizes (2^k)	k = 5,6,7,8,9,10
Number of Edges ($\approx 2^k m$)	m = 2,3,4,5,6
Total No. of Graphs	90
Degrade Level	Low, Medium, High, Random
Proportion of Degrade (p)	p = 1/2, 1/3, 1/4, 1/5, 1/7, 1/10, 1/20
No. of Degrade Settings per Graph	9

Specifically, within the networks simulated, the largest graph size, $k = 11$, was removed, resulting in 90 different graph combinations analyzed. In the degrade setting a proportion of $1/20^{th}$ was added. Further, within the degrade settings a new random level was added which randomly selects 20% from all nodes, and then a proportion, p, of those selected nodes are degraded. Finally, the proportion of degrade was centered around 1/10 since moments and network measures showed sensitivity at 1/10, the lowest level previous examined. The K-S Test was used to compare the CDF of the original non-degraded graph to the same graph after a particular degrade was applied.

The K-S Test is the same test described within research question 1a with the following difference. Instead of generating 500 random graphs and combining a particular moment for each graph simulated into an empirical distribution, the empirical distribution of a network measure from one non-degraded graph is tested to be equal to the empirical distribution of that same network measure after applying a particular degrade. This test was then replicated 50,000 times across each graph combination and degrade setting. The average number of times the degrade was detected (i.e. null hypothesis rejected), via the K-S Test, was reported as empirical power.

The second non-parametric test, the Sign Test [16], has the following assumptions: the difference in the random samples are mutually independent and each random sample comes from a continuous population with a common median, θ_0. The following hypothesis,

$$H_0 : \theta = \theta_0 \quad H_a : \theta \neq \theta_0, \tag{12}$$

is testing whether or not the medians from the two distributions are the same. In essence, the Sign Test is testing whether there is a location change based on the median. Large sample approximation is appropriate based on the smallest graph sizes and utilizes the following test statistic and rejection region:

$$B^* = \frac{B - (n/2)}{(n/4)^(1/2)}, \text{ where B} = \sum_{i=1}^{n} \phi_i \tag{13}$$

$$\text{Reject } H_0 \text{ if } |B^*| \geq z_{\alpha/2} \tag{14}$$

The test statistic, B^*, is the sum of the positive ranks from the random samples of the degraded graph after subtracting the median from the non-degraded graph.

The assumed alpha level for both of these tests was set to 0.05. Full results can be found in the Appendix A in Tables A16 - A27 and highlight that closeness achieves the highest power most consistently out of the three network measures across both the K-S and Sign Tests. Then, focusing on closeness, Tables 23 - 25 list the lowest proportion of degrade at which each test was able to detect a change with at least 0.80 power based on the network measure of closeness. These tables are structured as follows: the left most column represents each of the four degrade levels. For each of those levels the lowest proportion that achieves > 0.80 power in detecting the difference between the degraded and non-degraded graphs is broken down in the

second column by the number of nodes, k. Then edge density, m, is provided in each of the subsequent columns and is separated by the two tests, K-S and Sign Test. Blanks represent graph combinations where power was below the 0.80 threshold for in the largest proportions setting (1/2).

Table 23. Erdös-Rényi Smallest Proportion of Node Degrade to Achieve 0.80 Power Based on Closeness

	m	2		3		4		5		6	
Degrade	k	K-S	Sign	K-S	Sign	K-S	Sign	K-S	Sign	K-S	Sign
Low	5	1/3	1/3	1/3	1/4	1/4	1/4	1/4	1/4	1/4	1/7
	6	1/4	1/4	1/5	1/5	1/5	1/7	1/5	1/7	1/7	1/7
	7	1/5	1/7	1/7	1/10	1/10	1/10	1/7	1/10	1/7	1/10
	8	1/7	1/10	1/10	1/10	1/10	1/10	1/10	1/10	1/10	1/20
	9			1/20	1/20	1/20	1/20	1/20	1/20	1/20	1/20
	10			1/20	1/20	1/20	1/20	1/20	1/20	1/20	1/20
Medium	5			1/3	1/3	1/4	1/4	1/4	1/4	1/4	1/5
	6			1/4	1/4	1/5	1/5	1/5	1/5	1/7	1/7
	7			1/7	1/7	1/7	1/10	1/7	1/7	1/7	1/7
	8			1/10	1/10	1/10	1/10	1/10	1/10	1/10	1/10
	9			1/10	1/20	1/10	1/20	1/20	1/20	1/20	1/20
	10					1/20	1/20	1/20	1/20	1/20	1/20
High	5							1/3	1/3	1/3	1/4
	6					1/2	1/2	1/3	1/3	1/5	1/5
	7					1/4	1/5	1/5	1/5	1/5	1/5
	8					1/5	1/5	1/7	1/10	1/10	1/10
	9					1/7	1/10	1/10	1/10	1/10	1/20
	10					1/10	1/10	1/10	1/10	1/10	1/20
Random	5					1/2	1/3	1/3	1/3	1/3	1/3
	6			1/2	1/2	1/3	1/4	1/4	1/4	1/5	1/5
	7			1/3	1/4	1/5	1/5	1/5	1/7	1/5	1/7
	8			1/5	1/7	1/7	1/10	1/10	1/10	1/10	1/10
	9			1/7	1/10	1/10	1/10	1/10	1/20	1/20	1/20
	10					1/20	1/20	1/20	1/20	1/20	1/20

$1/7 \sim$ 4-6%, $1/10 \sim$ 2-5%, $1/20 \sim$ 1-3%, and K-S: Kolmogorov-Smirnov

For the Erdös-Rényi model, degradation of nodes with low degree was detected across more graph combinations than any other degrade level. Degradation in the nodes with high degrade was the least detectable (Table 23). Moreover, the detectable

graph combinations were concentrated in the higher node and edge density combinations. Except for when $k = 5 - 8$ in the low degrade, all degraded networks with $m = 2$ were undetectable at the proportions simulated. In addition, no proportion was detectable with prescribed power for the high degrade at $m = 3$, the medium degrade $k = 10$ and $m = 3$, or the random degrade $k = 5, 10$ and $m = 3$. The only graph combination not detectable at $m = 4$, was seen in the high degrade when $k = 5$. As size and density of the networks examined increased, the degraded proportion needed to detect the change was reduced on average. In the larger networks with a higher number of edges, detection at high power was achieved across all degrade levels with as little as $1 - 3\%$ of all nodes being removed. In every combination in which one of the proportions used for degrading the network was examined, the Sign Test detected the change at either the same or lower proportion of nodes than the K-S Test.

Table 24. Barabási-Albert Smallest Proportion of Node Degrade to Achieve 0.80 Power Based on Closeness

	m	2		3		4		5		6	
Degrade	k	KS	Sign	KS	Sign	KS	Sign	KS	Sign	KS	Sign
Low	5	1/4	1/5	1/3	1/5	1/3	1/4	1/3	1/4	1/3	1/4
	6	1/7	1/7	1/7	1/7	1/5	1/7	1/5	1/7	1/5	1/7
	7	1/10	1/10	1/10	1/10	1/10	1/10	1/10	1/7	1/10	1/7
	8	1/10	1/10	1/10	1/10	1/10	1/20	1/10	1/20	1/10	1/10
	9	1/20	1/20	1/20	1/20	1/20	1/20	1/20	1/20	1/20	1/20
	10	1/20	1/20	1/20	1/20	1/20	1/20	1/20	1/20	1/20	1/20
Medium	5	1/4	1/5	1/2	1/4	1/2	1/3	1/2	1/3	1/2	1/2
	6	1/7	1/7	1/5	1/7	1/5	1/5	1/4	1/5	1/3	1/4
	7	1/10	1/10	1/7	1/10	1/7	1/10	1/7	1/10	1/5	1/7
	8	1/20	1/20	1/10	1/10	1/10	1/10	1/10	1/10	1/10	1/10
	9	1/20	1/20	1/10	1/20	1/20	1/20	1/20	1/20	1/20	1/20
	10	1/20	1/20	1/20	1/20	1/20	1/20	1/20	1/20	1/20	1/20
High	5										
	6										
	7										
	8										
	9									1/4	1/5
	10							1/4		1/5	
Random	5				1/2		1/2	1/2	1/3	1/2	1/3
	6			1/2	1/3	1/3	1/4	1/3	1/4	1/3	1/4
	7			1/3	1/5	1/5	1/5	1/5	1/5	1/5	1/5
	8			1/5	1/5	1/7	1/10	1/10	1/10	1/10	1/10
	9			1/5	1/7	1/10	1/10	1/10	1/10	1/10	1/20
	10			1/10	1/10	1/10	1/10	1/10	1/20	1/20	1/20

$1/7 \sim$ 5-9%, $1/10 \sim$ 4-6%, $1/20 \sim$ 2-3%, and K-S: Kolmogorov-Smirnov

Table 24 displays the results from the Barabási-Albert network generating algorithm. Two very noticeable differences exist when comparing the Erdös-Rényi results to that of the Barabási-Albert. First, low and medium degrade were able to detect the change across all graph combinations. Second, detection dropped drastically for closeness in the high degrade level, with only four graph combinations able to detect the degradation at a power of 0.80 or higher. Within random degrade, detection never achieved prescribed power at $m = 2$ or for the K-S Test at $k = 5$ when $m = 3$ or 4. As

size and density of the networks examined increased, the degraded proportion needed to detect the change was reduced on average. In the larger networks with a higher number of edges, detection at high power was achieved across the low, medium, and random degrade levels with as little as $2-3\%$ of all nodes being removed. Once again in every category, the Sign Test achieved the desired power of 0.80 at the same or lower proportions than the K-S Test. Further, the Sign Test detected the change when the K-S Test did not in the random degrade at $k = 5$ when $m = 3$ or $m = 4$.

Table 25. Watts-Strogratz Smallest Proportion of Node Degrade to Achieve 0.80 Power Based on Closeness

	m	2		3		4		5		6	
Degrade	k	KS	Sign	KS	Sign	KS	Sign	KS	Sign	KS	Sign
Low	5	1/3	1/3	1/3	1/4	1/4	1/4	1/4	1/4	1/4	1/5
	6	1/4	1/5	1/5	1/5	1/5	1/7	1/7	1/7	1/7	1/7
	7	1/5	1/5	1/7	1/10	1/10	1/10	1/10	1/10	1/10	1/10
	8			1/10	1/10	1/10	1/20	1/20	1/20	1/10	1/20
	9			1/20	1/20	1/20	1/20	1/20	1/20	1/20	1/20
	10			1/20	1/20	1/20	1/20	1/20	1/20	1/20	1/20
Medium	5			1/3	1/3	1/4	1/4	1/4	1/5	1/4	1/5
	6			1/5	1/5	1/5	1/5	1/5	1/7	1/7	1/7
	7			1/7	1/7	1/10	1/10	1/10	1/10	1/10	1/10
	8			1/10	1/10	1/10	1/10	1/10	1/20	1/10	1/20
	9			1/20	1/20	1/20	1/20	1/20	1/20	1/20	1/20
	10			1/20	1/20	1/20	1/20	1/20	1/20	1/20	1/20
High	5					1/2	1/2	1/3	1/3	1/3	1/5
	6					1/3	1/3	1/3	1/4	1/5	1/5
	7					1/5	1/5	1/7	1/7	1/5	1/7
	8					1/5	1/7	1/10	1/10	1/10	1/10
	9					1/10	1/10	1/10	1/10	1/20	1/20
	10					1/10	1/20	1/20	1/20	1/20	1/20
Random	5				1/2	1/3	1/3	1/3	1/3	1/3	1/5
	6			1/2	1/2	1/4	1/4	1/4	1/4	1/5	1/5
	7			1/4	1/4	1/5	1/7	1/7	1/7	1/7	1/7
	8			1/7	1/7	1/10	1/10	1/10	1/10	1/10	1/10
	9			1/10	1/10	1/10	1/10	1/10	1/20	1/20	1/20
	10			1/10	1/20	1/20	1/20	1/20	1/20	1/20	1/20

$1/7 \sim$ 4-6%, $1/10 \sim$ 2-5%, $1/20 \sim$ 1-3%, and K-S: Kolmogorov-Smirnov

Lastly, Table 25 shows the smallest proportion of node degrade out of those examined to achieve 0.80 power based on closeness for the Watts-Strogratz network model. Across the medium, high and random degrade levels, when $m = 2$, power was not observed above 0.80. In the low degrade level, when $m = 2$ the change was not detectable at the prescribed power for $k = 8 - 10$. In addition, the high degrade levels, when $m = 3$, failed to detect the change as well. In the larger networks with a higher number of edges, detection at high power was achieved across all degrade levels with as little as $1 - 3\%$ of all nodes being removed. Once again the Sign Test was on par or detected the change at a lower proportion across all cases when compared to the K-S Test and specifically detected the change in the random degrade at $k = 5$ when $m = 2$ when the K-S test did not.

Out of the two measures not discussed here, betweenness had the lowest power across all settings, while degree had higher power than betweenness but lower than closeness. As seen within closeness, the Sign Test on average performed equal or superior to the K-S Test with respect to the network measure degree. Of note, degree on average out-performed closeness within the high degrade for large network sizes.

Highlighted within this section is a method for detecting change that is free of distributional assumptions of the underlying networks or network measures themselves. These tests can be implemented for a large number of networks. As this testing method works well across a number of degrades, graph combinations, and graph models it appears this test will work across real world networks that do not fully follow one particular network model. One last testing method, parametric, is examined next before applying these tests to real world datasets.

Method 3: Parametric Testing Methods.

In the final method, a parametric test between the degraded and non-degraded network is conducted using the mean network measure, as it was characteristically the most common sensitive moment observed from which change could be detected among the moments examined. In this parametric method, normality is assumed for the mean network measures, and the estimated mean from the degraded network is used to test whether or not the observed degraded graph is significantly different in its mean as compared to the original network. Let μ_0 equal the mean of the original network, and μ equal the mean of the degraded network. Then the following hypothesis was constructed:

$$H_0 : \mu = \mu_0, \quad H_a : \mu \neq \mu_0.$$

Two variations of this test were examined. The first test utilizes the variance of the non-degraded graph (denoted σ^2) and utilizes a score-based test statistic:

$$\frac{\bar{X} - \mu_0}{\sigma} \sim N(0, 1). \tag{15}$$

The next test utilizes the variance from the degraded graph (denoted s^2) and utilizes a Wald-based test statistic:

$$\frac{\bar{X} - \mu_0}{s} \sim N(0, 1) \tag{16}$$

As this final method requires no assumption of the network generation, this is best explored in real data applications. As such, the non-parametric methods (K-S and Sign Tests) and parametric methods (Score and Wald) are compared next using real world networks.

3.3 Research Question 1c: Which Combination of Network Measures and Tests are most Effective at Detecting Network Changes in Data Applications

After discussing the three potential methods, the tests based on normality and the non-parametric tests are viable options across a multitude of different graphs due to their relaxed assumptions, and not relying on characterization to a specific graph generating model. The next section focuses on these two methods concerning two different real world networks.

The parametric and non-parametric tests were performed on two real world data sets to assess the viability of these methods across a spectrum of real-world network data. The results for each method are compared followed by some concluding remarks. The first dataset utilizes an immunoglobulin protein network which mimics one of the graph generating models and parameters that were simulated, while the second dataset utilizes a social network of high school students and does not closely resemble any of the simulations.

Immunoglobulin Protein Network.

The first real world network examined is a simple and undirected network modeled from protein interactions. A network of the interaction in the immunoglobulin protein was generated by Gfeller for his PhD dissertation in 2007 [12]. It is comprised of the interactions in the Immunoglobulin protein. This particular network is made up of 1316 nodes and 6300 edges representing amino-acids. An edge is drawn between two amino-acids if the shortest distance between their C_{alpha} atoms is smaller than the threshold value $\theta = 8$ Angstrom [11].

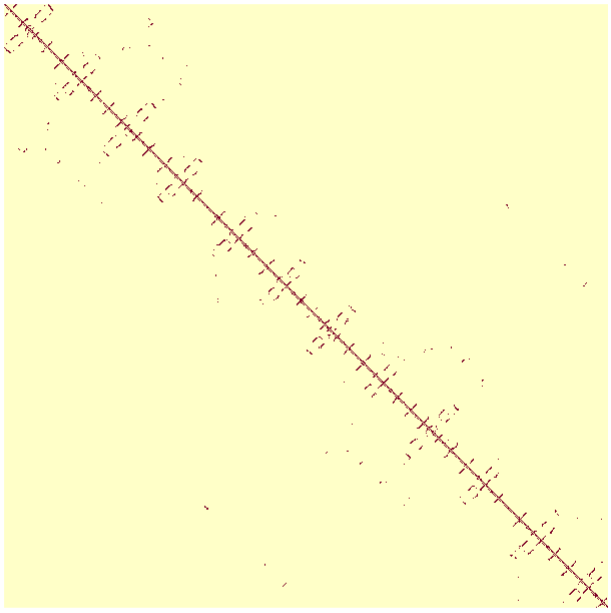

Figure 13. Adjacency Matrix for Immunoglobulin Protein Network

Figure 14. Distributions of Network Measures for the Immunoglobulin Protein Network

(a) closeness

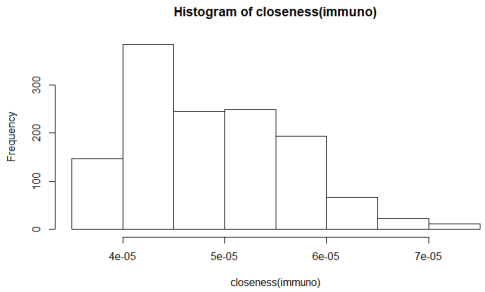

(b) betweenness

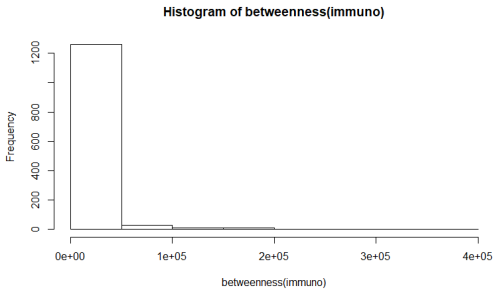

(c) degree

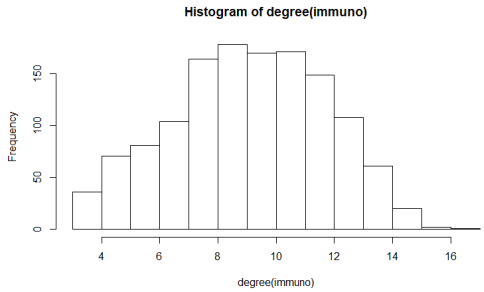

Figure 13 shows the adjacency matrix as a heat plot while Figure 14 shows the distributions for each of the three network measures (a-c). The adjacency matrix resembles a Watts-Strogratz model with very small rewiring, because the edges that are rewired appear highly correlated to closer nodes more so than random nodes. The degree distribution is not right skewed, Figure 14(c). Hence, it does not resemble the typical degree distribution of a Barabási-Albert network. Closeness and betweenness are both right-tailed with the majority of nodes having essentially the same value for betweenness. This suggests little to no randomness contained within the graph. While this network appears most closely aligned with the structure properties associated with a Watts-Strogratz network model its specific structure is not easily simulated using the Watts-Strogratz generation model, mainly due to the lack of randomness.

The full network of 1,316 nodes and 6,300 edges was degraded over four settings (low, medium, high, and random). The low, medium, and high degrade settings used the degree distribution for the degrade, while the random setting randomly selected from all nodes.

Table 26. Degrade Settings

Degrade	Number Selected	Proportion	Number Degraded
Low	292	1/10	29
Medium	348	1/10	34
High	341	1/10	34
Random	1316	1/10	26

Table 26 shows how many nodes were considered for degrade, and the number of nodes actually removed during each replication of the test at degrade proportion of $1/10^{th}$. In the low degrade setting, $1/10^{th}$ of all 292 nodes that fell in the bottom quintile of the degree distribution were removed from the network. In the medium degrade setting, $1/10^{th}$ of all 348 nodes that fell within 40^{th} or 60^{th} degree distribution percentile were removed, and in the high setting, $1/10^{th}$ of the 341 nodes in the highest quintile of the degree distribution were removed from the network. Recall the random degrade setting initially selected 1/5 across all nodes, then the proportion of 1/10 is selected from that, which results in 26 nodes being removed each replication. Across all degrade settings, the number of nodes removed varied from 26 to 34. Each degrade setting was replicated 200 times and selected 26 to 34 different nodes, depending on the degrade setting. The newly degraded graph was then tested against the initial graph using the Kolmogorov-Smirnov, Sign, Wald, and score tests outlined previously. The proportion of times out of 200 that the degrade was detected using the specified test was reported as the power and was summarized in Table 27.

Table 27. Degraded Immunoglobulin Protein Network detection power using $1/10^{th}$ proportion setting by statistical test and network measure

	closeness	betweenness	degree	Proportion of Nodes Removed
Kolmogorov-Smirnov				
Low	0.65	0.04	0.00	0.022
Medium	0.96	0.00	0.00	0.026
High	1.0	0.00	1.0	0.025
Random	0.78	0.00	0.00	0.02
Sign				
Low	0.39	0.04	0.96	0.022
Medium	0.83	0.00	1.00	0.026
High	0.91	0.00	1.00	0.025
Random	0.54	0.00	1.00	0.02
Score				
Low	0.04	0.00	0.00	0.022
Medium	0.00	0.00	0.00	0.026
High	0.00	0.00	0.00	0.025
Random	0.00	0.00	0.00	0.020
Wald				
Low	0.04	0.03	0.00	0.022
Medium	0.00	0.00	0.00	0.026
High	0.00	0.00	0.00	0.025
Random	0.00	0.00	0.00	0.020

The first column in Table 27 lists the degrade settings (low, medium, high, and random), while the next three columns list out which network measure was utilized in the hypothesis test. The last column puts into prospective the proportion of nodes removed as compared to the full non-degraded graph. Both parametric tests utilizing the mean (the Score and Wald) across all network measures had little to no power. The K-S performed fairly well and was consistent with the previous results, with closeness being the most sensitive network measure to the degrade. Both degree and closeness detected the degrade with 100% power in the high degrade category. Interestingly, closeness across all degrade levels for the Sign Test had lower power when compared to the K-S Test. However, the previous simulation comparing these tests in the common network models consistently showed that the Sign Test could detect

the degrade at equal or smaller proportions than the K-S Test. Further, the Sign Test was more sensitive in detecting the degrade when using degree than any other test. The results of the K-S and Sign Test based on the simulations ran suggested that a Watts-Strogratz $k = 10$, and $m = 5$, which is the closest match of the Watts-Strogratz network model to the Immunoglobulin network, could detect the degrade at $p = 1/20$ (Table 25). Table 28 shows the results when the degrade proportion was lowered to 1/20 for the K-S and Sign Test as they consistently had the highest power.

Table 28. Degraded Immunoglobulin Protein Network detection power using 1/20th proportion setting by statistical test and network measure

	closeness	betweenness	degree	Proportion of Nodes Removed
Kolmogorov-Smirnov				
Low	0.14	0.02	0.00	0.010
Medium	0.30	0.00	0.00	0.013
High	0.30	0.00	0.00	0.013
Random	0.01	0.00	0.00	0.010
Sign				
Low	0.06	0.02	0.99	0.010
Medium	0.00	0.00	1.00	0.013
High	0.03	0.00	1.00	0.013
Random	0.00	0.00	1.00	0.010

Recall that the proportion degraded is not affecting all nodes but only the subset selected by the degrade level. As shown in Table 28, the Sign Test was able to detect the degrade in the network using the network measure degree with approximately only 1 percent of all nodes being degraded. For this particular network, power to detect the degrade using closeness was reduced to near zero, counter to the previous simulation study results. For the K-S Test the power to detect the degrade using closeness was reduced to below a fifty-fifty chance.

High School Students Interaction.

The second network is one of a high school social network [10]. The social network is constructed of social interactions among high school students from four different classrooms throughout the day. The students are tracked for four days and each day represents a network. Such a network is ideal for this study as it has properties found in random, preferential attachment, and small world networks. Less social students will only have random encounters that would occur in the hall or during lunch, whereas more popular students would have more interactions exhibiting preferential attachment. Since all the students go to the same high school, short path lengths (small world effect) should be present as well. Figure 15 shows us the adjacency matrix for the four different days as a heat plot, where white represents an interaction between students and red represents no interaction. Within these networks each of the random graph models characteristics are present. Certain rows show a large concentration of connections (Barabási-Albert), while neighborhood pockets (Watts-Strogratz) with links to each other are seen as well, and throughout the edge matrix randomness (Erdös-Rényi) abounds.

Figure 15. Adjacency Matrix for High School Network Days 1-4

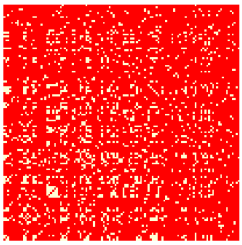

Day 1

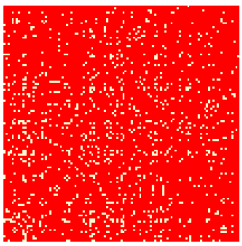

Day 2

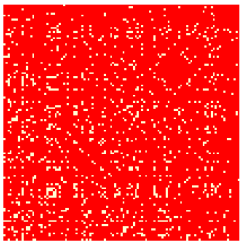

Day 3

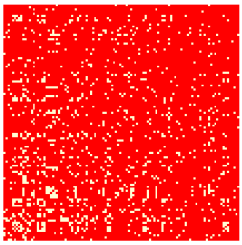

Day 4

Table 29 contains the number of students (nodes) and interactions (edges) within

the network for the four different days that data was collected. Based on the ratio of edges to nodes, all four of these networks have a much higher edge density than any of the network models that were simulated. The density for each network, which is the ratio of the number of edges divided by the total number of possible edges, was listed out as well for additional inference for this particular network.

Table 29. Graph Characteristics of Nodes & Edges

	Day 1	Day 2	Day 3	Day 4
Node Count	121	113	113	112
Edge Count	1950	1164	1190	1218
Density	0.1238	0.0739	0.0941	0.0785

Due to the edge density, the proportion for deletion was set to 1/2 in order to highlight measures and tests that were able to detect the change across a multitude of degrade settings. The same degrade settings (Low, Medium, High, Random) as with the first Immunoglobulin Protein network were replicated. Only the tests based on Normality are not shown, as they performed just as poorly, as seen in the protein network, even at the higher proportion of degrade.

Table 30. High School Networks Nodes Selected and Number Degraded for Each Degrade Level

	Number of Nodes Selected							
	Selected				Degraded			
Degrade	Day 1	Day 2	Day 3	Day 4	Day 1	Day 2	Day 3	Day 4
Low	25	28	28	30	12	14	14	15
Medium	10	14	8	10	5	7	4	5
High	26	23	25	29	13	11	12	14
Random	24	22	22	22	12	11	11	11

Table 30 shows the different node counts selected and actually degraded based on the degrade and proportion levels. Nodes targeted and the number removed were fairly consistent across all degrade levels except for medium degrade. For medium degrade about half the number of nodes are being selected. Based on this it was

assumed that the detection power across the medium degrade setting will be the lowest.

Table 31. Power to Detect Degraded High School Network for Day 1 at $p = 1/2$

	closeness	betweenness	degree	Proportion of Nodes Removed
Kolmogorov-Smirnov				
Low	1.00	0.00	0.00	0.10
Medium	0.15	0.00	0.00	0.04
High	0.06	0.00	0.99	0.11
Random	0.99	0.00	0.00	0.10
Sign				
Low	1.00	0.00	0.00	0.10
Medium	1.00	0.00	0.00	0.04
High	0.58	0.00	1.00	0.11
Random	1.00	0.00	0.01	0.10

The network based on the first day of the study reflects a much higher edge density than the proceeding three days. Results for the first day network can be found in Table 31. The medium degrade using closeness was not sensitive utilizing the K-S Test but did detect the degrade with high power for the Sign Test. Although closeness could not be used to detect the degrade in the high setting, the network measure degree detected the change with high power for both the K-S and Sign Tests. Similar to the results of the network models, the Sign Test performed as well or better than the K-S Test across every degrade level.

Table 32. Power to Detect Degraded High School Network for Day 2-4 at $p = 1/2$

	closeness	betweenness	degree	Proportion of Nodes Removed
Kolmogorov-Smirnov : Day 2				
Low	1.00	0.00	0.00	0.10
Medium	1.00	0.00	0.00	0.04
High	0.02	0.00	0.95	0.11
Random	0.99	0.00	0.00	0.10
Day 3				
Low	1.00	0.00	0.00	0.10
Medium	0.65	0.00	0.00	0.04
High	0.29	0.00	1.0	0.11
Random	1.0	0.00	0.00	0.10
Day 4				
Low	1.00	0.00	0.00	0.10
Medium	0.64	0.00	0.00	0.04
High	0.68	0.00	1.0	0.11
Random	1.0	0.00	0.00	0.10
Sign: Day 2				
Low	1.00	0.00	0.00	0.10
Medium	0.33	0.00	0.00	0.04
High	0.05	0.01	1.00	0.11
Random	0.94	0.01	0.00	0.10
Day 3				
Low	1.00	0.00	0.00	0.10
Medium	0.00	0.00	0.00	0.04
High	0.12	0.01	1.00	0.11
Random	0.99	0.00	0.06	0.10
Day 4				
Low	1.00	0.00	0.00	0.10
Medium	1.00	0.00	0.00	0.04
High	0.77	0.01	1.00	0.11
Random	0.99	0.00	0.01	0.10

The second, third, and fourth day results can be seen in Table 32 and show similar results to the first day with two notable exceptions. The K-S Test on day two was able to detect the change in medium degrade with high power versus all other days. As day two had the lowest density of the four days, it appears that the lower density increased the effect of the degradation enough for the change to be detected with high power. The other notable difference was seen within the Sign Test. Both day two and

three failed to detect the degradation at the medium degrade level. As day 3 had the second highest density, the same case that was made for the K-S test does not appear to hold for the Sign Test. The Sign Test is detecting changes in the central location based on the median, while the K-S Test is looking for a change in the location or dispersion, based on these differences different results from one test to the other are expected.

The same analysis of the High School Social Network at proportion of degrade equals 1/3 can be found in Tables A28 - A31 within the Appendix A. Lowering the proportion of nodes for the degrade resulted in the following overall changes to detection: 1) power for low degrade continued to meet at least 0.80 for closeness for both the K-S and Sign Test. 2) Power for the random degrade level dropped below 0.80 for both the K-S and Sign Test in day 2, and also in the K-S Test for day 3. 3) Power for medium degrade dropped below 0.80 across all categories. 4) Power for high degrade for degree dropped below 0.80 in all categories except for the Sign Test for the third and fourth days.

3.4 Statistical Testing Summary

The major contribution from this section lies in the power of the non-parametric test to detect changes across many network types and degrade levels. For anyone wanting to monitor a network for change, it is simple to implement the K-S or Sign Test utilizing one or multiple network measures. In particular, the Sign or K-S Test applied to network measure closeness would be quite sensitive to change in networks with similar properties and structure as those examined here, if it is known that low or random node degrade is being targeted in their network. If there is a potential for high degree nodes to be targeted, then either non-parametric test with the network measure degree may perform with more sensitivity to detect this change. Each of

the applied networks showed one Test as superior than the other, for applying to any number of networks its recommended to run both test simultaneously. The lack of detection of the network measure betweenness highlights the potential for focusing on this measures ability to withstand degradation from node attacks. This information might be beneficial when building or testing a network for vulnerabilities.

3.5 Contributions and Conclusions for Network Sensitivity

1. Across all graph models, for the network measure closeness, the mean, variance, skewness and L-scale appeared the most sensitive.

2. Across all graph models, for the network measure betweenness and closeness, the mean appeared the most sensitive.

3. Across all graph models, L-skewness and L-kurtosis had the lowest sensitivity overall.

4. On average as the graphs size and edge density increased sensitivity across moments increased as well.

5. Specifically for the Barabási-Albert model, skewness for closeness, and dispersion (both variance and L-scale) for betweenness were also sensitive.

6. Both the K-S and Sign Test achieved high power to detect node degrade, with as few as $1 - 2\%$ of all nodes being deleted using, using the network measure closeness and degree.

7. Betweenness was unable to detect the node degradation in either real world network, and appears a suitable choice when building a network that is robust against node degrade.

Although the mean was the most sensitive moment to detect change in network models, statistical test based on the mean were not sensitive at all in the real world networks. Without a network model it is possible that moments are not sensitive and that the empirical distribution of the network as a whole must be used to detect the change. With this in mind, the non-parametric test, K-S and Sign, were the most sensitive test and when paired with the network measures of closeness and betweenness they could detect the change with as few as $1 - 2\%$ of all nodes being removed. These results highlight the advantage of non-parametric statistical test being used to detect changes within networks. To use these results in real world applications it is recommended that interested parties implement a simultaneous of both the K-S and Sign test using both network measures of closeness and degree for detecting changes within their respective networks. When these test detect changes, an analyst should be informed to examine the network and making detailed inference based on the specific change noted.

With respect to network analysis in general, more attention needs to be paid to network measures other than degree. Much of the current research utilizes degree, possibly due to distributions being derived and the ease of calculations. Yet, degree might not always be the most sensitive network measure as this research has shown. Finally, based on this chapter, L-moments showed very little sensitivity to degradation within a network by themselves. To this end, the next chapters extend the theory for estimating L-moments in order to properly estimate them via sample size criteria (Chapter 4) and joint confidence estimation (Chapter 5).

IV. L-moments and L-moment ratios Sample Size Guidance

L-moments have been in use for decades, but very little guidance exists when it comes to deriving theory for sample size requirements, confidence intervals and effect sizes. The research here seeks to provide this guidance by developing exact variance and covariance estimates in order to derive sample size requirements and confidence intervals estimating L-moments and L-moment ratios. Recall, that sample L-moments may be calculated by Equation 5 yet another way to write that equation was derived by Hoskings [17] in 1985 and is the following:

$$l_r = \sum_{k=0}^{r-1} p^*_{r-1,k} b_k \tag{17}$$

$$\text{where } b_k = \frac{1}{n^{k+1}} \sum_{i=1}^{n} (i-1)^{(k)} X_{i:n}, \text{ and } p_{rk} = (-1)^{r-k} \binom{r}{k} \binom{r+k}{k},$$

where the r equals the r^{th} L-moment, n equals the sample size, and k is determined by r. This equation will be used to derive the variance and covariance of each L-moment.

Calculating Expectations and Variance of Sample L-moments.

Elamir and Schultz [8] laid the foundation needed for solving the exact variance of sample L-moments. Prior to their research, only asymptotic variances and covariances had been reported. Based on their work, one can now solve for the variance and covariance for any L-moment estimate, for known distributions. The core of their work combines equations and identities given by Downton [7] for calculating the expectations, joint expectations, and variance/covariance of order statistics. In doing so, they were able to evaluate the mean and variance of sample L-moments, l_r, by deriving the following formulas for the expectations and variance of b_k, the individual order statistic and its weights for a specific L-moment. Those formulas are

the following:

$$E[b_k] = \frac{1}{k-1} E(X_{k+1;k+1}), \tag{18}$$

$$E[b_k b_l] = \frac{1}{n^{(k+1)} n^{(l+1)}} \sum_{i=1}^{n} \sum_{j=1}^{n} (i-l)^{(k)} (j-1)^{(l)} E[X_{i:n} X_{j:n}], \tag{19}$$

$$\text{and } var[b_k, b_l] = \frac{1}{n^{(k+1)}} \sum_{s=0}^{k} (n-l-1)^{(s)} A_{kl}^{(s)} \tag{20}$$

$$\begin{aligned}
\text{where } A_{kl}^{(s)} =& \frac{k!l!E[X^2_{s+l+1;s+l+1}]}{(k-s)!(s+l+1)!s!(s+l+1)} \\
&+ \frac{k!l!(l+1)^{(k+l-s)}}{(k+l-s)!} \sum_{r=0}^{s-1} (-1)^r \frac{E[X_{l+1:l+2+r} X_{1+2:l+2+r}]}{(l+2+r)!(s-1-r)!} \\
&- \frac{k!l!(k+1)^{(k+l-s)}}{(k+1-s)!} \sum_{r=0}^{k} (-1)^r \frac{E[X_{s+l-k:s+l-k+1+r} X_{s+l-k+a:s+1-k+1+r}]}{(k-r)!(s+l-k+1+r)!} \\
&+ \frac{k!l!E[X_{k+l:k+1}](E[X_{s+l-k:s+l-k}] - E[X_{l+1:l+1}])}{(k+1-s)!(s+l-k)!s!}.
\end{aligned} \tag{21}$$

The mean, variance and covariance can now be exactly computed for each L-moment via Equations 18-21. These exact variance formulas are required to derive sample size guidance. Solving for the first four sample L-moments, one can derive the variance/-covariance matrix for these four sample L-moments simultaneously. Allowing $\boldsymbol{C}$ to be the matrix defined by the p_{rk} coefficient of Equation 17, and matrix $\boldsymbol{\Theta}$ based on the b_k portion (e.g. $\boldsymbol{var(b)}$ for $\boldsymbol{b} = (b_0, ..., b_{n-1})$) based on Equation 17, the matrix notation for the variance is:

$$\boldsymbol{var(l_r)} = \boldsymbol{C\Theta C^T} \tag{22}$$

$$\text{where } \boldsymbol{C} = \begin{bmatrix} 1 & 0 & 0 & 0 \\ -1 & 2 & 0 & 0 \\ 1 & -6 & 6 & 0 \\ -1 & 12 & -30 & 20 \end{bmatrix}, \text{ and } \boldsymbol{\Theta} = \begin{bmatrix} \Theta_{00} & \Theta_{01} & \Theta_{02} & \Theta_{03} \\ \Theta_{10} & \Theta_{11} & \Theta_{12} & \Theta_{13} \\ \Theta_{20} & \Theta_{21} & \Theta_{22} & \Theta_{33} \\ \Theta_{30} & \Theta_{31} & \Theta_{32} & \Theta_{33} \end{bmatrix} \tag{23}$$

Note that $\boldsymbol{\Theta_{kl}} = \boldsymbol{\Theta_{lk}} = var(b_k, b_l)$.

Evaluating this covariance matrix for the first four sample L-moments yields equations for the variances and covariances in terms of Θ_{kl} and subsequently in terms of $\text{var}(b_k, b_l)$, Equation 20. In Appendix B, Equation 20 is expanded for all combinations of k, l. Subsequently, special cases of Equation 21 are derived when $k = l$ as well as when $s = 0$. Full expansion of Equation 21 is also given for all needed values of k, l, and s in terms of expectations and joint expectations of order statistics.

The steps in solving these equations includes placing them all under a common divisor, the 2nd L-moment specifically utilizes $n(n-1)$, and then expanding all $A_{k,l}^{(s)}$ expressions in terms of the underlying order statistics. Lastly, expectations are grouped together. Complete steps to derive these variances are shown in Appendix B. Results are simplified to the greatest common factor, and the variance and covariance of the first four L-moments are shown as linear combinations of expectations and joint expectations of order statistics as a function of n, sample size. These equations follow. The first two equations were previously derived by Elmiar and Seheultz [8] while I derived the expressions for l_3 and l_4.

$$var(l_1) = \frac{1}{n}\left[E[Y_{1:1}^2] - E[Y_{1:1}]^2\right]. \tag{24}$$

$$
\begin{aligned}
&var(l_2) = \\
&\Big[\frac{4(n-2)}{3}\left[E(Y_{3:3}^2) + E(Y_{1:3}Y_{2:3}) + E(Y_{2:3}Y_{3:3})\right] - 2(n-3)E(Y_{1:2}Y_{2:2}) \\
&- 2(n-2)E(Y_{2:2}^2) + (n-1)E(Y_{1:1}^2) - 2(2n-3)E(Y_{2:2})^2 \\
&+ 4(2n-3)E(Y_{2:2})E(Y_{1:1}) - 5(n-1)E(Y_{1:1})^2\Big]/n(n-1).
\end{aligned} \tag{25}
$$

$$
\begin{aligned}
&var(l_3) = \\
&\Big[36/10(n^2-7n+12)\left[2E[Y_{5:5}^2] - E[Y_{3:5}Y_{4:5}] - E[Y_{2:5}Y_{3:5}]\right] + 4(4n^2-27n+44)E[Y_{3:3}^2] \\
&+ 12(-3n^2+15n-20)E[Y_{3:3}]^2 + 18(-n^2+7n-12)E[Y_{4:4}^2] + 18(-n^2+3)\big[E[Y_{3:4}Y_{4:4}] \\
&+ E[Y_{1:4}Y_{2:4}]\big] + 6(-5n^2+15n+8)E[Y_{1:2}Y_{2:2}] + 12(n^2-10)E[Y_{1:3}Y_{2:3}] \\
&+ 4(5n^2-6n-26)E[Y_{2:3}Y_{3:3}] + 6(n^2-11n+24)E[Y_{2:4}Y_{3:4}] \\
&+ 36(3n^2-15n+20)E[Y_{3:3}]E[Y_{2:2}] + 12(5n^2-24n+28)E[Y_{2:2}]E[Y_{1:1}] \\
&+ 54(-2n^2+9n-10)E[Y_{2:2}]^2 + 6(-n^2+6n-8)E[Y_{2:2}^2] \\
&+ 12(-n^2+9n-20)E[Y_{1:1}]E[Y_{3:3}] + 13(-n^2+3n-2)E[Y_{1:1}]^2 \\
&+ (n^2-3n+2)E[Y_{1:1}^2]\Big]/n(n-1)(n-2).
\end{aligned} \tag{26}
$$

$$
\begin{aligned}
&var(l_4) = \\
&\Big[400/35(n^3 - 15n^2 + 74n - 120)\left[[5E[Y^2_{7:7}] + E[Y_{3:7}Y_{4:7}] + E[Y_{4:7}Y_{5:7}]\right] \\
&+ (n^3 - 6n^2 + 11n - 6)\left[E[Y^2_{1:1}] - 25E[Y_{1:1}]^2\right] + 12(-n^3 + 12n^2 - 41n + 42)E[Y^2_{2:2}] \\
&+ 4(17n^3 - 234n^2 + 997n - 1344)E[Y^2_{3:3}] + 10(-19n^3 + 276n^2 - 1289n + 1956)E[Y^2_{4:4}] \\
&+ 12(23n^3 - 342n^2 + 1663n - 2652)E[Y^2_{5:5}] + 200(-n^3 + 15n^2 - 74n + 120)E[Y^2_{6:6}] \\
&+ 72(-12n^3 + 103n^2 - 287n + 258)E[Y_{2:2}]^2 + 300(-7n^3 + 72n^2 - 253n + 300)E[Y_{3:3}]^2 \\
&+ 200(-2n^3 + 21n^2 - 79n + 105)E[Y_{4:4}]^2 + 12(-11n^3 - 87n^2 + 769n - 827)E[Y_{1:2}Y_{2:2}] \\
&+ 8(-49n^3 + 708n^2 - 2534n + 1953)E[Y_{2:3}Y_{3:3}] + 30(18n^3 - 177n^2 + 498n - 307)E[Y_{3:4}Y_{4:4}] \\
&+ 24(2n^3 + 51n^2 - 268n + 91)E[Y_{1:3}Y_{2:3}] + 30(11n^3 - 114n^2 + 271n + 36)E[Y_{2:4}Y_{3:4}] \\
&+ 150(-3n^2 + 6n + 25)E[Y_{1:4}Y_{2:4}] + 48(-3n^3 + 27n^2 - 68n + 32)E[Y_{4:5}Y_{5:5}] \\
&+ 18(-9n^3 + 66n^2 - 49n - 284)E[Y_{3:5}Y_{4:5}] + 90(-n^3 + 6n^2 + 11n - 76)E[Y_{2:5}Y_{3:5}] \\
&+ 480(n - 4)E[Y_{1:5}Y_{2:5}] + 120(n^2 - 9n + 20)\left[E[Y_{4:6}Y_{5:6}] + E[Y_{2:6}Y_{3:6}]\right] \\
&+ 20(-n^3 + 24n^2 - 155n + 300)E[Y_{3:6}Y_{4:6}] + 12(19n^3 - 186n^2 + 59n - 546)E[Y_{1:1}]E[Y_{2:2}] \\
&+ 100(-n^3 + 24n^2 - 143n + 240)E[Y_{1:1}]E[Y_{3:3}] + 40(n^3 - 6n^2 + 71n - 246)E[Y_{1:1}]E[Y_{4:4}] \\
&+ 60(35n^3 - 366n^2 + 1315n - 1596)E[Y_{2:2}]E[Y_{3:3}] \\
&+ 120(-4n^3 + 45n^2 - 209n + 360)E[Y_{2:2}]E[Y_{4:4}] \\
&+ 800(2n^3 - 21n^2 + 79n - 105)E[Y_{3:3}]E[Y_{4:4}]\Big]/n(n)(n-1)(n-2).
\end{aligned}
\tag{27}
$$

Exact covariance equations are derived next for each of the first four L-moments. Equation (28) was previously derived by Elamir and Seheultz [8] while I derived the remaining five covariance equations, Equations 29-33. The covariance among the second (l_2), third (l_3), and fourth (l_4) L-moments are used subsequently to estimate

variance for L-moment ratios as well as build confidence intervals for L-moments and L-moment ratios. The derivations for these equations can be found in Appendix B.

$$cov(l_1, l_2) = \\ \Big[\frac{1}{2}E[Y_{2:2}^2] - \frac{1}{2}E[Y_{1:2}Y_{2:2}] + 2E[Y_{1:1}]^2 - E[Y_{1:1}]E[Y_{2:2}] - E[Y_{1:1}^2]\Big]/n. \tag{28}$$

$$cov(l_1, l_3) = \\ \Big[2E[Y_{3:3}^2] - 2E[Y_{2:3}Y_{3:3}] + 12E[Y_{1:1}]E[Y_{2:2}] - 6E[Y_{1:1}]E[Y_{3:3}] - 3E[Y_{2:2}^2] \\ + 3E[Y_{1:2}Y_{2:2}] - 7E[Y_{1:1}]^2 + E[Y_{1:1}^2]\Big]/n. \tag{29}$$

$$cov(l_1, l_4) = \\ \Big[5E[Y_{4:4}^2] - 5E[Y_{3:4}Y_{4:4}] + 50E[Y_{1:1}]E[Y_{3:3}] - 20E[Y_{1:1}]E[Y_{4:4}] - 10E[Y_{3:3}^2] \\ - 10E[Y_{2:3}Y_{3:3}] - 42E[Y_{1:1}]E[Y_{2:2}] + 30E[Y_{1:1}]E[Y_{3:3}] + 6E[Y_{2:2}^2] \\ - 6E[Y_{1:2}Y_{2:2}] + 13E[Y_{1:1}]^2 - E[Y_{1:1}]^2\Big]/n. \tag{30}$$

$$cov(l_2, l_3) = \\ \Big[(n-3)\left[3E[Y_{4:4}^2] - 6E[Y_{3:3}^2] + 3E[Y_{3:4}Y_{4:4}] + 2E[Y_{2:4}Y_{3:4}] - 10E[Y_{2:3}Y_{3:3}] - 4E[Y_{1:3}Y_{2:3}]\right] \\ + (n-1)\left[9E[Y_{1:1}]^2 - E[Y_{1:1}^2] + 6E[Y_{1:1}]E[Y_{3:3}]\right] + 2(2n-5)E[Y_{2:2}^2] + 6(4n-9)E[Y_{2:2}]^2 \\ + 8(n-4)E[Y_{1:2}Y_{2:2}] - 2(13n-25)E[Y_{1:1}]E[Y_{2:2}] - 12(n-2)E[Y_{2:2}]E[Y_{3:3}]\Big]/n(n-1). \tag{31}$$

$$
\begin{aligned}
&cov(l_2, l_4) = \\
&\Big[(n-1)\left[E[Y_{1:1}^2] - 15E[Y_{1:1}]^2 - 10E[Y_{1:1}](E[Y_{3:3}] - 2E[Y_{4:4}])\right] \\
&+ (n-4)\big[8E[Y_{5:5}^2] - 20E[Y_{4:4}^2] - 30E[Y_{3:4}Y_{4:4}] - 10E[Y_{2:4}Y_{3:4}] + 8E[Y_{4:5}Y_{5:5}] \\
&+ 4E[Y_{3:5}Y_{4:5}]\big] + (-7n+19)E[Y_{2:2}^2] + 6(3n-11)E[Y_{3:3}^2] - 4(21n-69)E[Y_{2:2}]^2 \\
&- (17n+101)E[Y_{1:2}Y_{2:2}] + 2(19n-83)E[Y_{2:3}Y_{3:3}] + 4(2n-9)E[Y_{1:3}Y_{2:3}] \\
&+ 4(17n-38)E[Y_{1:1}]E[Y_{2:2}] + 20(5n-14)E[Y_{2:2}]E[Y_{3:3}] - 20(2n-5)E[Y_{2:2}]E[Y_{4:4}]\Big] \\
&/n(n-1).
\end{aligned}
\tag{32}
$$

$$
\begin{aligned}
&cov(l_3, l_4) = \\
&\Big[(n^3 - 12n^2 + 47n - 60)\big[20E[Y_{6:6}^2] - 8E[Y_{4:6}Y_{5:6}] - 6E[Y_{3:6}Y_{4:6}] + 24E[Y_{4:5}Y_{5:5}] \\
&+ 42E[Y_{3:5}Y_{4:5}] + 18E[Y_{2:5}Y_{3:5}] - 60E[Y_{5:5}^2]\big] + (n^3 - 6n^2 + 11n - 6)\big[-E[Y_{1:1}^2] \\
&+ 19E[Y_{1:1}]^2 - 20E[Y_{1:1}]E[Y_{4:4}]\big] + 9(n^3 - 10n^2 + 31n - 30)E[Y_{2:2}^2] \\
&+ 12(-3n^3 + 34n^2 - 123n + 144)E[Y_{3:3}^2] + 4(17n^3 - 201n^2 + 772n - 966)E[Y_{4:4}^2] \\
&+ 36(9n^3 - 74n^2 + 199n - 174)E[Y_{2:2}]^2 + 60(5n^3 - 48n^2 + 159n - 180)E[Y_{3:3}]^2 \\
&+ 9(7n^3 - 18n^2 - 143n + 402)E[Y_{1:2}Y_{2:2}] + 120(-5n^2 + 34n - 57)E[Y_{2:3}Y_{3:3}] \\
&+ 2(-31n^3 + 438n^2 - 1916n + 2643)E[Y_{3:4}Y_{4:4}] \\
&+ 12(-2n^3 - 9n^2 + 133n - 264)E[Y_{1:3}Y_{2:3}] + 6(-8n^3 + 119n^2 - 533n + 744)E[Y_{2:4}Y_{3:4}] \\
&+ 30(3n^2 - 20n + 33)E[Y_{1:4}Y_{2:4}] + 18(-7n^3 + 60n^2 - 167n + 150)E[Y_{1:1}]E[Y_{2:2}] \\
&+ 8(7n^3 - 87n^2 + 377n - 537)E[Y_{1:1}]E[Y_{3:3}] \\
&+ 12(-46n^3 + 417n^2 - 1301n + 1392)E[Y_{2:2}]E[Y_{3:3}] \\
&+ 60(2n^3 - 15n^2 + 37n - 30)E[Y_{2:2}]E[Y_{4:4}] + 120(-n^3 + 9n^2 - 28n + 30)E[Y_{3:3}]E[Y_{4:4}]\Big] \\
&/n(n)(n-1)(n-2).
\end{aligned}
\tag{33}
$$

Notice that each of these variance and covariance expressions is a function of sample size, n, in the denominator. Therefore, as sample size increases, the variance and covariance among the first four L-moments decrease.

4.1 L-Moments and L-moment Ratios Sample Size Requirements for Common Distributions

To derive guidance for the required sample size for estimating a sample L-moment or L-moment ratio from a particular distribution, mean square error (MSE) was utilized. In doing so, the sample size which adequately minimizes MSE of the L-moment estimator is highlighted. For statistic l estimating parameter λ, MSE is expressed as the sum of (squared) bias and and variance of the estimator:

$$\text{MSE}_\lambda l \ = E_\lambda(l-\lambda)^2 = var_\lambda l + (Bias_\lambda l)^2. \tag{34}$$

Since sample L-moments are unbiased estimates of population L-moments [8], MSE_λ reduces down to the variance of the estimator, which for the r^{th} sample L-moment, l_r, is:

$$\text{MSE}_\lambda l_r = var(l_r).$$

Thus, sample size guidance for estimating population L-moments through sample L-moments only relies on the variance calculated for each r^{th} L-moment. With the exact variance formulas for statistics l_r derived in Equations 24-27, the variance for the first four sample L-moments can be calculated directly for any known distribution.

In addition, sample L-moment ratios (t_r) are formed where $t_r = l_r/l_2$. The ratios for $r = 3$ and 4 are known as L-skewness and L-kurtosis and are widely used. While exact formulas for the variance have not been derived for any L-moment ratios, a Taylor series expansion can be used to estimate the variance of the ratio of two random variables and can be approximated using the following form:

$$var(l_r/l_2) \sim \left[\frac{E[l_r]}{E[l_2]}\right]^2 \left[\frac{var(l_r)}{E[l_r]^2} + \frac{var(l_2)}{E[l_2]^2} - 2\frac{cov(l_r,l_2)}{E[l_r]E[l_2]}\right]. \tag{35}$$

Combining exact variance equations, covariance equations, and known expectations, the variance of L-moment ratios may be approximated using Equation 35 and sample size guidance provided for these estimators as well. The expected value for the second, third, and fourth L-moments, which are required for approximating the variance of L-moment ratios have been reported [18], and they are provided in Table 33 for the common distributions examined.

Table 33. Expected Values of L-moments for Common distributions [18]

	normal(0,1)	uniform(0,1)	exponential(1)	gumbel(0,1)	pareto($\frac{3}{\sqrt{2}}$, 4)
$E[l_2]$	0.56418	1/6	1/2	log(2)	0.4040610
$E[l_3]$	0	0	1/6	0.1177657	0.1836641
$E[l_4]$	0.06916964	0	1/12	0.1042493	0.1101985

The following sections derive and plot var(l_r) for sample L-moments and approximate variance for L-moment ratios for the following distributions: normal(0,1), uniform(0,1), exponential(1), gumbel(0,1) and pareto($\frac{3}{\sqrt{2}}$,4). The exact variance was calculated using Equations 24-27 for sample L-moments, and Equation 35 was used to derive the approximate variance of the L-moment ratios for each of the distributions. Plots of the exact variance as a function of sample size from n = 4 to 50 are provided for each distribution and used to compare the first four L-moments in relation to each other. Plots of the approximate variance as a function of sample size from n = 4 to 50 are shown as well for both L-skewness (t_3) and L-kurtosis (t_4) for each of the distributions. The last subsection gives general inference and sample size guidance for L-moments and L-moment ratios for each of the given distributions when appropriate.

normal distributions(0,1).

The expressions for the expected value of an order statistic for a standard normal random variable and the covariance between two order statistics both from a standard

normal distribution are as follows:

$$E[X^r_{j,n}] = {}_nC_j \int_{-\infty}^{\infty} x^r \Phi(x)^{j-1}(1-\Phi(x))^{n-j}\Phi(x)dx. \tag{36}$$

$$E[X_{i,n}X_{j:n}] = {}_nC_{ij} \int_{-\infty}^{\infty}\int_{-\infty}^{v} uv\Phi(u)^{i-1}[\Phi(v)-\Phi(x)]^{(j-i-1)}(1-\Phi(v))^{n-j}\Phi(u)\Phi(v)dudv. \tag{37}$$

$${}_nC_j = \frac{n!}{(j-1)!(n-j)!} \text{ and } {}_nC_{ij} = \frac{n!}{(i-1)!(j-i-1)!(n-j)!} \tag{38}$$

In these equations i, j represent the i^{th} and j^{th} order statistics, and Φ denotes the inverse cumulative normal distribution. Numerical approximation techniques are required to estimate these expectations and covariances. Numerical approximated tables calculated by Teichroew [37] were used with Equations 24-27, and 35 for deriving the approximated variances for the standard normal distribution (Table 34). Table 34 which details these exact variances of L-moments and approximate variances for L-moment ratios are based on a sample size of n.

Table 34. Exact and Approximate Variances for normal(0,1)

	normal(0,1)	Divisor
var(l_1)	1	$n^{(1)}$
var(l_2)	$0.16275n + 0.03787$	$n^{(2)}$
var(l_3)	$0.05938n^2 + 0.04905n + 0.01037$	$n^{(3)}$
var(l_4)	$0.02829n^3 + 0.05650n^2 + 0.05482n + 0.01214$	$n^{(4)}$
$\hat{var}(t_3)$	-	-
$\hat{var}(t_4)$	$0.08824n^3 + 0.18233n^2 + 0.16032n + 0.04785$	$n^{(4)}$

*divisor: $n^{(r)} = n(n-1)(n-r+1)$ -: does not exist

Table 34 and subsequent tables of exact and approximate variances for all the distributions examined have the following layout. The distribution is listed in the center column on the top row. The first column lists the estimators, the first four L-moments followed by third and fourth L-moment ratios. The center column gives

the variance as a function of sample size. The last column denotes the divisor for each of the functions, with the equation to solve for the divisor listed as a note at the bottom of the table.

For all distributions, the variance of the first L-moment is equal to the variance of the distribution. Each higher order L-moment has an approximate factor of n increase in the divisor. Any population L-moment that equals zero, yields the approximated variance equation unsolvable. Specifically, notice that the variance of τ_3 for normal(0,1) does not exist using the approximation of Equation 35 as the $\mathrm{E}[l_3] = 0$ for the standard normal distribution.

Figure 16. Plot of Exact Variance Sample L-moments for the standard normal distribution, Sample Size 4-50

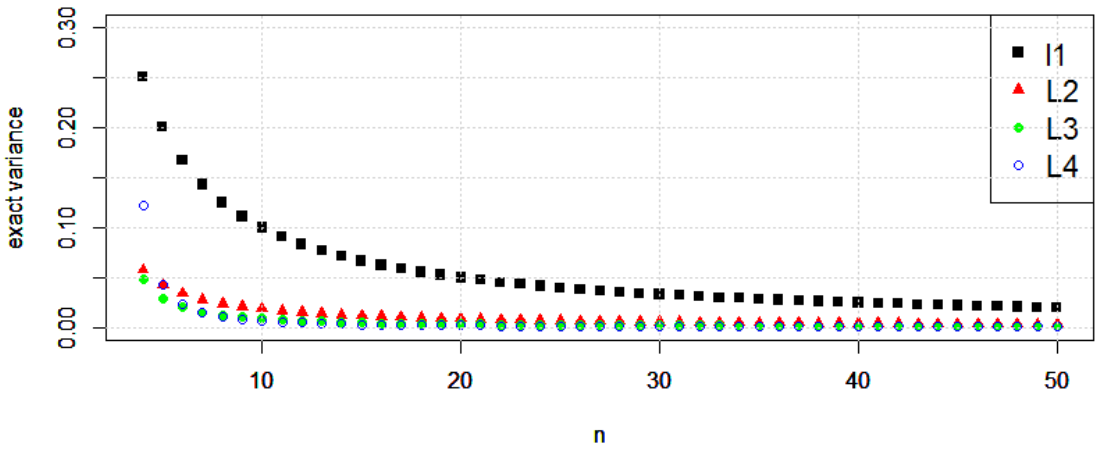

The exact variance for the first four L-moments from a standard normal distribution are shown in Figure 16. The x-axis is plotted for sample sizes 4-50, while the y-axis lists the exact variance for a given sample size. For the standard normal distribution, the mean levels off around a sample size of 30, while the higher order L-moments level off around samples sizes of 10. Of note, the L-moment estimators, for $l_2 - l_4$ have considerably less variance than the mean.

Figure 17. Plots of Approximate Variance L-moment ratios for the standard normal distribution, Sample Size 4-50

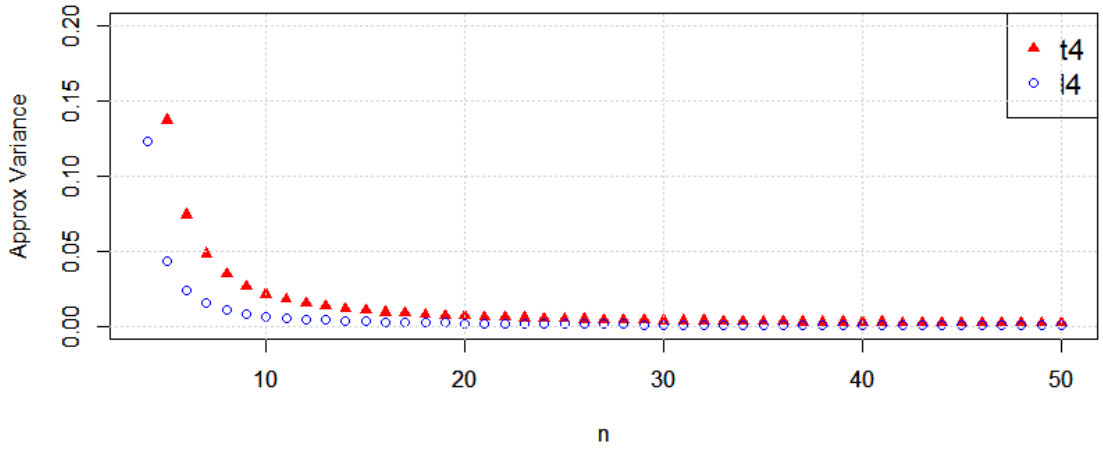

The approximate variance for estimator L-kurtosis (t_4) from a standard normal distribution is shown in Figure 17 and is compared with its un-scaled L-moment (l_4). The L-moment ratio t_4 has slightly higher variance than the un-scaled L-moment l_4 with approximate variance stable at about a sample size of 15. In addition, the variance of l_4 and t_4 are nearly equivalent at about a sample size of 25.

uniform distributions (0,1).

The expressions for the expected value of an order statistic for a standard uniform random variable and the covariance between two order statistics both from a standard uniform distribution can be found in *Records via Probability Theory* [2] Equations (2.3.14 and 2.3.15) and are the following:

$$E[X^r_{j,n}] = \frac{n!\Gamma(r+j)}{(j-1)!\Gamma(r+n+1)}. \tag{39}$$

$$E[X_{i:n}X_{j:n}] = \frac{i(j+1)}{(n+1)(n+2)} \text{ for } 1 \leq i < j \leq n. \tag{40}$$

Once again i, j represents the i^{th} and j^{th} order statistics and the gamma function (Γ) is defined as $(n-1)!$. The closed forms of Equations 39-40 were used with Equations 24-27 to derive the exact variances for the uniform(0,1) distribution (Table 35).

Table 35. Exact and Approximate Variance for uniform(0,1)

	uniform(0,1)	Divisor
var(l_1)	1/12	$n^{(1)}$
var(l_2)	0.00555n+0.01666	$n^{(2)}$
var(l_3)	$0.00476n^2 + 0.02380$	$n^{(3)}$
var(l_4)	$0.00158n^3 + 0.00476n^2 + 0.01746n + 0.05238$	$n^{(4)}$

*divisor $n^{(r)} = n(n-1)(n-r+1)$

Once again, the population variance is the variance of the first L-moment. The divisors remain the same regardless of the distribution, as they are only dependent on the L-moment estimator for which the variance is derived. Due to the expected values of both l_3 and l_4 being equal to zero in the uniform(0,1) distribution, it is not possible to approximate the variance of the L-moment ratios for the uniform distribution using Equation 35. As such, no plots or inference is made concerning L-moment ratios for this distribution.

Figure 18. Plot of Exact Variance Sample L-moments for the standard uniform distribution, Sample Size 4-50

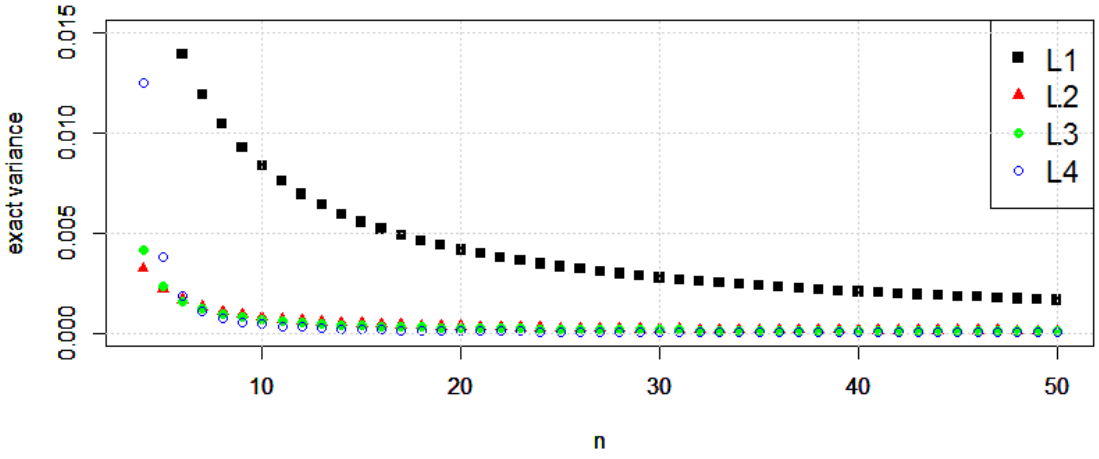

The exact variance for the first four L-moments from a standard uniform distribution are shown in Figure 18. Similar to the standard normal distribution, the variance of the first L-moment of the uniform(0,1) distribution levels off around 30, while the higher order L-moments level off around 10. The y-axis range is about half that of the normal distribution and is expected as the variance within the population is considerably smaller than that for the normal distribution.

exponential distributions (1).

The expressions for the expected value of an order statistic for an exponential random variable and the covariance between two order statistics both from an exponential distribution are given in Equations 41 and 42. The expected value has a closed form solution that is found within *Records via Probability Theory* [2] Equation (2.3.23) while the covariance is calculated using integration techniques.

$$E[X_{j,n}^r] = {}_nC_j \sum_{s=0}^{j-1} (-1)^s \binom{j-1}{s} \frac{\Gamma(r+1)}{(n-j+s+1)^{r+1}}. \tag{41}$$

$$E[X_{i:n}X_{j:n}] =$$
$$_nC_{ij}\int_0^\infty \int_0^v (u)(v)e^{-u}(1-e^{-u})^{i-1}[e^{-u}-e^{-v}]^{j-1-i}(e^{-v})^{n-j+1}dudv. \quad (42)$$

Once again i, j represents the i^{th} and j^{th} order statistics. These expressions for the expected values of the order statistics were used with Equations 24-27 and Equation 35 to derive the exact and approximate variances for the exponential(1) distribution (Table 36).

Table 36. Exact and Approximate Variance for exponential(1)

	exponential(1)	Divisor
var(l_1)	1	$n^{(1)}$
var(l_2)	0.33333n - 0.16666	$n^{(2)}$
var(l_3)	$0.13333n^2 - 0.10000n - 0.06666$	$n^{(3)}$
var(l_4)	$0.07142n^3 - 0.07142n^2 - 0.04761n - 0.07142$	$n^{(4)}$
$\hat{var}(\tau_3)$	$0.23703n^2 + 0.11851n - 0.11851$	$n^{(3)}$
$\hat{var}(\tau_4)$	$0.21164n^3 + 0.06613n^2 - 0.05423n - 0.04932$	$n^{(4)}$

*divisor $n^{(r)} = n(n-1)(n-r+1)$

Unlike the normal and uniform distributions the exponential distribution is a non-symmetric distribution and as such, the expected values for the upper L-moments (l_3 and l_4) are not equal to zero. Therefore, Equation 35 was used to approximate both L-moment ratios for t_3 and t_4.

Figure 19. Plot of Exact Variance Sample L-moments for the exponential(1) distribution, Sample Size 4-50

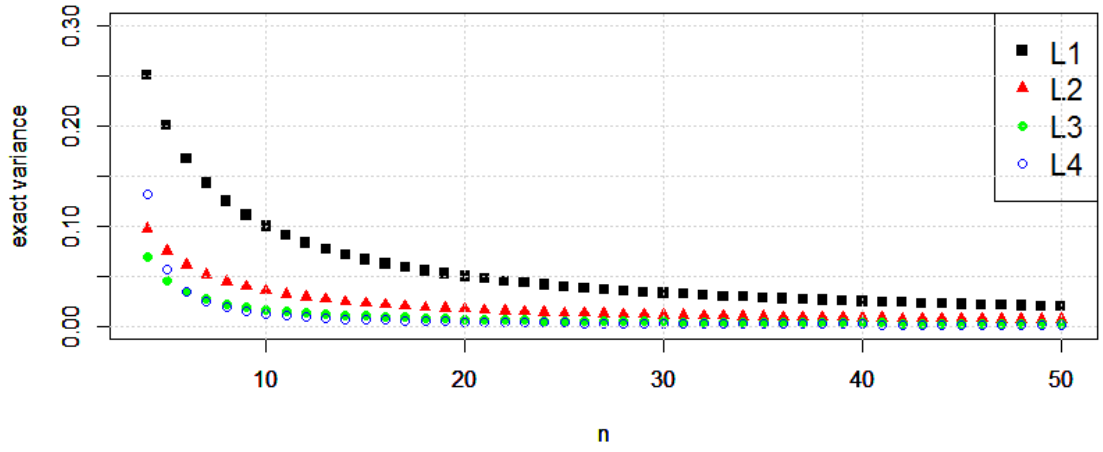

The exact variance for the first four L-moments from an exponential distribution are shown in Figure 19. Once again, the variance of the first L-moment levels off at about 30, while the higher order L-moments level off around 10.

Figure 20. Plots of Approximate Variance L-moment ratios for the exponential(1) distribution, Sample Size 4-50

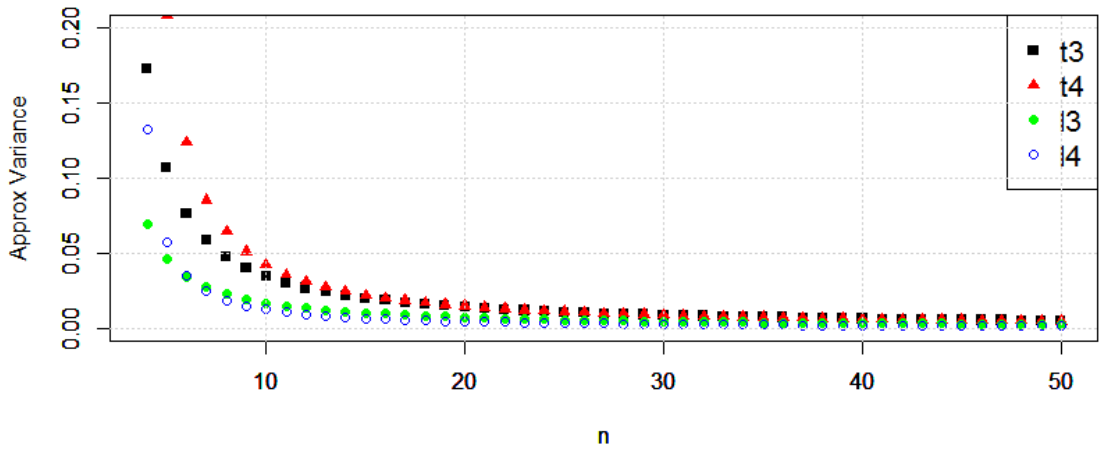

The approximate variance for L-skewness (t_3) and L-kurtosis (t_4) from an ex-

ponential distribution is shown in Figure 20 and is compared with their un-scaled L-moments (l_3 and l_4). The L-moment ratios have slightly higher variance than their un-scaled L-moments and seem to level off considerably by a sample size of about 15, similar to the normal distribution. It does appear that there is more variation in the variance in small sample sizes than what was observed in the normal distribution, but this was expected as the exponential is a skewed distribution. Further, the L-moments and their L-moment ratio counter parts have near equivalent variance about a sample size of 25.

gumbel distributions (u,v).

The expressions for the expected value of an order statistic for a standard gumbel random variable and the covariance between two order statistics both from a standard gumbel distribution were derived as follows:

$$E[X^r_{j:n}] =_n C_j \int_{-\infty}^{\infty} x^r e^{-(x+e^{-x})}[e^{-e^{-x}}]^{j-1}[1-e^{-e^{-x}}]^{n-j}dx. \tag{43}$$

$$E[X_{i:n}X_{j:n}] = \\ {}_nC_{ij}\int_{-\infty}^{\infty}\int_{-\infty}^{v}(u)(v)e^{-(u+e^{-u})}e^{-(v+e^{-v})}[e^{-e^{-u}}]^{i-1}[e^{-e^{-v}}-e^{-e^{-u}}]^{j-1-i}[e^{-e^{-v}}]^{n-j}dudv. \tag{44}$$

Once again i, j represents the i^{th} and j^{th} order statistics. These expressions were used with Equations 24-27 and Equation 35 to derive exact and approximate variances for the gumbel(0,1) distribution (Table 37).

Table 37. Exact and Approximate Variance for gumbel(0,1)

	gumbel(0,1)	Divisor
$\text{var}(l_1)$	$\pi^2/6$	$n^{(1)}$
$\text{var}(l_2)$	$0.38658n - 0.08913$	$n^{(2)}$
$\text{var}(l_3)$	$0.15395n^2 - 0.04810n - 0.02506$	$n^{(3)}$
$\text{var}(l_4)$	$0.08114n^3 - 0.26966n^2 + 0.03536n - 0.02153$	$n^{(4)}$
$\hat{var}(\tau_3)$	$0.23265n^2 + 0.07006n - 0.04134$	$n^{(3)}$
$\hat{var}(\tau_4)$	$0.13737n^3 + 0.10090n^2 - 0.11258n - 0.04837$	$n^{(4)}$

*divisor $n^{(r)} = n(n-1)(n-r+1)$

Once again the population variance is the variance of the first L-moments and the divisors remain the same. As a non symmetric distribution, the gumbel(0,1) distribution also has variance approximations for both L-moment ratios.

Figure 21. Plot of Exact Variance Sample L-moments for the gumbel(0,1) distribution, Sample Size 4-50

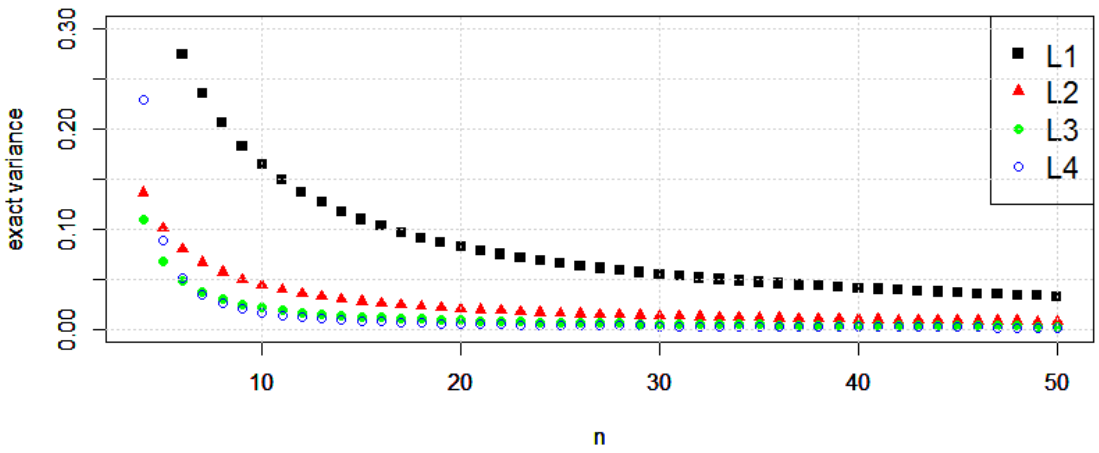

The exact variances for the first four L-moments from a standard gumbel distribution are shown in Figure 21. Once again the variance of the first L-moment levels off around 30, while the higher order L-moments levels off around 10. The y-axis range is identical to that of all the other distributions with a population variance equal to 1.

Figure 22. Plots of Approximate Variance L-moment ratios for the gumbel(0,1) distribution, Sample Size 4-50

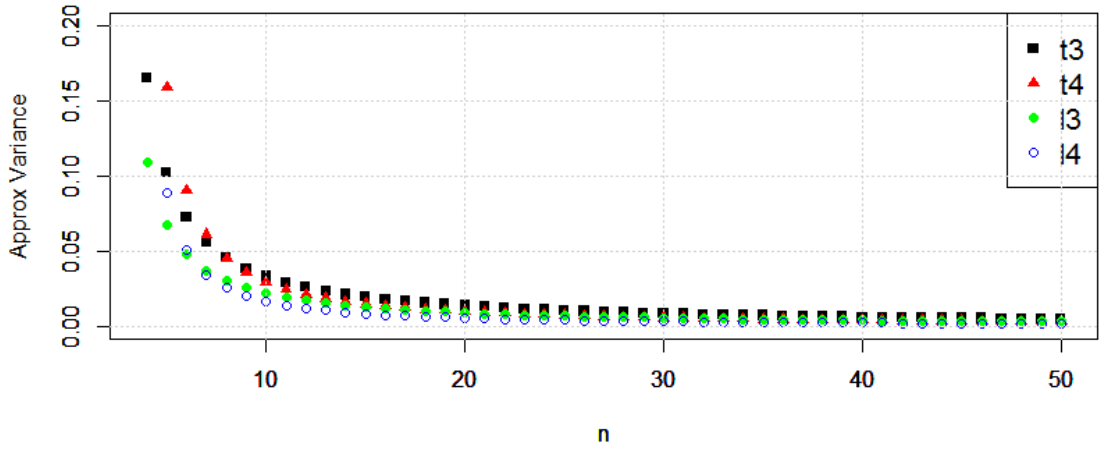

The approximate variance for L-skewness (t_3) and L-kurtosis (t_4) from a standard gumbel distribution is shown in Figure 22 and is compared with their un-scaled L-moments (l_3 and l_4). The L-moment ratios have slightly higher variance than the un-scaled L-moments and seems to level off considerably by a sample size of about 15. The L-moment ratios appear to have a closer bound to the un-scaled version than seen in the exponential, and the result more closely follows what was seen in results coming from the normal distribution. Once more the L-moments ratio achieves the variance of the unscaled L-moment at about a sample size of 25.

pareto distributions (a, v).

As a lesser known distribution, the probability distribution function of a random variable (X) that follows pareto(a, v) is given.

$$f(x) = \frac{va^v}{x^{v+1}}, \quad \text{where } a, v > 0 \text{ and } x \in [a, \infty). \tag{45}$$

The expressions for the expected value of an order statistic for a pareto(a, v) ran-

dom variable and the covariance between two order statistics, both from a pareto(a, v) distribution, were derived by Huang [20] and are the following:

$$E[(X_{j,n})^r] = a^r \frac{n!}{(n-j)!} \frac{\Gamma(n-j+1-r/v)}{\Gamma(n+1-r/v)}. \tag{46}$$

$$E[X_{i,n}^r X_{j,n}^s] = a^{(r+s)} \frac{n!}{(n-j)!} \frac{\Gamma(n-i+1-(r+s)/v)}{\Gamma(n+1-(r+s)/v)} \frac{\Gamma(n-j+1-\beta/v)}{\Gamma(n-i+1-\beta/v)}. \tag{47}$$

Since no standard form exists for the pareto distribution, exact solutions to the variance equations were derived by placing Equations 46 and 47 into Equations 24-27. The derivation of these equations can be found in Appendix B and result in the following:

$$\text{pareto } var(l_1) = \frac{a^2 v}{n(v-1)^2(v-2)}. \tag{48}$$

$$\begin{aligned}&\text{pareto } var(l_2) = \\ &\Big[\frac{8a^2v^2(n-2)[6v^3-16v^2+13v-4]}{(3v-2)(2v-2)(v-2)(2v-1)(v-1)} + \frac{4a^2v^2(3-n)}{(2v-2)(v-1)} + \frac{4a^2v^2(2-n)}{(2v-2)(v-2)} \\ &+ \frac{a^2v(n-1)}{(v-2)} + \frac{8a^2v^4(3-2n)}{(2v-1)^2(v-1)^2} + \frac{8a^2v^3(2n-3)}{(2v-1)(v-1)^2} + \frac{5a^2v^2(1-n)}{(v-1)^2}\Big]/(n(n-1)).\end{aligned} \tag{49}$$

pareto $var(l_3) =$

$$\Big[\frac{432a^2v^3(n^2-7n+12)[35v^3-51v^2+24v-4]}{(5v-2)(4v-2)(3v-2)(2v-2)(2v-1)(v-2)(3v-1)}+\frac{24a^2v^3(4n^2-27n+44)}{(3v-2)(2v-2)(v-2)}$$
$$-\frac{432a^2v^6(3n^2-15n+20)}{(3v-1)^2(2v-1)^2(v-1)^2}+\frac{432a^2v^4(-n^2+7n-12)}{(4v-2)(3v-2)(2v-2)(v-2)}$$
$$+\frac{432a^2v^2(-n+3)[6v^3-9v^2+7v-2]}{(4v-2)(3v-2)(2v-2)(3v-1)(v-1)}+\frac{12a^2v^2(-5n^2+15n+8)}{(2v-2)(v-1)}$$
$$+\frac{72a^2v^2(n^2-10)}{(3v-2)(2v-1)}+\frac{24a^2v^3(5n^2-6n-26)}{(3v-2)(2v-2)(v-1)}+\frac{144a^2v^3(n^2-11n+24)}{(4v-2)(3v-2)(2v-1)}$$
$$+\frac{432a^2v^5(3n^2-15n+20)}{(3v-1)(2v-1)^2(v-1)^2}+\frac{24a^2v^3(5n^2-24n+28)}{(2v-1)(v-1)^2}+\frac{216a^2v^4(-2n^2+9n-10)}{(2v-1)^2(v-1)^2}$$
$$+\frac{12a^2v^2(-n^2+6n-8)}{(2v-2)(v-2)}+\frac{72a^2v^4(-n^2+9n-20)}{(3v-1)(2v-1)(v-1)^2}+\frac{a^2v(-n^2+3n-2)[12v^2-24v-1]}{(v-1)^2(v-2)}\Big]$$

$$/n(n-1)(n-2).$$

(50)

pareto $var(l_4) =$

$$\Big[\frac{384000a^2v^4(n^3-15n^2+74n-120)[126v^5-204v^4+226v^3-146v^2+38v-4]}{(7v-2)(6v-2)(5v-2)(4v-2)(3v-2)(2v-2)(v-2)(4v-1)(3v-1)}$$
$$+\frac{a^2v(n^3-6n^2+11n-6)[-24v^2+48v+1]}{(v-1)^2(v-2)}+\frac{24a^2v^2(-n^3+12n^2-41n+42)}{(2v-2)(v-2)}$$
$$+\frac{24a^2v^3(17n^3-234n^2+997n-1344)}{(3v-2)(2v-2)(v-2)}+\frac{240a^2v^4(-19n^3+276n^2-1289n+1956)}{(4v-2)(3v-2)(2v-2)(v-2)}$$
$$+\frac{1440a^2v^5(23n^3-342n^2+1663n-2652)}{(5v-2)(4v-2)(3v-2)(2v-2)(v-2)}+\frac{144000a^2v^6(-n^3+15n^2-74n+120)}{(6v-2)(5v-2)(4v-2)(3v-2)(2v-2)(v-2)}$$
$$+\frac{288a^2v^4(-12n^3+103n^2-287n+258)}{(2v-1)^2(v-1)^2}+\frac{10800a^2v^6(-7n^3+72n^2-253n+300)}{(3v-1)^2(2v-1)^2(v-1)^2}$$
$$+\frac{24a^2v^2(-11n^3-87n^2+769n-827)}{(2v-2)(v-1)}+\frac{48a^2v^3(-49n^3+708n^2-2534n+1953)}{(3v-2)(2v-2)(v-1)}$$
$$+\frac{720a^2v^4(18n^3-177n^2+498n-307)}{(4v-2)(3v-2)(2v-2)(v-1)}+\frac{144a^2v^2(2n^3+51n^2-268n+91)}{(3v-2)(2v-1)}$$
$$+\frac{720a^2v^3(11n^3-114n^2+271n+36)}{(4v-2)(3v-2)(2v-1)}+\frac{1800a^2v^2(-3n^2+6n+25)}{(4v-2)(3v-1)}$$
$$+\frac{5760a^2v^5(-3n^3+27n^2-68n+32)}{(2v-2)(3v-2)(4v-2)(5v-2)(v-1)}+\frac{2160a^2v^4(-9n^3+66n^2-49n-284)}{(3v-2)(4v-2)(5v-2)(2v-1)}$$
$$+\frac{5400a^2v^3(-n^3+6n^2+11n-76)}{(4v-2)(5v-2)(3v-1)}+\frac{9600a^2v^2(n-4)}{(5v-2)(4v-1)}$$
$$+\frac{7200a^2v^4(-n^3+24n^2-155n+300)}{(4v-2)(5v-2)(6v-2)(3v-1)}+\frac{14400a^2v^3(n^2-9n+20)[48v^3-46v^2+22v-4]}{(5v-2)(6v-2)(4v-1)}$$
$$+\frac{24a^2v^3(19n^3-186n^2+569n-546)}{(2v-1)(v-1)^2}+\frac{600a^2v^4(-n^3+24n^2-143n+240)}{(3v-1)(2v-1)(v-1)^2}$$
$$+\frac{960a^2v^5(n^3-6n^2+71n-246)}{(v-1)^2(4v-1)(3v-1)(2v-1)}+\frac{720a^2v^5(35n^3-366n^2+1315n-1596)}{(3v-1)(2v-1)^2(v-1)^2}$$
$$+\frac{5760a^2v^6(-4n^3+45n^2-209n+360)}{(4v-1)(3v-1)(2v-1)^2(v-1)^2}+\frac{115200a^2v^7(2n^3-21n^2+79n-105)}{(4v-1)^2(3v-1)(2v-1)^2(v-1)^2}\Big]$$

$$/n(n-1)(n-2)(n-3).$$

(51)

For the purpose of sample size guidance and inference, a pareto with $\alpha = \frac{3}{\sqrt{2}}$ and $v = 4$ was chosen to be examined as it has a variance = 1. Subsequently, Equations

46 and 47 reduce to the following:

$$E[(Z_{j,n})^r] = (\frac{3}{\sqrt{2}})^r \frac{n!}{(n-j)!} \frac{\Gamma(n-j+1-r/4)}{\Gamma(n+1-r/4)}. \tag{52}$$

$$E[Z_{i,n}Z_{j,n}] = \frac{9}{2} \frac{n!}{(n-j)!} \frac{\Gamma(n-i+2/4)}{\Gamma(n+2/4)} \frac{\Gamma(n-j+3/4)}{\Gamma(n-i+3/4)}. \tag{53}$$

Once again i, j represents the i^{th} and j^{th} order statistics. These expressions were used with Equations 24-27 and Equation 35 to derive exact and approximate variances for the pareto($\frac{3}{\sqrt{2}}, 4$) distribution (Table 38).

Table 38. Exact and Approximate Variance for pareto($\frac{3}{\sqrt{2}}, 4$)

	pareto($\frac{3}{\sqrt{2}}, 4$)	Divisor
var(l_1)	1	$n^{(1)}$
var(l_2)	0.57551n - 0.47755	$n^{(2)}$
var(l_3)	$0.35800n^2 - 0.81413n + 0.33226$	$n^{(3)}$
var(l_4)	$0.25863n^3 - 1.14400n^2 + 1.46285n - 0.56405$	$n^{(4)}$
$\hat{var}(\tau_3)$	$0.55537n^2 - 0.69421n$	$n^{(3)}$
$\hat{var}(\tau_4)$	$0.75828n^3 - 2.38429^2 + 1.53701n - 0.49325$	$n^{(4)}$

*divisor $n^{(r)} = n(n-1)(n-r+1)$

The variance of the first L-moment equaling 1 confirms the choice of parameters resulting in a population that has a variance equal to 1. Based on the parameter choices for the pareto distribution, approximated variance estimates exist for L-skewness (t_3) and L-kurtosis (t_4).

Figure 23. Plot of Exact Variance Sample L-moments for the pareto($\frac{3}{\sqrt{2}}, 4$) distribution, Sample Size 4-50

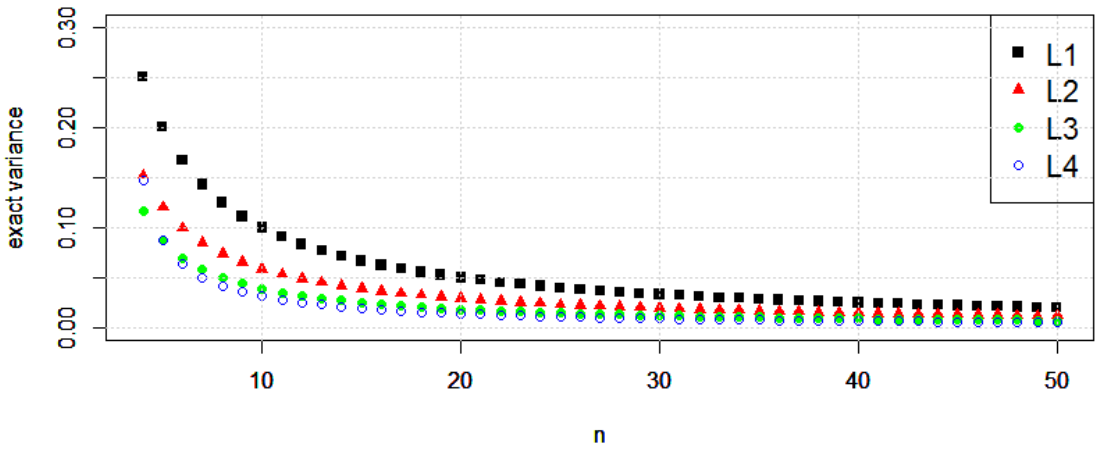

The exact variance for the first four L-moments from a pareto($\frac{3}{\sqrt{2}}, 4$) distribution are shown in Figure 23. Once again the variance of the first L-moment is constant around a sample size of 30, while the higher order L-moments become constant at about $n = 10$. The y-axis range is consistent with other distributions with a variance equal to 1.

Figure 24. Plots of Approximate Variance L-moment ratios for the pareto($\frac{3}{\sqrt{2}}, 4$) distribution, Sample Size 4-50

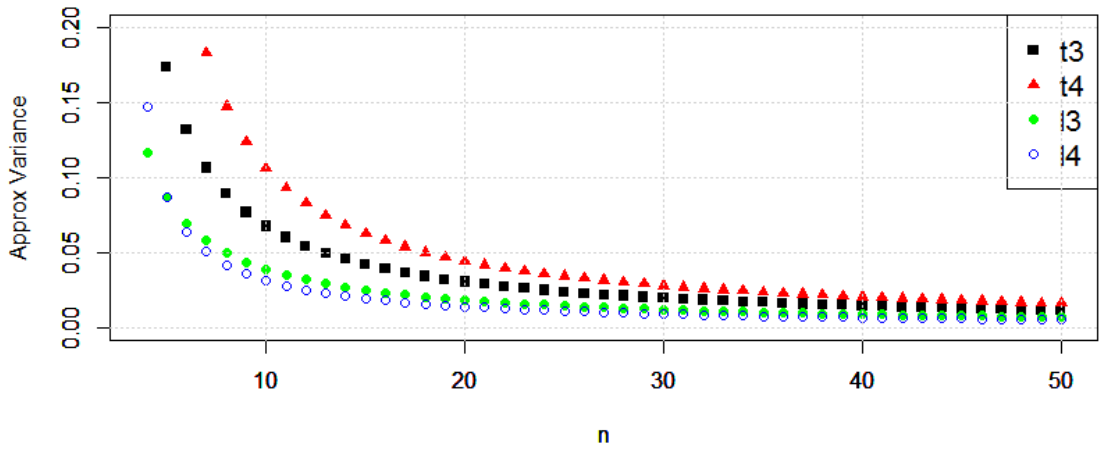

The approximate variance for L-skewness (t_3) and L-kurtosis (t_4) from a pareto($\frac{3}{\sqrt{2}}, 4$) distribution is shown in Figure 24 and is compared with their un-scaled L-moments (l_3 and l_4). The L-moment ratios have slightly higher variance, as seen across all previous distributions, than the un-scaled L-moments and appear to level off considerably by a sample size of about 25. Consistent with this larger sample size estimate is the fact that the spread from the un-scaled estimators appear larger from the pareto distribution when compared to the previous distributions examined. Further, the L-moment and its L-moment ratio counterpart achieve a similar variance estimate at about a sample size of 45.

Inference and Sample Size Guidance Summary.

The variance for l_1-l_4 decreases consistently as a function of sample size for all the distributions considered. For each distribution and L-moment, the exact variance minimizes quickly for the three highest L-moments (l_2, l_3, l_4), while the mean (l_1) retains a higher variance across all samples and distributions. All distributions and

L-moments appear to have a similar leveling point, and notably, the variance of l_1 of the pareto is more similar to the upper L-moments of the pareto than the variance of l_1 in any other distribution examined. General guidance for l_1 demonstrates reasonable minimization of the variance for the mean at about a sample size of 30, and the remaining L-moments (l_2,l_3,l_4) show that the variance is reasonably reduced at about a sample size of 10, possibly a little higher for the pareto distribution. The findings about the mean, (l_1) is consistent with what others have found concerning sample sizes requirements. Unlike conventional moments, L-moments ($l_2 - l_4$) seem to require smaller sample sizes for convergence of their variance.

The variance estimates for the L-moment ratios (t_3 and t_4) are slightly higher than the variance for their un-scaled L-moments (l_3 and l_4). This is expected since these are ratios of variance estimates, each requiring its own variance estimate. However, the variance estimates for the L-moment ratios decrease as a function of sample size and carry the same divisor as their un-scaled variances. With respect to L-moment ratios, a sample size of 15 still seems adequate for minimizing the MSE of τ_3 and τ_4 for all distributions except for the pareto. Within the pareto, a sample of size of 25 seems to minimize the variance. When needed, exact sample sizes, based on precision requirements and application needs, can be calculated from the equations found in each of the Tables 34-38 for each of the distributions examined.

In summary, the derived exact and approximate variance expressions for L-moments and L-moment ratios along with the figures that plot these variances as a function of sample size can be used as general guidelines to determine appropriate sample sizes when estimating L-moments and L-moment ratios. In general for all distributions a sample size of about 10 for L-moments (l_2, l_3, l_4) and about 15 for L-moment ratios (t_3 and τ_4) seems appropriate based on the research, with the exception of 25 for L-moment ratios for the pareto distribution. Noting that when possible, sam-

ple sizes should be chosen to reduce variance as much as possible. To compute a specific variance, the variance formulas given for each distribution may be used to calculate the exact or approximate variance and to determine a more precise sample size requirement.

V. L-moments and L-moment ratios Confidence Interval Estimation

5.1 Methods of Interval Estimations for L-Moments

The exact and approximate variance equations may be used to create confidence intervals for the estimation of L-moments and L-moment ratios. This chapter utilizes these equations and derives two methods for estimating confidence intervals for L-moments and L-moment ratios. Two additional methods are also derived for estimating joint confidence intervals and compared with previous research. Two methods currently exist for confidence interval estimation, although no practitioners appear to be utilizing confidence intervals within their L-moment research. Potentially, this is due to the computational intensity and high computational time required of these methods in addition to the lack of standard packages available within any software. These two methods are reviewed next and followed by four newly derived methods.

Exact Bootstrap For L-moment estimation.

The first existing method for creating a confidence interval is an exact bootstrapped method derived by Hutson and Wang [21]. In this method, the mean ($\hat{\mu}^k_{r:k}$, where $k = 1$), variance ($\hat{\sigma}^2_{r:n}$), and covariance ($\hat{\sigma}_{rs:n}$), of each order statistics are derived as follows:

$$\hat{\boldsymbol{\mu}} = \hat{\mu}^k_{r:n} = \sum_{j=1}^{n} W_{j(r)} X^k_{j:n}, \tag{54}$$

$$\hat{\sigma}^2_{r:n} = \sum_{j=1}^{n} W_{j(r)} (X_{j:n} - \hat{\mu}_{r:n})^2, \tag{55}$$

$$\hat{\sigma}_{rs:n} = \sum_{j-2}^{n} \sum_{i=1}^{j-1} W_{ij(rs)}(X_{i:n} - \hat{\mu}_{r:n})(X_{j:n} - \hat{\mu}_{s:n}) + \sum_{j=1}^{n} V_{j(rs)}(X_{j:n} - \hat{\mu}_{r:n})(X_{j:n} - \hat{\mu}_{s:n}), \tag{56}$$

where n equals the sample size and r, s equal the r^{th} and s^{th} order statistic, and k represents the k^{th} moment being estimated. $W_{j(r)}$ represents weights utilized in the mean and variance equations and are based on an incomplete beta distribution (Equation 57). $W_{ij(rs)}$ and $V_{j(rs)}$ are the weights utilized in the covariance equation and both are based on a joint uniform distribution (Equations 58 and 59).

$$W_{j(r)} = r\binom{n}{r} \int_{(j-1)/n}^{j/n} t^{r-1}(1-t)^{n-r} dt, \tag{57}$$

$$W_{ij(rs)} = \int_{(j-1)/n}^{j/n} \int_{(i-1)/n}^{i/n} f_{rs}(u_r, u_s) du_r du_s, \tag{58}$$

$$V_{j(rs)} = \int_{(j-1)/n}^{j/n} \int_{(j-1)/n}^{u_s} f_{rs}(u_r, u_s) du_r du_s, \tag{59}$$

$$\text{where } f_{rs}(u_r, u_s) =_n C_{rs} u_r^{r-1}(u_s - u_r)^{s-r-1}(1 - U_s)^{n-s}. \tag{60}$$

The pdf given in Equations 58-59, $f_{rs}(u_r, u_s)$, is the joint distribution of two uniform order statistics (Equation 60). In order to derive estimates for L-moments, the sample estimate of each L-moment (l_r) is applied to the estimates of mean ($\hat{\boldsymbol{\mu}}$), and covariance ($\hat{\boldsymbol{\Sigma}}$) for each order statistics and shown below:

$$\hat{\boldsymbol{\eta}} = \boldsymbol{l_r'}\hat{\boldsymbol{\mu}} \quad \text{and} \quad \hat{\boldsymbol{\Lambda}} = \boldsymbol{l_r'}\hat{\boldsymbol{\Sigma}}\boldsymbol{l_r}, \tag{61}$$

where $\hat{\boldsymbol{\Sigma}}$ is comprised of the variance and covariance (Equation 55 and 56) of each order statistic. Then, the exact bootstrapped estimate for each L-moment is $\hat{\boldsymbol{\eta}}$, and the covariance structure for any L-moment(s) is $\hat{\boldsymbol{\Lambda}}$. The exact bootstrap method is preferable to a traditional bootstrap by eliminating the error caused from re-sampling in a simulated setting. However, this method does not overcome the high computa-

tional cost of a bootstrap method. A Wald-based interval was then derived using these estimates for creating the confidence interval for the L-moment.

Numerical Inversion of Characteristic Generating Function for L-moment Estimation.

The second existing method for creating a confidence interval estimates the cumulative distribution function (CDF) of the L-moments through numerical inversion of the characteristic generating function, and then applies an α level confidence interval based on quantiles of the inverted CDF [38]. The characteristic generating function is given in Equations 62-64 and utilizes the exact bootstrap L-moment estimators for the mean ($\hat{\boldsymbol{\eta}}$) and covariance ($\hat{\boldsymbol{\Lambda}}$).

$$\phi_{l_r}(t) =$$
$$exp(it\hat{\boldsymbol{\eta}} - \frac{1}{2}t^2\hat{\boldsymbol{\Lambda}})(1 + \frac{1}{6}\sum_{j=1}^{n}(it)^3 l_{j(r)}^3 \hat{k}_{3j} + \frac{1}{24}\sum_{j=1}^{n}(it)^4 l_{j(r)}^4 \hat{k}_{4j} + \frac{1}{72}\sum_{h=1}^{n}\sum_{j=1}^{n}(it)^6 l_{j(r)}^3 l_{h(r)}^3 \hat{k}_{3h}\hat{k}_{3j}) \tag{62}$$

$$\text{where } \hat{k}_{3j} = 2(\hat{\mu}_{j:n})^3 - 3\hat{\mu}_{j:n}\hat{\mu}_{j:n}^2 + \hat{\mu}_{j:n}^3, \tag{63}$$

$$\text{where } \hat{k}_{4j} = -6(\hat{\mu}_{j:n})^4 + 12(\hat{\mu}_{j:n})^2\hat{\mu}_{j:n}^2 - 3(\hat{\mu}_{j:n}^2)^2 - 4\hat{\mu}_{j:n}\hat{\mu}_{j:n}^3 + \hat{\mu}_{j:n}^4. \tag{64}$$

The higher ordered cumulants ($\hat{k_3}$ and $\hat{k_4}$) are derived by Equation 63 and 64 which utilize Equation 54 for estimating the higher ordered moments. The characteristic generating function is used to generate a kernel estimate for the CDF using the Inversion Theorem (Equation 65).

$$\hat{F}_{l_r}(X) = \frac{1}{2} + \frac{1}{2\pi}\int_0^\infty \frac{exp(itx)\hat{\phi}_{l_r}(-t) - exp(-itx)\hat{\phi}_{l_r}(t)}{it}dt. \tag{65}$$

The kernel estimate for the CDF is then inverted, and quantiles are selected for building confidence intervals of the specific L-moment (Equation 66).

$$\hat{F}_{l_r}^{-1}(\alpha) \leq l_r \leq \hat{F}_{l_r}^{-1}(1-\alpha). \tag{66}$$

Both of these methods are extremely computationally intense and rely on bootstrapped estimates for the mean, variance, and covariance. Therefore, multiple confidence intervals using exact and approximate variances were derived and examined for improved L-moment and L-moment ratio estimations as well as computational efficiency. The first derived confidence interval estimate follows.

5.2 Wald Based Exact Variance Confidence Intervals for L-moments

The first confidence interval estimator derived for use with L-moments was based on a Wald interval using the exact variance for each known distribution. Thus, the (1-α)100% confidence interval for the rth L-moment was calculated as:

$$l_r \pm z_{\alpha/2}\sqrt{var(l_r)}. \tag{67}$$

Coverage for the confidence interval in Equation 67 was examined for $\alpha = 0.10$, 0.05, and 0.02 through a simulation which drew 10,000 samples from each of the following distributions: normal(0,1), uniform(0,1), exponential(1), gumbel(0,1), and pareto($\frac{3}{\sqrt{2}}, 4$). L-moments, $l_1 - l_4$, exact variance, and the confidence interval for each moment were estimated for each sample. For each distribution, L-moment, and sample size, the proportion of times out of 10,000 that the true parameter was contained within the interval was recorded and rounded to two decimal places. In addition, right and left coverage of the confidence interval was examined to further investigate skewness resulting from this estimated interval. For L-moments $l_2 - l_4$,

Tables 39-41 provide coverage results based on the simulation by sample size for each distribution and α level tested ($\alpha = 0.10$, 0.05, and 0.02 respectively). Figures 25-29 examine skewness (computed as right - left coverage) of the confidence interval for $\alpha = 0.10$, 0.05, and 0.02 respectively. Right - left coverage was calculated as the number of times right coverage was obtained minus the number of times left coverage was obtained divided by the number of replications, 10,000.

Table 39 provides the coverage results of the simulation for each distribution at $\alpha = 0.10$ level. In this table, since $\alpha = 0.10$, a coverage coefficient of 0.90 is desired with values above 0.90 denoting confidence intervals that were conservative and values below 0.90 denoting confidence intervals that did not meet coverage.

The normal distribution was consistently meeting coverage across all L-moments and sample sizes from $n = 4$ through $n = 100$ (Table 39). For the exponential distribution, confidence intervals tend to be slightly conservative in smaller sample sizes and higher L-moments. For the exponential distribution, sample size requirements for α level coverage increased as the L-moments increased, and the fourth L-moment, l_4, remains slightly conservative even at a sample size of 100. For the uniform distribution, by a sample size of 10, α level coverage was met and maintained through sample size 100 with slight deviations at $n < 7$. For the pareto distribution, coverage was high, creating conservative intervals across all sample sizes. As sample size increased, coverage approached 0.90, however coverage over 0.90 was still maintained especially for the higher L-moments. The gumbel distribution was similar to the exponential distribution in that the mean (l_1) produces consistent α level coverage across all samples. The other L-moments all display coverage over 0.90 with the higher L-moments being the most conservative. As sample size approached 100, the higher order L-moments ($l_2 - l_4$) converged to α, 0.90.

Table 40 provides the coverage results of the simulation for each distribution at

an $\alpha = 0.05$ level. Here, in this table, since $\alpha = 0.05$, a confidence coefficient of 0.95 represents exact coverage. At $\alpha = 0.05$, more L-moments across all distributions equal α level coverage. For the normal, uniform and exponential distributions, all L-moments appear to consistently achieve exact coverage. All coverage estimates are $\pm$ 0.01 from $\alpha = 0.05$, except for small sample sizes in l_2 and l_4 from the uniform distribution. The pareto distribution appeared to give conservative coverage results at 0.96 across all sample sizes and L-moments with a few exceptions for the mean. The gumbel distribution consistently gave exact coverage for the first three L-moments at a sample sizes about 40, while the fourth L-moment (l_4) and smaller sample sizes for higher ordered L-moments ($l_2 - l_4$) provided coverage values around 0.96.

Table 41 provides the coverage results of the simulation for each distribution and L-moment at an $\alpha = 0.02$ level. Here, in this table, since $\alpha = 0.02$, a confidence coefficient of 0.98 represents exact coverage. Coverage seems to be closer to exact as α level decreased. For the normal, uniform, exponential and gumbel distribution, all L-moments appear to consistently achieve exact coverage. There was slight under-coverage at smaller sample sizes for l_3 and l_4 of the exponential and l_4 from the gumbel. The pareto distribution appears to give exact coverage results for the first L-moment (l_1) and at slightly higher sample sizes for the second L-moment (l_2). The third and fourth L-moments (l_3 and l_4) stay under-coverage, yet near 0.98 across almost all sample sizes, yielding a confidence coefficient of about 0.97.

Table 39. Coverage of Wald-based Exact Variance Confidence Interval for L-moments at $\alpha = 0.10$

	normal				exponential				uniform				pareto				gumbel			
Size	l_1	l_2	l_3	l_4	l_1	l_2	l_3	l_4	l_1	l_2	l_3	l_4	l_1	l_2	l_3	l_4	l_1	l_2	l_3	l_4
4	0.90	0.91	0.90	0.91	0.92	0.93	0.92	0.91	0.90	0.91	0.89	0.92	0.94	0.95	0.95	0.93	0.91	0.94	0.93	0.93
7	0.90	0.91	0.90	0.91	0.91	0.93	0.93	0.93	0.90	0.90	0.90	0.89	0.94	0.94	0.95	0.95	0.90	0.92	0.93	0.92
10	0.90	0.90	0.90	0.91	0.91	0.92	0.92	0.92	0.90	0.90	0.90	0.90	0.94	0.94	0.95	0.95	0.91	0.92	0.92	0.92
13	0.89	0.90	0.90	0.90	0.91	0.92	0.92	0.92	0.90	0.90	0.90	0.90	0.94	0.94	0.94	0.95	0.90	0.92	0.92	0.92
16	0.90	0.90	0.90	0.90	0.91	0.92	0.93	0.93	0.90	0.90	0.90	0.90	0.93	0.94	0.94	0.95	0.90	0.92	0.92	0.92
19	0.90	0.90	0.90	0.91	0.91	0.91	0.92	0.92	0.89	0.90	0.90	0.90	0.93	0.94	0.95	0.95	0.90	0.91	0.92	0.92
22	0.90	0.90	0.90	0.90	0.91	0.91	0.92	0.92	0.90	0.91	0.90	0.90	0.93	0.94	0.94	0.94	0.90	0.91	0.91	0.92
25	0.90	0.90	0.90	0.90	0.91	0.91	0.91	0.92	0.90	0.90	0.90	0.90	0.93	0.94	0.95	0.95	0.90	0.91	0.92	0.92
28	0.90	0.90	0.90	0.90	0.90	0.90	0.91	0.91	0.90	0.90	0.90	0.90	0.93	0.94	0.95	0.95	0.90	0.91	0.91	0.91
31	0.90	0.90	0.90	0.90	0.90	0.90	0.91	0.92	0.90	0.90	0.90	0.90	0.92	0.93	0.94	0.94	0.90	0.90	0.91	0.91
34	0.90	0.90	0.90	0.90	0.90	0.90	0.91	0.92	0.90	0.90	0.90	0.90	0.92	0.94	0.94	0.94	0.90	0.91	0.92	0.92
37	0.90	0.90	0.90	0.90	0.91	0.91	0.91	0.92	0.90	0.90	0.91	0.90	0.92	0.94	0.94	0.94	0.91	0.91	0.91	0.91
40	0.90	0.90	0.90	0.90	0.90	0.91	0.91	0.92	0.90	0.90	0.90	0.90	0.92	0.93	0.94	0.94	0.90	0.91	0.91	0.92
43	0.90	0.90	0.90	0.90	0.90	0.90	0.91	0.92	0.90	0.90	0.90	0.90	0.92	0.93	0.94	0.94	0.90	0.90	0.91	0.91
46	0.90	0.90	0.90	0.90	0.90	0.90	0.90	0.91	0.90	0.90	0.90	0.90	0.91	0.92	0.94	0.94	0.90	0.90	0.91	0.91
49	0.90	0.90	0.90	0.90	0.90	0.90	0.91	0.91	0.90	0.90	0.90	0.90	0.92	0.93	0.94	0.94	0.90	0.90	0.91	0.91
52	0.90	0.90	0.90	0.91	0.90	0.91	0.91	0.92	0.90	0.90	0.90	0.90	0.92	0.93	0.94	0.94	0.90	0.90	0.91	0.91
55	0.90	0.90	0.90	0.90	0.90	0.90	0.91	0.91	0.89	0.90	0.90	0.90	0.92	0.93	0.94	0.94	0.90	0.91	0.91	0.91
58	0.90	0.90	0.90	0.90	0.90	0.90	0.90	0.90	0.90	0.90	0.90	0.90	0.92	0.93	0.95	0.95	0.90	0.91	0.91	0.91
61	0.90	0.90	0.90	0.90	0.90	0.90	0.90	0.91	0.90	0.90	0.90	0.90	0.92	0.93	0.94	0.94	0.90	0.90	0.91	0.91
64	0.90	0.90	0.90	0.90	0.90	0.90	0.91	0.92	0.90	0.90	0.90	0.91	0.91	0.93	0.93	0.94	0.91	0.91	0.91	0.91
67	0.90	0.90	0.90	0.89	0.90	0.90	0.90	0.91	0.91	0.90	0.90	0.90	0.92	0.93	0.94	0.94	0.90	0.91	0.91	0.92
70	0.90	0.90	0.90	0.90	0.90	0.90	0.90	0.91	0.90	0.90	0.89	0.90	0.91	0.92	0.93	0.94	0.90	0.90	0.91	0.91
73	0.90	0.90	0.90	0.90	0.90	0.90	0.90	0.91	0.90	0.90	0.90	0.90	0.92	0.93	0.94	0.94	0.90	0.90	0.90	0.91
76	0.90	0.89	0.90	0.90	0.90	0.90	0.91	0.91	0.90	0.90	0.90	0.90	0.91	0.92	0.94	0.94	0.90	0.91	0.91	0.91
79	0.90	0.91	0.90	0.90	0.90	0.91	0.90	0.91	0.90	0.90	0.90	0.90	0.91	0.92	0.94	0.94	0.90	0.90	0.90	0.91
82	0.90	0.90	0.90	0.90	0.90	0.90	0.90	0.91	0.90	0.90	0.90	0.90	0.92	0.93	0.94	0.95	0.90	0.90	0.91	0.91
85	0.90	0.90	0.90	0.90	0.90	0.90	0.90	0.91	0.90	0.90	0.90	0.90	0.91	0.92	0.94	0.94	0.90	0.90	0.91	0.91
88	0.90	0.90	0.91	0.90	0.90	0.90	0.91	0.91	0.90	0.90	0.91	0.90	0.92	0.93	0.94	0.94	0.90	0.89	0.90	0.90
91	0.90	0.89	0.90	0.90	0.90	0.91	0.91	0.91	0.90	0.89	0.90	0.90	0.92	0.93	0.94	0.94	0.90	0.90	0.90	0.90
94	0.90	0.90	0.90	0.90	0.90	0.90	0.90	0.91	0.89	0.90	0.90	0.90	0.91	0.92	0.93	0.94	0.90	0.90	0.90	0.90
97	0.89	0.90	0.90	0.90	0.90	0.90	0.90	0.91	0.91	0.90	0.91	0.90	0.92	0.92	0.94	0.94	0.90	0.90	0.90	0.90
100	0.90	0.90	0.90	0.90	0.90	0.90	0.90	0.91	0.90	0.90	0.90	0.90	0.91	0.92	0.93	0.94	0.90	0.90	0.91	0.91

Table 40. Coverage of Wald-based Exact Variance Confidence Interval for L-moments at $\alpha = 0.05$

	normal				exponential				uniform				pareto				gumbel			
Size	l_1	l_2	l_3	l_4	l_1	l_2	l_3	l_4	l_1	l_2	l_3	l_4	l_1	l_2	l_3	l_4	l_1	l_2	l_3	l_4
4	0.95	0.96	0.95	0.95	0.95	0.95	0.95	0.94	0.95	0.96	0.94	0.97	0.96	0.96	0.96	0.96	0.95	0.96	0.96	0.96
7	0.95	0.96	0.95	0.95	0.95	0.96	0.96	0.95	0.95	0.96	0.95	0.94	0.96	0.96	0.96	0.96	0.95	0.96	0.96	0.96
10	0.95	0.95	0.95	0.95	0.95	0.95	0.95	0.95	0.95	0.95	0.95	0.95	0.96	0.96	0.96	0.96	0.95	0.96	0.96	0.95
13	0.94	0.95	0.95	0.95	0.96	0.96	0.96	0.95	0.95	0.95	0.95	0.95	0.96	0.96	0.96	0.96	0.95	0.96	0.96	0.95
16	0.95	0.95	0.95	0.95	0.96	0.96	0.96	0.96	0.95	0.96	0.95	0.95	0.96	0.96	0.96	0.96	0.95	0.96	0.96	0.96
19	0.95	0.95	0.95	0.95	0.95	0.95	0.96	0.95	0.95	0.95	0.95	0.95	0.96	0.96	0.96	0.96	0.95	0.95	0.96	0.96
22	0.95	0.95	0.95	0.94	0.95	0.95	0.95	0.95	0.95	0.95	0.95	0.95	0.96	0.96	0.95	0.96	0.95	0.96	0.95	0.95
25	0.95	0.95	0.95	0.95	0.96	0.96	0.96	0.96	0.95	0.95	0.95	0.95	0.96	0.96	0.96	0.96	0.95	0.95	0.96	0.96
28	0.95	0.95	0.95	0.95	0.95	0.95	0.95	0.95	0.95	0.95	0.95	0.95	0.97	0.96	0.96	0.96	0.95	0.95	0.96	0.96
31	0.95	0.95	0.95	0.95	0.95	0.95	0.95	0.95	0.95	0.95	0.95	0.95	0.95	0.96	0.96	0.96	0.95	0.95	0.95	0.95
34	0.95	0.95	0.95	0.95	0.95	0.95	0.95	0.96	0.95	0.95	0.95	0.95	0.96	0.96	0.96	0.96	0.95	0.96	0.96	0.96
37	0.95	0.95	0.95	0.95	0.95	0.95	0.96	0.96	0.95	0.95	0.95	0.95	0.96	0.96	0.96	0.96	0.95	0.96	0.96	0.96
40	0.95	0.95	0.95	0.95	0.95	0.95	0.96	0.95	0.95	0.95	0.95	0.95	0.96	0.96	0.96	0.96	0.95	0.95	0.96	0.96
43	0.95	0.95	0.95	0.95	0.95	0.95	0.96	0.96	0.95	0.96	0.95	0.95	0.95	0.96	0.96	0.96	0.95	0.95	0.95	0.95
46	0.95	0.95	0.95	0.95	0.95	0.95	0.95	0.95	0.95	0.95	0.95	0.95	0.95	0.95	0.96	0.96	0.94	0.95	0.95	0.95
49	0.95	0.95	0.95	0.95	0.95	0.95	0.95	0.95	0.95	0.95	0.95	0.95	0.96	0.96	0.96	0.96	0.95	0.95	0.95	0.95
52	0.95	0.96	0.95	0.95	0.95	0.95	0.96	0.96	0.95	0.95	0.95	0.95	0.95	0.96	0.96	0.96	0.95	0.95	0.95	0.95
55	0.95	0.95	0.95	0.95	0.95	0.95	0.95	0.95	0.95	0.95	0.95	0.95	0.96	0.96	0.96	0.96	0.95	0.96	0.95	0.95
58	0.95	0.95	0.95	0.95	0.95	0.95	0.95	0.95	0.95	0.95	0.95	0.95	0.96	0.96	0.96	0.97	0.95	0.95	0.96	0.95
61	0.95	0.95	0.95	0.95	0.95	0.95	0.95	0.95	0.95	0.95	0.95	0.95	0.96	0.96	0.96	0.96	0.95	0.95	0.95	0.95
64	0.95	0.95	0.95	0.95	0.95	0.95	0.95	0.96	0.95	0.95	0.95	0.95	0.95	0.96	0.96	0.96	0.95	0.95	0.95	0.95
67	0.95	0.95	0.95	0.95	0.95	0.95	0.95	0.95	0.96	0.95	0.95	0.95	0.96	0.96	0.96	0.96	0.95	0.95	0.96	0.96
70	0.95	0.95	0.95	0.95	0.95	0.95	0.95	0.95	0.95	0.95	0.95	0.95	0.96	0.96	0.96	0.96	0.95	0.95	0.95	0.95
73	0.95	0.95	0.95	0.95	0.95	0.95	0.95	0.95	0.95	0.95	0.95	0.95	0.96	0.96	0.96	0.96	0.95	0.95	0.95	0.96
76	0.95	0.95	0.95	0.95	0.95	0.95	0.96	0.95	0.95	0.95	0.95	0.95	0.95	0.96	0.96	0.96	0.95	0.95	0.95	0.95
79	0.95	0.95	0.95	0.95	0.95	0.95	0.95	0.95	0.95	0.95	0.95	0.95	0.95	0.96	0.96	0.96	0.95	0.95	0.95	0.95
82	0.95	0.95	0.95	0.95	0.95	0.95	0.95	0.95	0.95	0.95	0.95	0.95	0.96	0.96	0.96	0.96	0.95	0.95	0.96	0.96
85	0.95	0.95	0.95	0.95	0.95	0.95	0.95	0.95	0.95	0.95	0.95	0.95	0.95	0.96	0.96	0.96	0.95	0.95	0.95	0.95
88	0.95	0.95	0.95	0.95	0.95	0.95	0.95	0.96	0.95	0.95	0.96	0.95	0.96	0.96	0.96	0.96	0.95	0.95	0.95	0.95
91	0.95	0.95	0.95	0.95	0.95	0.95	0.95	0.95	0.95	0.95	0.95	0.95	0.96	0.96	0.96	0.96	0.95	0.95	0.95	0.95
94	0.95	0.95	0.95	0.95	0.95	0.95	0.95	0.95	0.95	0.95	0.95	0.95	0.95	0.96	0.96	0.96	0.95	0.95	0.95	0.95
97	0.94	0.95	0.95	0.95	0.95	0.95	0.95	0.95	0.96	0.95	0.95	0.95	0.96	0.96	0.96	0.96	0.95	0.95	0.95	0.95
100	0.95	0.95	0.95	0.95	0.95	0.95	0.95	0.95	0.95	0.95	0.95	0.95	0.95	0.96	0.96	0.96	0.95	0.95	0.95	0.95

Table 41. Coverage of Wald-based Exact Variance Confidence Interval for L-moments at = 0.02

	normal				exponential				uniform				pareto				gumbel			
Size	l_1	l_2	l_3	l_4	l_1	l_2	l_3	l_4	l_1	l_2	l_3	l_4	l_1	l_2	l_3	l_4	l_1	l_2	l_3	l_4
4	0.98	0.98	0.97	0.98	0.97	0.97	0.97	0.97	0.98	0.99	0.98	0.99	0.97	0.97	0.97	0.97	0.98	0.98	0.98	0.98
7	0.98	0.98	0.98	0.98	0.98	0.97	0.97	0.97	0.98	0.99	0.98	0.98	0.97	0.97	0.97	0.97	0.98	0.98	0.98	0.97
10	0.98	0.98	0.98	0.98	0.98	0.97	0.97	0.97	0.98	0.98	0.98	0.98	0.97	0.97	0.97	0.97	0.98	0.98	0.98	0.97
13	0.98	0.98	0.98	0.98	0.98	0.98	0.97	0.97	0.98	0.98	0.98	0.98	0.97	0.97	0.97	0.97	0.98	0.98	0.98	0.97
16	0.98	0.98	0.98	0.98	0.98	0.98	0.98	0.97	0.98	0.98	0.98	0.98	0.97	0.97	0.97	0.97	0.98	0.98	0.98	0.98
19	0.98	0.98	0.98	0.98	0.98	0.98	0.97	0.97	0.98	0.98	0.98	0.98	0.97	0.97	0.97	0.97	0.98	0.98	0.98	0.98
22	0.98	0.98	0.98	0.98	0.98	0.98	0.98	0.97	0.98	0.98	0.98	0.98	0.98	0.97	0.97	0.97	0.98	0.98	0.98	0.97
25	0.98	0.98	0.98	0.98	0.98	0.98	0.98	0.98	0.98	0.98	0.98	0.98	0.98	0.97	0.97	0.97	0.98	0.98	0.98	0.98
28	0.98	0.98	0.98	0.98	0.98	0.98	0.97	0.97	0.98	0.98	0.98	0.98	0.98	0.98	0.98	0.98	0.98	0.98	0.98	0.98
31	0.98	0.98	0.98	0.98	0.98	0.98	0.98	0.97	0.98	0.98	0.98	0.98	0.97	0.97	0.97	0.97	0.98	0.98	0.98	0.98
34	0.98	0.98	0.98	0.98	0.98	0.98	0.98	0.97	0.98	0.98	0.98	0.98	0.98	0.98	0.97	0.97	0.98	0.98	0.98	0.98
37	0.98	0.98	0.98	0.98	0.98	0.98	0.98	0.98	0.98	0.98	0.98	0.98	0.98	0.97	0.97	0.97	0.98	0.98	0.98	0.98
40	0.98	0.98	0.98	0.98	0.98	0.98	0.98	0.98	0.98	0.98	0.98	0.98	0.98	0.97	0.97	0.97	0.98	0.98	0.98	0.98
43	0.98	0.98	0.98	0.98	0.98	0.98	0.98	0.98	0.98	0.98	0.98	0.98	0.98	0.97	0.97	0.97	0.98	0.98	0.98	0.98
46	0.98	0.98	0.98	0.98	0.98	0.98	0.98	0.97	0.98	0.98	0.98	0.98	0.97	0.97	0.97	0.97	0.98	0.98	0.98	0.98
49	0.98	0.98	0.98	0.98	0.98	0.98	0.98	0.98	0.98	0.98	0.98	0.98	0.98	0.97	0.97	0.97	0.98	0.98	0.98	0.98
52	0.98	0.98	0.98	0.98	0.98	0.98	0.98	0.98	0.98	0.98	0.98	0.98	0.97	0.97	0.97	0.97	0.98	0.98	0.98	0.98
55	0.98	0.98	0.98	0.98	0.98	0.98	0.98	0.98	0.98	0.98	0.98	0.98	0.98	0.98	0.97	0.97	0.98	0.98	0.98	0.98
58	0.98	0.98	0.98	0.98	0.98	0.98	0.98	0.97	0.98	0.98	0.98	0.98	0.98	0.98	0.98	0.98	0.98	0.98	0.98	0.98
61	0.98	0.98	0.98	0.98	0.98	0.98	0.98	0.98	0.98	0.98	0.98	0.98	0.98	0.98	0.97	0.97	0.98	0.98	0.98	0.98
64	0.98	0.98	0.98	0.98	0.98	0.98	0.98	0.98	0.98	0.98	0.98	0.98	0.98	0.97	0.97	0.97	0.98	0.98	0.98	0.98
67	0.98	0.98	0.98	0.98	0.98	0.98	0.98	0.98	0.98	0.98	0.98	0.98	0.98	0.98	0.97	0.97	0.98	0.98	0.98	0.98
70	0.98	0.98	0.98	0.98	0.98	0.98	0.98	0.98	0.98	0.98	0.98	0.98	0.98	0.97	0.97	0.97	0.98	0.98	0.98	0.98
73	0.98	0.98	0.98	0.98	0.98	0.98	0.98	0.98	0.98	0.98	0.98	0.98	0.98	0.98	0.97	0.97	0.98	0.98	0.98	0.98
76	0.98	0.98	0.98	0.98	0.98	0.98	0.98	0.98	0.98	0.98	0.98	0.98	0.98	0.98	0.97	0.97	0.98	0.98	0.98	0.98
79	0.98	0.98	0.98	0.98	0.98	0.98	0.98	0.98	0.98	0.98	0.98	0.98	0.98	0.97	0.97	0.97	0.98	0.98	0.98	0.98
82	0.98	0.98	0.98	0.98	0.98	0.98	0.98	0.98	0.98	0.98	0.98	0.98	0.98	0.98	0.98	0.97	0.98	0.98	0.98	0.98
85	0.98	0.98	0.98	0.98	0.98	0.98	0.98	0.98	0.98	0.98	0.98	0.98	0.98	0.98	0.97	0.97	0.98	0.98	0.98	0.98
88	0.98	0.98	0.98	0.98	0.98	0.98	0.98	0.98	0.98	0.98	0.98	0.98	0.98	0.98	0.98	0.98	0.98	0.98	0.98	0.98
91	0.98	0.98	0.98	0.98	0.98	0.98	0.98	0.98	0.98	0.98	0.98	0.98	0.98	0.98	0.98	0.97	0.98	0.98	0.98	0.98
94	0.98	0.98	0.98	0.98	0.98	0.98	0.98	0.98	0.98	0.98	0.98	0.98	0.98	0.98	0.97	0.97	0.98	0.98	0.98	0.98
97	0.98	0.98	0.98	0.98	0.98	0.98	0.98	0.98	0.98	0.98	0.98	0.98	0.98	0.98	0.97	0.97	0.98	0.98	0.98	0.98
100	0.98	0.98	0.98	0.98	0.98	0.98	0.98	0.98	0.98	0.98	0.98	0.98	0.98	0.98	0.97	0.97	0.98	0.98	0.98	0.98

Figure 25 contains 3 plots of skewness for the normal distribution separated by the assumed α level. The y-axis details the excess or under coverage amounts that exist between the two tails of the confidence interval. The x-axis is the sample size range, size 4-100. Any result above 0, indicates right skewness, while results below 0, indicate left skewness. For the normal distribution the α level has very little effect on the resulting skewness of the confidence interval. The first (l_1) and third (l_3) L-moments have equal coverage in the two tails, which is seen by the green and black dots oscillating about zero for all sample sizes. The second (l_2) and fourth (l_4) L-moments both have more coverage (conservative) in the right tail, this skewness decreased as sample size increased.

Figure 26 contains three plots of skewness for the uniform distribution by α level. The first (l_1) and third (l_3) L-moments exhibit no skewness having equal coverage in the two tails of the confidence interval, which is seen by the green and black dots oscillating about zero for all sample sizes. The second (l_2) and fourth (l_4) L-moments both have more coverage (are conservative) in the left tail (left skewed), yet the skewness decreased as sample size increased. The magnitude of the skewness in the uniform distribution especially at lower sample sizes was slightly larger than the magnitude of the skewness recorded for the normal distribution.

Figure 27 contains three plots of skewness for the exponential distribution by α level. All L-moments have more coverage in the right tail (right skewed), and although skewness decreased as sample size increased, these intervals maintained a right skewness, being conservative in the upper confidence interval for all L-moments at each α level.

Figure 28 contains three plots of skewness for the gumbel distribution by α level. Similar to the exponential distribution, all L-moments have more coverage in the right tail (right skewed), and although skewness decreased as sample size increased

the intervals remained right skewed, being conservative in the upper bound of the confidence interval for all L-moments at each α level.

Figure 25. Skewness of Wald Based Exact Variance Confidence Intervals for the normal distribution

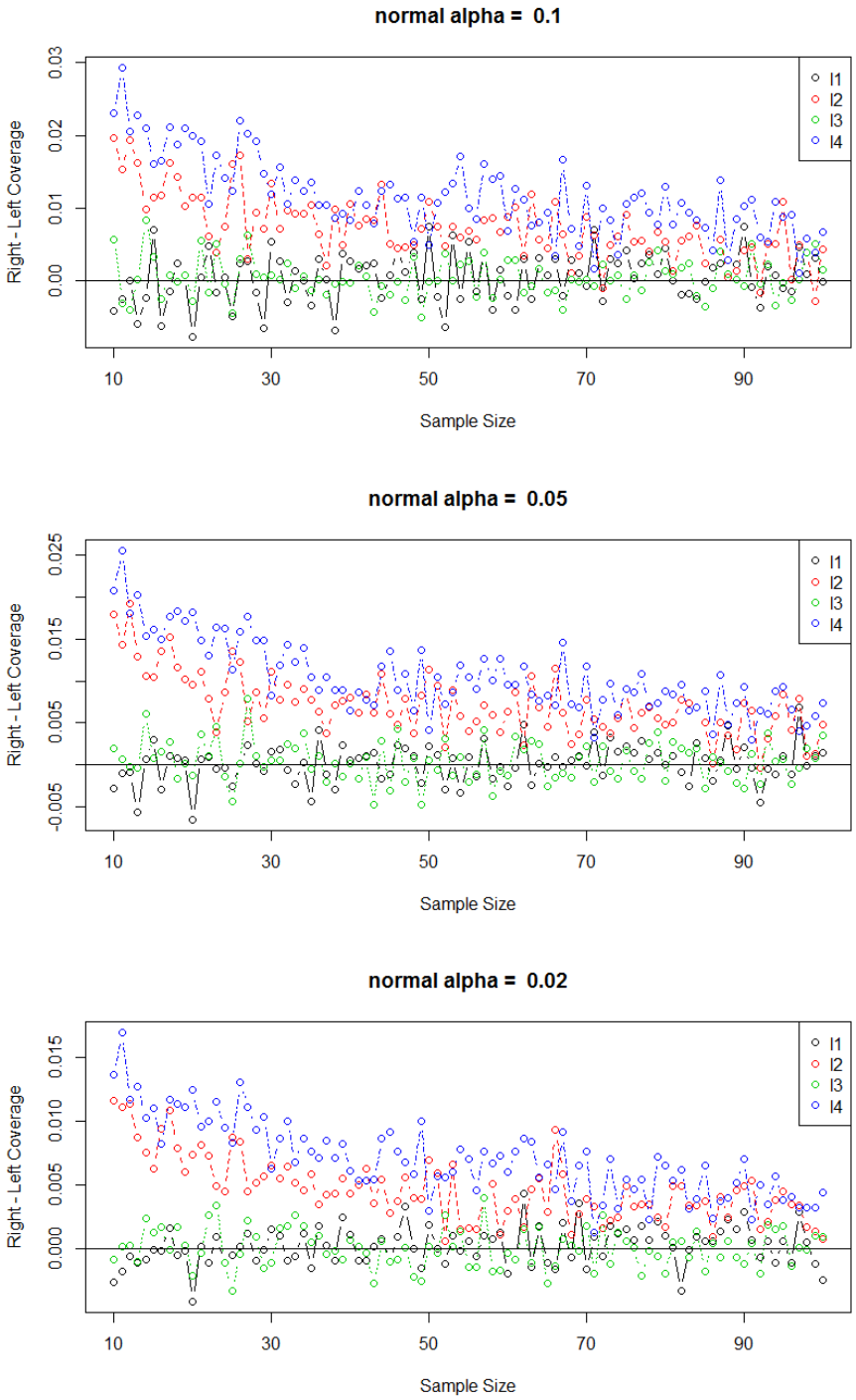

Figure 26. Skewness of Wald Based Exact Variance Confidence Intervals for the uniform distribution

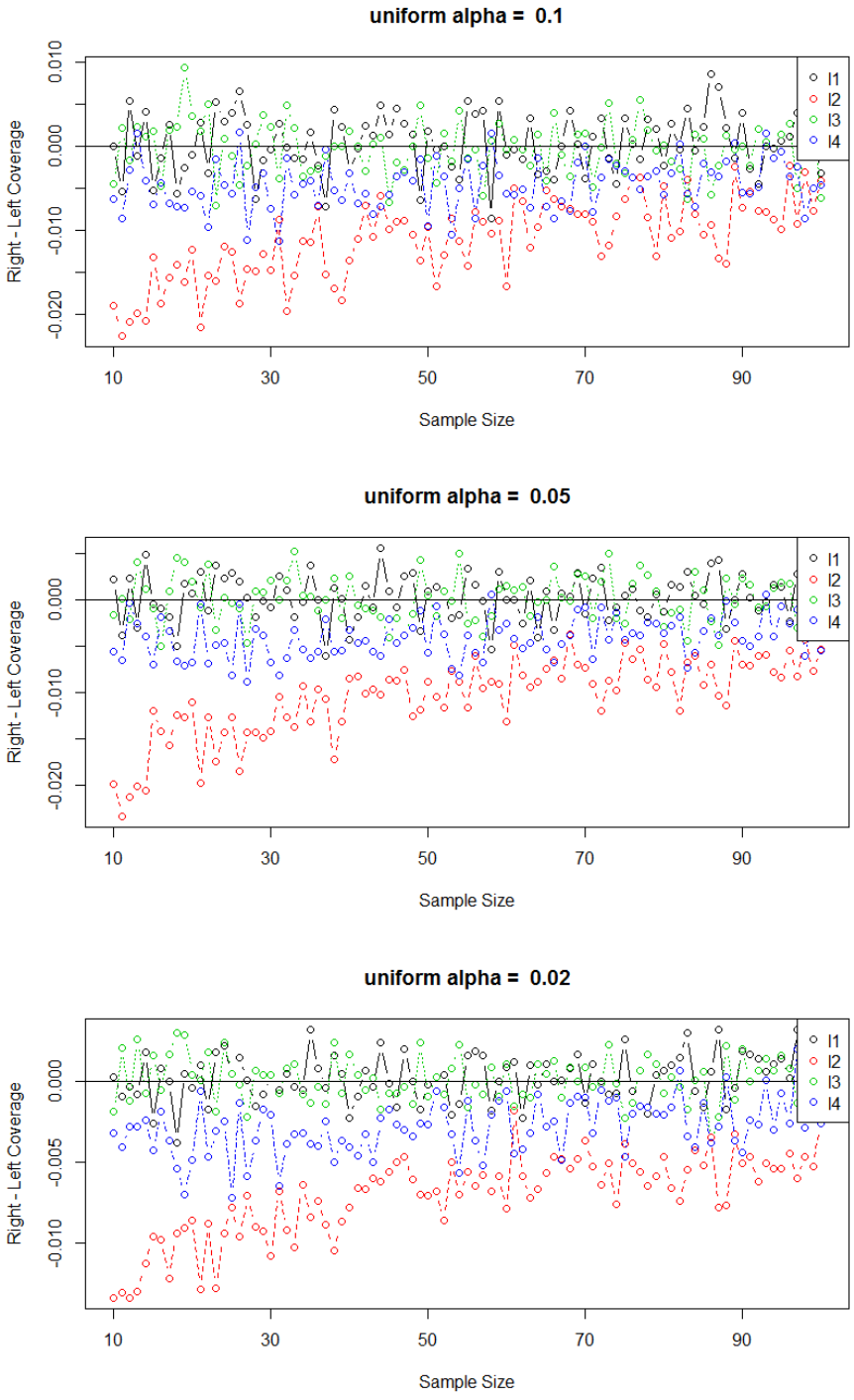

Figure 27. Skewness of Wald Based Exact Variance Confidence Intervals for the exponential distribution

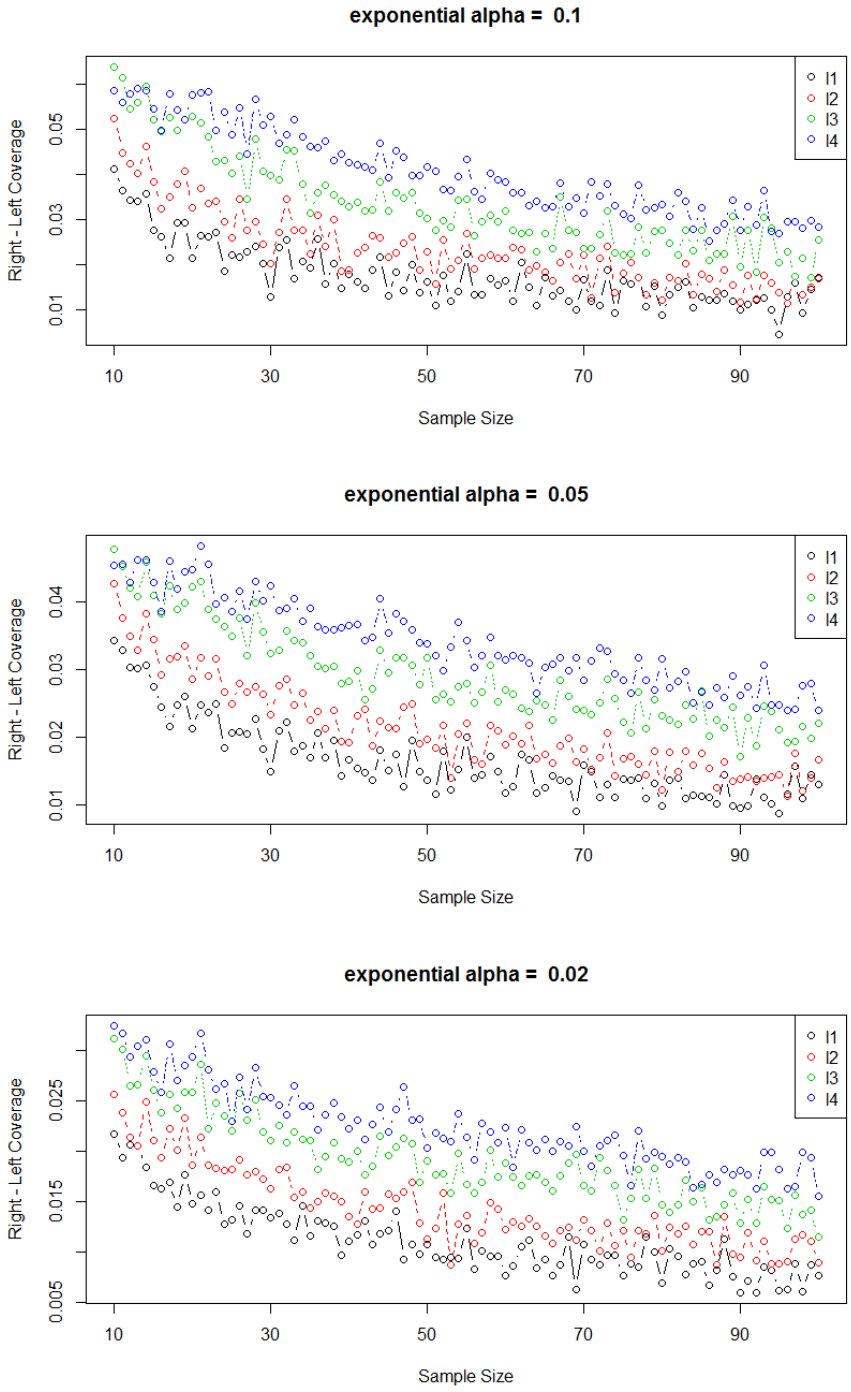

Figure 28. Skewness of Wald Based Exact Variance Confidence Intervals for the gumbel distribution

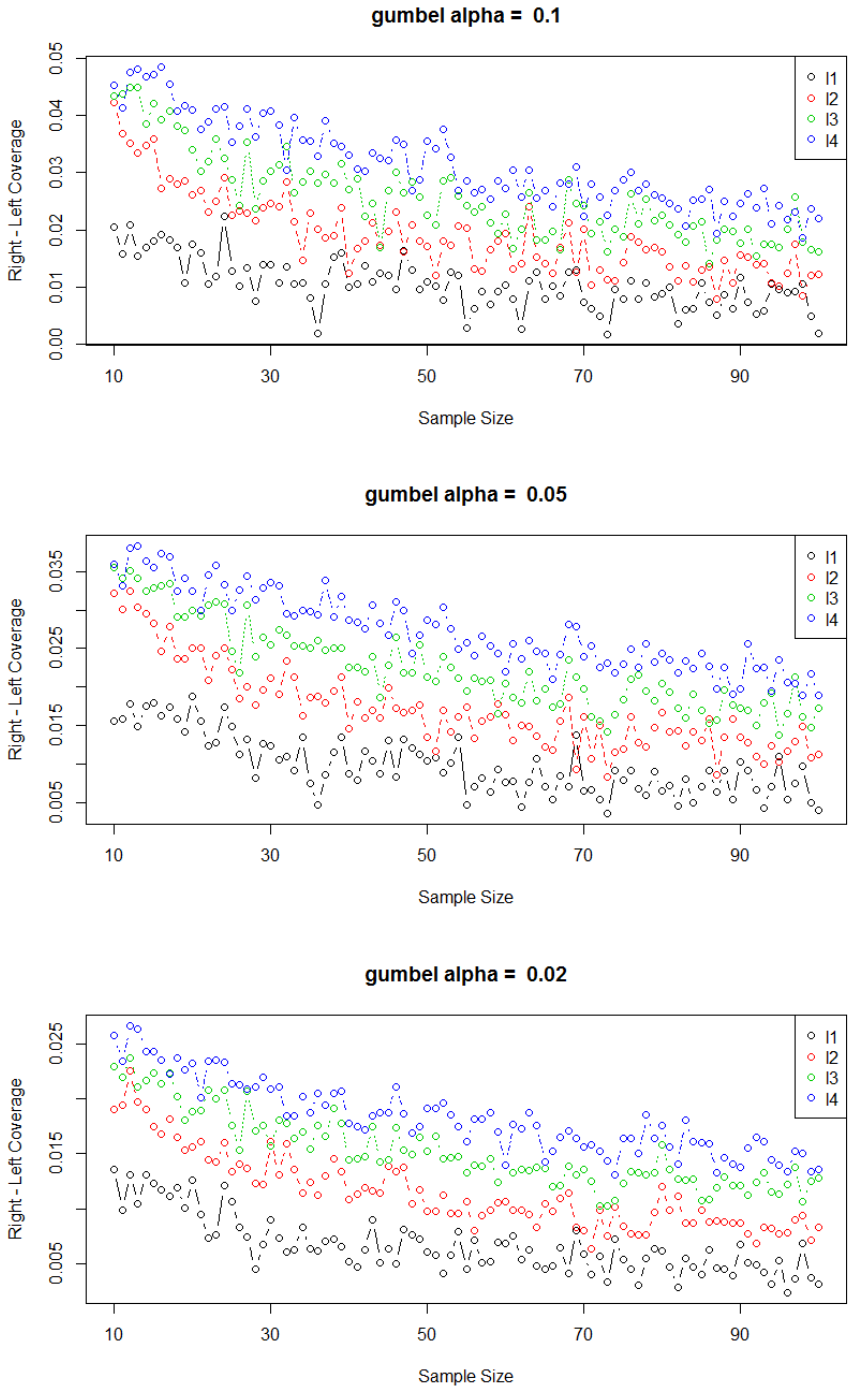

Figure 29 contains three plots of skewness for the pareto distribution by α level. All L-moments have more coverage in the right tail (right skewed). In contrast to all

other distributions examined, as sample size increased skewness only decreased for the first two L-moments (l_1 and l_2), while the last two L-moments (l_3 and l_4) either remain constant or slightly increased.

Figure 29. Skewness of Wald Based Exact Variance Confidence Intervals for the pareto distribution

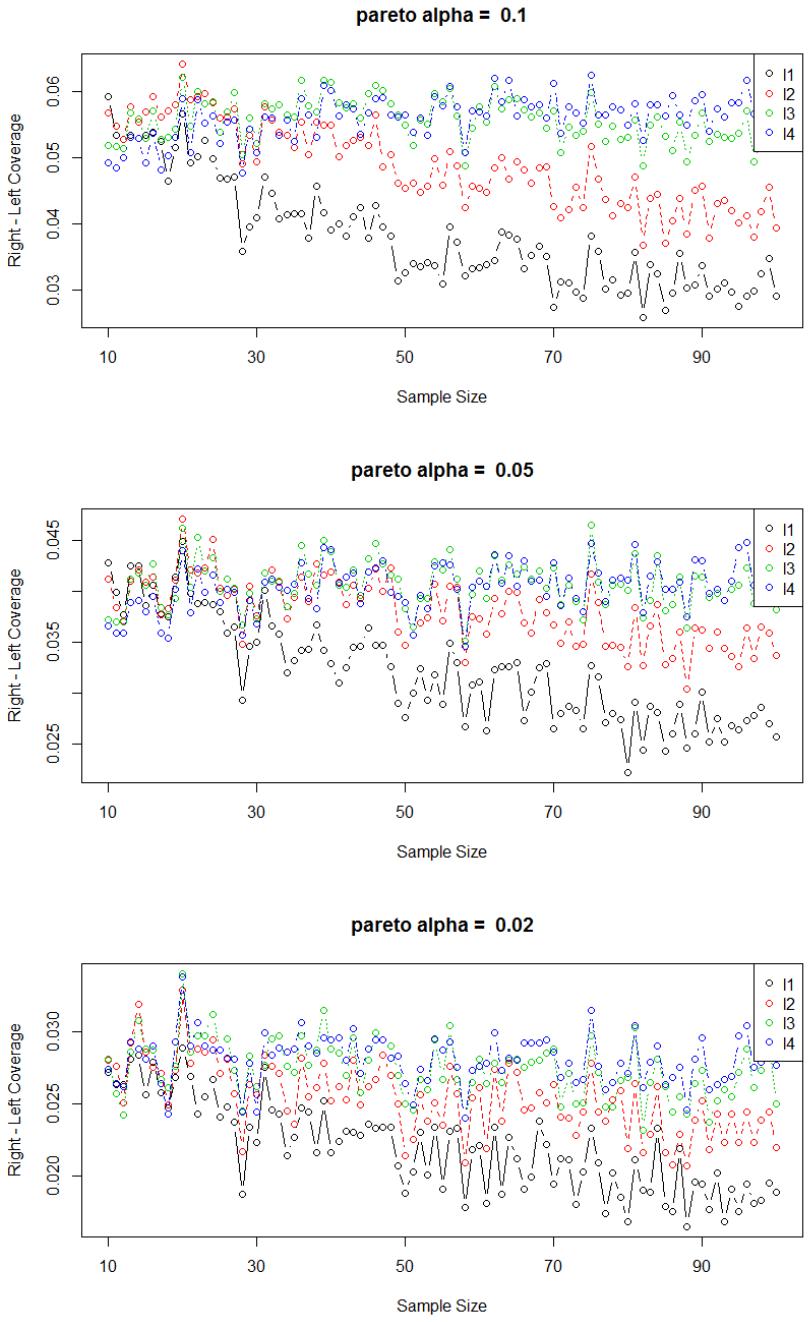

Summary of Wald Based Exact Variance Interval Estimates of L-moments.

For all but the pareto distribution at α level 0.02, coverage was generally achieved or slightly conservative for each L-moment across all sample sizes above 30. This is possibly due to the underlying distributions of the L-moments and the application of a normal quantile for confidence interval estimation via Equation 67. The Wald assumes normality for each L-moment, which may not be accurate even for large sample sizes. The results for the normal and uniform distributions are very similar across L-moments with the normal being right skewed, maintaining coverage on the right not the left, and the uniform having left skewness, maintaining coverage on the left, not the right. For both of these distributions, right-left coverage for the mean and l_3 remains symmetric across all sample sizes while l_2 and l_4 decreased in skewness as the sample increased, but does not achieve symmetry by a sample size of 100. The gumbel and exponential distributions show decreased skewness as sample size increased across all α levels and L-moments, yet symmetry was not obtained by a sample size of 100. The skewness converges in the higher sample sizes, slightly above zero, and maintains conservative right coverage, whereas left coverage was not maintained. For each of these four distributions, the general trends hold across all α levels. For the pareto distribution, right-left coverage for the mean (l_1) and second L-moment (l_2) decreased with sample size, yet never approached symmetry across all α levels. Right-left coverage for upper L-moments of the pareto, l_3 and l_4 appear to increase slightly in skewness as sample size increased at $\alpha = 0.05$ and 0.10, while remaining stable in skewness for $\alpha = 0.02$. While coverage was maintained in general for the two-sided interval, many of the estimator's distributions are not symmetric with respect to coverage when using the quick Wald confidence interval (Equation 67). This means that for the right skewed intervals, coverage was conservatively maintained in the upper bound, but not the lower bound, despite overall coverage

(α) being maintained.

5.3 Wald Based Approximate Variance Confidence Intervals for L-moment Ratios

The second confidence interval estimator derived, for use with L-moment ratios, was based on a Wald interval using the approximate variance for each known distribution. Thus, the (1-α)100% confidence interval for the rth L-moment ratio was calculated as:

$$t_r \pm z_{\alpha/2}\sqrt{\widehat{var(t_r)}}. \tag{68}$$

The exact simulation settings used for L-moments were replicated for the L-moment ratios using Equation 68. Tables 42-44 show the coverage results for t_3 and t_4 for $\alpha = 0.10$, 0.05, and 0.02 respectively. Figures 30-33 show the skewness of the confidence interval via left and right coverage. Undefined L-moment ratios could not be estimated and are not included in these tables and figures.

Table 42 provides the coverage results of the simulation for each distribution and L-moment ratios at an $\alpha = 0.10$ level. The normal distribution was consistently meeting coverage for L-kurtosis (t_4) across all sample sizes $n = 7$ through $n = 100$. At $n = 4$, the normal was conservative with a coefficient of 0.95. For the exponential distribution, the confidence intervals tend to be slightly conservative in smaller sample sizes and higher L-moments. For the exponential distribution, sample size requirements for α level coverage increased as the L-moments increased. L-skewness (t_3) and L-kurtosis (t_4) achieve α level at a sample size of 10 and 40, respectively. Similarly, the gumbel distribution L-moment ratios (t_3 and t_4) achieve α level coverage at sample sizes of 7 and 22, respectively. For the pareto distribution, coverage of both L-moment ratios (t_3 and t_4) remained conservative across all sample sizes,

Table 42. Coverage of Wald-based Approximate Variance Confidence Interval for L-moment Ratios at = 0.10

	normal	exponential		pareto		gumbel	
Size	t_4	t_3	t_4	t_3	t_4	t_3	t_4
4	0.95	0.93	0.95	0.96	1.00	0.92	0.95
7	0.91	0.92	0.95	0.97	1.00	0.91	0.93
10	0.91	0.91	0.94	0.97	0.99	0.91	0.93
13	0.90	0.91	0.93	0.96	0.99	0.91	0.92
16	0.90	0.91	0.93	0.96	0.98	0.91	0.92
19	0.90	0.90	0.92	0.96	0.98	0.90	0.92
22	0.89	0.90	0.92	0.95	0.98	0.90	0.91
25	0.90	0.90	0.92	0.95	0.98	0.90	0.91
28	0.90	0.90	0.92	0.95	0.97	0.90	0.91
31	0.90	0.90	0.91	0.95	0.97	0.90	0.91
34	0.90	0.91	0.92	0.95	0.97	0.91	0.91
37	0.90	0.90	0.92	0.95	0.97	0.90	0.91
40	0.90	0.90	0.91	0.95	0.96	0.90	0.91
43	0.89	0.90	0.91	0.94	0.96	0.90	0.91
46	0.90	0.90	0.91	0.94	0.96	0.90	0.91
49	0.89	0.91	0.91	0.94	0.96	0.90	0.91
52	0.91	0.91	0.91	0.94	0.96	0.90	0.90
55	0.90	0.91	0.90	0.94	0.96	0.90	0.90
58	0.90	0.90	0.91	0.95	0.96	0.90	0.90
61	0.90	0.90	0.91	0.94	0.96	0.90	0.90
64	0.90	0.90	0.91	0.93	0.95	0.90	0.91
67	0.90	0.90	0.91	0.93	0.95	0.90	0.91
70	0.90	0.91	0.91	0.94	0.95	0.91	0.90
73	0.90	0.89	0.91	0.94	0.95	0.90	0.91
76	0.90	0.91	0.91	0.93	0.95	0.90	0.90
79	0.90	0.90	0.90	0.93	0.95	0.90	0.90
82	0.90	0.90	0.90	0.93	0.95	0.90	0.90
85	0.90	0.90	0.91	0.94	0.95	0.90	0.90
88	0.90	0.91	0.91	0.94	0.95	0.90	0.90
91	0.90	0.90	0.91	0.94	0.95	0.90	0.90
94	0.90	0.90	0.91	0.93	0.95	0.90	0.90
97	0.90	0.90	0.91	0.93	0.94	0.90	0.90
100	0.90	0.90	0.91	0.93	0.95	0.90	0.90

achieving 0.93 and 0.95 at a sample size of 100.

Table 43 provides the coverage results of the simulation for each distribution and L-moment ratios at an $\alpha = 0.05$ level. Identical to the previous α level (0.10), the normal distribution was consistently meeting coverage for L-kurtosis (t_4) across all sample sizes $n = 7$ through $n = 100$. One again, at $n = 4$ the normal was conservative with a coefficient of 1.0. For the exponential distribution, the confidence intervals are α level for L-skewness (t_3) and conservative for L-kurtosis (t_4) at smaller sample sizes. L-kurtosis (t_4) achieves α level at a sample size of 19. The gumbel distribution L-moment ratios (t_3 and t_4) are both conservative in small sample sizes, and achieve α level coverage at sample sizes of 7 and 13, respectively. For the pareto distribution, coverage of both L-moment ratios (t_3 and t_4) remained conservative across all sample sizes, ranging from 0.99 and 1.0 in the smallest sample sizes, to 0.97 and 0.98 at a sample size of 100.

Table 44 provides the coverage results of the simulation for each distribution and L-moment ratios at an $\alpha = 0.02$ level. Identical to both previous α levels (0.10 and 0.05), the normal distribution was consistently meeting coverage across L-kurtosis (t_4) for sample sizes $n = 7$ through $n = 100$. At $n = 4$ the normal was conservative with a coefficient of 1.0. For both the exponential and gumbel distribution, the confidence intervals are at the α level for L-skewness (t_3) and conservative for L-kurtosis (t_4) at smaller sample sizes. For the exponential distribution L-kurtosis (t_4) achieves α at a sample size of 10 while the gumbel distribution achieves α at a sample size of 7. For the pareto distribution, coverage of both L-moment ratios (t_3 and t_4) remained conservative across all sample sizes, ranging from 0.99 to 1.0

Figure 30 contains 3 plots of skewness for the normal distribution separated by the assumed α level. For the normal distribution, the α level has very little effect on the resulting skewness of the confidence interval. L-kurtosis (t_4) had more coverage

Table 43. Coverage of Wald-based Approximate Variance Confidence Interval for L-moment Ratios at = 0.05

	normal	exponential		pareto		gumbel	
Size	t_4	t_3	t_4	t_3	t_4	t_3	t_4
4	1.00	0.96	1.00	0.98	1.00	0.97	1.00
7	0.96	0.96	0.99	0.99	1.00	0.96	0.97
10	0.95	0.96	0.97	0.99	1.00	0.96	0.97
13	0.95	0.96	0.97	0.99	1.00	0.96	0.96
16	0.95	0.96	0.97	0.99	1.00	0.95	0.96
19	0.95	0.96	0.96	0.99	0.99	0.95	0.96
22	0.95	0.95	0.96	0.98	0.99	0.95	0.96
25	0.95	0.95	0.96	0.98	0.99	0.95	0.96
28	0.95	0.95	0.96	0.98	0.99	0.95	0.96
31	0.95	0.95	0.96	0.98	0.99	0.95	0.96
34	0.95	0.95	0.96	0.98	0.99	0.96	0.96
37	0.95	0.95	0.96	0.98	0.99	0.95	0.96
40	0.95	0.95	0.96	0.98	0.98	0.95	0.96
43	0.95	0.95	0.96	0.98	0.98	0.95	0.96
46	0.95	0.95	0.96	0.98	0.98	0.95	0.95
49	0.95	0.95	0.96	0.98	0.98	0.95	0.95
52	0.95	0.95	0.96	0.97	0.98	0.95	0.95
55	0.95	0.95	0.96	0.97	0.98	0.95	0.96
58	0.95	0.95	0.95	0.98	0.98	0.95	0.95
61	0.95	0.95	0.96	0.97	0.98	0.95	0.95
64	0.95	0.95	0.96	0.97	0.98	0.95	0.95
67	0.95	0.95	0.95	0.97	0.98	0.95	0.96
70	0.95	0.95	0.96	0.97	0.98	0.95	0.95
73	0.95	0.95	0.96	0.97	0.98	0.95	0.96
76	0.95	0.95	0.96	0.97	0.98	0.95	0.95
79	0.95	0.95	0.95	0.97	0.98	0.95	0.95
82	0.95	0.95	0.95	0.97	0.98	0.95	0.95
85	0.95	0.95	0.96	0.97	0.98	0.95	0.95
88	0.95	0.95	0.95	0.97	0.98	0.95	0.95
91	0.95	0.95	0.96	0.97	0.98	0.95	0.95
94	0.95	0.95	0.95	0.97	0.98	0.95	0.95
97	0.95	0.95	0.95	0.97	0.98	0.95	0.95
100	0.95	0.95	0.96	0.97	0.98	0.95	0.95

Table 44. Coverage of Wald-based Approximate Variance Confidence Interval for L-moment Ratios at = 0.02

	normal	exponential		pareto		gumbel	
Size	t_4	t_3	t_4	t_3	t_4	t_3	t_4
4	1.00	0.99	1.00	0.99	1.00	0.99	1.00
7	0.99	0.99	1.00	1.00	1.00	0.99	0.99
10	0.98	0.99	0.99	1.00	1.00	0.98	0.99
13	0.98	0.98	0.99	1.00	1.00	0.98	0.98
16	0.98	0.98	0.99	1.00	1.00	0.98	0.99
19	0.98	0.98	0.99	1.00	1.00	0.98	0.98
22	0.98	0.98	0.99	1.00	1.00	0.98	0.98
25	0.98	0.98	0.99	1.00	1.00	0.98	0.98
28	0.98	0.98	0.99	0.99	1.00	0.98	0.98
31	0.98	0.98	0.98	0.99	1.00	0.98	0.98
34	0.98	0.98	0.99	1.00	1.00	0.98	0.98
37	0.98	0.98	0.99	0.99	0.99	0.98	0.98
40	0.98	0.98	0.98	0.99	0.99	0.98	0.98
43	0.98	0.98	0.98	0.99	0.99	0.98	0.98
46	0.98	0.98	0.98	0.99	0.99	0.98	0.98
49	0.98	0.98	0.98	0.99	0.99	0.98	0.98
52	0.98	0.98	0.98	0.99	0.99	0.98	0.98
55	0.98	0.98	0.98	0.99	0.99	0.98	0.98
58	0.98	0.98	0.98	0.99	0.99	0.98	0.98
61	0.98	0.98	0.98	0.99	0.99	0.98	0.98
64	0.98	0.98	0.98	0.99	0.99	0.98	0.98
67	0.98	0.98	0.98	0.99	0.99	0.98	0.98
70	0.98	0.98	0.98	0.99	0.99	0.98	0.98
73	0.98	0.98	0.98	0.99	0.99	0.98	0.98
76	0.98	0.98	0.98	0.99	0.99	0.98	0.98
79	0.98	0.98	0.98	0.99	0.99	0.98	0.98
82	0.98	0.98	0.98	0.99	0.99	0.98	0.98
85	0.98	0.98	0.98	0.99	0.99	0.98	0.98
88	0.98	0.98	0.98	0.99	0.99	0.98	0.98
91	0.98	0.98	0.98	0.99	0.99	0.98	0.98
94	0.98	0.98	0.98	0.99	0.99	0.98	0.98
97	0.98	0.98	0.98	0.99	0.99	0.98	0.98
100	0.98	0.98	0.98	0.99	0.99	0.98	0.98

Figure 30. Skewness of Wald Based Approximate Variance Confidence Intervals for the normal distribution

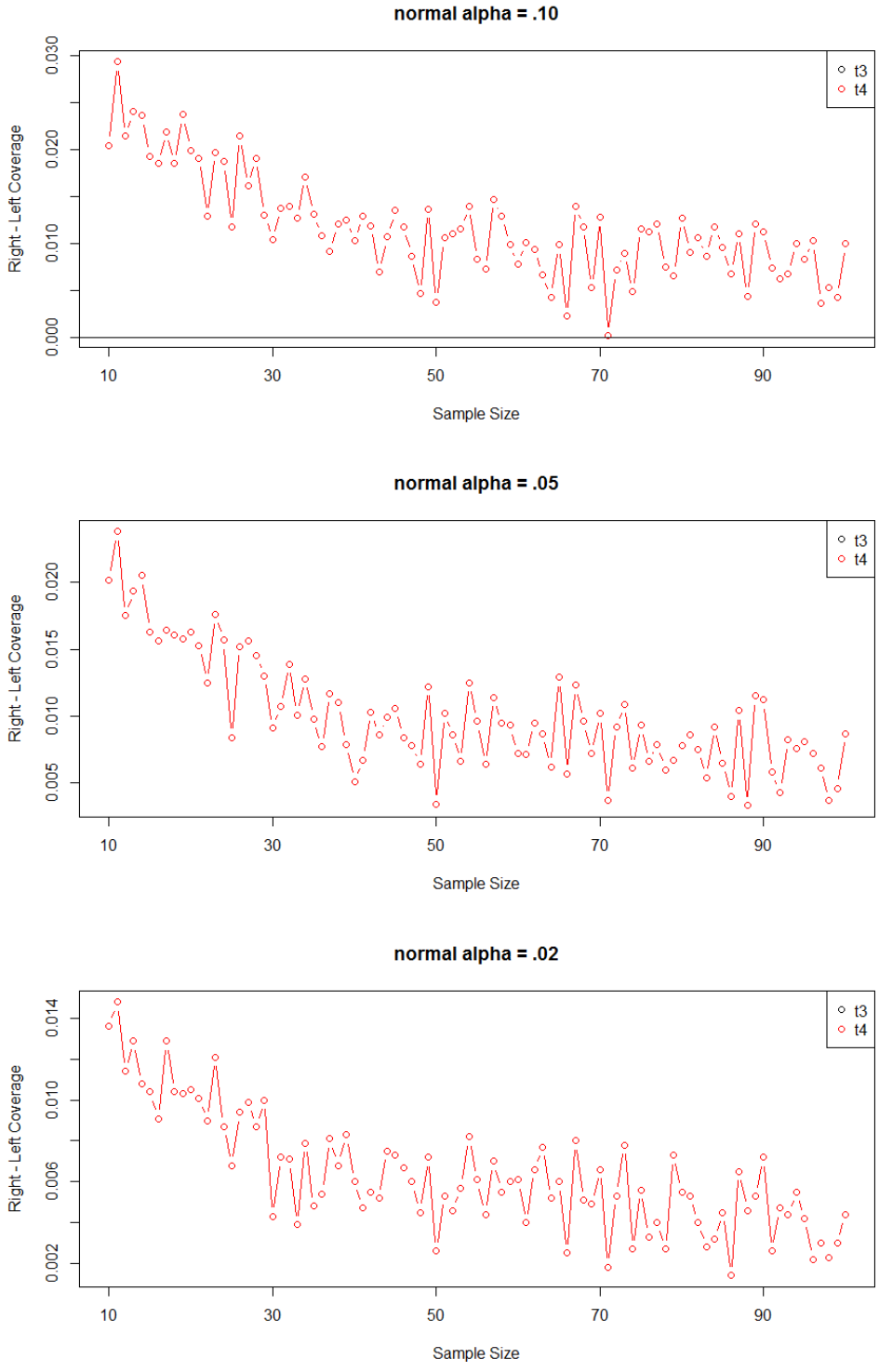

(conservative) in the right tail, this skewness decreased as sample size increased.

Figure 31 contains 3 plots of skewness for the exponential distribution separated by the assumed α level. For the exponential distribution, the α level has very little effect on the resulting skewness of the confidence intervals. L-skewness (t_3) had more coverage (conservative) in the left tail, yet this skewness decreased as sample size increased. While L-kurtosis (t_4) had more coverage (conservative) in the right tail, this skewness decreased as sample size increased.

Figure 32 contains 3 plots of skewness for the gumbel distribution separated by the assumed α level. Similar to both the normal and exponential distribution, α level has very little effect on the resulting skewness of the confidence intervals for the gumbel distributions. L-skewness (t_3) had more coverage (conservative) in the left tail, yet this skewness decreased as sample size increased. While L-kurtosis (t_4) had more coverage (conservative) in the right tail, this skewness decreased as sample size increased.

Figure 33 contains 3 plots of skewness for the pareto distribution separated by the assumed α level. For the pareto distribution, the α level had some effect on the resulting skewness of the confidence intervals. L-skewness (t_3) had more coverage (conservative) in the left tail at smaller sample sizes, yet this skewness increased as sample size increased and eventually became right tailed in the larger sample sizes. The point where the interval moved from left tailed conservative to right tailed conservative differed based on α. This trend happened at $\alpha = 0.10$, 0.05, and 0.02 at sample sizes around 90, 50, and 35, respectively. L-kurtosis (t_4) had more coverage (conservative) in the right tail, and this skewness increased as sample size increased.

Figure 31. Skewness of Wald Based Approximate Variance Confidence Intervals for the exponential distribution

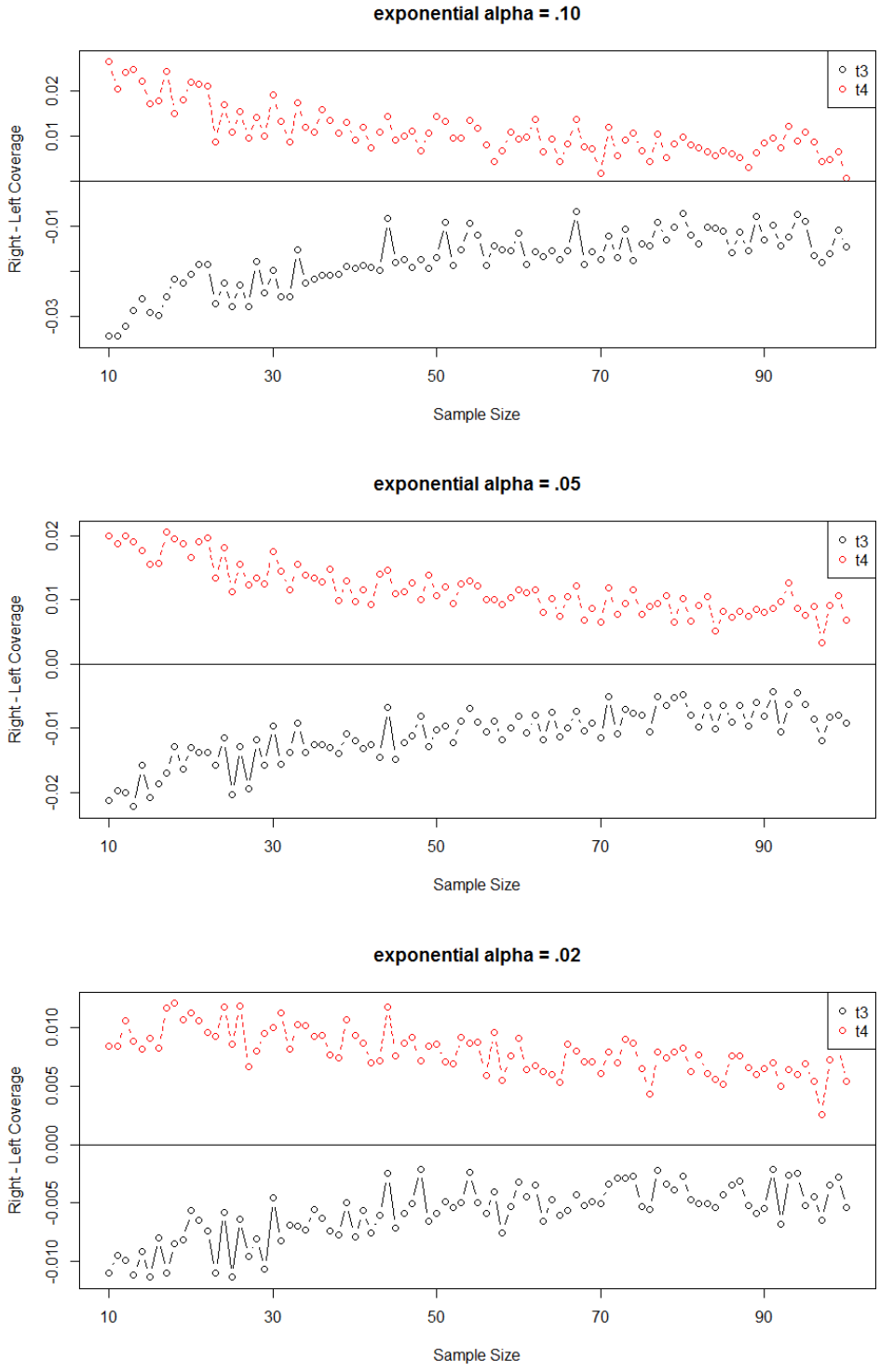

Figure 32. Skewness of Wald Based Approximate Variance Confidence Intervals for the gumbel distribution

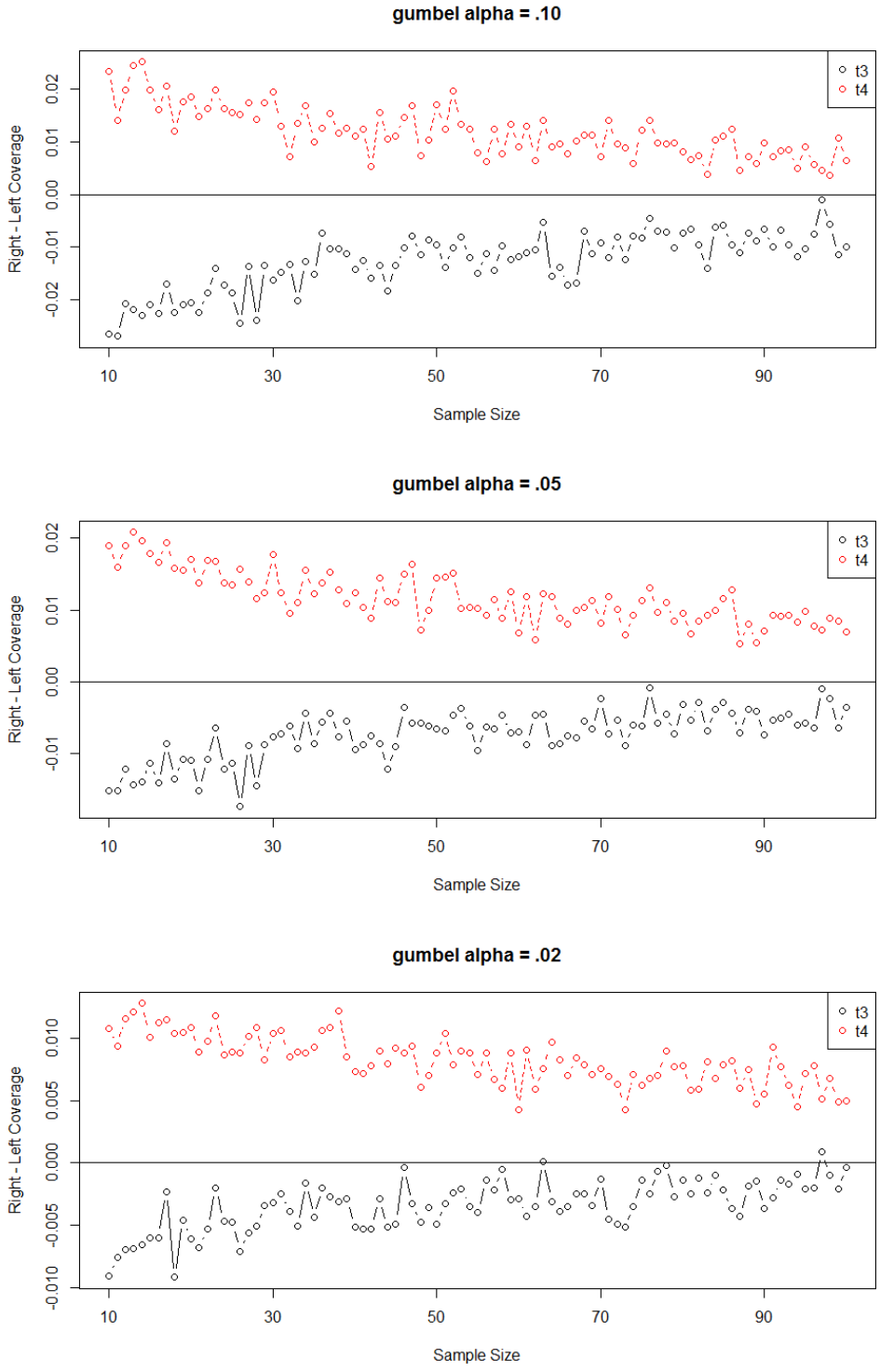

Figure 33. Skewness of Wald Based Approximate Variance Confidence Intervals for the pareto distribution

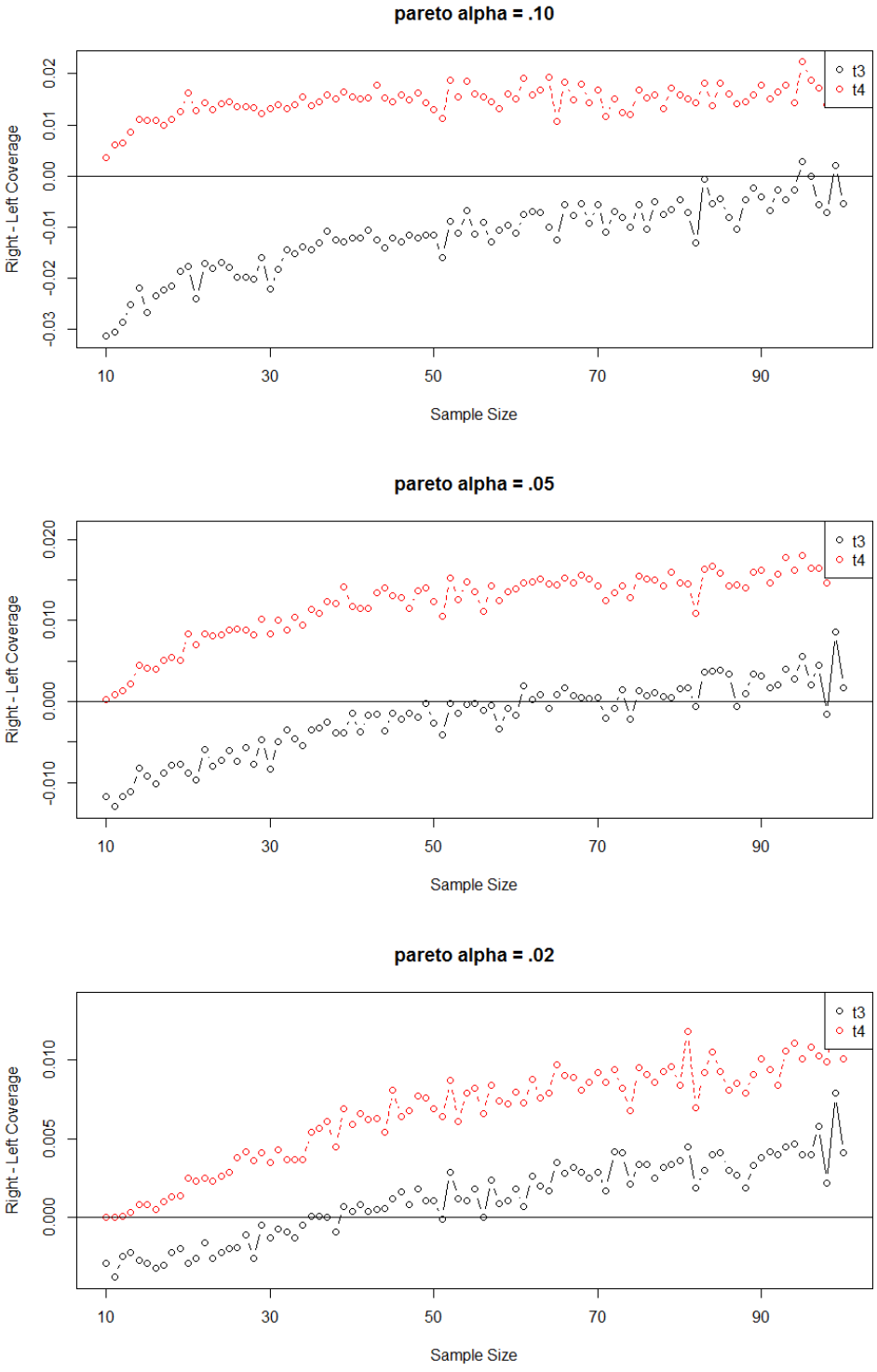

Summary of Wald Based Approximate Variance Interval Estimates of L-moment Ratios.

Of note, α level coverage for the two-sided interval was exact or conservative for all distributions and L-moment ratios across all sample sizes. The right-left coverage plots for all distributions except the pareto distribution, show L-kurtosis (t_4) was right skewed, while L-skewness (t_3) was left skewed. As the sample size increased, skewness decreased. In all cases except for the gumbel distribution at $\alpha = 0.02$, symmetry was not achieved as sample size increased. Only the confidence interval of L-skewness (t_3) for the gumbel distribution seemed to approach symmetry. For the pareto distribution, L-kurtosis (t_4) was right skewed for small sample sizes while L-skewness (t_3) was left skewed. However, as sample size increased the skewness increased for both L-moment ratios, and L-skewness (t_3) became right skewed. The pareto distribution seemed to have the most problems when applying the normal approximation. Therefore, while coverage was maintained in general for the Wald based approximate variance confidence interval, computed from Equation 68 for L-moment ratios, the intervals are not symmetric (consistently over or under coveraged in the bounds), and in the case of the pareto distribution, skewness increased as a function of sample size.

5.4 Interval Estimates of Joint L-moment Ratios

A few methods exist to generate joint confidence intervals for L-moment ratios, (t_3 and t_4). However, none of these methods use the exact variance formulas derived in Chapter 4. Therefore, joint coverage was investigated by deriving two confidence interval estimators for use with joint L-moment ratios, t_3 and t_4.

Multivariate Wald Based Exact Variance Confidence Intervals for Joint L-moment Ratios.

The first method derived utilizes a multivariate Wald when constructing the joint confidence interval and is described as the following:

$$\frac{(\boldsymbol{\eta}-\hat{\boldsymbol{\eta}})'\boldsymbol{\Lambda}^{-1}(\boldsymbol{\eta}-\hat{\boldsymbol{\eta}}) \leq \chi^2_{2,\alpha}}{l_2} \tag{69}$$

$$\text{where } \hat{\boldsymbol{\eta}} = (l_3, l_4)^T \text{ and } \boldsymbol{\eta} = (\lambda_3, \lambda_4)^T, \tag{70}$$

$$\text{and } \boldsymbol{\Lambda} = \begin{pmatrix} var(l_3) & covar(l_3, l_4) \\ covar(l_3, l_4) & var(l_4) \end{pmatrix}. \tag{71}$$

$\chi^2_{2,\alpha}$ is based on a χ^2_2 distribution at the designated α level. The estimates of $\boldsymbol{\eta}$, population L-moments (λ_r), are found in Table 33 and $\hat{\boldsymbol{\eta}}$, sample L-moments (l_r), are based on Equation 17. The variance estimates in Equation 71, are the exact variance equations solved for in Chapter 4. Exact covariance estimates in Equation 71, for each of the distributions examined were derived and reported in Table 45.

Table 45. Covariance l_3 and l_4 for common distributions

Distributions	Covariance	Divisor
normal	0.00	$n^{(3)}$
uniform	0.00	$n^{(3)}$
exponential	$0.08333n^2$	$n^{(3)}$
gumbel	$0.07927n^2 - 0.00298n + 0.00048$	$n^{(3)}$
pareto	$0.29330n^2 - 0.59656n + 0.24659$	$n^{(3)}$

*divisor $n^{(r)} = n(n-1)(n-r+1)$

The left column lists the distribution, and the center column gives the exact covariance. The last column is identical to the variance tables and lists out the divisor for each equation. As seen in the exact variance equations, the equations for exact covariance are given as a function of sample size, n.

The corresponding confidence ellipse created by Equation 69 is then scaled by the

estimate of l_2. Thus, this (1-α)100% confidence interval for the joint L-moment ratio of L-skewness and L-kurtosis was calculated as:

$$\frac{(\boldsymbol{\eta} - \hat{\boldsymbol{\eta}})' \boldsymbol{\Lambda}^{-1} (\boldsymbol{\eta} - \hat{\boldsymbol{\eta}}) \leq \chi^2_{2,\alpha}}{l_2}. \tag{72}$$

The exact simulation settings for L-moments and L-moment ratios were replicated for joint L-moment ratios using Equation 72 for creating the confidence ellipse. Tables 46-48 show the coverage results for the joint L-moment ratios (t_3 and t_4) ellipse at α equal to (0.10, 0.05, and 0.02) respectively.

Table 46 provides the coverage results of the simulation for each distribution and joint L-moment ratio at an $\alpha = 0.10$ level. The normal and uniform distribution consistently meet coverage across all sample sizes $n = 4$ through $n = 100$. For both the exponential and gumbel distribution, the confidence intervals were the most conservative ranging from 0.93 to 0.94 (respectively) in the smallest sample sizes, to 0.96 for both within the higher sample sizes. The pareto distribution was conservative as well, with a range of 0.92 to 0.93 in all sample sizes.

Table 47 provides the coverage results of the simulation for each distribution and joint L-moment ratio at an $\alpha = 0.05$ level. The normal and uniform distribution consistently meet coverage across all sample sizes $n = 4$ through $n = 100$. For the exponential distribution, the confidence interval was the most conservative ranging from 0.95 in the smallest sample sizes, to 0.98 within the higher sample sizes. While, the gumbel and pareto distributions were both conservative as well ranging from 0.96 to 0.97 in all sample sizes.

Table 48 provides the coverage results of the simulation for each distribution and joint L-moment ratio at an $\alpha = 0.02$ level. The normal, uniform, exponential, and pareto distributions consistently meet coverage across all sample sizes $n = 4$ through $n = 100$, except for the exponential distribution at a sample size of 100. For the

Table 46. Coverage for Joint Confidence Interval $\alpha = 0.10$

Size	normal	uniform	exponential	gumbel	pareto
4	0.90	0.91	0.93	0.93	0.94
7	0.90	0.89	0.95	0.93	0.95
10	0.90	0.90	0.94	0.93	0.95
13	0.90	0.90	0.95	0.93	0.96
16	0.90	0.90	0.95	0.93	0.96
19	0.90	0.89	0.95	0.93	0.95
22	0.89	0.89	0.95	0.93	0.95
25	0.89	0.90	0.95	0.93	0.96
28	0.89	0.89	0.95	0.93	0.96
31	0.90	0.90	0.95	0.93	0.96
34	0.90	0.89	0.95	0.93	0.96
37	0.90	0.90	0.95	0.93	0.96
40	0.89	0.90	0.95	0.93	0.96
43	0.90	0.89	0.95	0.93	0.95
46	0.90	0.89	0.95	0.92	0.96
49	0.89	0.90	0.95	0.92	0.96
52	0.90	0.90	0.96	0.93	0.96
55	0.90	0.89	0.95	0.93	0.96
58	0.90	0.90	0.95	0.92	0.96
61	0.89	0.89	0.95	0.93	0.95
64	0.90	0.90	0.96	0.93	0.95
67	0.90	0.90	0.95	0.93	0.95
70	0.90	0.90	0.95	0.93	0.96
73	0.90	0.90	0.95	0.93	0.96
76	0.90	0.90	0.96	0.92	0.96
79	0.90	0.90	0.95	0.92	0.96
82	0.90	0.90	0.95	0.93	0.96
85	0.90	0.90	0.96	0.93	0.96
88	0.90	0.90	0.96	0.92	0.96
91	0.90	0.89	0.96	0.92	0.96
94	0.90	0.89	0.95	0.92	0.95
97	0.90	0.90	0.95	0.92	0.96
100	0.90	0.90	0.95	0.93	0.95

Table 47. Coverage for Joint Confidence Interval $\alpha = 0.05$

Size	normal	uniform	exponential	gumbel	pareto
4	0.94	0.95	0.95	0.96	0.96
7	0.94	0.94	0.97	0.96	0.96
10	0.94	0.95	0.96	0.96	0.97
13	0.94	0.95	0.97	0.96	0.97
16	0.95	0.95	0.97	0.97	0.97
19	0.94	0.95	0.96	0.96	0.97
22	0.94	0.95	0.97	0.96	0.97
25	0.94	0.95	0.97	0.97	0.97
28	0.94	0.94	0.97	0.96	0.97
31	0.95	0.95	0.97	0.96	0.97
34	0.95	0.94	0.97	0.97	0.97
37	0.95	0.95	0.97	0.97	0.97
40	0.95	0.95	0.97	0.97	0.97
43	0.95	0.95	0.97	0.97	0.97
46	0.95	0.94	0.97	0.96	0.97
49	0.94	0.95	0.97	0.96	0.97
52	0.95	0.95	0.97	0.96	0.97
55	0.95	0.94	0.97	0.97	0.97
58	0.95	0.95	0.97	0.96	0.97
61	0.94	0.95	0.97	0.96	0.97
64	0.95	0.95	0.97	0.96	0.97
67	0.95	0.95	0.97	0.97	0.97
70	0.94	0.95	0.97	0.96	0.97
73	0.94	0.95	0.97	0.97	0.97
76	0.95	0.95	0.97	0.96	0.97
79	0.95	0.95	0.97	0.96	0.97
82	0.95	0.95	0.98	0.97	0.97
85	0.95	0.94	0.98	0.97	0.97
88	0.95	0.95	0.97	0.96	0.97
91	0.95	0.95	0.97	0.96	0.97
94	0.95	0.94	0.97	0.96	0.97
97	0.95	0.95	0.97	0.96	0.97
100	0.95	0.95	0.98	0.96	0.97

Table 48. Coverage for Joint Confidence Interval $\alpha = 0.02$

Size	normal	uniform	exponential	gumbel	pareto
4	0.97	0.98	0.97	0.98	0.97
7	0.97	0.98	0.98	0.98	0.98
10	0.97	0.98	0.98	0.98	0.98
13	0.97	0.98	0.98	0.98	0.98
16	0.97	0.98	0.98	0.98	0.98
19	0.97	0.97	0.98	0.98	0.98
22	0.97	0.98	0.98	0.98	0.98
25	0.97	0.98	0.98	0.98	0.98
28	0.97	0.98	0.98	0.98	0.98
31	0.97	0.98	0.98	0.98	0.98
34	0.97	0.98	0.98	0.99	0.98
37	0.97	0.98	0.98	0.99	0.98
40	0.98	0.98	0.99	0.99	0.98
43	0.98	0.98	0.98	0.99	0.98
46	0.98	0.97	0.98	0.98	0.98
49	0.97	0.98	0.98	0.98	0.98
52	0.98	0.98	0.98	0.98	0.98
55	0.98	0.97	0.98	0.98	0.98
58	0.97	0.98	0.98	0.98	0.98
61	0.97	0.98	0.98	0.99	0.98
64	0.98	0.98	0.98	0.98	0.98
67	0.98	0.98	0.98	0.99	0.98
70	0.98	0.98	0.98	0.99	0.98
73	0.97	0.98	0.98	0.99	0.98
76	0.98	0.98	0.99	0.99	0.98
79	0.98	0.98	0.98	0.98	0.98
82	0.98	0.98	0.99	0.98	0.98
85	0.98	0.97	0.98	0.99	0.98
88	0.98	0.98	0.98	0.98	0.98
91	0.98	0.97	0.98	0.98	0.98
94	0.97	0.97	0.98	0.98	0.98
97	0.98	0.98	0.98	0.99	0.98
100	0.98	0.98	0.99	0.99	0.98

gumbel distribution, the confidence interval was conservative at times starting at a sample size of 34 and continuing to 100 with a maximum coefficient of 0.99.

Multivariate Wald Based Unbiased Variance Confidence Intervals for Joint L-moment Ratios.

The second joint confidence interval estimator derived for use with joint L-moment ratios, was based on the unbiased estimator (UBE) of variance detailed by Elamir and Seheult [8] and is shown below:

$$\widehat{\boldsymbol{var}(\boldsymbol{l})} = \boldsymbol{C}\hat{\boldsymbol{\Theta}}\boldsymbol{C}^T. \tag{73}$$

Where $\hat{\boldsymbol{\Theta}} =$

$$b_k b_l - \frac{1}{n^{(k+l+2)}} \sum_{1\le i<j\le n} [(i-l)^{(k)}(j-k-2)^{(l)} + (i-1)^{(l)}(j-l-2)^{(k)}]X_{i:n}X_{j:n}, \tag{74}$$

$$\text{and } b_k b_l = \frac{1}{n^{(k+1)}n^{(l+1)}} \sum_{i=1}^{n}\sum_{j=1}^{n}(i-1)^{(k)}(j-1)^{(l)}X_{i:n}X_{j:n}, \tag{75}$$

where i, j represents the i^{th} and j^{th} order statistics and n represents the sample size. Thus, the (1-α)100% distribution free joint confidence interval for L-moment ratios of L-skewness and L-kurtosis was calculated as:

$$\frac{(\boldsymbol{\eta}-\hat{\boldsymbol{\eta}})'\hat{\boldsymbol{\Theta}}^{-1}(\boldsymbol{\eta}-\hat{\boldsymbol{\eta}}) \le \chi^2_{2,\alpha}}{l_2}. \tag{76}$$

This confidence interval was not simulated as the three previously derived confidence intervals. Instead, the next section compares the four joint confidence interval methods, two that I derived (Equations 72 and 76) with two previously researched (Equations 77 and 78), at select sample sizes.

Exact Bootstrap and Characteristic Generating Function Confidence Intervals for Joint L-moment Ratios.

Both of the previous methods discussed at the beginning of this chapter were used in deriving joint confidence interval estimates for the L-moment ratios, L-skewness and L-kurtosis. [21][38] The Exact Bootstrap (EB) method constructed its joint confidence interval based on the same multivariate assumption, yet utilized the exact bootstrapped estimators for the multivariate Wald expression.

$$(\boldsymbol{\eta} - \hat{\boldsymbol{\eta}})' \hat{\boldsymbol{\Lambda}}^{-1} (\boldsymbol{\eta} - \hat{\boldsymbol{\eta}}) \leq \chi^2_{2,\alpha}. \tag{77}$$

Recall, the bootstrapped estimators, $\hat{\boldsymbol{\eta}}$ and $\hat{\boldsymbol{\Lambda}}$, for L-moments are derived in Equation 61. The second method for estimating a joint confidence interval was derived from the characteristic generating function (CGF) utilizing a Bonferrnoi corrected interval for the pair of L-moment ratios:

$$\frac{\hat{F}^{-1}_{l_r}(\alpha/4)}{l_2} \leq l_r \leq \frac{\hat{F}^{-1}_{l_r}(1-\alpha/4)}{l_2}. \tag{78}$$

Comparison between the four methods is shown in Table 49 where the first three columns list the distribution and true population parameters for the L-moment ratios (τ_3,τ_4). The fourth column highlights the method, while the last four columns specify the sample sizes simulated (10, 35, 50, 100, 150). All four methods were simulated across all sample sizes at α equals 0.05 and replicated 1,000 times for each distribution.

Table 49. Empirical Joint Coverage Comparison at $\alpha = 0.05$

	τ_3	τ_4	Method	10	35	50	100	150
normal	0	0.123	EB	0.95	0.90	0.90	0.91	0.92
			CGF	0.99	0.95	0.94	0.94	0.94
			UBE	0.85	0.82	0.87	0.91	0.92
			Exact	0.93	0.94	0.94	0.94	0.94
uniform	0	0	EB	0.98	0.95	0.94	0.94	0.94
			CGF	0.98	0.96	0.95	0.94	0.94
			UBE	0.83	0.78	0.84	0.90	0.92
			Exact	0.94	0.94	0.94	0.94	0.94
exponential	0.333	0.167	EB	0.90	0.858	0.84	0.83	0.82
			CGF	0.98	0.92	0.92	0.93	0.93
			UBE	0.84	0.83	0.87	0.93	0.94
			Exact	0.96	0.97	0.97	0.97	0.97
gumbel	0.170	0.150	EB	0.93	0.87	0.89	0.89	0.90
			CGF	0.98	0.92	0.93	0.92	0.93
			UBE	0.85	0.82	0.87	0.91	0.93
			Exact	0.96	0.96	0.96	0.96	0.96

EB - Exact Bootstrap, CGF - Characteristic Generating Function, UBE - Unbiased estimator of variance

For the normal distribution, the UBE method failed to meet coverage (α) at all sample sizes. The EB method at a sample size of 10 was slightly conservative, but as sample size grew, coverage dropped below α and even at a sample size of 150, only rose to 0.92. The CGF and Exact method compared almost identically for sample sizes of 50, 100, and 150, while CGF was conservative and the Exact method failed to meet coverage for sample sizes of 10 and 35.

Figure 34 shows an example of a standard normal random sample of size 50. The x-axis shows the range for t_3, while the y-axis shows the range of t_4. Each method is color coded showing the UBE method in red, the EB method in blue, the Exact method in green, and lastly, the CGF method is shown in black as a box since it is a Bonferroni corrected method.

Figure 34. Joint Confidence Interval L-moment Ratios: sample size 50 for the normal distribution

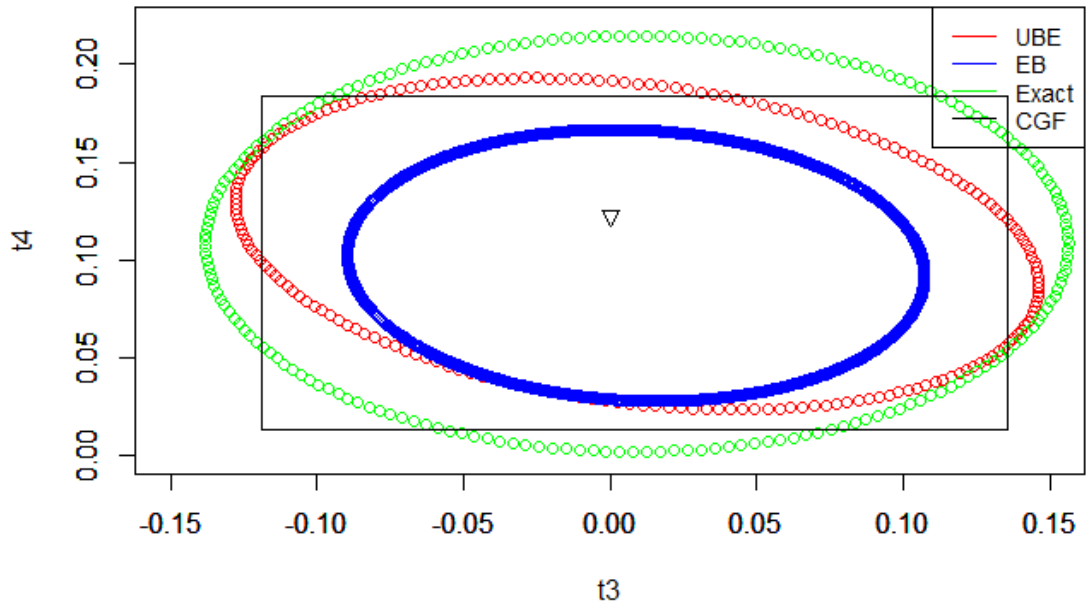

Based on the simulation, the UBE and EB methods performed the poorest, failing to meet coverage, and for this particular sample they give the smallest ellipse (Figure 34). However, the Exact method and CGF performed almost identically, providing (conservative) coverage. Although they provide similar coverage, the Exact method accounts for covariance while the CGF method over-corrects for it in the form of a box.

For the uniform distribution, the UBE method performed the poorest, remaining substantially below α in smaller sample sizes and only achieving a power of 0.92 at the largest sample size. The EB, CFG, and Exact methods all performed close to α for all sample sizes except 10. At a sample size of 10, CGF and EB were conservative while the Exact method performed close to α, at 0.95.

When data was simulated from an exponential distribution, the UBE method

performed the poorest at sample sizes of 10 and 35. By sample size of 150, the UBE method achieved power close to α, at 0.94. The EB method performed the poorest for sample sizes of 50, 100, 150 and by sample size of 150, power has dropped to 0.82. The CGF method was conservative at a sample size of 10, with empirical power equal to 0.98, yet fails to meet coverage for all other sample sizes, slowly climbing from 0.92 to 0.93 for sample sizes of 35 and 150, respectively. The Exact method moves from 0.96 to 0.97 as it progresses through the sample sizes. The Exact method was the only method that consistently achieves power closest to α, and was not found to drop below coverage.

Figure 35 shows one replication from an exponential random sample of size 150. This figure highlights the fact that the Exact method was conservative, which is easily seen by the large ellipse provided. It also highlights the EB method generally failing to meet coverage as shown by having the smallest ellipse. The CGF and UBE both come close, but for both of these estimators they fail to encompass the true parameter, which is shown as a black triangle.

Figure 35. Joint Confidence Interval L-moment Ratios: sample size 150 for the exponential distribution

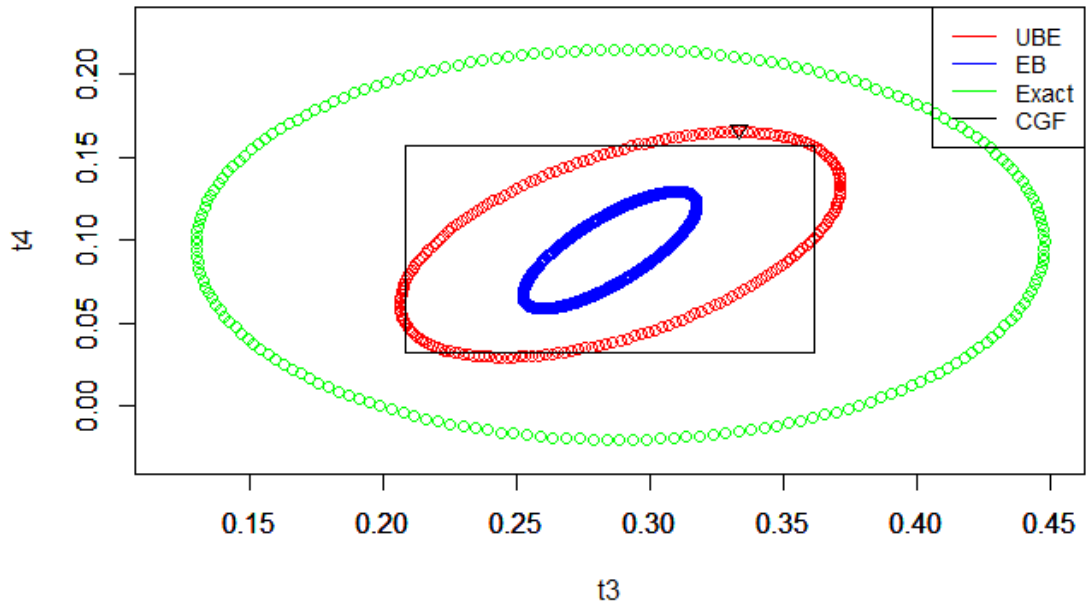

For the last distribution, the gumbel, the UBE method performed the poorest in sample sizes of 10 - 50, consistently staying below α and achieved at most 0.93 coverage at a sample size of 150. The EB method performed the poorest at sample sizes of 100 and 150, and has power below α across all sample sizes. The CGF was conservative in the smallest sample sizes and fails to meet coverage across increasing sample sizes. The CGF method achieves coverage as high as 0.93 at a sample size of 150. The Exact method consistently stays at 0.96 for all samples and was the closest interval estimator across all sample sizes.

Table 50 lists the computational timing required for estimating the mean and covariance based on each joint interval method. MatLab code for estimating all parameters needed for each of the four methods can be found in Appendix C. All scripts were executed on an Intel i7-6700HQ CPU single core at 2.60 GHz. The first

column lists sample size, while the remaining four columns give timing results for each of the four methods compared. The exact bootstrap method (EB) was exponentially time challenged as a function of sample size. The characteristic generating function (CGF) method builds off the EB estimates and only adds about 4 seconds regardless of sample size. The unbiased estimator of variance has a linear growth as a function of sample size. The best performance from a timing perspective was the exact method, which was achievable due to the derived equations found in Chapter 4. By deriving exact variance as a function of sample size, the timing requirements remain fixed. Theoretically, one could partition the matrix across multiple scripts and save time by running each script on a different core. However, overall these comparisons remain the same. Discretizing the largest calculation still results in a run time of over 30 minutes for sample sizes of 150. This was still 1800 times slower than the exact method.

Table 50. Time in Seconds to Calculate Mean and Covariance Estimates for Building Intervals

Sample Size	EB	CGF	UBE	Exact
10	<1	5	<1	<1
35	487	581	<1	<1
50	2066	2070	1	<1
100	24,123.47	24,127	45	<1
150	122,221.32	122,225	67	<1

Summary of Interval Estimates of Joint L-moment Ratios.

The confidence interval estimates derived from the Exact Bootstrap (EB) and Unbaised Estimator of Variance (UBE) only meets coverage in a single distribution and sample size. The EB method meets coverage in a sample size of 10 for the normal distribution, while the UBE method meets coverage at a sample size of 150 for the exponential distribution. The Exact method provides either α level or conservative coverage in all sample sizes and distributions. It also out performed all methods in skewed distributions. The CGF method provided conservative coverage in the

smallest sample size for all distributions. The fact that the Exact method either meets or exceeds coverage while being computationally efficient makes it a superior choice when a parametric assumption is valid.

5.5 Conclusion

In this chapter, I derived quick confidence intervals for estimating L-moments, L-moment ratios, and joint L-moment ratios that generally maintains coverage, and often conservative coverage, in all distributions. Although the Wald based Exact variance confidence interval maintains two-sided coverage in general for each distribution and L-moment examined, these interval estimates are at times skewed, providing either conservative right coverage at the expense of left coverage or vice versa. However, these confidence intervals meet general α level requirements for a two-sided interval. This interval provides quick and reasonable estimation. Further, the Exact joint interval meets coverage at almost all sample sizes and distributions. In addition, the joint interval was computationally more efficient than the other research based methods that fail to meet coverage across sample sizes and distributions. I acknowledge that other methods are less restrictive and perform better in specific situations, but they come with high implementation and computational costs. If practitioners are going to incorporate uncertainty along with their estimates of L-moments and L-moment ratios, they need a quick and reasonable method.

The contributions of this work provide a two-sided confidence interval, based on distribution, for L-moments and L-moment ratios that are quick and reasonable. In addition, the exact joint confidence interval, based on the exact variances derived in Chapter 2, are quick and reasonable across all sample sizes. These contributions allow for the statistic community, and by in large those scientific fields, utilizing L-moments and L-moment ratios to build appropriate interval estimates.

VI. Conclusions

As we become more dependent on technology and the networks that power and run the future, so must the fields of network analysis and statistics grow to help researchers characterize and monitor these networks. The results of this work provided contributions in network analysis and across research in general, in the form of theoretical contributions toward the estimation of L-moments and L-moment ratios. The following contributions are related to network analysis:

1. Across all graph models, for the network measure closeness, the mean, variance, skewness and L-scale appeared the most sensitive.

2. Across all graph models, for the network measure betweenness and closeness, the mean appeared the most sensitive.

3. Across all graph models, L-skewness and L-kurtosis had the lowest sensitivity overall.

4. On average as the graphs size and edge density increased sensitivity across moments increased as well.

5. Specifically for the Barabási-Albert model, skewness for closeness, and dispersion (both variance and L-scale) for betweenness were also sensitive.

6. Both the K-S and Sign Test achieved high power to detect node degrade, with as few as $1 - 2\%$ of all nodes being deleted using, using the network measure closeness and degree.

7. Betweenness was unable to detect the node degradation in either real world network, and appears a suitable choice when building a network that is robust against node degrade.

The following contributions are related to the theoretical work on estimation of L-moments and L-moment ratios:

1. Distribution free exact variance and covariance equations for the first four L-moments were derived, for which previously only the first two L-moments were reported.

2. Exact variance equations of L-moments for any general Pareto(a, v) distribution were derived.

3. Formulas for the exact variance of L-moments for the normal(0,1), and exponential(1) distributions were verified and corrections were made to previously reported formulas to correct errors.

4. Formulas for the exact variance of L-moments for the uniform(0,1), pareto$(\frac{3}{\sqrt{2}}, 4)$, and gumbel(0,1) were derived.

5. Formulas for the approximated variance of L-moment ratios for the normal(0,1), uniform(0,1), exponential(1), gumbel(0,1) and pareto$(\frac{3}{\sqrt{2}}, 4)$ distributions were derived.

6. Sample size estimation for the variance of both L-moments and L-moment ratios were provided and recommendations made for the normal, uniform, exponential, gumbel and pareto distributions.

7. Two confidence interval estimates were derived for L-moments and L-moment ratios utilizing the exact and approximate variance equations respectively.

8. Two confidence interval estimates were derived for joint L-moment ratios utilizing the exact variance equations and an unbiased estimator of the variance.

I intend to accomplish the following future work with respect to network analysis and L-moment estimation. Building off the success of the non-parametric methods, I intend to research a two-dimensional Kolmogorov-Smirnov test utilizing various combinations of network measures for sensitivity to network degradation, since they are free from distributional and correlational complications. In a similar vein I intend to research growing a network as I suspect similar results in the ability to detect the change, much as was seen in degradation of networks. I also intend to expand sample size guidance and interval estimations for additional distributions. In addition, I will be implementing my code as a software package that provide interval estimation for L-moments, L-moment ratios, and joint L-moment ratios for use within R.

Appendix A. Appendix A: Chapter 3 Algorithm, Tables, and Figures

Appendix A has full details from each of the research questions listed out in Chapter 3. Algorithm details, full tables, and figures from all simulations are shown within this Appendix.

Algorithm 1

Result: Moments from select Network Measures Simulated 50,000 for select Graph and Node Degrade Settings
initialization;
for *Each Graph Setting: Table 3* **do**
  for *50,000 iterations* **do**
    simulated network (nondegraded graph);
    remove any isolates ;
    calculate network measures: degree, betweenness, and closeness from each graph;
    calculate moments: $m_{1,2,3,4}$, λ_2, $\tau_{3,4}$ for each network measure;
    store all values;
    for *Each Degrade Setting: Table 3* **do**
      calculate degree value selected for removal based on degrade level;
      select nodes for removal based on proportion of degrade;
      remove selected vertices and remaining isolates;
      calculate network measures: degree, betweenness, and closeness from each degraded graph;
      calculate moments: $m_{1,2,3,4}$, λ_2, $\tau_{3,4}$ for each network measure;
      store all values;
    end
  end
end

Algorithm 1: Simulated Moments for all Graphs and Degrades

Table A1. Erdös-Rényi Average Number of Nodes Degraded within Simulation

Degrade & & Proportion	$k=5$					$k=6$					$k=7$					$k=8$				
	m																			
	2	3	4	5	6	2	3	4	5	6	2	3	4	5	6	2	3	4	5	6
Low 1/2	5.0	4.4	4.3	4.2	4.2	9.3	8.4	8.4	8.1	7.9	17.5	17.4	17.7	16.2	15.4	32.1	35.6	36.5	31.2	30.4
Low 1/3	3.2	2.8	2.7	2.6	2.6	6.1	5.5	5.4	5.2	5.1	11.6	11.5	11.6	10.6	10.1	21.5	23.6	24.2	20.6	20.1
Low 1/4	2.3	2.0	1.9	1.9	1.8	4.5	4.0	4.0	3.8	3.7	8.6	8.5	8.6	7.8	7.4	16.1	17.6	18.0	15.4	14.9
Low 1/5	1.7	1.4	1.4	1.3	1.3	3.5	3.1	3.0	2.9	2.8	6.8	6.7	6.8	6.2	5.9	12.8	14.0	14.3	12.2	11.9
Low 1/7	1.2	1.1	1.0	1.0	1.0	2.4	2.1	2.0	2.0	1.9	4.7	4.6	4.7	4.2	4.1	9.0	9.8	10.1	8.5	8.3
Low 1/10	0.6	0.4	0.3	0.3	0.3	1.5	1.2	1.2	1.2	1.2	3.1	3.1	3.1	2.8	2.7	6.2	6.7	6.9	5.8	5.7
Med 1/2	7.3	5.9	5.4	5.1	5.0	14.0	11.2	9.8	9.0	8.4	27.9	21.9	18.7	16.8	15.4	56.4	43.4	36.3	32.1	29.2
Med 1/3	4.5	3.8	3.4	3.3	3.1	8.9	7.2	6.4	5.8	5.4	18.0	14.4	12.3	11.0	10.1	36.7	28.6	23.9	21.2	19.3
Med 1/4	3.2	2.7	2.5	2.3	2.2	6.5	5.3	4.7	4.3	3.9	13.2	10.6	9.1	8.1	7.4	27.0	21.2	17.8	15.8	14.4
Med 1/5	2.4	2.0	1.9	1.7	1.7	5.1	4.1	3.6	3.3	3.1	10.4	8.3	7.2	6.4	5.9	21.3	16.8	14.2	12.5	11.4
Med 1/7	1.6	1.3	1.2	1.1	1.1	3.4	2.8	2.5	2.2	2.0	7.3	5.8	5.0	4.4	4.0	15.0	11.8	10.0	8.8	8.0
Med 1/10	0.9	0.8	0.8	0.7	0.6	2.1	1.8	1.6	1.4	1.3	4.8	3.9	3.3	3.0	2.7	10.3	8.1	6.8	6.0	5.4
High 1/2	6.4	4.5	4.2	4.2	4.1	12.4	8.5	8.1	7.9	7.7	23.9	17.2	17.0	16.1	15.3	44.8	34.9	35.1	31.8	29.7
High 1/3	3.7	2.8	2.6	2.6	2.6	7.4	5.4	5.2	5.1	5.0	14.7	11.2	11.1	10.5	10.0	27.7	22.7	23.1	21.0	19.6
High 1/4	2.5	2.0	1.9	1.8	1.8	5.3	3.9	3.8	3.7	3.6	10.6	8.2	8.2	7.7	7.4	20.0	16.8	17.2	15.7	14.6
High 1/5	1.9	1.4	1.3	1.3	1.3	4.0	3.0	2.9	2.8	2.8	8.2	6.4	6.4	6.1	5.8	15.5	13.3	13.6	12.4	11.6
High 1/7	1.3	1.1	1.0	1.0	1.0	2.7	2.0	1.9	1.9	1.9	5.5	4.4	4.4	4.2	4.0	10.9	9.3	9.6	8.7	8.1
High 1/10	0.6	0.3	0.3	0.3	0.3	1.7	1.1	1.1	1.1	1.1	3.6	3.0	2.9	2.7	2.6	7.2	6.3	6.6	6.0	5.5

Degrade & & Proportion	$k=9$					$k=10$					$k=11$				
	m														
	2	3	4	5	6	2	3	4	5	6	2	3	4	5	6
Low 1/2	59.7	72.0	74.2	58.6	60.9	114.0	144.9	151.8	113.0	122.9	225.2	290.8	312.1	224.7	247.1
Low 1/3	40.0	47.9	49.3	38.9	40.5	76.4	96.9	101.0	75.2	81.8	151.3	194.1	207.8	149.7	164.6
Low 1/4	30.0	35.8	36.9	29.0	30.2	57.7	72.5	75.7	56.3	61.2	114.3	145.5	156.0	112.2	123.3
Low 1/5	23.9	28.6	29.4	23.1	24.1	46.2	57.9	60.4	44.9	48.9	91.5	116.5	124.6	89.6	98.5
Low 1/7	17.0	20.3	20.9	16.4	17.1	32.8	41.3	43.0	31.9	34.8	65.4	83.1	89.0	63.8	70.2
Low 1/10	11.8	14.0	14.5	11.3	11.8	22.9	28.7	30.0	22.2	24.2	45.5	57.9	62.1	44.5	49.0
Med 1/2	115.8	85.9	71.0	62.5	57.1	235.8	170.7	140.2	123.5	113.2	476.6	341.6	276.2	245.6	225.6
Med 1/3	75.7	56.7	47.0	41.5	37.9	154.6	112.6	93.0	82.1	75.3	310.7	225.8	183.8	163.4	150.2
Med 1/4	56.1	42.3	35.2	31.0	28.3	114.9	84.2	69.6	61.5	56.4	230.3	169.2	137.4	122.5	112.5
Med 1/5	44.4	33.7	28.1	24.7	22.5	91.1	67.4	55.5	49.1	45.0	184.4	135.0	110.0	97.9	89.9
Med 1/7	31.7	23.9	19.9	17.5	16.0	64.7	47.8	39.4	34.9	32.0	130.4	96.3	78.2	69.8	64.1
Med 1/10	21.5	16.5	13.8	12.1	11.0	44.4	33.3	27.5	24.3	22.2	89.6	67.4	54.7	48.7	44.7
High 1/2	83.6	70.8	71.8	60.8	58.0	161.0	142.5	145.9	116.0	115.9	319.3	285.4	294.6	223.1	232.7
High 1/3	52.4	46.2	47.5	40.3	38.5	102.8	93.2	96.6	77.1	77.1	201.6	186.3	195.7	148.4	154.9
High 1/4	38.3	34.3	35.4	30.2	28.8	73.8	69.3	72.2	57.7	57.7	147.9	138.5	146.0	111.3	116.1
High 1/5	29.7	27.1	28.2	24.0	22.9	59.0	55.0	57.6	46.0	46.0	116.8	110.6	116.6	88.9	92.8
High 1/7	20.9	19.2	20.0	17.0	16.2	41.4	39.0	41.2	32.7	32.8	81.1	78.5	83.2	63.3	66.1
High 1/10	14.3	13.2	13.9	11.7	11.2	28.3	27.3	28.5	22.7	22.8	56.8	54.4	58.0	44.2	46.1

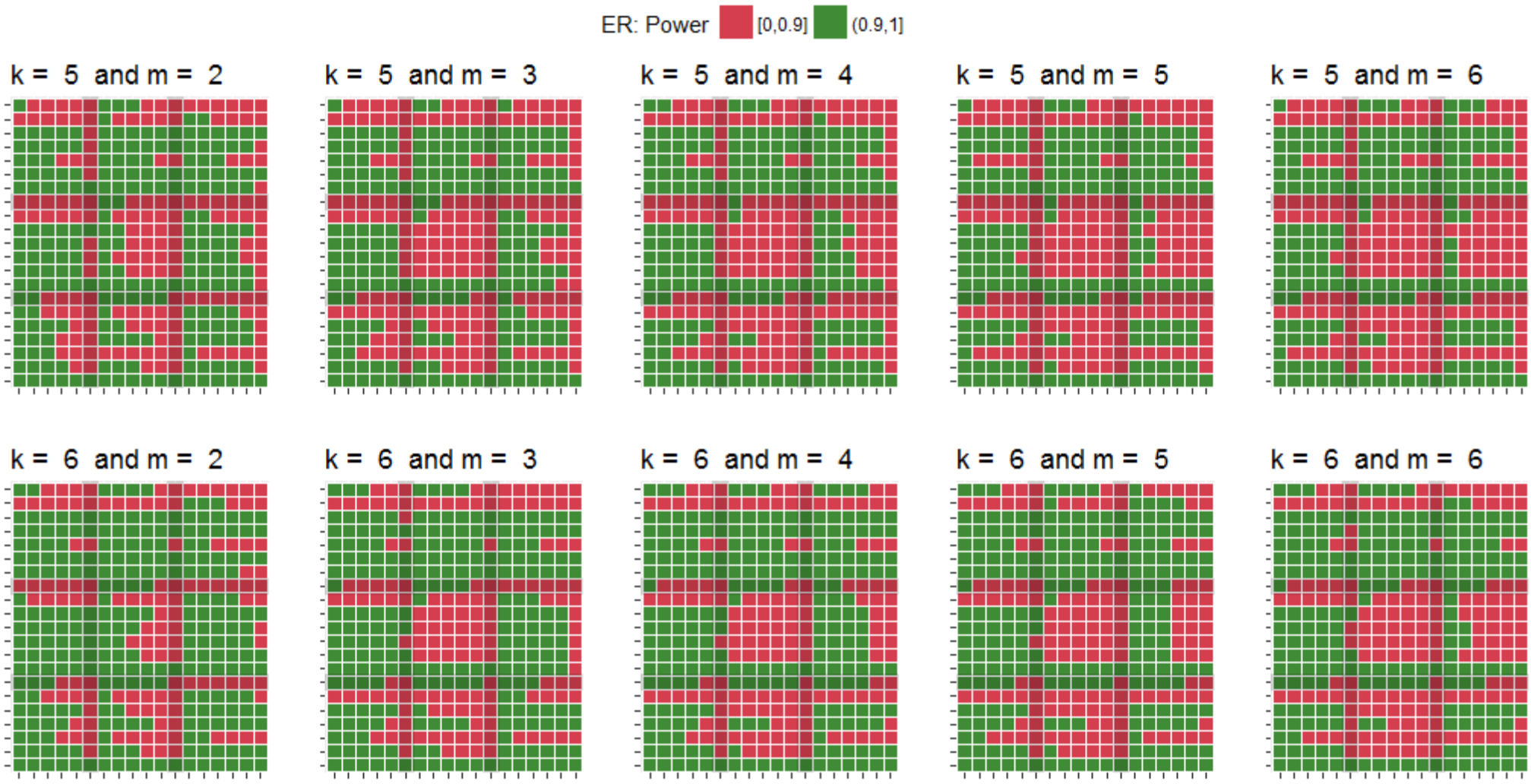

Figure A1. Power results for the Erdös-Rényi model for k = 5 and 6 across network measures, moments, degrade setting and proportions according to the key from Figure 9

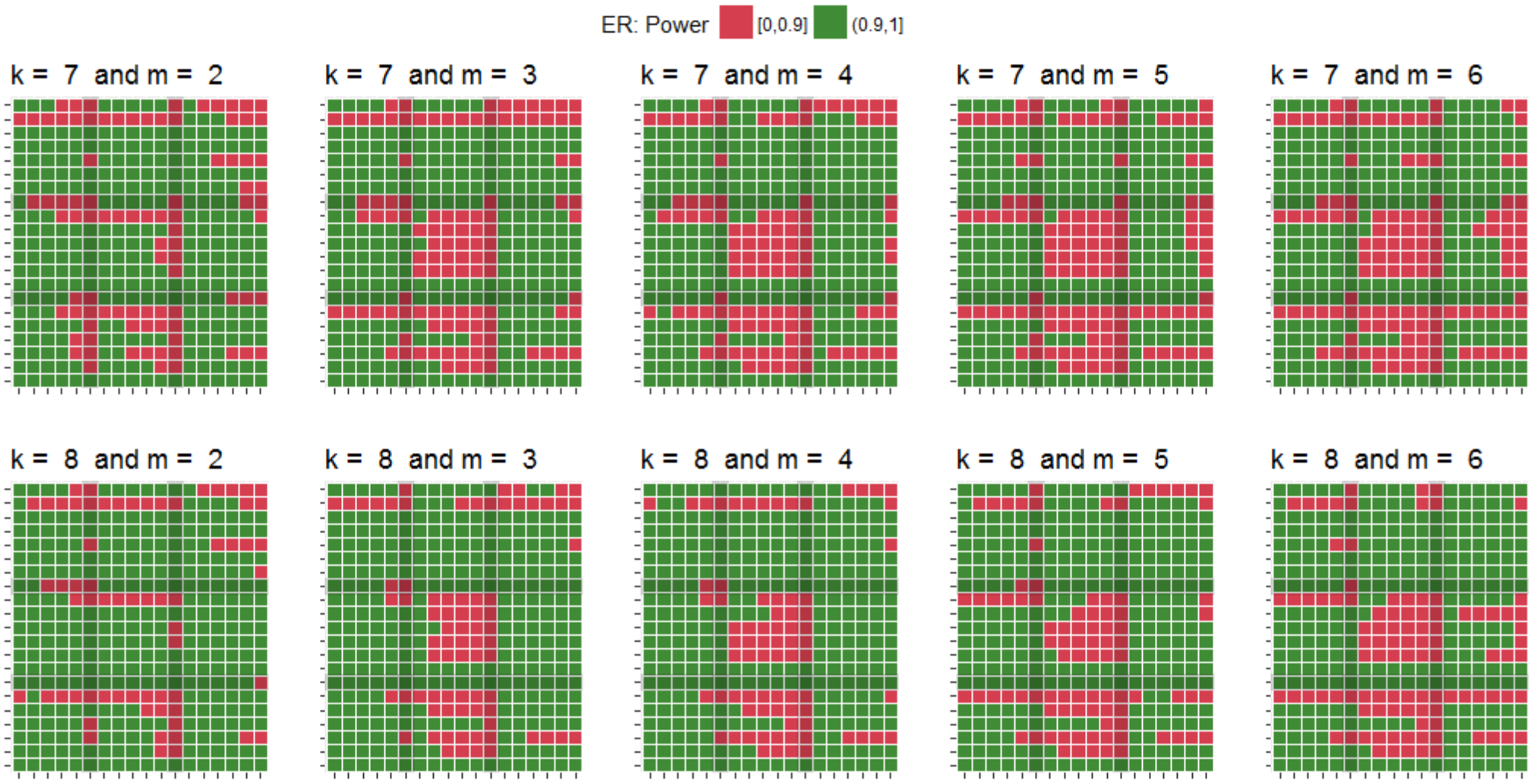

Figure A2. Power results for the Erdös-Rényi model for k = 7 and 8 across network measures, moments, degrade setting and proportions according to the key from Figure 9

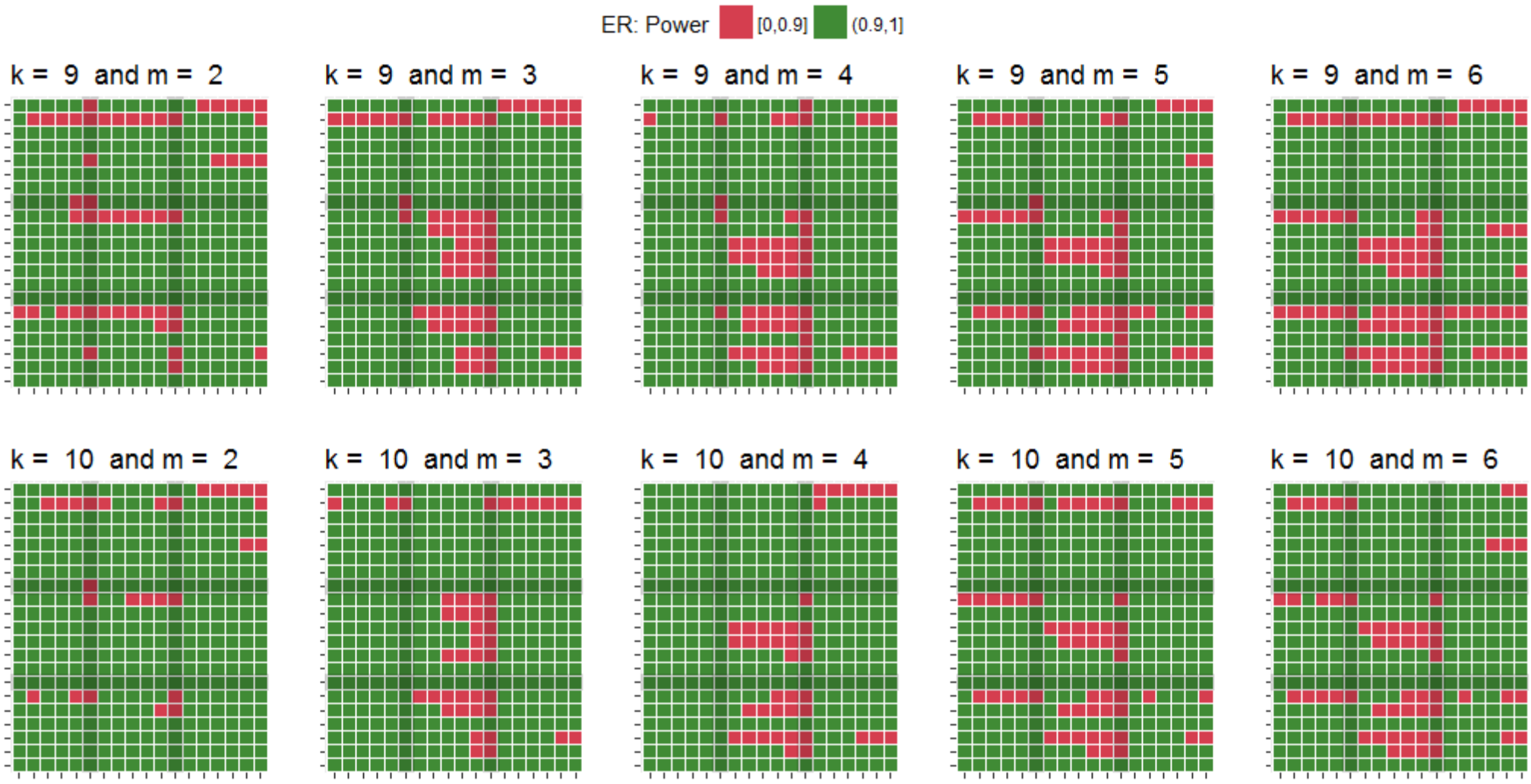

Figure A3. Power results for the Erdös-Rényi model for k = 9 and 10 across network measures, moments, degrade setting and proportions according to the key from Figure 9

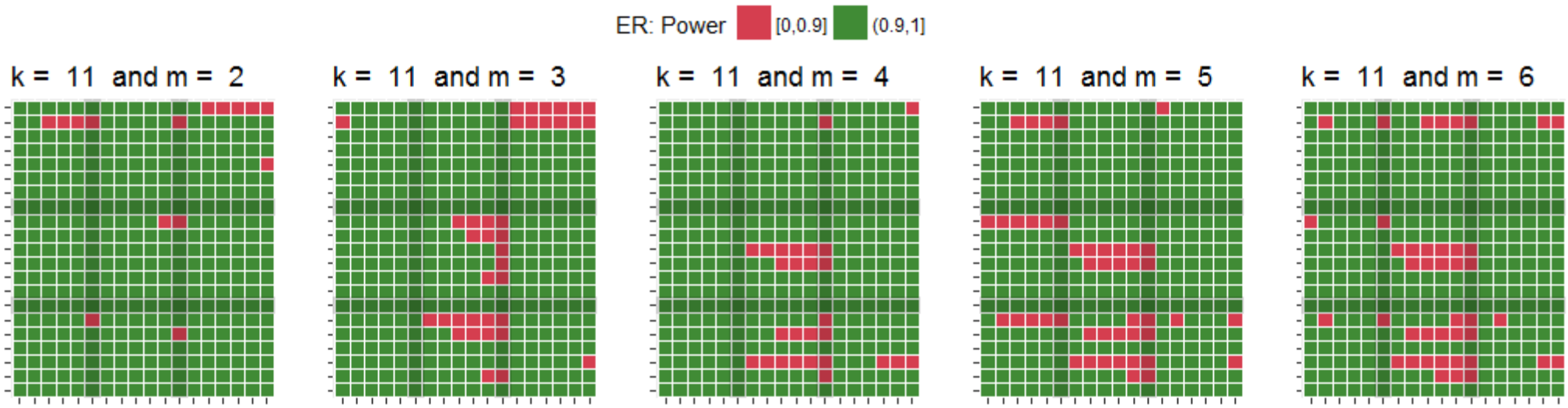

Figure A4. Power results for the Erdös-Rényi model for k = 11 across network measures, moments, degrade setting and proportions according to the key from Figure 9

Table A2. Barabási-Albert Average Number of Nodes Degraded within Simulation

Degrade & Proportion	$k=5$					$k=6$					$k=7$					$k=8$				
	m																			
	2	3	4	5	6	2	3	4	5	6	2	3	4	5	6	2	3	4	5	6
Low 1/2	6.7	5.2	4.5	4.3	4.3	14.0	11.1	9.2	8.2	8.2	28.5	22.9	19.1	16.5	15.9	57.6	46.4	38.9	33.5	30.5
Low 1/3	4.3	3.3	2.8	2.7	2.7	9.1	7.2	6.0	5.3	5.3	18.8	15.1	12.6	10.8	10.4	38.2	30.8	25.8	22.2	20.2
Low 1/4	3.1	2.4	2.0	1.9	1.9	6.7	5.3	4.3	3.9	3.8	14.0	11.2	9.3	8.0	7.7	28.5	23.0	19.2	16.5	15.0
Low 1/5	2.4	1.8	1.5	1.4	1.4	5.3	4.1	3.4	3.0	3.0	11.1	8.8	7.3	6.3	6.1	22.7	18.3	15.3	13.1	11.9
Low 1/7	1.6	1.1	1.0	1.0	1.0	3.6	2.8	2.2	2.0	2.1	7.8	6.2	5.1	4.4	4.2	16.1	12.9	10.8	9.2	8.3
Low 1/10	1.0	0.8	0.4	0.3	0.4	2.3	1.9	1.4	1.1	1.2	5.3	4.2	3.4	2.9	2.8	11.1	8.9	7.4	6.3	5.7
Med 1/2	9.1	5.7	4.4	3.7	3.1	19.2	10.9	9.1	7.9	6.3	40.6	21.1	18.8	16.1	13.0	84.4	41.8	38.5	32.7	26.8
Med 1/3	5.9	3.6	2.8	2.3	1.9	12.6	7.1	5.9	5.1	4.1	26.8	13.9	12.4	10.6	8.5	56.0	27.6	25.5	21.6	17.7
Med 1/4	4.3	2.6	2.0	1.6	1.3	9.3	5.2	4.3	3.7	2.9	20.0	10.3	9.2	7.8	6.3	41.9	20.6	19.0	16.1	13.2
Med 1/5	3.4	2.0	1.5	1.2	0.9	7.3	4.1	3.3	2.9	2.2	15.9	8.1	7.2	6.2	4.9	33.4	16.4	15.1	12.8	10.4
Med 1/7	2.2	1.2	0.9	0.8	0.5	5.1	2.7	2.2	1.9	1.4	11.2	5.7	5.0	4.3	3.4	23.7	11.5	10.7	9.0	7.3
Med 1/10	1.6	0.8	0.4	0.2	0.1	3.5	1.8	1.4	1.1	0.9	7.7	3.8	3.4	2.8	2.2	16.4	7.9	7.3	6.1	5.0
High 1/2	6.0	3.7	3.5	3.4	3.5	12.2	7.5	6.8	6.6	6.5	25.6	16.0	14.2	13.8	13.6	50.9	33.2	29.1	27.9	27.5
High 1/3	2.9	2.2	2.2	2.1	2.1	6.3	4.6	4.3	4.2	4.2	13.4	9.8	9.1	8.9	8.8	27.2	20.4	18.9	18.3	18.1
High 1/4	1.8	1.5	1.4	1.4	1.4	4.1	3.3	3.1	3.1	3.1	9.0	7.1	6.7	6.5	6.4	18.4	14.9	14.0	13.7	13.5
High 1/5	1.2	1.1	1.0	1.0	1.0	3.0	2.4	2.3	2.2	2.2	6.7	5.5	5.3	5.2	5.1	13.8	11.7	11.0	10.8	10.6
High 1/7	1.0	1.0	1.0	1.0	1.0	1.9	1.7	1.6	1.5	1.4	4.4	3.7	3.6	3.5	3.4	9.1	8.1	7.7	7.5	7.4
High 1/10	0.2	0.1	0.0	0.0	0.0	1.1	1.0	1.0	1.0	1.0	2.8	2.4	2.3	2.2	2.1	5.9	5.6	5.3	5.1	5.1

Degrade & Proportion	$k=9$					$k=10$					$k=11$				
	m														
	2	3	4	5	6	2	3	4	5	6	2	3	4	5	6
Low 1/2	115.7	93.5	78.6	67.8	59.8	232.0	187.9	158.1	136.4	120.1	464.8	376.5	316.9	273.7	241.0
Low 1/3	77.0	62.2	52.2	45.0	39.7	154.5	125.1	105.2	90.8	79.9	309.7	250.8	211.1	182.3	160.5
Low 1/4	57.6	46.5	39.1	33.6	29.7	115.8	93.7	78.8	68.0	59.8	232.1	188.0	158.2	136.6	120.3
Low 1/5	46.0	37.1	31.1	26.8	23.6	92.5	74.8	62.9	54.3	47.7	185.6	150.3	126.5	109.2	96.1
Low 1/7	32.7	26.4	22.1	19.0	16.7	65.9	53.3	44.8	38.6	34.0	132.4	107.2	90.2	77.9	68.5
Low 1/10	22.7	18.3	15.3	13.2	11.6	46.0	37.2	31.2	26.9	23.6	92.6	74.9	63.0	54.3	47.8
Med 1/2	170.3	82.8	78.2	66.0	54.5	341.4	164.9	157.8	132.7	109.5	683.5	330.4	316.7	266.1	219.4
Med 1/3	113.2	54.9	51.9	43.8	36.2	227.2	109.5	105.0	88.3	72.8	455.1	219.4	210.9	177.3	146.1
Med 1/4	84.7	41.0	38.8	32.7	27.0	170.1	81.9	78.6	66.1	54.5	340.9	164.3	158.1	132.8	109.5
Med 1/5	67.6	32.7	31.0	26.1	21.5	135.9	65.4	62.8	52.8	43.5	272.4	131.3	126.3	106.2	87.5
Med 1/7	48.1	23.2	22.0	18.5	15.2	96.9	46.5	44.7	37.6	30.9	194.3	93.6	90.1	75.7	62.3
Med 1/10	33.5	16.1	15.2	12.8	10.5	67.6	32.4	31.2	26.1	21.5	135.7	65.3	62.9	52.8	43.5
High 1/2	99.7	67.4	58.7	55.3	54.9	197.7	135.6	119.3	109.4	109.2	395.4	271.2	244.6	217.5	216.7
High 1/3	54.0	41.7	38.2	36.6	36.4	107.7	84.0	77.8	72.5	72.6	215.7	167.9	159.5	144.2	144.1
High 1/4	36.7	30.4	28.4	27.3	27.1	73.6	61.3	58.0	54.2	54.3	147.5	122.8	118.9	107.9	108.0
High 1/5	27.7	24.0	22.6	21.7	21.6	55.7	48.5	46.2	43.2	43.3	111.8	97.1	94.9	86.2	86.3
High 1/7	18.5	16.8	16.0	15.4	15.3	37.3	34.1	32.8	30.7	30.8	75.2	68.5	67.5	61.4	61.5
High 1/10	12.2	11.6	11.0	10.6	10.6	24.8	23.6	22.8	21.3	21.4	50.2	47.6	47.1	42.9	42.9

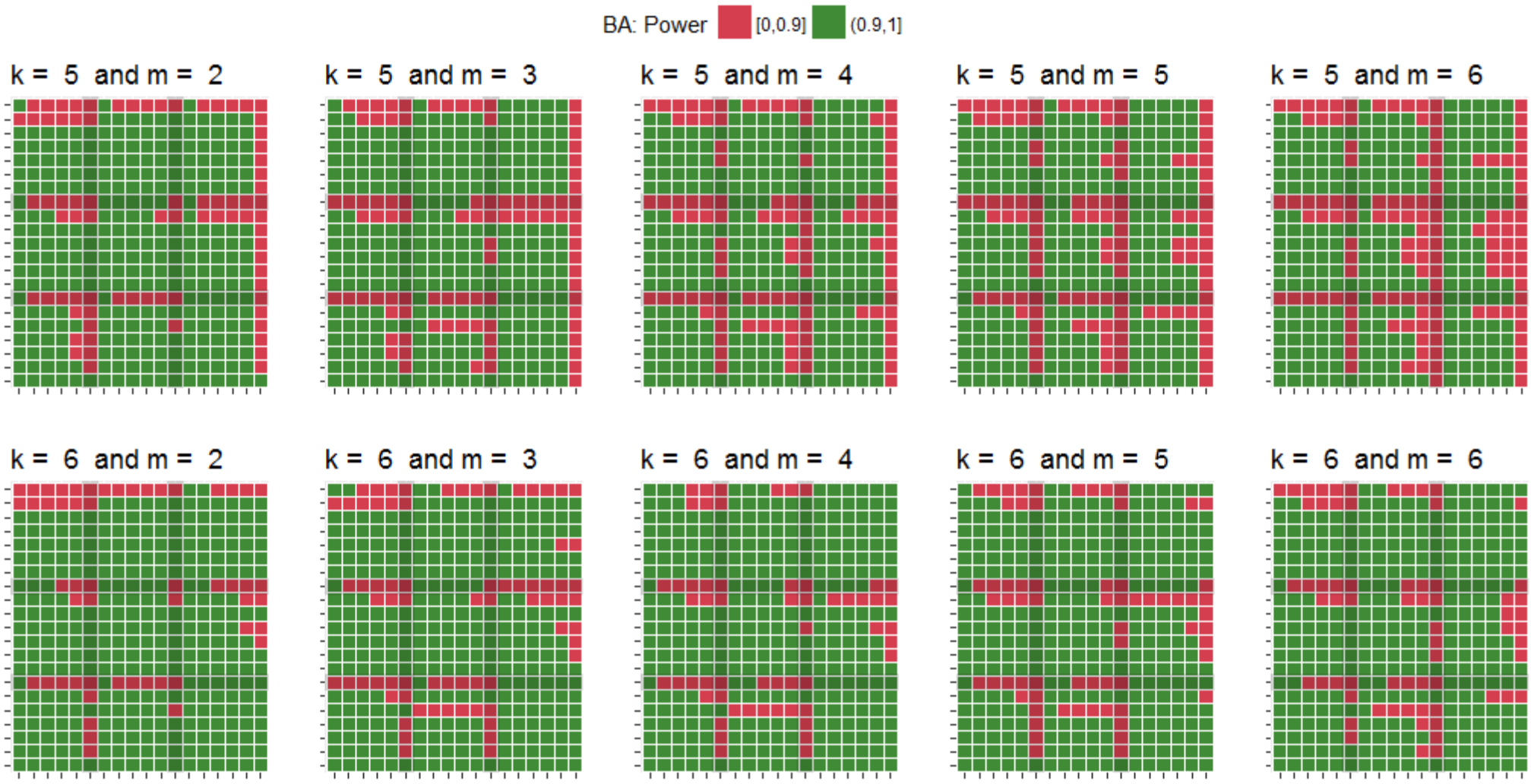

Figure A5. Power results for the Barabási-Albert model for k = 5 and 6 across network measures, moments, degrade setting and proportions according to the key from Figure 9

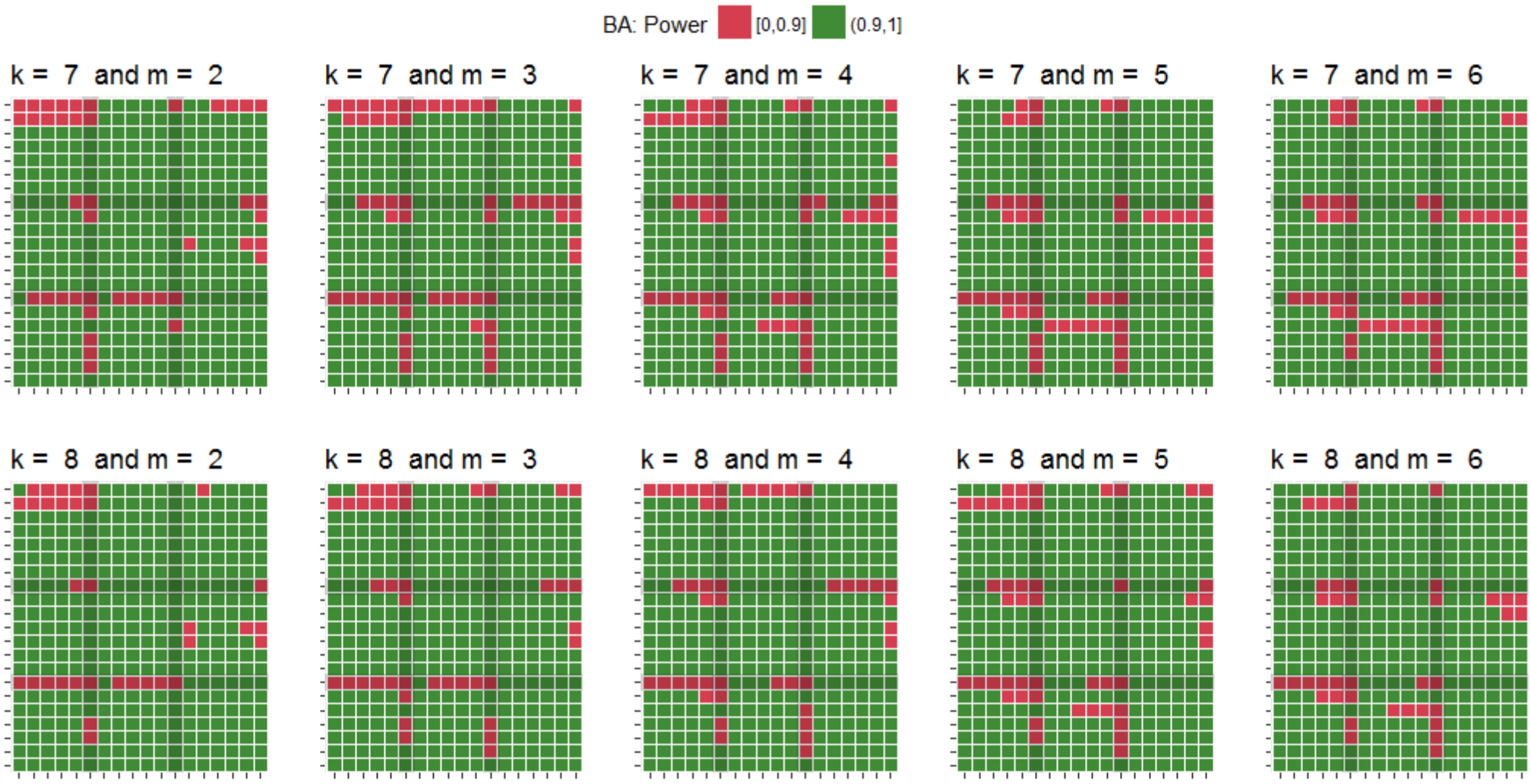

Figure A6. Power results for the Barabási-Albert model for k = 7 and 8 across network measures, moments, degrade setting and proportions according to the key from Figure 9

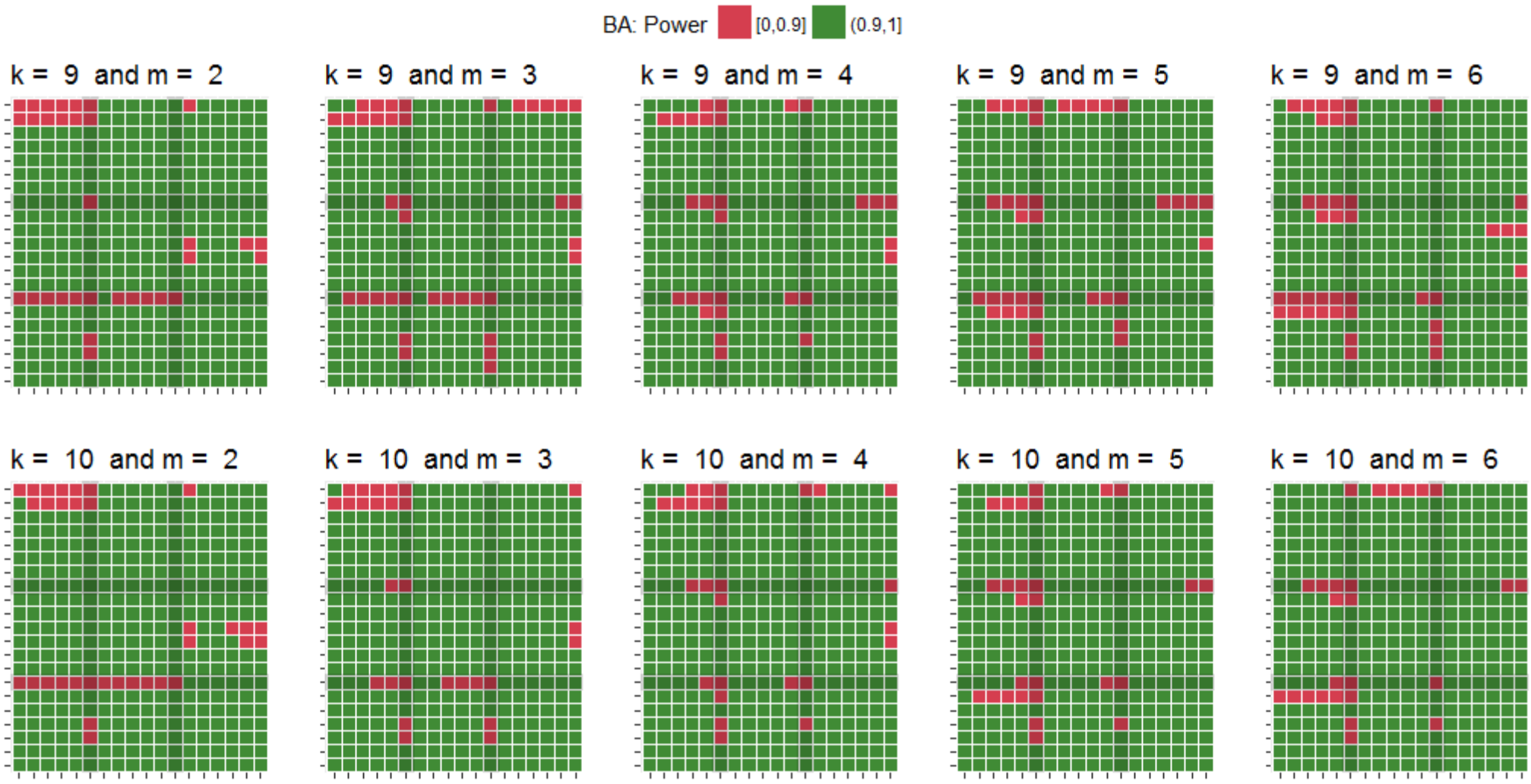

Figure A7. Power results for the Barabási-Albert model for k = 9 and 10 across network measures, moments, degrade setting and proportions according to the key from Figure 9

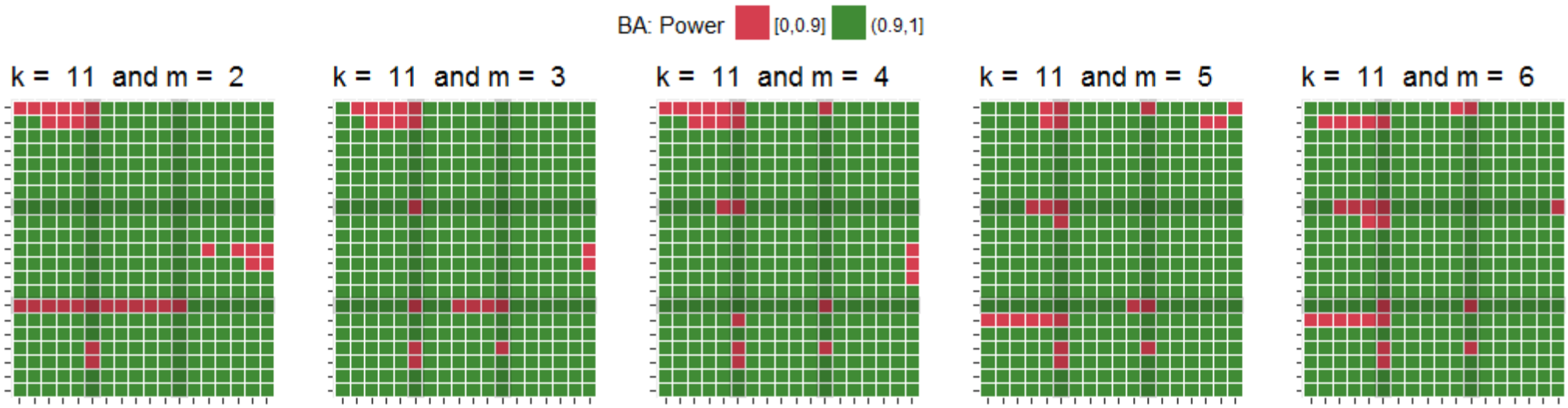

Figure A8. Power results for the Barabási-Albert model for k = 11 across network measures, moments, degrade setting and proportions according to the key from Figure 9

Table A3. Watts-Strogratz Average Number of Nodes Degraded within Simulation

Degrade & Proportion	$k=5$					$k=6$					$k=7$					$k=8$				
	m																			
	2	3	4	5	6	2	3	4	5	6	2	3	4	5	6	2	3	4	5	6
Low 1/2	5.4	4.6	4.3	4.2	4.2	10.7	8.4	8.3	8.4	8.2	22.7	16.1	17.2	17.6	16.7	46.5	31.4	35.1	36.6	33.4
Low 1/3	3.4	2.9	2.7	2.7	2.6	7.1	5.4	5.4	5.4	5.3	15.0	10.6	11.3	11.5	10.9	31.0	20.8	23.2	24.3	22.1
Low 1/4	2.5	2.1	1.9	1.9	1.9	5.2	3.9	3.9	3.9	3.8	11.2	7.8	8.3	8.5	8.1	23.3	15.4	17.3	18.1	16.5
Low 1/5	1.8	1.5	1.4	1.3	1.3	4.0	3.0	3.0	3.0	2.9	8.9	6.1	6.6	6.7	6.4	18.5	12.2	13.7	14.3	13.1
Low 1/7	1.2	1.1	1.1	1.0	1.0	2.7	2.1	2.0	2.0	2.0	6.2	4.2	4.5	4.6	4.4	13.1	8.6	9.7	10.1	9.2
Low 1/10	0.7	0.4	0.3	0.3	0.3	1.7	1.2	1.2	1.2	1.2	4.1	2.8	3.0	3.1	2.9	9.0	5.9	6.6	6.9	6.3
Med 1/2	7.5	6.3	5.7	5.4	5.2	14.0	11.9	10.7	9.9	9.2	27.0	23.3	20.9	18.9	17.3	52.9	47.3	41.2	36.6	33.3
Med 1/3	4.7	4.0	3.6	3.4	3.3	8.9	7.7	7.0	6.4	6.0	17.3	15.3	13.7	12.5	11.4	34.3	31.1	27.3	24.3	22.0
Med 1/4	3.3	2.9	2.6	2.5	2.3	6.4	5.6	5.1	4.7	4.3	12.8	11.3	10.2	9.2	8.4	25.3	23.1	20.3	18.1	16.4
Med 1/5	2.5	2.2	2.0	1.8	1.8	5.0	4.4	4.0	3.6	3.4	10.0	8.9	8.0	7.3	6.6	20.1	18.3	16.1	14.3	13.0
Med 1/7	1.7	1.4	1.3	1.2	1.1	3.4	3.0	2.7	2.5	2.3	6.9	6.2	5.6	5.0	4.6	13.9	12.9	11.4	10.1	9.2
Med 1/10	0.9	0.9	0.8	0.8	0.7	2.2	1.9	1.8	1.6	1.4	4.6	4.2	3.8	3.4	3.1	9.6	8.9	7.8	6.9	6.3
High 1/2	6.6	4.7	4.3	4.2	4.2	13.5	8.6	8.1	8.1	8.0	28.5	16.5	16.3	16.9	16.5	59.5	31.7	33.0	34.9	33.5
High 1/3	3.8	2.9	2.7	2.6	2.6	8.0	5.5	5.2	5.2	5.2	17.2	10.8	10.7	11.1	10.8	36.0	20.7	21.8	23.1	22.1
High 1/4	2.6	2.0	1.9	1.9	1.8	5.6	3.9	3.8	3.8	3.8	12.3	7.9	7.9	8.2	7.9	25.8	15.3	16.2	17.2	16.5
High 1/5	2.0	1.5	1.4	1.3	1.3	4.3	3.0	2.9	2.9	2.9	9.6	6.2	6.2	6.4	6.3	20.3	12.2	12.9	13.7	13.1
High 1/7	1.3	1.1	1.1	1.0	1.0	2.9	2.1	2.0	1.9	1.9	6.5	4.3	4.3	4.4	4.3	13.9	8.5	9.0	9.6	9.2
High 1/10	0.7	0.4	0.3	0.3	0.3	1.9	1.2	1.1	1.1	1.1	4.2	2.8	2.9	2.9	2.8	9.6	5.8	6.2	6.6	6.3

Degrade & Proportion	$k=9$					$k=10$					$k=11$				
	m														
	2	3	4	5	6	2	3	4	5	6	2	3	4	5	6
Low 1/2	97.5	62.7	70.8	75.1	64.7	203.0	126.0	142.2	152.7	124.4	419.0	252.5	285.1	307.7	240.4
Low 1/3	65.4	41.7	47.0	49.9	43.0	136.2	83.8	94.7	101.7	82.8	281.6	168.4	189.9	205.0	160.1
Low 1/4	49.0	31.2	35.2	37.3	32.1	102.5	62.9	70.9	76.1	62.0	212.1	126.0	142.3	153.6	120.0
Low 1/5	39.2	24.8	28.0	29.7	25.6	82.0	50.2	56.6	60.8	49.5	169.9	100.9	113.7	122.8	95.9
Low 1/7	27.9	17.6	19.9	21.1	18.1	58.7	35.7	40.3	43.3	35.2	121.5	71.8	81.1	87.6	68.3
Low 1/10	19.4	12.2	13.8	14.6	12.5	40.7	24.9	28.1	30.1	24.5	85.0	50.2	56.6	61.1	47.7
Med 1/2	107.2	95.9	81.2	71.7	65.2	218.8	192.9	161.0	141.4	129.2	450.3	385.4	320.0	280.1	257.4
Med 1/3	70.0	63.3	53.9	47.6	43.3	142.1	127.3	107.0	94.1	85.9	293.3	255.2	213.0	186.6	171.5
Med 1/4	51.1	47.1	40.3	35.6	32.3	105.1	95.4	80.2	70.4	64.3	217.9	190.3	159.4	139.8	128.5
Med 1/5	40.8	37.6	32.2	28.4	25.8	83.8	75.8	64.0	56.3	51.4	172.7	152.3	127.5	111.8	102.7
Med 1/7	28.7	26.7	22.8	20.1	18.3	59.0	54.2	45.5	40.0	36.5	122.1	108.4	90.9	79.7	73.2
Med 1/10	20.0	18.5	15.8	13.9	12.6	41.0	37.8	31.7	27.9	25.4	85.3	75.7	63.4	55.6	51.1
High 1/2	125.5	61.6	66.5	71.2	66.5	259.0	123.1	133.3	143.7	132.8	533.0	245.7	267.8	288.3	269.4
High 1/3	75.4	40.4	44.1	47.2	44.2	157.2	80.8	88.6	95.6	88.4	323.5	162.7	177.9	191.8	179.4
High 1/4	54.8	30.1	32.9	35.3	33.0	114.0	60.3	66.3	71.5	66.2	233.5	121.3	133.2	143.7	134.4
High 1/5	42.8	23.9	26.2	28.2	26.3	88.8	48.0	52.9	57.1	52.9	181.2	96.6	106.3	114.9	107.5
High 1/7	29.5	16.9	18.6	20.0	18.6	62.0	34.0	37.6	40.7	37.6	127.6	68.7	75.7	81.9	76.6
High 1/10	20.4	11.6	12.8	13.8	12.9	42.8	23.6	26.2	28.3	26.1	88.0	47.6	53.0	57.2	53.5

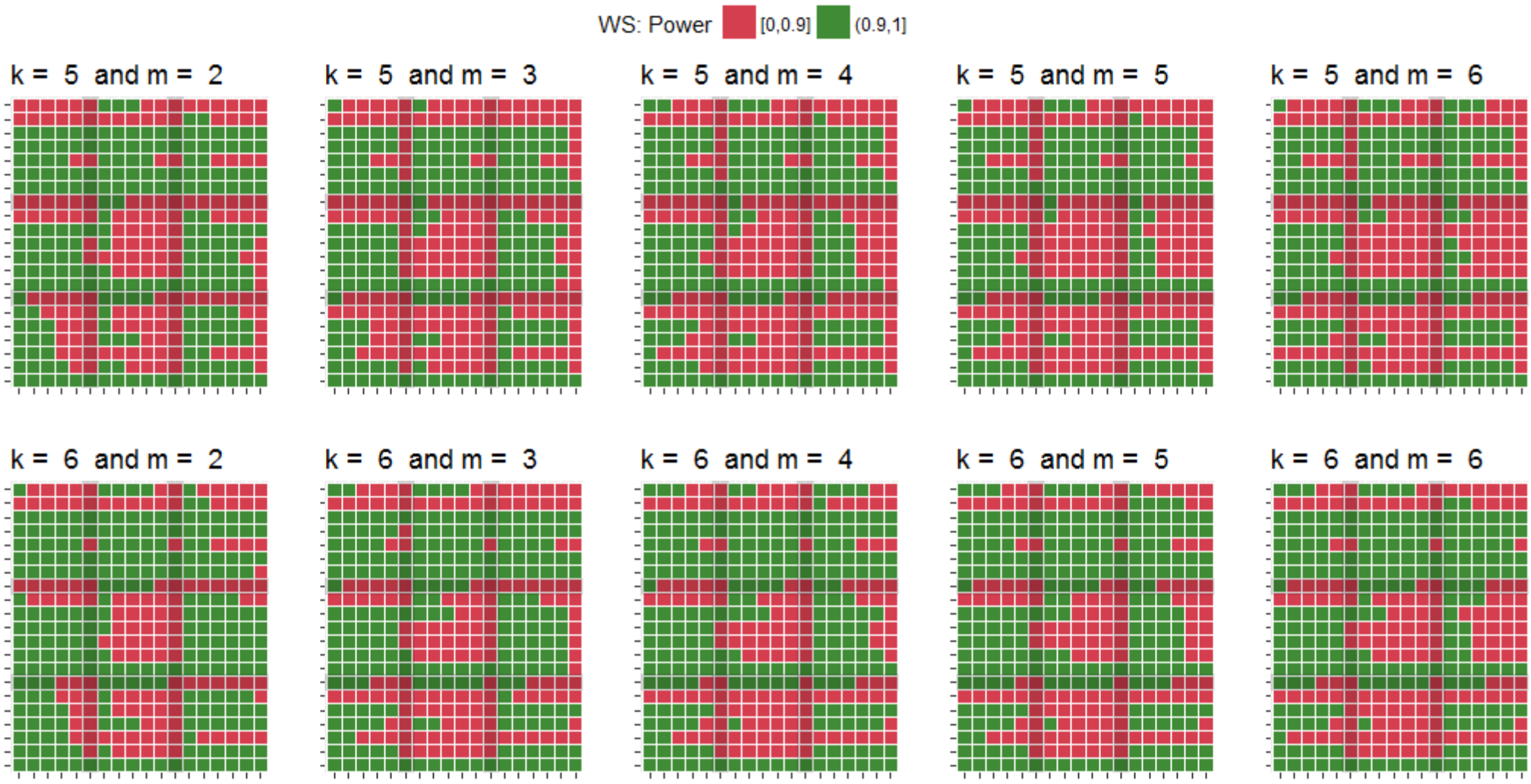

Figure A9. Power results for the Watts-Strogratz model for k = 5 and 6 across network measures, moments, degrade setting and proportions according to the key from Figure 9

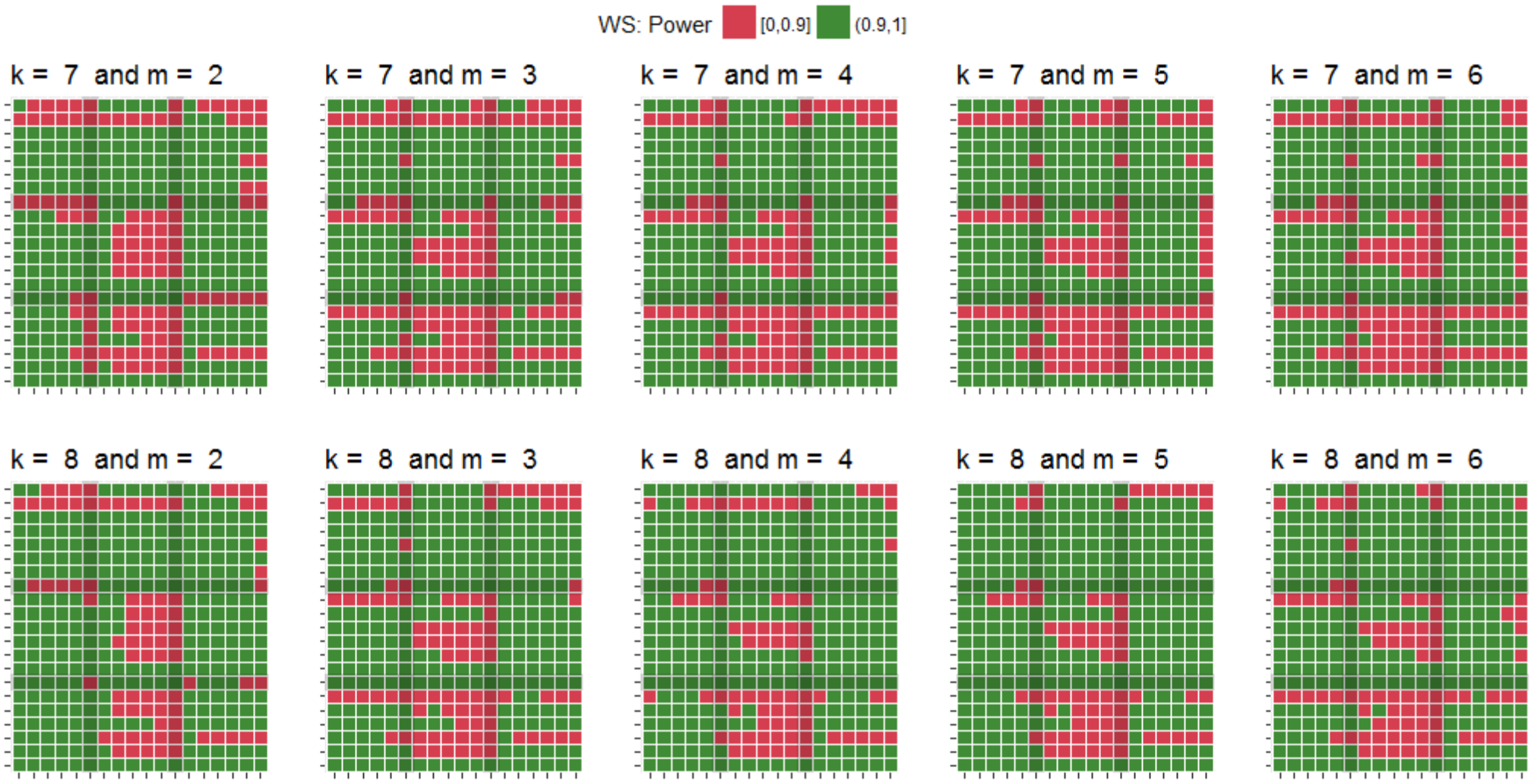

Figure A10. Power results for the Watts-Strogratz model for k = 7 and 8 across network measures, moments, degrade setting and proportions according to the key from Figure 9

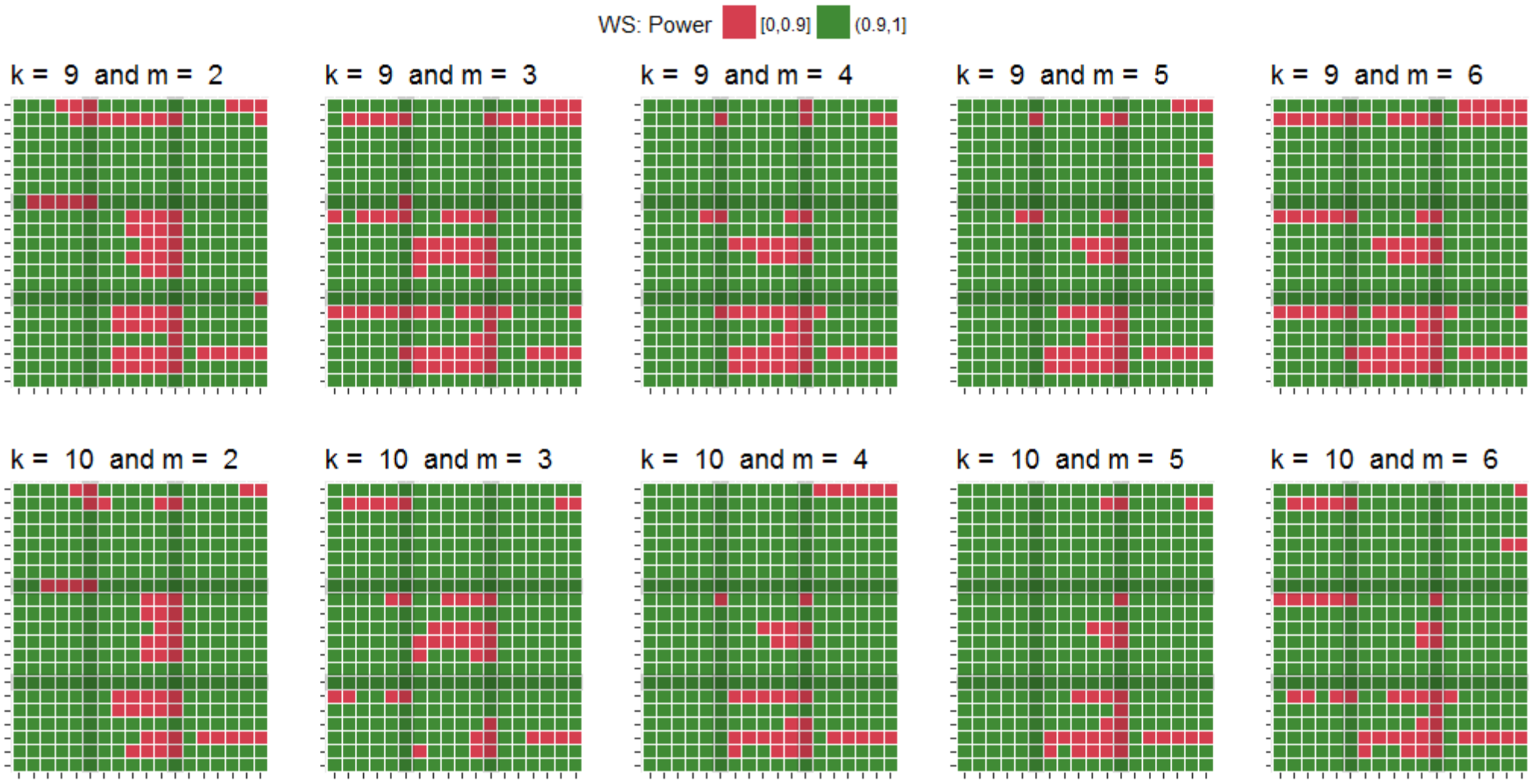

Figure A11. Power results for the Watts-Strogratz model for k = 9 and 10 across network measures, moments, degrade setting and proportions according to the key from Figure 9

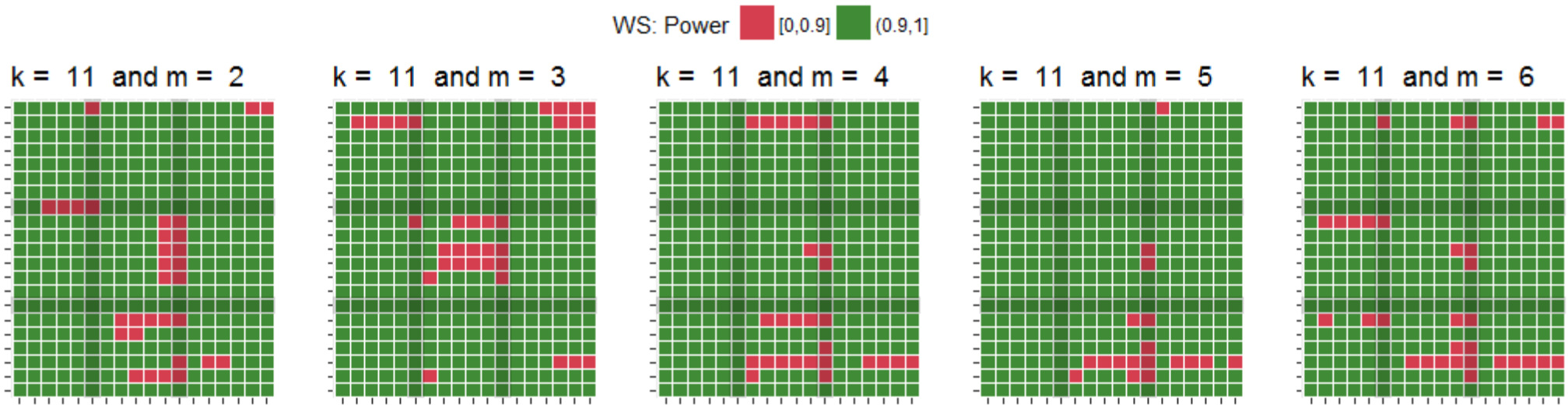

Figure A12. Power results for the Watts-Strogratz model for k = 11 across network measures, moments, degrade setting and proportions according to the key from Figure 9

Table A4. Tukey's Pairwise comparison for Erdös-Rényi model

		Difference	t ratio	Prob > |t|	Lower 95%	Upper 95%
Network Measures: All Pairwise Comparison						
betweenness	closeness	-0.1284	-13.55	<0.0001	-0.1507	-0.1062
betweenness	degree	0.0292	3.08	<0.0001	0.0069	0.0514
closeness	degree	0.1577	16.63	<0.0001	0.1354	0.1799
Moments: All Pairwise with Mean						
Mean	Variance	0.2906	20.07	<0.0001	0.2479	0.3334
Mean	Skewness	0.7212	49.80	<0.0001	0.6784	0.7639
Mean	Kurtosis	0.4219	29.13	<0.0001	0.3791	0.4646
Mean	L-scale	0.2902	20.04	<0.0001	0.2474	0.3329
Mean	L-skewness	0.5453	37.65	<0.0001	0.5025	0.5880
Mean	L-kurtosis	0.2909	20.09	<0.0001	0.2482	0.3337
Moments: Pairwise Traditional Moment vs L-moment						
Variance	L-scale	0.0000	0.03	1.00	-	-
Skewness	L-Skewness	0.1758	12.14	<0.0001	0.1331	0.2186
Kurtosis	L-kurtosis	0.1309	9.04	<0.0001	0.0881	0.1736

Table A5. Tukey's Pairwise comparison for Barabási-Albert model

		Difference	t ratio	Prob > |t|	Lower 95%	Upper 95%
Network Measures: All Pairwise Comparison						
betweenness	closeness	-0.0629	-6.84	<0.0001	-0.8461	-0.0413
betweenness	degree	0.0787	8.55	<0.0001	0.0571	0.1000
closeness	degree	0.1417	15.38	<0.0001	0.1201	0.1633
Moments: All Pairwise with Mean						
Mean	Variance	0.087	6.21	<0.0001	0.0458	0.1289
Mean	Skewness	0.2118	15.05	<0.0001	0.1703	0.2534
Mean	Kurtosis	0.2478	17.61	<0.0001	0.2063	0.2894
Mean	L-scale	0.0822	5.84	<0.0001	0.0406	0.1237
Mean	L-skewness	0.3716	26.40	<0.0001	0.3300	0.4131
Mean	L-kurtosis	0.6057	43.04	<0.0001	0.5641	0.6473
Moments: Pairwise Traditional Moment vs L-moment						
Variance	L-scale	-0.0051	-0.37	1.0	-	-
Skewness	L-Skewness	0.1597	11.35	<0.0001	0.1181	0.2013
Kurtosis	L-kurtosis	0.3578	25.43	<0.0001	0.3163	0.3994

Table A6. Tukey's Pairwise comparison for Watts-Strogratz model

		Difference	t ratio	Prob > $\|t\|$	Lower 95%	Upper 95%
Network Measures: All Pairwise Comparison						
betweenness	closeness	-0.1348	-14.62	<0.0001	-0.1564	-0.1131
betweenness	degree	0.0464	5.04	<0.0001	0.0248	0.0681
closeness	degree	0.1813	19.67	<0.0001	0.1596	0.2029
Moments: All Pairwise with Mean						
Mean	Variance	0.2762	19.61	<0.0001	0.2346	0.3178
Mean	Skewness	0.5325	37.82	<0.0001	0.4909	0.5741
Mean	Kurtosis	0.3360	23.87	<0.0001	0.2945	0.3776
Mean	L-scale	0.2410	17.12	<0.0001	0.1994	0.2826
Mean	L-skewness	0.6814	48.39	<0.0001	0.6398	0.7230
Mean	L-kurtosis	0.4322	30.70	<0.0001	0.3907	0.4738
Moments: Pairwise Traditional Moment vs L-moment						
Variance	L-scale	-0.0351	-2.5	0.1607	-	-
Skewness	L-Skewness	0.1489	10.57	<0.0001	0.1073	0.1904
Kurtosis	L-kurtosis	0.0961	6.83	<0.0001	0.0546	0.1377

Table A7. Erdös-Rényi Power based on Empirical Quantile Degrade Detection Low Degrade

		degree							betweenness							closeness						
k	m	m_1	m_2	m_3	m_4	l_2	t_3	t_4	m_1	m_2	m_3	m_4	l_2	t_3	t_4	m_1	m_2	m_3	m_4	l_2	t_3	t_4
5	2	0.20	0.06	0.05	0.05	0.06	0.05	0.05	0.07	0.07	0.06	0.06	0.07	0.05	0.05	0.07	0.05	0.06	0.06	0.05	0.05	0.05
5	3	0.24	0.05	0.05	0.05	0.05	0.05	0.05	0.12	0.06	0.05	0.06	0.06	0.05	0.05	0.12	0.06	0.06	0.05	0.06	0.05	0.05
5	4	0.30	0.05	0.05	0.05	0.05	0.05	0.05	0.25	0.05	0.05	0.05	0.05	0.05	0.05	0.37	0.06	0.06	0.05	0.06	0.05	0.05
5	5	0.30	0.05	0.05	0.05	0.05	0.05	0.05	0.33	0.05	0.05	0.05	0.05	0.05	0.05	0.36	0.05	0.06	0.05	0.05	0.05	0.05
5	6	0.30	0.05	0.05	0.05	0.05	0.05	0.05	0.32	0.05	0.05	0.05	0.05	0.05	0.05	0.35	0.05	0.06	0.05	0.05	0.05	0.05
6	2	0.12	0.06	0.05	0.06	0.06	0.05	0.05	0.10	0.08	0.06	0.07	0.08	0.05	0.05	0.11	0.06	0.06	0.06	0.06	0.05	0.05
6	3	0.51	0.05	0.05	0.05	0.05	0.05	0.05	0.18	0.06	0.05	0.06	0.06	0.05	0.05	0.24	0.06	0.06	0.06	0.06	0.05	0.05
6	4	0.82	0.05	0.05	0.05	0.05	0.05	0.05	0.67	0.06	0.05	0.06	0.06	0.05	0.05	0.96	0.06	0.06	0.06	0.06	0.05	0.05
6	5	0.89	0.05	0.05	0.05	0.05	0.05	0.05	0.69	0.06	0.05	0.06	0.06	0.05	0.05	0.99	0.06	0.06	0.05	0.06	0.05	0.05
6	6	0.93	0.06	0.05	0.05	0.05	0.05	0.05	0.72	0.06	0.05	0.06	0.06	0.05	0.05	1.00	0.06	0.06	0.05	0.06	0.05	0.05
7	2	0.09	0.06	0.05	0.06	0.06	0.05	0.05	0.16	0.10	0.07	0.08	0.11	0.05	0.05	0.19	0.06	0.06	0.06	0.06	0.05	0.05
7	3	0.46	0.06	0.05	0.06	0.06	0.05	0.06	0.60	0.09	0.06	0.07	0.10	0.05	0.05	0.82	0.07	0.07	0.06	0.08	0.05	0.06
7	4	0.80	0.06	0.05	0.06	0.06	0.05	0.06	0.96	0.09	0.06	0.07	0.10	0.05	0.06	1.00	0.07	0.07	0.06	0.07	0.05	0.05
7	5	0.94	0.06	0.05	0.06	0.06	0.05	0.05	1.00	0.08	0.06	0.07	0.09	0.05	0.05	1.00	0.07	0.07	0.05	0.07	0.06	0.05
7	6	0.97	0.06	0.05	0.06	0.06	0.06	0.05	1.00	0.07	0.06	0.07	0.08	0.05	0.05	1.00	0.07	0.07	0.06	0.07	0.06	0.05
8	2	0.08	0.06	0.06	0.06	0.06	0.06	0.05	0.30	0.14	0.08	0.09	0.18	0.06	0.05	0.35	0.07	0.06	0.06	0.07	0.05	0.05
8	3	0.49	0.07	0.06	0.06	0.07	0.06	0.06	0.97	0.15	0.08	0.09	0.19	0.06	0.06	1.00	0.09	0.07	0.07	0.09	0.06	0.06
8	4	0.89	0.07	0.05	0.06	0.07	0.06	0.06	1.00	0.14	0.08	0.09	0.17	0.06	0.05	1.00	0.09	0.07	0.07	0.08	0.06	0.06
8	5	0.98	0.07	0.05	0.06	0.07	0.05	0.06	1.00	0.12	0.07	0.09	0.14	0.05	0.05	1.00	0.07	0.07	0.06	0.06	0.06	0.06
8	6	1.00	0.06	0.05	0.06	0.07	0.05	0.06	1.00	0.11	0.06	0.08	0.12	0.05	0.05	1.00	0.08	0.07	0.05	0.08	0.05	0.06
9	2	0.10	0.07	0.06	0.06	0.07	0.06	0.06	0.49	0.20	0.09	0.10	0.31	0.06	0.05	0.56	0.07	0.06	0.06	0.07	0.05	0.06
9	3	0.40	0.08	0.06	0.07	0.08	0.06	0.07	1.00	0.25	0.10	0.11	0.37	0.06	0.05	1.00	0.11	0.07	0.08	0.11	0.06	0.06
9	4	0.94	0.08	0.06	0.07	0.09	0.06	0.07	1.00	0.24	0.10	0.12	0.33	0.06	0.06	1.00	0.12	0.07	0.08	0.11	0.06	0.06
9	5	0.99	0.08	0.05	0.07	0.08	0.06	0.06	1.00	0.18	0.08	0.10	0.22	0.05	0.06	1.00	0.08	0.07	0.06	0.08	0.06	0.06
9	6	1.00	0.08	0.05	0.07	0.09	0.05	0.06	1.00	0.17	0.08	0.10	0.21	0.05	0.06	1.00	0.09	0.07	0.06	0.09	0.06	0.06
10	2	0.18	0.09	0.06	0.07	0.09	0.06	0.07	0.79	0.31	0.12	0.12	0.57	0.06	0.05	0.86	0.08	0.06	0.06	0.08	0.05	0.06
10	3	0.35	0.11	0.07	0.08	0.11	0.06	0.08	1.00	0.42	0.14	0.15	0.66	0.06	0.06	1.00	0.15	0.08	0.10	0.14	0.06	0.07
10	4	0.96	0.12	0.07	0.08	0.13	0.06	0.08	1.00	0.40	0.13	0.14	0.57	0.06	0.06	1.00	0.17	0.09	0.11	0.16	0.06	0.07
10	5	1.00	0.11	0.05	0.08	0.12	0.06	0.07	1.00	0.30	0.10	0.12	0.41	0.06	0.06	1.00	0.11	0.07	0.07	0.10	0.06	0.07
10	6	1.00	0.12	0.06	0.08	0.13	0.06	0.08	1.00	0.30	0.10	0.13	0.40	0.06	0.06	1.00	0.15	0.08	0.08	0.14	0.06	0.08
11	2	0.30	0.12	0.07	0.08	0.14	0.06	0.10	0.98	0.51	0.16	0.15	0.87	0.06	0.06	0.99	0.09	0.06	0.08	0.09	0.05	0.07
11	3	0.39	0.17	0.08	0.10	0.18	0.07	0.11	1.00	0.67	0.20	0.20	0.93	0.07	0.06	1.00	0.21	0.11	0.14	0.19	0.06	0.08
11	4	0.98	0.18	0.09	0.11	0.20	0.08	0.11	1.00	0.66	0.20	0.21	0.86	0.07	0.07	1.00	0.33	0.14	0.17	0.32	0.07	0.09
11	5	1.00	0.18	0.06	0.11	0.20	0.06	0.10	1.00	0.51	0.14	0.16	0.70	0.05	0.07	1.00	0.13	0.08	0.09	0.12	0.06	0.08
11	6	1.00	0.20	0.07	0.11	0.22	0.06	0.11	1.00	0.54	0.14	0.18	0.71	0.06	0.07	1.00	0.19	0.08	0.10	0.18	0.06	0.10

m_1 (mean), m_2 (variance), m_3 (skewness), m_4 (kurtosis), l_2 (L-scale), t_3 (L-skewness), and t_4 (L-kurtosis)

Table A8. Erdös-Rényi Power based on Empirical Quantile Degrade Detection Med Degrade

		degree							betweenness							closeness						
k	m	m_1	m_2	m_3	m_4	l_2	t_3	t_4	m_1	m_2	m_3	m_4	l_2	t_3	t_4	m_1	m_2	m_3	m_4	l_2	t_3	t_4
5	2	0.62	0.05	0.04	0.05	0.05	0.04	0.05	0.06	0.05	0.05	0.05	0.05	0.05	0.05	0.07	0.09	0.08	0.08	0.09	0.05	0.05
5	3	0.81	0.05	0.04	0.05	0.05	0.05	0.05	0.08	0.05	0.05	0.05	0.05	0.05	0.05	0.08	0.08	0.08	0.07	0.09	0.05	0.05
5	4	0.76	0.05	0.05	0.05	0.05	0.05	0.05	0.27	0.05	0.05	0.05	0.05	0.05	0.05	0.75	0.08	0.07	0.06	0.08	0.05	0.05
5	5	0.69	0.05	0.04	0.05	0.05	0.05	0.05	0.54	0.05	0.05	0.05	0.05	0.05	0.05	0.71	0.07	0.07	0.05	0.07	0.05	0.05
5	6	0.65	0.05	0.05	0.05	0.05	0.05	0.05	0.65	0.05	0.05	0.05	0.05	0.05	0.05	0.67	0.06	0.07	0.06	0.06	0.05	0.05
6	2	0.59	0.05	0.04	0.06	0.05	0.04	0.06	0.08	0.05	0.05	0.05	0.05	0.05	0.06	0.11	0.11	0.08	0.08	0.12	0.05	0.05
6	3	0.97	0.05	0.04	0.05	0.05	0.05	0.05	0.13	0.05	0.05	0.05	0.05	0.05	0.05	0.28	0.10	0.08	0.07	0.10	0.05	0.05
6	4	1.00	0.05	0.05	0.05	0.05	0.05	0.05	0.48	0.05	0.05	0.05	0.05	0.05	0.05	0.90	0.09	0.07	0.06	0.09	0.05	0.05
6	5	0.99	0.05	0.05	0.05	0.05	0.05	0.05	0.45	0.05	0.05	0.05	0.05	0.05	0.05	0.93	0.08	0.07	0.05	0.09	0.05	0.05
6	6	0.99	0.05	0.05	0.05	0.05	0.05	0.05	0.47	0.05	0.05	0.05	0.05	0.05	0.05	0.97	0.08	0.07	0.05	0.08	0.05	0.05
7	2	0.66	0.05	0.04	0.06	0.05	0.04	0.06	0.12	0.05	0.05	0.05	0.04	0.05	0.06	0.19	0.15	0.08	0.10	0.16	0.05	0.06
7	3	1.00	0.05	0.04	0.05	0.05	0.04	0.06	0.29	0.05	0.05	0.05	0.05	0.05	0.06	0.64	0.14	0.08	0.08	0.16	0.05	0.05
7	4	1.00	0.05	0.05	0.05	0.05	0.05	0.05	0.76	0.05	0.05	0.05	0.05	0.05	0.06	0.98	0.12	0.08	0.07	0.12	0.05	0.06
7	5	1.00	0.05	0.05	0.05	0.05	0.05	0.05	0.93	0.05	0.05	0.05	0.05	0.05	0.05	1.00	0.10	0.07	0.06	0.10	0.05	0.05
7	6	1.00	0.05	0.05	0.05	0.05	0.05	0.05	0.90	0.05	0.05	0.05	0.05	0.05	0.05	1.00	0.10	0.07	0.06	0.10	0.05	0.05
8	2	0.82	0.05	0.05	0.06	0.05	0.04	0.08	0.24	0.05	0.05	0.06	0.05	0.05	0.06	0.37	0.22	0.09	0.13	0.24	0.05	0.06
8	3	1.00	0.05	0.05	0.06	0.05	0.04	0.07	0.63	0.05	0.05	0.05	0.05	0.05	0.06	0.95	0.20	0.08	0.10	0.23	0.05	0.06
8	4	1.00	0.05	0.05	0.06	0.05	0.05	0.06	0.95	0.05	0.05	0.05	0.05	0.05	0.06	1.00	0.20	0.08	0.09	0.23	0.05	0.06
8	5	1.00	0.05	0.05	0.05	0.05	0.05	0.06	1.00	0.05	0.05	0.05	0.05	0.05	0.05	1.00	0.16	0.07	0.07	0.18	0.05	0.06
8	6	1.00	0.05	0.05	0.05	0.05	0.05	0.06	1.00	0.05	0.05	0.05	0.05	0.05	0.06	1.00	0.12	0.07	0.06	0.13	0.05	0.05
9	2	0.96	0.05	0.05	0.06	0.05	0.04	0.11	0.46	0.06	0.06	0.06	0.07	0.05	0.07	0.68	0.35	0.10	0.18	0.38	0.05	0.07
9	3	1.00	0.05	0.05	0.06	0.05	0.04	0.08	0.94	0.05	0.05	0.05	0.05	0.05	0.06	1.00	0.35	0.10	0.15	0.39	0.05	0.06
9	4	1.00	0.05	0.05	0.06	0.05	0.04	0.07	1.00	0.05	0.05	0.05	0.05	0.05	0.06	1.00	0.26	0.08	0.11	0.29	0.05	0.05
9	5	1.00	0.05	0.05	0.06	0.05	0.05	0.07	1.00	0.05	0.05	0.05	0.06	0.05	0.06	1.00	0.31	0.08	0.09	0.36	0.05	0.06
9	6	1.00	0.05	0.05	0.05	0.05	0.05	0.07	1.00	0.05	0.05	0.05	0.05	0.05	0.06	1.00	0.27	0.08	0.08	0.32	0.05	0.06
10	2	1.00	0.06	0.06	0.07	0.05	0.05	0.18	0.81	0.09	0.08	0.08	0.11	0.05	0.09	0.95	0.55	0.14	0.28	0.59	0.06	0.08
10	3	1.00	0.05	0.05	0.07	0.05	0.04	0.13	1.00	0.05	0.05	0.06	0.05	0.04	0.08	1.00	0.54	0.13	0.22	0.59	0.05	0.07
10	4	1.00	0.05	0.04	0.06	0.05	0.04	0.09	1.00	0.05	0.05	0.05	0.05	0.05	0.07	1.00	0.48	0.12	0.17	0.53	0.05	0.07
10	5	1.00	0.05	0.05	0.06	0.05	0.05	0.09	1.00	0.05	0.05	0.05	0.06	0.05	0.07	1.00	0.34	0.08	0.13	0.37	0.05	0.06
10	6	1.00	0.05	0.05	0.06	0.05	0.05	0.09	1.00	0.05	0.05	0.05	0.06	0.05	0.07	1.00	0.46	0.08	0.11	0.53	0.06	0.08
11	2	1.00	0.06	0.07	0.09	0.05	0.06	0.32	0.98	0.13	0.09	0.09	0.19	0.06	0.12	1.00	0.80	0.24	0.47	0.83	0.06	0.10
11	3	1.00	0.05	0.05	0.07	0.05	0.04	0.23	1.00	0.05	0.05	0.06	0.05	0.04	0.11	1.00	0.80	0.22	0.39	0.84	0.06	0.10
11	4	1.00	0.05	0.04	0.07	0.05	0.04	0.13	1.00	0.05	0.05	0.05	0.07	0.05	0.09	1.00	0.78	0.14	0.27	0.85	0.05	0.10
11	5	1.00	0.05	0.05	0.06	0.05	0.05	0.13	1.00	0.05	0.05	0.05	0.06	0.06	0.09	1.00	0.65	0.16	0.22	0.70	0.08	0.07
11	6	1.00	0.05	0.05	0.06	0.05	0.05	0.12	1.00	0.05	0.05	0.05	0.06	0.06	0.10	1.00	0.45	0.08	0.14	0.48	0.05	0.07

m_1 (mean), m_2 (variance), m_3 (skewness), m_4 (kurtosis), l_2 (L-scale), t_3 (L-skewness), and t_4 (L-kurtosis)

Table A9. Erdös-Rényi Power based on Empirical Quantile Degrade Detection High Degrade

		degree							betweenness							closeness						
k	m	m_1	m_2	m_3	m_4	l_2	t_3	t_4	m_1	m_2	m_3	m_4	l_2	t_3	t_4	m_1	m_2	m_3	m_4	l_2	t_3	t_4
5	2	0.50	0.07	0.04	0.06	0.07	0.05	0.06	0.08	0.06	0.05	0.05	0.06	0.05	0.05	0.07	0.06	0.06	0.06	0.06	0.05	0.05
5	3	0.34	0.06	0.04	0.06	0.06	0.05	0.05	0.06	0.05	0.05	0.05	0.05	0.05	0.05	0.05	0.06	0.06	0.05	0.06	0.05	0.05
5	4	0.29	0.05	0.04	0.05	0.05	0.05	0.05	0.07	0.05	0.05	0.05	0.05	0.05	0.05	0.28	0.06	0.06	0.05	0.06	0.05	0.05
5	5	0.29	0.05	0.04	0.05	0.05	0.05	0.05	0.15	0.05	0.05	0.05	0.05	0.05	0.05	0.33	0.06	0.06	0.05	0.06	0.05	0.05
5	6	0.29	0.05	0.05	0.05	0.05	0.05	0.05	0.28	0.05	0.05	0.05	0.05	0.05	0.05	0.33	0.06	0.06	0.05	0.05	0.05	0.05
6	2	0.84	0.07	0.04	0.07	0.07	0.06	0.06	0.10	0.07	0.06	0.05	0.08	0.05	0.05	0.08	0.07	0.07	0.06	0.07	0.05	0.05
6	3	1.00	0.06	0.04	0.06	0.06	0.05	0.05	0.08	0.06	0.06	0.05	0.06	0.05	0.05	0.08	0.06	0.07	0.06	0.06	0.05	0.05
6	4	1.00	0.05	0.04	0.06	0.05	0.05	0.05	0.09	0.06	0.05	0.05	0.06	0.05	0.05	0.45	0.07	0.07	0.06	0.07	0.05	0.05
6	5	1.00	0.06	0.04	0.06	0.05	0.05	0.06	0.11	0.06	0.05	0.05	0.05	0.05	0.05	0.69	0.08	0.07	0.05	0.08	0.06	0.05
6	6	1.00	0.06	0.04	0.06	0.06	0.05	0.05	0.17	0.05	0.05	0.05	0.05	0.05	0.05	0.89	0.08	0.07	0.05	0.08	0.05	0.05
7	2	0.93	0.09	0.04	0.08	0.09	0.06	0.06	0.12	0.08	0.06	0.06	0.10	0.06	0.06	0.09	0.08	0.07	0.06	0.08	0.05	0.05
7	3	1.00	0.07	0.04	0.08	0.08	0.06	0.05	0.13	0.07	0.06	0.05	0.08	0.06	0.06	0.10	0.09	0.07	0.06	0.10	0.05	0.05
7	4	1.00	0.07	0.04	0.07	0.08	0.05	0.06	0.11	0.06	0.05	0.05	0.06	0.06	0.06	0.61	0.09	0.07	0.06	0.09	0.06	0.05
7	5	1.00	0.07	0.04	0.07	0.08	0.06	0.06	0.32	0.06	0.05	0.05	0.06	0.06	0.05	0.97	0.07	0.07	0.06	0.07	0.06	0.06
7	6	1.00	0.07	0.04	0.07	0.07	0.06	0.06	0.30	0.06	0.06	0.05	0.06	0.06	0.05	0.99	0.08	0.08	0.06	0.08	0.06	0.05
8	2	1.00	0.14	0.05	0.10	0.15	0.07	0.06	0.17	0.11	0.07	0.06	0.15	0.06	0.06	0.10	0.09	0.07	0.07	0.10	0.06	0.05
8	3	1.00	0.12	0.04	0.10	0.12	0.06	0.06	0.19	0.09	0.06	0.06	0.10	0.06	0.06	0.12	0.11	0.07	0.07	0.12	0.05	0.06
8	4	1.00	0.11	0.04	0.09	0.11	0.06	0.06	0.13	0.07	0.06	0.05	0.07	0.06	0.06	0.83	0.15	0.08	0.08	0.17	0.06	0.05
8	5	1.00	0.10	0.04	0.09	0.11	0.06	0.06	0.60	0.06	0.06	0.05	0.06	0.06	0.06	1.00	0.13	0.07	0.07	0.13	0.06	0.05
8	6	1.00	0.09	0.04	0.08	0.10	0.06	0.06	0.94	0.06	0.06	0.05	0.05	0.06	0.06	1.00	0.08	0.07	0.06	0.07	0.06	0.07
9	2	1.00	0.22	0.05	0.13	0.26	0.07	0.06	0.24	0.15	0.09	0.07	0.23	0.08	0.07	0.12	0.11	0.07	0.07	0.12	0.06	0.05
9	3	1.00	0.20	0.04	0.13	0.22	0.06	0.06	0.29	0.12	0.07	0.06	0.14	0.07	0.07	0.15	0.17	0.07	0.09	0.19	0.06	0.05
9	4	1.00	0.18	0.04	0.12	0.20	0.06	0.07	0.16	0.09	0.07	0.06	0.10	0.07	0.07	0.98	0.16	0.08	0.09	0.16	0.06	0.08
9	5	1.00	0.16	0.04	0.11	0.17	0.06	0.07	0.49	0.07	0.06	0.06	0.06	0.06	0.07	1.00	0.21	0.08	0.08	0.24	0.07	0.05
9	6	1.00	0.15	0.04	0.11	0.16	0.06	0.06	0.99	0.06	0.06	0.05	0.06	0.06	0.07	1.00	0.26	0.08	0.08	0.29	0.05	0.05
10	2	1.00	0.41	0.05	0.17	0.49	0.09	0.07	0.40	0.25	0.12	0.08	0.39	0.09	0.08	0.18	0.13	0.06	0.08	0.14	0.06	0.05
10	3	1.00	0.36	0.04	0.18	0.40	0.07	0.08	0.42	0.19	0.10	0.08	0.25	0.09	0.09	0.17	0.23	0.08	0.11	0.23	0.06	0.07
10	4	1.00	0.33	0.04	0.18	0.37	0.07	0.09	0.33	0.14	0.09	0.07	0.14	0.10	0.09	1.00	0.37	0.11	0.15	0.39	0.07	0.06
10	5	1.00	0.28	0.04	0.16	0.30	0.06	0.08	0.73	0.08	0.07	0.06	0.07	0.07	0.08	1.00	0.10	0.08	0.09	0.09	0.06	0.10
10	6	1.00	0.26	0.04	0.15	0.29	0.06	0.08	0.99	0.07	0.07	0.06	0.07	0.07	0.08	1.00	0.30	0.08	0.09	0.34	0.10	0.05
11	2	1.00	0.70	0.06	0.27	0.80	0.11	0.09	0.62	0.42	0.17	0.11	0.64	0.13	0.12	0.30	0.18	0.07	0.10	0.18	0.06	0.05
11	3	1.00	0.63	0.04	0.29	0.70	0.10	0.11	0.60	0.34	0.16	0.11	0.42	0.14	0.13	0.19	0.37	0.11	0.17	0.39	0.06	0.05
11	4	1.00	0.58	0.04	0.28	0.64	0.09	0.12	0.30	0.25	0.15	0.10	0.26	0.14	0.13	1.00	0.62	0.10	0.23	0.68	0.12	0.05
11	5	1.00	0.49	0.05	0.25	0.53	0.06	0.10	1.00	0.09	0.09	0.07	0.07	0.08	0.11	1.00	0.33	0.17	0.17	0.31	0.16	0.09
11	6	1.00	0.49	0.04	0.25	0.53	0.06	0.11	1.00	0.08	0.09	0.07	0.07	0.08	0.11	1.00	0.09	0.08	0.09	0.08	0.06	0.16

m_1 (mean), m_2 (variance), m_3 (skewness), m_4 (kurtosis), l_2 (L-scale), t_3 (L-skewness), and t_4 (L-kurtosis)

Table A10. Barabási-Albert Power based on Empirical Quantile Degrade Detection Low Degrade

		degree							betweenness							closeness						
k	m	m_1	m_2	m_3	m_4	l_2	t_3	t_4	m_1	m_2	m_3	m_4	l_2	t_3	t_4	m_1	m_2	m_3	m_4	l_2	t_3	t_4
5	2	0.99	0.05	0.05	0.05	0.06	0.06	0.05	0.12	0.08	0.06	0.06	0.11	0.05	0.05	0.25	0.10	0.08	0.07	0.12	0.06	0.06
5	3	0.80	0.05	0.05	0.05	0.05	0.05	0.05	0.27	0.06	0.06	0.06	0.07	0.05	0.06	0.62	0.13	0.07	0.06	0.17	0.05	0.06
5	4	0.44	0.04	0.05	0.05	0.04	0.05	0.05	0.29	0.05	0.05	0.05	0.05	0.05	0.05	0.46	0.10	0.06	0.06	0.13	0.05	0.05
5	5	0.35	0.05	0.05	0.05	0.05	0.05	0.05	0.32	0.06	0.05	0.06	0.06	0.05	0.05	0.38	0.07	0.06	0.05	0.10	0.05	0.05
5	6	0.42	0.05	0.05	0.06	0.05	0.05	0.05	0.43	0.06	0.06	0.06	0.07	0.05	0.05	0.45	0.07	0.06	0.05	0.10	0.05	0.05
6	2	1.00	0.06	0.05	0.05	0.06	0.05	0.05	0.22	0.10	0.07	0.07	0.40	0.05	0.05	0.38	0.13	0.10	0.08	0.12	0.05	0.05
6	3	1.00	0.05	0.05	0.05	0.05	0.05	0.05	0.36	0.08	0.06	0.07	0.17	0.05	0.05	0.72	0.16	0.11	0.09	0.16	0.05	0.05
6	4	1.00	0.05	0.05	0.05	0.05	0.05	0.05	0.37	0.07	0.06	0.06	0.10	0.05	0.05	0.61	0.18	0.10	0.07	0.20	0.05	0.06
6	5	1.00	0.05	0.05	0.05	0.05	0.05	0.05	0.33	0.07	0.06	0.06	0.08	0.05	0.05	0.75	0.16	0.07	0.06	0.18	0.05	0.05
6	6	1.00	0.06	0.06	0.06	0.06	0.06	0.05	0.55	0.08	0.06	0.07	0.10	0.05	0.05	0.95	0.17	0.07	0.06	0.20	0.06	0.05
7	2	1.00	0.06	0.06	0.06	0.06	0.06	0.05	0.33	0.13	0.09	0.08	0.94	0.06	0.06	0.54	0.14	0.14	0.11	0.13	0.05	0.05
7	3	1.00	0.06	0.05	0.05	0.06	0.05	0.05	0.49	0.10	0.07	0.07	0.57	0.05	0.05	0.82	0.19	0.14	0.11	0.17	0.05	0.05
7	4	1.00	0.06	0.05	0.05	0.06	0.05	0.05	0.64	0.09	0.07	0.07	0.31	0.05	0.05	0.93	0.25	0.15	0.13	0.20	0.05	0.05
7	5	1.00	0.06	0.06	0.05	0.06	0.05	0.05	0.70	0.08	0.07	0.07	0.22	0.05	0.05	0.95	0.33	0.18	0.13	0.28	0.05	0.05
7	6	1.00	0.06	0.06	0.06	0.06	0.05	0.05	0.71	0.09	0.07	0.07	0.20	0.05	0.05	0.96	0.45	0.19	0.14	0.41	0.05	0.06
8	2	1.00	0.06	0.06	0.06	0.08	0.06	0.05	0.51	0.14	0.09	0.08	1.00	0.06	0.06	0.75	0.15	0.17	0.15	0.14	0.05	0.05
8	3	1.00	0.06	0.06	0.06	0.07	0.06	0.05	0.69	0.12	0.08	0.08	1.00	0.06	0.05	0.94	0.24	0.24	0.17	0.19	0.05	0.05
8	4	1.00	0.06	0.05	0.06	0.06	0.05	0.05	0.81	0.11	0.08	0.07	0.85	0.05	0.05	0.99	0.30	0.22	0.17	0.22	0.05	0.05
8	5	1.00	0.06	0.05	0.05	0.06	0.05	0.05	0.91	0.09	0.07	0.07	0.59	0.05	0.05	1.00	0.38	0.26	0.20	0.25	0.05	0.05
8	6	1.00	0.06	0.05	0.05	0.06	0.05	0.05	0.93	0.09	0.07	0.07	0.45	0.05	0.05	1.00	0.51	0.34	0.26	0.33	0.05	0.05
9	2	1.00	0.06	0.06	0.06	0.09	0.07	0.05	0.70	0.15	0.09	0.08	1.00	0.06	0.06	0.89	0.16	0.17	0.19	0.15	0.05	0.05
9	3	1.00	0.06	0.06	0.06	0.08	0.06	0.05	0.86	0.13	0.09	0.08	1.00	0.06	0.06	0.99	0.24	0.32	0.24	0.20	0.05	0.05
9	4	1.00	0.06	0.06	0.06	0.08	0.05	0.05	0.92	0.12	0.08	0.08	1.00	0.05	0.05	1.00	0.36	0.37	0.25	0.28	0.05	0.06
9	5	1.00	0.06	0.06	0.05	0.07	0.05	0.05	0.97	0.11	0.08	0.07	0.99	0.05	0.05	1.00	0.43	0.33	0.25	0.27	0.06	0.05
9	6	1.00	0.06	0.06	0.06	0.07	0.05	0.05	0.99	0.10	0.08	0.07	0.91	0.05	0.05	1.00	0.49	0.38	0.30	0.28	0.05	0.05
10	2	1.00	0.07	0.06	0.06	0.13	0.08	0.06	0.88	0.16	0.10	0.09	1.00	0.06	0.06	0.97	0.17	0.15	0.21	0.18	0.05	0.05
10	3	1.00	0.06	0.06	0.06	0.11	0.06	0.06	0.97	0.14	0.09	0.08	1.00	0.06	0.06	1.00	0.26	0.35	0.35	0.22	0.05	0.05
10	4	1.00	0.06	0.06	0.06	0.10	0.06	0.06	0.98	0.13	0.09	0.08	1.00	0.06	0.05	1.00	0.35	0.56	0.37	0.28	0.05	0.05
10	5	1.00	0.06	0.06	0.06	0.09	0.05	0.06	0.99	0.12	0.09	0.08	1.00	0.06	0.05	1.00	0.49	0.56	0.35	0.35	0.05	0.06
10	6	1.00	0.06	0.06	0.05	0.08	0.05	0.06	1.00	0.11	0.08	0.08	1.00	0.05	0.05	1.00	0.53	0.48	0.35	0.32	0.06	0.06
11	2	1.00	0.07	0.06	0.06	0.19	0.10	0.05	0.97	0.16	0.10	0.08	1.00	0.07	0.06	1.00	0.20	0.15	0.23	0.21	0.05	0.05
11	3	1.00	0.06	0.06	0.06	0.16	0.07	0.06	1.00	0.14	0.09	0.08	1.00	0.06	0.06	1.00	0.29	0.32	0.42	0.27	0.05	0.05
11	4	1.00	0.06	0.06	0.06	0.14	0.06	0.06	1.00	0.13	0.09	0.08	1.00	0.06	0.05	1.00	0.34	0.58	0.54	0.28	0.05	0.05
11	5	1.00	0.06	0.06	0.06	0.12	0.05	0.06	1.00	0.13	0.09	0.08	1.00	0.06	0.05	1.00	0.47	0.75	0.53	0.37	0.05	0.05
11	6	1.00	0.06	0.06	0.05	0.11	0.05	0.06	1.00	0.12	0.09	0.08	1.00	0.06	0.05	1.00	0.62	0.76	0.49	0.46	0.05	0.06

m_1 (mean), m_2 (variance), m_3 (skewness), m_4 (kurtosis), l_2 (L-scale), t_3 (L-skewness), and t_4 (L-kurtosis)

Table A11. Barabási-Albert Power based on Empirical Quantile Degrade Detection Med Degrade

		degree							betweenness							closeness						
k	m	m_1	m_2	m_3	m_4	l_2	t_3	t_4	m_1	m_2	m_3	m_4	l_2	t_3	t_4	m_1	m_2	m_3	m_4	l_2	t_3	t_4
5	2	0.93	0.04	0.05	0.05	0.05	0.07	0.05	0.32	0.08	0.06	0.07	0.15	0.06	0.06	0.58	0.25	0.12	0.10	0.32	0.08	0.06
5	3	0.75	0.05	0.05	0.05	0.04	0.06	0.05	0.18	0.05	0.05	0.05	0.04	0.05	0.05	0.45	0.17	0.08	0.07	0.24	0.07	0.05
5	4	0.44	0.05	0.05	0.05	0.05	0.05	0.05	0.18	0.05	0.05	0.05	0.05	0.05	0.05	0.42	0.13	0.06	0.06	0.19	0.05	0.05
5	5	0.23	0.05	0.05	0.05	0.05	0.05	0.05	0.19	0.05	0.05	0.05	0.05	0.05	0.05	0.26	0.09	0.06	0.06	0.12	0.05	0.05
5	6	0.09	0.05	0.05	0.05	0.05	0.05	0.05	0.11	0.05	0.05	0.05	0.05	0.05	0.05	0.13	0.06	0.05	0.05	0.07	0.05	0.05
6	2	1.00	0.05	0.06	0.06	0.05	0.07	0.05	0.40	0.13	0.09	0.09	0.60	0.06	0.06	0.68	0.28	0.16	0.14	0.29	0.08	0.06
6	3	1.00	0.05	0.05	0.05	0.04	0.07	0.05	0.25	0.06	0.06	0.06	0.08	0.05	0.05	0.48	0.21	0.11	0.09	0.23	0.07	0.05
6	4	1.00	0.05	0.05	0.05	0.05	0.06	0.05	0.27	0.06	0.06	0.06	0.06	0.05	0.05	0.58	0.25	0.10	0.09	0.29	0.06	0.05
6	5	0.99	0.05	0.05	0.05	0.05	0.06	0.05	0.25	0.06	0.06	0.06	0.05	0.05	0.05	0.62	0.23	0.08	0.07	0.29	0.06	0.05
6	6	0.88	0.05	0.05	0.05	0.05	0.05	0.05	0.26	0.05	0.05	0.05	0.05	0.05	0.05	0.74	0.19	0.06	0.06	0.24	0.06	0.05
7	2	1.00	0.06	0.06	0.06	0.06	0.09	0.05	0.56	0.18	0.11	0.10	0.95	0.07	0.06	0.83	0.31	0.21	0.20	0.30	0.07	0.06
7	3	1.00	0.05	0.06	0.06	0.05	0.09	0.05	0.29	0.07	0.06	0.06	0.22	0.06	0.06	0.59	0.24	0.12	0.11	0.23	0.08	0.05
7	4	1.00	0.05	0.06	0.05	0.06	0.08	0.05	0.50	0.07	0.06	0.06	0.14	0.05	0.05	0.86	0.33	0.14	0.14	0.30	0.07	0.05
7	5	1.00	0.05	0.05	0.05	0.05	0.07	0.05	0.52	0.07	0.06	0.06	0.11	0.05	0.05	0.90	0.40	0.18	0.15	0.37	0.06	0.05
7	6	1.00	0.05	0.05	0.05	0.05	0.06	0.05	0.40	0.06	0.06	0.06	0.07	0.05	0.05	0.80	0.46	0.18	0.14	0.43	0.05	0.05
8	2	1.00	0.07	0.07	0.06	0.07	0.13	0.06	0.79	0.22	0.13	0.11	1.00	0.07	0.07	0.96	0.35	0.26	0.31	0.33	0.08	0.06
8	3	1.00	0.05	0.06	0.06	0.05	0.13	0.05	0.40	0.08	0.07	0.07	0.58	0.06	0.06	0.75	0.29	0.17	0.16	0.25	0.07	0.05
8	4	1.00	0.06	0.06	0.06	0.06	0.11	0.05	0.67	0.09	0.07	0.07	0.46	0.06	0.06	0.95	0.42	0.19	0.19	0.35	0.07	0.05
8	5	1.00	0.05	0.05	0.05	0.05	0.09	0.05	0.80	0.08	0.07	0.07	0.30	0.06	0.05	0.99	0.45	0.23	0.21	0.34	0.06	0.05
8	6	1.00	0.05	0.05	0.05	0.05	0.08	0.05	0.69	0.07	0.06	0.06	0.16	0.05	0.05	0.96	0.49	0.29	0.24	0.35	0.05	0.05
9	2	1.00	0.07	0.07	0.06	0.07	0.20	0.06	0.94	0.23	0.13	0.11	1.00	0.08	0.07	1.00	0.39	0.26	0.42	0.37	0.09	0.06
9	3	1.00	0.06	0.06	0.06	0.07	0.20	0.05	0.57	0.09	0.07	0.07	0.97	0.07	0.06	0.88	0.29	0.19	0.23	0.25	0.08	0.05
9	4	1.00	0.06	0.06	0.06	0.07	0.17	0.05	0.81	0.10	0.08	0.07	0.97	0.06	0.06	0.99	0.51	0.33	0.27	0.42	0.06	0.05
9	5	1.00	0.06	0.06	0.06	0.06	0.13	0.05	0.90	0.09	0.07	0.07	0.79	0.06	0.06	1.00	0.57	0.28	0.26	0.43	0.07	0.05
9	6	1.00	0.05	0.06	0.05	0.05	0.10	0.05	0.88	0.08	0.07	0.07	0.51	0.06	0.06	1.00	0.53	0.31	0.27	0.36	0.07	0.05
10	2	1.00	0.08	0.07	0.07	0.07	0.32	0.06	0.99	0.24	0.13	0.11	1.00	0.10	0.08	1.00	0.42	0.23	0.48	0.43	0.12	0.06
10	3	1.00	0.06	0.06	0.06	0.09	0.34	0.05	0.76	0.10	0.07	0.07	1.00	0.07	0.07	0.97	0.31	0.19	0.34	0.28	0.12	0.06
10	4	1.00	0.06	0.06	0.06	0.08	0.30	0.05	0.94	0.11	0.08	0.08	1.00	0.08	0.07	1.00	0.48	0.49	0.42	0.39	0.06	0.05
10	5	1.00	0.06	0.06	0.06	0.06	0.21	0.05	0.96	0.10	0.08	0.07	1.00	0.07	0.06	1.00	0.64	0.50	0.37	0.52	0.06	0.05
10	6	1.00	0.06	0.06	0.05	0.06	0.16	0.05	0.92	0.09	0.07	0.07	0.96	0.06	0.06	1.00	0.67	0.36	0.32	0.48	0.07	0.05
11	2	1.00	0.08	0.07	0.06	0.09	0.53	0.06	1.00	0.24	0.14	0.11	1.00	0.13	0.10	1.00	0.49	0.22	0.52	0.51	0.16	0.07
11	3	1.00	0.06	0.06	0.06	0.13	0.57	0.05	0.92	0.10	0.07	0.07	1.00	0.09	0.08	1.00	0.34	0.17	0.41	0.33	0.14	0.06
11	4	1.00	0.06	0.06	0.06	0.10	0.51	0.05	0.99	0.12	0.08	0.08	1.00	0.09	0.08	1.00	0.46	0.47	0.61	0.39	0.10	0.05
11	5	1.00	0.06	0.06	0.06	0.07	0.35	0.05	0.99	0.11	0.08	0.07	1.00	0.08	0.07	1.00	0.58	0.71	0.57	0.46	0.06	0.05
11	6	1.00	0.06	0.06	0.05	0.07	0.27	0.05	0.95	0.09	0.08	0.07	1.00	0.07	0.06	1.00	0.75	0.65	0.48	0.62	0.05	0.05

m_1 (mean), m_2 (variance), m_3 (skewness), m_4 (kurtosis), l_2 (L-scale), t_3 (L-skewness), and t_4 (L-kurtosis)

Table A12. Barabási-Albert Power based on Empirical Quantile Degrade Detection High Degrade

		degree							betweenness							closeness						
k	m	m_1	m_2	m_3	m_4	l_2	t_3	t_4	m_1	m_2	m_3	m_4	l_2	t_3	t_4	m_1	m_2	m_3	m_4	l_2	t_3	t_4
5	2	0.17	0.06	0.06	0.06	0.08	0.06	0.06	0.09	0.05	0.05	0.05	0.08	0.05	0.05	0.08	0.08	0.06	0.06	0.09	0.08	0.05
5	3	0.08	0.06	0.05	0.05	0.07	0.05	0.05	0.06	0.05	0.05	0.05	0.05	0.05	0.05	0.06	0.06	0.05	0.05	0.07	0.06	0.05
5	4	0.04	0.05	0.05	0.05	0.06	0.05	0.05	0.05	0.05	0.05	0.05	0.05	0.05	0.05	0.06	0.06	0.05	0.05	0.06	0.05	0.05
5	5	0.03	0.06	0.05	0.05	0.06	0.05	0.05	0.05	0.05	0.05	0.05	0.05	0.05	0.05	0.07	0.05	0.05	0.05	0.05	0.05	0.05
5	6	0.03	0.05	0.05	0.05	0.06	0.05	0.05	0.04	0.05	0.05	0.05	0.05	0.05	0.05	0.08	0.05	0.05	0.05	0.05	0.05	0.05
6	2	1.00	0.13	0.09	0.09	0.23	0.12	0.08	0.24	0.05	0.05	0.05	0.29	0.06	0.05	0.20	0.12	0.12	0.08	0.13	0.19	0.05
6	3	1.00	0.15	0.09	0.09	0.28	0.09	0.07	0.22	0.06	0.05	0.05	0.13	0.06	0.05	0.17	0.13	0.09	0.08	0.14	0.12	0.07
6	4	1.00	0.17	0.09	0.09	0.31	0.08	0.08	0.21	0.06	0.05	0.05	0.08	0.06	0.05	0.15	0.16	0.10	0.08	0.17	0.08	0.07
6	5	1.00	0.18	0.09	0.09	0.35	0.07	0.08	0.20	0.06	0.05	0.05	0.07	0.06	0.06	0.16	0.19	0.09	0.08	0.20	0.08	0.05
6	6	1.00	0.20	0.09	0.09	0.36	0.07	0.08	0.18	0.06	0.06	0.05	0.07	0.06	0.06	0.23	0.18	0.07	0.06	0.21	0.07	0.05
7	2	1.00	0.20	0.12	0.11	0.39	0.23	0.10	0.33	0.05	0.05	0.05	0.53	0.08	0.06	0.26	0.15	0.18	0.10	0.15	0.27	0.06
7	3	1.00	0.23	0.13	0.11	0.48	0.17	0.10	0.30	0.06	0.06	0.05	0.25	0.07	0.06	0.22	0.18	0.13	0.10	0.18	0.23	0.06
7	4	1.00	0.25	0.13	0.11	0.53	0.13	0.09	0.27	0.06	0.06	0.06	0.11	0.06	0.06	0.21	0.19	0.14	0.12	0.17	0.19	0.09
7	5	1.00	0.28	0.13	0.12	0.58	0.10	0.09	0.25	0.06	0.06	0.06	0.08	0.06	0.06	0.21	0.23	0.18	0.14	0.20	0.09	0.11
7	6	1.00	0.32	0.14	0.12	0.63	0.09	0.10	0.25	0.06	0.06	0.05	0.07	0.06	0.06	0.22	0.31	0.26	0.18	0.23	0.08	0.10
8	2	1.00	0.25	0.15	0.12	0.58	0.40	0.16	0.40	0.06	0.06	0.06	0.76	0.12	0.07	0.30	0.17	0.25	0.12	0.17	0.40	0.06
8	3	1.00	0.32	0.17	0.13	0.72	0.33	0.14	0.37	0.06	0.06	0.06	0.50	0.09	0.06	0.26	0.23	0.19	0.13	0.22	0.22	0.05
8	4	1.00	0.38	0.19	0.15	0.80	0.26	0.13	0.35	0.06	0.06	0.06	0.20	0.08	0.06	0.26	0.27	0.18	0.14	0.27	0.41	0.10
8	5	1.00	0.43	0.20	0.16	0.85	0.21	0.13	0.32	0.06	0.06	0.06	0.09	0.07	0.06	0.30	0.24	0.22	0.17	0.17	0.38	0.11
8	6	1.00	0.48	0.22	0.17	0.89	0.17	0.14	0.30	0.07	0.06	0.06	0.08	0.07	0.07	0.34	0.30	0.28	0.24	0.23	0.14	0.21
9	2	1.00	0.31	0.16	0.13	0.80	0.62	0.26	0.48	0.06	0.06	0.05	0.89	0.17	0.10	0.36	0.18	0.29	0.15	0.19	0.55	0.10
9	3	1.00	0.39	0.19	0.15	0.90	0.54	0.22	0.43	0.06	0.06	0.06	0.75	0.14	0.08	0.29	0.24	0.25	0.17	0.23	0.28	0.06
9	4	1.00	0.47	0.23	0.17	0.95	0.43	0.20	0.40	0.07	0.06	0.06	0.41	0.12	0.08	0.28	0.33	0.21	0.17	0.33	0.17	0.09
9	5	1.00	0.54	0.25	0.19	0.97	0.35	0.18	0.38	0.07	0.06	0.06	0.14	0.11	0.08	0.31	0.40	0.25	0.18	0.46	0.69	0.20
9	6	1.00	0.61	0.29	0.22	0.99	0.31	0.18	0.34	0.07	0.06	0.06	0.08	0.10	0.08	0.42	0.27	0.32	0.22	0.20	0.71	0.13
10	2	1.00	0.38	0.18	0.14	0.96	0.86	0.44	0.58	0.06	0.06	0.06	0.95	0.25	0.14	0.43	0.19	0.31	0.16	0.21	0.72	0.14
10	3	1.00	0.48	0.22	0.16	0.99	0.78	0.36	0.50	0.07	0.06	0.06	0.93	0.20	0.11	0.32	0.27	0.26	0.22	0.27	0.43	0.06
10	4	1.00	0.57	0.26	0.19	1.00	0.67	0.31	0.44	0.07	0.06	0.06	0.64	0.19	0.11	0.29	0.28	0.25	0.23	0.25	0.11	0.08
10	5	1.00	0.65	0.31	0.22	1.00	0.57	0.27	0.46	0.07	0.06	0.06	0.36	0.17	0.11	0.30	0.51	0.24	0.22	0.54	0.15	0.21
10	6	1.00	0.72	0.35	0.25	1.00	0.49	0.27	0.42	0.07	0.06	0.06	0.11	0.16	0.10	0.37	0.67	0.34	0.23	0.82	0.88	0.40
11	2	1.00	0.47	0.21	0.15	1.00	0.98	0.68	0.68	0.07	0.06	0.06	0.98	0.36	0.20	0.51	0.23	0.30	0.18	0.26	0.86	0.18
11	3	1.00	0.58	0.24	0.17	1.00	0.95	0.56	0.59	0.07	0.06	0.06	0.98	0.29	0.16	0.37	0.30	0.23	0.25	0.31	0.41	0.12
11	4	1.00	0.68	0.30	0.20	1.00	0.88	0.47	0.49	0.08	0.07	0.06	0.82	0.27	0.15	0.30	0.29	0.28	0.30	0.27	0.47	0.09
11	5	1.00	0.76	0.35	0.23	1.00	0.79	0.40	0.49	0.08	0.07	0.06	0.54	0.26	0.15	0.31	0.30	0.31	0.28	0.26	0.10	0.10
11	6	1.00	0.82	0.39	0.26	1.00	0.71	0.38	0.50	0.08	0.07	0.06	0.31	0.24	0.14	0.33	0.77	0.31	0.30	0.81	0.15	0.37

m_1 (mean), m_2 (variance), m_3 (skewness), m_4 (kurtosis), l_2 (L-scale), t_3 (L-skewness), and t_4 (L-kurtosis)

Table A13. Watts-Strogratz Power based on Empirical Quantile Degrade Detection Low Degrade

		degree							betweenness							closeness						
k	m	m_1	m_2	m_3	m_4	l_2	t_3	t_4	m_1	m_2	m_3	m_4	l_2	t_3	t_4	m_1	m_2	m_3	m_4	l_2	t_3	t_4
5	2	0.41	0.06	0.05	0.05	0.05	0.05	0.06	0.10	0.07	0.05	0.06	0.07	0.05	0.05	0.13	0.06	0.07	0.06	0.06	0.05	0.05
5	3	0.36	0.06	0.05	0.05	0.05	0.05	0.05	0.24	0.06	0.05	0.06	0.06	0.05	0.05	0.42	0.05	0.06	0.05	0.05	0.05	0.05
5	4	0.31	0.05	0.05	0.05	0.05	0.05	0.05	0.27	0.05	0.05	0.06	0.05	0.05	0.05	0.37	0.06	0.06	0.05	0.06	0.05	0.05
5	5	0.31	0.05	0.05	0.05	0.05	0.05	0.05	0.34	0.05	0.05	0.05	0.05	0.05	0.05	0.36	0.05	0.06	0.05	0.05	0.05	0.05
5	6	0.31	0.05	0.05	0.05	0.05	0.05	0.05	0.32	0.05	0.05	0.05	0.05	0.05	0.05	0.35	0.06	0.06	0.05	0.06	0.05	0.05
6	2	0.30	0.06	0.05	0.06	0.06	0.05	0.06	0.13	0.08	0.06	0.07	0.08	0.06	0.05	0.17	0.07	0.07	0.06	0.06	0.05	0.05
6	3	0.61	0.05	0.05	0.05	0.05	0.05	0.05	0.27	0.06	0.05	0.06	0.06	0.05	0.05	0.33	0.06	0.06	0.05	0.06	0.05	0.05
6	4	0.86	0.05	0.05	0.05	0.05	0.05	0.05	0.67	0.06	0.05	0.06	0.06	0.05	0.05	0.97	0.06	0.06	0.05	0.07	0.05	0.05
6	5	0.92	0.05	0.05	0.05	0.05	0.05	0.05	0.70	0.06	0.05	0.06	0.06	0.05	0.05	0.99	0.07	0.06	0.06	0.07	0.05	0.05
6	6	0.96	0.05	0.05	0.05	0.05	0.05	0.05	0.75	0.06	0.05	0.06	0.06	0.05	0.05	1.00	0.06	0.06	0.05	0.06	0.05	0.05
7	2	0.30	0.06	0.06	0.06	0.06	0.06	0.05	0.30	0.11	0.07	0.08	0.12	0.06	0.05	0.39	0.08	0.07	0.07	0.08	0.05	0.05
7	3	0.68	0.05	0.05	0.06	0.05	0.06	0.05	0.74	0.08	0.06	0.07	0.08	0.05	0.05	0.89	0.07	0.07	0.06	0.07	0.05	0.06
7	4	0.95	0.06	0.05	0.06	0.06	0.05	0.06	0.99	0.08	0.06	0.07	0.08	0.05	0.05	1.00	0.08	0.07	0.06	0.08	0.05	0.05
7	5	0.98	0.06	0.05	0.06	0.06	0.05	0.05	1.00	0.08	0.06	0.07	0.08	0.05	0.05	1.00	0.08	0.07	0.06	0.08	0.05	0.05
7	6	0.99	0.06	0.05	0.06	0.06	0.05	0.06	1.00	0.07	0.06	0.07	0.07	0.05	0.05	1.00	0.07	0.07	0.06	0.07	0.05	0.05
8	2	0.29	0.06	0.06	0.06	0.06	0.06	0.06	0.60	0.16	0.09	0.10	0.21	0.06	0.05	0.74	0.11	0.07	0.08	0.11	0.06	0.05
8	3	0.75	0.06	0.05	0.06	0.06	0.05	0.06	0.99	0.12	0.07	0.09	0.14	0.05	0.05	1.00	0.08	0.06	0.06	0.08	0.05	0.06
8	4	0.99	0.06	0.05	0.06	0.06	0.06	0.06	1.00	0.11	0.06	0.08	0.13	0.05	0.05	1.00	0.10	0.07	0.07	0.10	0.05	0.06
8	5	1.00	0.06	0.05	0.06	0.06	0.06	0.06	1.00	0.11	0.07	0.08	0.12	0.05	0.05	1.00	0.11	0.07	0.06	0.10	0.06	0.06
8	6	1.00	0.06	0.05	0.06	0.07	0.06	0.06	1.00	0.11	0.06	0.08	0.12	0.06	0.05	1.00	0.08	0.07	0.06	0.08	0.06	0.06
9	2	0.39	0.07	0.06	0.07	0.07	0.07	0.06	0.91	0.27	0.11	0.12	0.41	0.06	0.05	0.95	0.16	0.08	0.10	0.16	0.06	0.06
9	3	0.79	0.07	0.06	0.06	0.08	0.05	0.07	1.00	0.18	0.08	0.10	0.26	0.05	0.05	1.00	0.09	0.07	0.07	0.09	0.05	0.06
9	4	1.00	0.08	0.06	0.06	0.08	0.06	0.07	1.00	0.18	0.08	0.10	0.23	0.06	0.06	1.00	0.13	0.08	0.08	0.13	0.06	0.06
9	5	1.00	0.08	0.06	0.07	0.08	0.06	0.07	1.00	0.18	0.08	0.10	0.21	0.06	0.06	1.00	0.17	0.08	0.08	0.17	0.06	0.06
9	6	1.00	0.08	0.06	0.07	0.08	0.06	0.07	1.00	0.15	0.07	0.10	0.18	0.06	0.06	1.00	0.11	0.08	0.07	0.10	0.06	0.06
10	2	0.59	0.09	0.08	0.08	0.09	0.08	0.06	0.99	0.46	0.16	0.16	0.72	0.07	0.05	1.00	0.26	0.10	0.15	0.27	0.06	0.06
10	3	0.87	0.10	0.06	0.07	0.11	0.06	0.08	1.00	0.32	0.10	0.12	0.48	0.06	0.06	1.00	0.12	0.07	0.08	0.11	0.06	0.06
10	4	1.00	0.10	0.06	0.08	0.11	0.06	0.08	1.00	0.32	0.10	0.13	0.43	0.06	0.06	1.00	0.19	0.10	0.11	0.18	0.06	0.07
10	5	1.00	0.10	0.07	0.08	0.11	0.06	0.08	1.00	0.30	0.10	0.13	0.39	0.06	0.06	1.00	0.23	0.09	0.11	0.22	0.07	0.08
10	6	1.00	0.11	0.06	0.08	0.11	0.06	0.08	1.00	0.25	0.09	0.12	0.31	0.06	0.06	1.00	0.16	0.09	0.11	0.14	0.06	0.07
11	2	0.80	0.14	0.10	0.10	0.14	0.12	0.07	1.00	0.70	0.23	0.21	0.94	0.08	0.05	1.00	0.44	0.16	0.25	0.44	0.06	0.06
11	3	0.95	0.14	0.06	0.09	0.17	0.06	0.11	1.00	0.53	0.15	0.16	0.78	0.06	0.07	1.00	0.16	0.09	0.10	0.15	0.06	0.08
11	4	1.00	0.15	0.07	0.10	0.17	0.07	0.11	1.00	0.53	0.15	0.18	0.71	0.06	0.07	1.00	0.31	0.12	0.15	0.30	0.06	0.09
11	5	1.00	0.16	0.08	0.10	0.18	0.08	0.11	1.00	0.53	0.15	0.18	0.67	0.06	0.08	1.00	0.41	0.15	0.17	0.40	0.09	0.10
11	6	1.00	0.16	0.07	0.10	0.17	0.06	0.10	1.00	0.42	0.11	0.16	0.53	0.06	0.07	1.00	0.18	0.08	0.11	0.16	0.06	0.10

m_1 (mean), m_2 (variance), m_3 (skewness), m_4 (kurtosis), l_2 (L-scale), t_3 (L-skewness), and t_4 (L-kurtosis)

Table A14. Watts-Strogratz Power based on Empirical Quantile Degrade Detection Med Degrade

		degree							betweenness							closeness						
k	m	m_1	m_2	m_3	m_4	l_2	t_3	t_4	m_1	m_2	m_3	m_4	l_2	t_3	t_4	m_1	m_2	m_3	m_4	l_2	t_3	t_4
5	2	0.73	0.05	0.04	0.05	0.05	0.04	0.05	0.07	0.05	0.05	0.05	0.05	0.05	0.05	0.10	0.09	0.08	0.07	0.10	0.05	0.05
5	3	0.85	0.05	0.04	0.05	0.05	0.05	0.05	0.21	0.05	0.05	0.05	0.05	0.05	0.06	0.67	0.09	0.08	0.07	0.09	0.05	0.05
5	4	0.81	0.05	0.05	0.05	0.05	0.05	0.05	0.33	0.05	0.05	0.05	0.05	0.05	0.06	0.80	0.08	0.08	0.06	0.09	0.05	0.05
5	5	0.75	0.05	0.05	0.05	0.05	0.05	0.05	0.62	0.05	0.05	0.05	0.05	0.05	0.05	0.76	0.07	0.07	0.06	0.07	0.05	0.05
5	6	0.69	0.05	0.05	0.05	0.05	0.05	0.05	0.70	0.05	0.05	0.05	0.05	0.05	0.05	0.71	0.07	0.07	0.06	0.06	0.05	0.05
6	2	0.76	0.05	0.04	0.05	0.05	0.04	0.05	0.09	0.05	0.05	0.05	0.05	0.05	0.06	0.13	0.12	0.08	0.08	0.12	0.05	0.05
6	3	0.99	0.05	0.04	0.05	0.05	0.04	0.06	0.23	0.05	0.05	0.05	0.05	0.05	0.05	0.52	0.11	0.08	0.07	0.12	0.05	0.05
6	4	1.00	0.05	0.04	0.05	0.05	0.04	0.05	0.60	0.05	0.05	0.05	0.05	0.05	0.05	0.95	0.10	0.08	0.06	0.10	0.05	0.05
6	5	1.00	0.05	0.05	0.05	0.05	0.05	0.05	0.56	0.05	0.05	0.05	0.05	0.05	0.05	0.96	0.10	0.08	0.06	0.11	0.05	0.05
6	6	1.00	0.05	0.05	0.05	0.05	0.05	0.05	0.58	0.05	0.05	0.05	0.05	0.05	0.05	0.99	0.09	0.07	0.06	0.10	0.05	0.05
7	2	0.90	0.05	0.04	0.05	0.05	0.04	0.06	0.14	0.04	0.05	0.05	0.05	0.05	0.06	0.24	0.16	0.08	0.10	0.18	0.05	0.05
7	3	1.00	0.05	0.04	0.05	0.05	0.04	0.06	0.53	0.05	0.05	0.05	0.05	0.05	0.06	0.87	0.17	0.08	0.09	0.19	0.05	0.05
7	4	1.00	0.05	0.05	0.05	0.05	0.04	0.06	0.92	0.05	0.05	0.05	0.05	0.05	0.05	1.00	0.15	0.08	0.07	0.16	0.05	0.05
7	5	1.00	0.05	0.05	0.05	0.05	0.05	0.05	0.98	0.05	0.05	0.05	0.05	0.05	0.05	1.00	0.12	0.08	0.07	0.12	0.05	0.06
7	6	1.00	0.05	0.05	0.05	0.05	0.05	0.05	0.95	0.05	0.05	0.05	0.05	0.05	0.06	1.00	0.12	0.08	0.08	0.12	0.05	0.05
8	2	0.96	0.05	0.04	0.05	0.05	0.04	0.08	0.27	0.04	0.05	0.05	0.04	0.05	0.06	0.45	0.23	0.09	0.13	0.25	0.05	0.06
8	3	1.00	0.05	0.04	0.05	0.05	0.04	0.07	0.89	0.05	0.05	0.05	0.05	0.04	0.06	0.99	0.27	0.09	0.12	0.30	0.05	0.06
8	4	1.00	0.05	0.04	0.05	0.05	0.04	0.06	1.00	0.05	0.05	0.05	0.05	0.05	0.06	1.00	0.27	0.09	0.10	0.30	0.05	0.06
8	5	1.00	0.05	0.05	0.05	0.05	0.05	0.06	1.00	0.05	0.05	0.05	0.05	0.05	0.06	1.00	0.24	0.08	0.08	0.26	0.05	0.06
8	6	1.00	0.05	0.05	0.05	0.05	0.05	0.06	1.00	0.05	0.05	0.05	0.05	0.05	0.06	1.00	0.16	0.08	0.08	0.17	0.05	0.06
9	2	1.00	0.05	0.04	0.06	0.05	0.04	0.11	0.49	0.04	0.05	0.05	0.04	0.05	0.07	0.68	0.35	0.10	0.18	0.38	0.05	0.06
9	3	1.00	0.05	0.05	0.05	0.05	0.04	0.09	0.99	0.05	0.05	0.05	0.05	0.05	0.07	1.00	0.47	0.12	0.19	0.51	0.05	0.06
9	4	1.00	0.05	0.05	0.05	0.05	0.04	0.07	1.00	0.05	0.05	0.05	0.06	0.04	0.06	1.00	0.36	0.10	0.14	0.38	0.05	0.06
9	5	1.00	0.05	0.05	0.05	0.05	0.05	0.07	1.00	0.06	0.05	0.05	0.06	0.05	0.06	1.00	0.42	0.08	0.11	0.47	0.05	0.06
9	6	1.00	0.05	0.05	0.05	0.05	0.05	0.07	1.00	0.05	0.05	0.05	0.06	0.05	0.06	1.00	0.42	0.09	0.12	0.47	0.05	0.06
10	2	1.00	0.05	0.04	0.06	0.05	0.04	0.18	0.71	0.04	0.05	0.06	0.04	0.05	0.09	0.83	0.53	0.15	0.28	0.56	0.05	0.07
10	3	1.00	0.05	0.05	0.05	0.06	0.05	0.15	1.00	0.05	0.05	0.05	0.06	0.05	0.10	1.00	0.68	0.18	0.30	0.72	0.07	0.06
10	4	1.00	0.05	0.04	0.05	0.05	0.04	0.09	1.00	0.06	0.05	0.05	0.07	0.04	0.07	1.00	0.69	0.16	0.24	0.74	0.06	0.07
10	5	1.00	0.05	0.05	0.05	0.05	0.05	0.09	1.00	0.06	0.05	0.05	0.07	0.05	0.07	1.00	0.45	0.09	0.15	0.47	0.05	0.06
10	6	1.00	0.05	0.05	0.05	0.05	0.05	0.09	1.00	0.06	0.05	0.05	0.07	0.05	0.08	1.00	0.59	0.09	0.22	0.64	0.06	0.07
11	2	1.00	0.05	0.04	0.06	0.06	0.04	0.32	0.85	0.05	0.05	0.06	0.04	0.05	0.11	0.94	0.74	0.25	0.47	0.76	0.06	0.09
11	3	1.00	0.06	0.06	0.06	0.07	0.06	0.26	1.00	0.05	0.05	0.05	0.07	0.05	0.15	1.00	0.93	0.32	0.52	0.96	0.08	0.10
11	4	1.00	0.05	0.04	0.05	0.06	0.04	0.15	1.00	0.07	0.05	0.05	0.11	0.04	0.10	1.00	0.91	0.18	0.39	0.94	0.05	0.09
11	5	1.00	0.05	0.05	0.05	0.06	0.05	0.12	1.00	0.07	0.05	0.05	0.09	0.06	0.10	1.00	0.87	0.22	0.31	0.90	0.09	0.07
11	6	1.00	0.05	0.05	0.05	0.06	0.05	0.13	1.00	0.07	0.05	0.05	0.09	0.06	0.10	1.00	0.59	0.10	0.23	0.61	0.05	0.07

m_1 (mean), m_2 (variance), m_3 (skewness), m_4 (kurtosis), l_2 (L-scale), t_3 (L-skewness), and t_4 (L-kurtosis)

Table A15. Watts-Strogratz Power based on Empirical Quantile Degrade Detection High Degrade

		degree							betweenness							closeness						
k	m	m_1	m_2	m_3	m_4	l_2	t_3	t_4	m_1	m_2	m_3	m_4	l_2	t_3	t_4	m_1	m_2	m_3	m_4	l_2	t_3	t_4
5	2	0.66	0.06	0.04	0.06	0.06	0.05	0.06	0.09	0.06	0.05	0.05	0.06	0.05	0.05	0.08	0.07	0.07	0.06	0.07	0.05	0.05
5	3	0.43	0.06	0.04	0.06	0.06	0.05	0.06	0.07	0.05	0.05	0.05	0.05	0.05	0.05	0.23	0.06	0.07	0.05	0.06	0.05	0.05
5	4	0.32	0.05	0.05	0.05	0.05	0.05	0.05	0.09	0.05	0.05	0.05	0.05	0.05	0.05	0.32	0.06	0.06	0.05	0.06	0.05	0.05
5	5	0.30	0.05	0.05	0.05	0.05	0.05	0.05	0.18	0.05	0.05	0.05	0.05	0.05	0.05	0.33	0.06	0.06	0.05	0.06	0.05	0.05
5	6	0.30	0.05	0.05	0.05	0.05	0.05	0.05	0.29	0.05	0.05	0.05	0.05	0.05	0.05	0.34	0.06	0.06	0.05	0.05	0.05	0.05
6	2	0.96	0.06	0.04	0.07	0.06	0.06	0.06	0.12	0.07	0.06	0.05	0.09	0.06	0.06	0.10	0.08	0.08	0.07	0.08	0.05	0.05
6	3	1.00	0.06	0.04	0.06	0.06	0.06	0.05	0.08	0.06	0.05	0.05	0.06	0.05	0.05	0.08	0.06	0.07	0.06	0.06	0.05	0.05
6	4	1.00	0.05	0.04	0.06	0.05	0.05	0.05	0.10	0.05	0.05	0.05	0.06	0.05	0.05	0.54	0.07	0.07	0.06	0.07	0.05	0.05
6	5	1.00	0.05	0.04	0.06	0.05	0.05	0.05	0.12	0.05	0.05	0.05	0.06	0.05	0.05	0.72	0.08	0.08	0.06	0.08	0.05	0.05
6	6	1.00	0.05	0.04	0.06	0.05	0.05	0.05	0.21	0.05	0.05	0.05	0.05	0.05	0.05	0.92	0.09	0.07	0.06	0.09	0.05	0.05
7	2	0.99	0.08	0.04	0.08	0.08	0.06	0.06	0.17	0.10	0.07	0.06	0.14	0.06	0.06	0.11	0.11	0.08	0.07	0.12	0.06	0.05
7	3	1.00	0.06	0.04	0.07	0.06	0.06	0.05	0.12	0.07	0.06	0.05	0.07	0.06	0.05	0.13	0.10	0.07	0.06	0.10	0.05	0.05
7	4	1.00	0.07	0.04	0.06	0.06	0.05	0.05	0.18	0.06	0.05	0.05	0.06	0.06	0.06	0.92	0.10	0.07	0.06	0.10	0.05	0.05
7	5	1.00	0.07	0.04	0.06	0.07	0.05	0.06	0.48	0.06	0.06	0.05	0.06	0.06	0.06	1.00	0.08	0.08	0.07	0.08	0.05	0.06
7	6	1.00	0.06	0.04	0.06	0.07	0.05	0.06	0.43	0.06	0.06	0.05	0.06	0.05	0.06	0.99	0.08	0.08	0.07	0.08	0.06	0.05
8	2	1.00	0.12	0.04	0.10	0.13	0.07	0.06	0.25	0.17	0.09	0.08	0.25	0.08	0.07	0.12	0.16	0.08	0.09	0.17	0.06	0.05
8	3	1.00	0.09	0.04	0.08	0.09	0.06	0.06	0.18	0.09	0.07	0.06	0.10	0.06	0.06	0.18	0.11	0.07	0.07	0.12	0.06	0.05
8	4	1.00	0.08	0.04	0.08	0.09	0.06	0.06	0.17	0.08	0.06	0.06	0.08	0.06	0.06	0.97	0.16	0.08	0.08	0.17	0.06	0.05
8	5	1.00	0.08	0.04	0.07	0.09	0.06	0.06	0.89	0.06	0.06	0.05	0.06	0.06	0.06	1.00	0.20	0.08	0.08	0.21	0.06	0.06
8	6	1.00	0.08	0.04	0.07	0.09	0.06	0.06	0.99	0.06	0.06	0.05	0.05	0.06	0.06	1.00	0.10	0.08	0.08	0.09	0.06	0.07
9	2	1.00	0.19	0.04	0.12	0.21	0.10	0.07	0.38	0.30	0.12	0.09	0.46	0.11	0.07	0.14	0.24	0.09	0.12	0.26	0.06	0.05
9	3	1.00	0.13	0.04	0.10	0.14	0.06	0.06	0.32	0.12	0.08	0.06	0.14	0.07	0.06	0.19	0.17	0.07	0.09	0.18	0.05	0.05
9	4	1.00	0.13	0.04	0.09	0.14	0.06	0.07	0.31	0.10	0.07	0.06	0.10	0.07	0.06	1.00	0.16	0.08	0.10	0.15	0.06	0.07
9	5	1.00	0.12	0.04	0.09	0.13	0.06	0.07	0.90	0.09	0.07	0.06	0.09	0.07	0.07	1.00	0.32	0.09	0.10	0.36	0.07	0.05
9	6	1.00	0.12	0.05	0.09	0.13	0.06	0.07	1.00	0.06	0.06	0.06	0.05	0.07	0.07	1.00	0.42	0.10	0.13	0.45	0.05	0.05
10	2	1.00	0.34	0.05	0.17	0.40	0.16	0.07	0.57	0.55	0.21	0.14	0.77	0.18	0.10	0.19	0.39	0.10	0.18	0.43	0.07	0.06
10	3	1.00	0.22	0.04	0.13	0.25	0.06	0.07	0.49	0.19	0.10	0.08	0.23	0.08	0.08	0.22	0.21	0.09	0.11	0.21	0.06	0.07
10	4	1.00	0.21	0.04	0.13	0.23	0.07	0.08	0.59	0.14	0.09	0.07	0.14	0.08	0.08	1.00	0.43	0.13	0.17	0.45	0.06	0.06
10	5	1.00	0.20	0.04	0.12	0.22	0.07	0.09	1.00	0.12	0.09	0.07	0.11	0.09	0.09	1.00	0.19	0.09	0.12	0.18	0.06	0.11
10	6	1.00	0.20	0.04	0.12	0.21	0.06	0.09	1.00	0.08	0.08	0.07	0.07	0.08	0.09	1.00	0.40	0.08	0.16	0.42	0.11	0.05
11	2	1.00	0.60	0.05	0.26	0.69	0.29	0.08	0.80	0.84	0.38	0.22	0.97	0.34	0.14	0.30	0.62	0.13	0.30	0.66	0.07	0.06
11	3	1.00	0.40	0.04	0.20	0.45	0.07	0.10	0.71	0.33	0.16	0.11	0.39	0.10	0.11	0.25	0.41	0.12	0.17	0.43	0.06	0.05
11	4	1.00	0.36	0.04	0.19	0.41	0.07	0.11	0.50	0.25	0.15	0.11	0.25	0.12	0.12	1.00	0.57	0.09	0.22	0.61	0.10	0.06
11	5	1.00	0.36	0.04	0.19	0.40	0.08	0.12	1.00	0.17	0.13	0.10	0.14	0.13	0.13	1.00	0.78	0.28	0.32	0.77	0.15	0.09
11	6	1.00	0.34	0.05	0.18	0.37	0.08	0.12	1.00	0.11	0.11	0.08	0.08	0.11	0.13	1.00	0.14	0.09	0.13	0.11	0.06	0.16

m_1 (mean), m_2 (variance), m_3 (skewness), m_4 (kurtosis), l_2 (L-scale), t_3 (L-skewness), and t_4 (L-kurtosis)

Table A16. Erdös-Rényi Power Based on Non-parametric Tests with Low Degrade

		p=1/7						p=1/10						p=1/20					
		KS Test			Sign Test			KS Test			Sign Test			KS Test			Sign Test		
k	m	C	B	D	C	B	D	C	B	D	C	B	D	C	B	D	C	B	D
5	2	0.08	0.00	0.00	0.22	0.00	0.00	0.01	0.00	0.00	0.08	0.00	0.01	0.00	0.00	0.00	0.00	0.00	0.01
5	3	0.08	0.00	0.00	0.32	0.00	0.00	0.01	0.00	0.00	0.09	0.00	0.00	0.00	0.00	0.00	0.00	0.00	0.00
5	4	0.32	0.00	0.00	0.36	0.00	0.00	0.08	0.00	0.00	0.10	0.00	0.00	0.00	0.00	0.00	0.00	0.00	0.00
5	5	0.32	0.00	0.00	0.59	0.00	0.00	0.09	0.00	0.00	0.18	0.00	0.00	0.00	0.00	0.00	0.00	0.00	0.00
5	6	0.33	0.00	0.00	0.91	0.00	0.01	0.08	0.00	0.00	0.28	0.00	0.00	0.00	0.00	0.00	0.00	0.00	0.00
6	2	0.30	0.00	0.00	0.50	0.00	0.01	0.04	0.00	0.00	0.18	0.00	0.01	0.00	0.00	0.00	0.01	0.00	0.01
6	3	0.52	0.00	0.00	0.77	0.00	0.01	0.06	0.00	0.00	0.22	0.00	0.01	0.00	0.00	0.00	0.01	0.00	0.01
6	4	0.59	0.00	0.00	0.83	0.00	0.00	0.11	0.00	0.00	0.37	0.00	0.00	0.00	0.00	0.00	0.04	0.00	0.00
6	5	0.74	0.00	0.00	0.85	0.00	0.00	0.20	0.00	0.00	0.43	0.00	0.00	0.01	0.00	0.00	0.05	0.00	0.00
6	6	0.91	0.00	0.00	0.93	0.00	0.00	0.56	0.00	0.00	0.66	0.00	0.00	0.08	0.00	0.00	0.09	0.00	0.00
7	2	0.65	0.00	0.00	0.82	0.00	0.00	0.25	0.00	0.00	0.50	0.00	0.00	0.00	0.00	0.00	0.05	0.00	0.00
7	3	0.97	0.00	0.00	0.97	0.00	0.01	0.67	0.00	0.00	0.91	0.00	0.01	0.00	0.00	0.00	0.04	0.00	0.01
7	4	0.99	0.00	0.00	0.99	0.00	0.01	0.82	0.00	0.00	0.93	0.00	0.01	0.04	0.00	0.00	0.22	0.00	0.01
7	5	1.00	0.00	0.00	1.00	0.00	0.01	0.70	0.00	0.00	0.93	0.00	0.01	0.05	0.00	0.00	0.22	0.00	0.00
7	6	1.00	0.00	0.00	1.00	0.00	0.01	0.78	0.00	0.00	0.94	0.00	0.00	0.04	0.00	0.00	0.16	0.00	0.00
8	2	0.80	0.00	0.00	0.80	0.00	0.01	0.74	0.00	0.00	0.84	0.00	0.01	0.05	0.00	0.00	0.18	0.00	0.01
8	3	0.93	0.00	0.00	0.93	0.00	0.01	0.95	0.00	0.00	0.95	0.00	0.01	0.08	0.00	0.00	0.68	0.00	0.01
8	4	0.99	0.00	0.00	0.99	0.00	0.04	0.99	0.00	0.00	0.99	0.00	0.02	0.47	0.00	0.00	0.79	0.00	0.01
8	5	1.00	0.00	0.00	1.00	0.00	0.04	1.00	0.00	0.00	1.00	0.00	0.02	0.40	0.00	0.00	0.78	0.00	0.01
8	6	1.00	0.00	0.00	1.00	0.00	0.04	1.00	0.00	0.00	1.00	0.00	0.02	0.61	0.00	0.00	0.90	0.00	0.01
9	2	0.67	0.00	0.00	0.67	0.00	0.02	0.75	0.00	0.00	0.75	0.00	0.03	0.11	0.00	0.00	0.71	0.00	0.03
9	3	0.87	0.00	0.00	0.87	0.00	0.08	0.90	0.00	0.00	0.90	0.00	0.07	0.95	0.00	0.00	0.95	0.00	0.06
9	4	0.97	0.00	0.00	0.97	0.01	0.17	0.98	0.00	0.00	0.98	0.00	0.11	0.97	0.00	0.00	0.99	0.00	0.07
9	5	1.00	0.00	0.00	1.00	0.01	0.14	1.00	0.00	0.00	1.00	0.00	0.09	1.00	0.00	0.00	1.00	0.00	0.05
9	6	1.00	0.00	0.00	1.00	0.02	0.19	1.00	0.00	0.00	1.00	0.00	0.10	1.00	0.00	0.00	1.00	0.00	0.04
10	2	0.48	0.00	0.00	0.48	0.00	0.13	0.58	0.00	0.00	0.58	0.00	0.14	0.76	0.00	0.00	0.76	0.00	0.15
10	3	0.75	0.00	0.00	0.75	0.02	0.35	0.81	0.00	0.00	0.81	0.00	0.34	0.90	0.00	0.00	0.90	0.00	0.32
10	4	0.94	0.00	0.00	0.94	0.11	0.57	0.96	0.00	0.00	0.96	0.01	0.45	0.98	0.00	0.00	0.98	0.00	0.31
10	5	0.99	0.00	0.00	0.99	0.07	0.46	0.99	0.00	0.00	0.99	0.00	0.34	1.00	0.00	0.00	1.00	0.00	0.21
10	6	1.00	0.00	0.00	1.00	0.16	0.64	1.00	0.00	0.00	1.00	0.01	0.43	1.00	0.00	0.00	1.00	0.00	0.21

KS test - Kolmogorov-Smirnov test, C - closeness, B - betweenness, D - degree

Table A17. Erdös-Rényi Power Based on Non-parametric Tests with Medium Degrade

		p=1/7						p=1/10						p=1/20					
		KS Test			Sign Test			KS Test			Sign Test			KS Test			Sign Test		
k	m	C	B	D	C	B	D	C	B	D	C	B	D	C	B	D	C	B	D
5	2	0.04	0.00	0.00	0.13	0.00	0.01	0.00	0.00	0.00	0.03	0.00	0.01	0.00	0.00	0.00	0.00	0.00	0.01
5	3	0.09	0.00	0.00	0.23	0.00	0.01	0.00	0.00	0.00	0.07	0.00	0.00	0.00	0.00	0.00	0.00	0.00	0.00
5	4	0.25	0.00	0.00	0.25	0.00	0.01	0.11	0.00	0.00	0.10	0.00	0.01	0.00	0.00	0.00	0.00	0.00	0.00
5	5	0.21	0.00	0.00	0.45	0.00	0.02	0.10	0.00	0.00	0.31	0.00	0.01	0.00	0.00	0.00	0.00	0.00	0.00
5	6	0.19	0.00	0.00	0.72	0.00	0.03	0.12	0.00	0.00	0.53	0.00	0.01	0.00	0.00	0.00	0.00	0.00	0.00
6	2	0.13	0.00	0.00	0.24	0.00	0.01	0.02	0.00	0.00	0.09	0.00	0.01	0.00	0.00	0.00	0.00	0.00	0.01
6	3	0.44	0.00	0.00	0.57	0.00	0.01	0.08	0.00	0.00	0.25	0.00	0.00	0.00	0.00	0.00	0.02	0.00	0.00
6	4	0.45	0.00	0.00	0.63	0.00	0.02	0.08	0.00	0.00	0.33	0.00	0.00	0.00	0.00	0.00	0.06	0.00	0.00
6	5	0.47	0.00	0.00	0.68	0.00	0.02	0.16	0.00	0.00	0.34	0.00	0.01	0.00	0.00	0.00	0.06	0.00	0.00
6	6	0.83	0.00	0.00	0.83	0.00	0.03	0.40	0.00	0.00	0.48	0.00	0.01	0.11	0.00	0.00	0.13	0.00	0.00
7	2	0.36	0.00	0.00	0.42	0.00	0.03	0.14	0.00	0.00	0.29	0.00	0.02	0.00	0.00	0.00	0.02	0.00	0.01
7	3	0.81	0.00	0.00	0.84	0.00	0.08	0.40	0.00	0.00	0.63	0.00	0.03	0.00	0.00	0.00	0.09	0.00	0.01
7	4	0.94	0.00	0.00	0.96	0.00	0.09	0.57	0.00	0.00	0.81	0.00	0.02	0.02	0.00	0.00	0.18	0.00	0.01
7	5	0.93	0.00	0.00	0.96	0.00	0.10	0.60	0.00	0.00	0.79	0.00	0.02	0.02	0.00	0.00	0.12	0.00	0.00
7	6	0.91	0.00	0.00	0.95	0.00	0.10	0.54	0.00	0.00	0.71	0.00	0.02	0.01	0.00	0.00	0.06	0.00	0.00
8	2	0.32	0.00	0.00	0.33	0.00	0.09	0.38	0.00	0.00	0.41	0.00	0.06	0.01	0.00	0.00	0.16	0.00	0.03
8	3	0.84	0.00	0.00	0.84	0.00	0.39	0.85	0.00	0.00	0.87	0.00	0.18	0.05	0.00	0.00	0.39	0.00	0.05
8	4	0.97	0.00	0.00	0.97	0.00	0.50	0.96	0.00	0.00	0.97	0.00	0.21	0.10	0.00	0.00	0.42	0.00	0.04
8	5	1.00	0.00	0.00	1.00	0.00	0.49	0.99	0.00	0.00	1.00	0.00	0.21	0.24	0.00	0.00	0.66	0.00	0.03
8	6	1.00	0.00	0.00	1.00	0.00	0.45	1.00	0.00	0.00	1.00	0.00	0.19	0.26	0.00	0.00	0.59	0.00	0.03
9	2	0.12	0.00	0.00	0.12	0.00	0.12	0.22	0.00	0.00	0.23	0.00	0.13	0.22	0.00	0.00	0.40	0.00	0.11
9	3	0.70	0.00	0.00	0.70	0.00	0.69	0.78	0.00	0.00	0.78	0.00	0.60	0.63	0.00	0.00	0.82	0.00	0.26
9	4	0.95	0.00	0.00	0.95	0.00	0.91	0.96	0.00	0.00	0.96	0.00	0.75	0.65	0.00	0.00	0.91	0.00	0.28
9	5	0.99	0.00	0.00	0.99	0.00	0.94	0.99	0.00	0.00	0.99	0.00	0.72	0.80	0.00	0.00	0.95	0.00	0.24
9	6	1.00	0.00	0.00	1.00	0.00	0.92	1.00	0.00	0.00	1.00	0.00	0.66	0.98	0.00	0.00	1.00	0.00	0.19
10	2	0.01	0.00	0.00	0.01	0.00	0.20	0.05	0.00	0.00	0.05	0.00	0.23	0.24	0.00	0.00	0.24	0.00	0.29
10	3	0.48	0.00	0.01	0.48	0.00	0.63	0.61	0.00	0.00	0.61	0.00	0.73	0.79	0.00	0.00	0.79	0.00	0.75
10	4	0.89	0.00	0.03	0.89	0.01	0.91	0.92	0.00	0.00	0.92	0.00	0.93	0.96	0.00	0.00	0.96	0.00	0.81
10	5	0.98	0.00	0.05	0.98	0.01	0.98	0.99	0.00	0.00	0.99	0.00	0.98	0.99	0.00	0.00	0.99	0.00	0.74
10	6	1.00	0.00	0.06	1.00	0.02	1.00	1.00	0.00	0.00	1.00	0.00	0.98	1.00	0.00	0.00	1.00	0.00	0.66

KS test - Kolmogorov-Smirnov test, C - closeness, B - betweenness, D - degree

Table A18. Erdös-Rényi Power Based on Non-parametric Tests with High Degrade

		p=1/7						p=1/10						p=1/20					
		KS Test			Sign Test			KS Test			Sign Test			KS Test			Sign Test		
k	m	C	B	D	C	B	D	C	B	D	C	B	D	C	B	D	C	B	D
5	2	0.00	0.00	0.00	0.01	0.00	0.01	0.00	0.00	0.00	0.00	0.00	0.01	0.00	0.00	0.00	0.00	0.00	0.01
5	3	0.00	0.00	0.00	0.02	0.00	0.02	0.00	0.00	0.00	0.01	0.00	0.01	0.00	0.00	0.00	0.00	0.00	0.00
5	4	0.07	0.00	0.00	0.06	0.00	0.03	0.02	0.00	0.00	0.01	0.00	0.01	0.00	0.00	0.00	0.00	0.00	0.00
5	5	0.07	0.00	0.00	0.31	0.00	0.04	0.02	0.00	0.00	0.08	0.00	0.01	0.00	0.00	0.00	0.00	0.00	0.00
5	6	0.08	0.00	0.00	0.62	0.00	0.06	0.03	0.00	0.00	0.17	0.00	0.01	0.00	0.00	0.00	0.00	0.00	0.00
6	2	0.00	0.00	0.00	0.02	0.00	0.12	0.00	0.00	0.00	0.01	0.00	0.03	0.00	0.00	0.00	0.00	0.00	0.01
6	3	0.01	0.00	0.00	0.04	0.00	0.12	0.00	0.00	0.00	0.01	0.00	0.02	0.00	0.00	0.00	0.00	0.00	0.01
6	4	0.02	0.00	0.00	0.13	0.00	0.12	0.00	0.00	0.00	0.03	0.00	0.01	0.00	0.00	0.00	0.00	0.00	0.00
6	5	0.06	0.00	0.00	0.26	0.00	0.13	0.01	0.00	0.00	0.06	0.00	0.01	0.00	0.00	0.00	0.00	0.00	0.00
6	6	0.56	0.00	0.00	0.63	0.00	0.15	0.18	0.00	0.00	0.27	0.00	0.02	0.02	0.00	0.00	0.02	0.00	0.00
7	2	0.01	0.00	0.00	0.04	0.00	0.27	0.00	0.00	0.00	0.01	0.00	0.14	0.00	0.00	0.00	0.00	0.00	0.02
7	3	0.01	0.00	0.00	0.04	0.00	0.57	0.00	0.00	0.00	0.02	0.00	0.22	0.00	0.00	0.00	0.00	0.00	0.02
7	4	0.28	0.00	0.00	0.56	0.00	0.67	0.03	0.00	0.00	0.26	0.00	0.23	0.00	0.00	0.00	0.01	0.00	0.01
7	5	0.48	0.00	0.00	0.73	0.00	0.63	0.11	0.00	0.00	0.37	0.00	0.20	0.00	0.00	0.00	0.02	0.00	0.01
7	6	0.47	0.00	0.00	0.76	0.00	0.60	0.13	0.00	0.00	0.37	0.00	0.19	0.00	0.00	0.00	0.02	0.00	0.01
8	2	0.03	0.00	0.00	0.10	0.00	0.28	0.01	0.00	0.00	0.05	0.00	0.28	0.00	0.00	0.00	0.01	0.00	0.09
8	3	0.01	0.00	0.00	0.06	0.00	0.79	0.00	0.00	0.00	0.03	0.00	0.71	0.00	0.00	0.00	0.00	0.00	0.21
8	4	0.60	0.00	0.02	0.74	0.00	0.95	0.15	0.00	0.00	0.44	0.00	0.86	0.00	0.00	0.00	0.03	0.00	0.20
8	5	0.98	0.00	0.07	0.99	0.00	0.97	0.70	0.00	0.00	0.91	0.00	0.79	0.03	0.00	0.00	0.22	0.00	0.14
8	6	1.00	0.00	0.06	1.00	0.00	0.97	0.94	0.00	0.00	0.99	0.00	0.73	0.04	0.00	0.00	0.28	0.00	0.11
9	2	0.05	0.00	0.00	0.08	0.00	0.13	0.03	0.00	0.00	0.10	0.00	0.22	0.00	0.00	0.00	0.02	0.00	0.28
9	3	0.02	0.00	0.16	0.06	0.00	0.64	0.00	0.00	0.00	0.03	0.00	0.74	0.00	0.00	0.00	0.00	0.00	0.67
9	4	0.85	0.00	0.75	0.89	0.00	0.92	0.60	0.00	0.01	0.81	0.00	0.94	0.00	0.00	0.00	0.18	0.00	0.78
9	5	0.98	0.00	0.41	0.98	0.00	0.99	0.82	0.00	0.03	0.93	0.00	0.98	0.10	0.00	0.00	0.33	0.00	0.64
9	6	1.00	0.00	0.64	1.00	0.00	1.00	1.00	0.00	0.01	1.00	0.00	0.99	0.58	0.00	0.00	0.91	0.00	0.56
10	2	0.01	0.00	0.01	0.01	0.00	0.20	0.03	0.00	0.00	0.04	0.00	0.22	0.01	0.00	0.00	0.07	0.00	0.36
10	3	0.01	0.00	0.37	0.04	0.00	0.55	0.00	0.00	0.08	0.03	0.00	0.65	0.00	0.00	0.00	0.00	0.00	0.81
10	4	0.82	0.00	0.82	0.82	0.00	0.85	0.87	0.00	0.74	0.88	0.00	0.90	0.35	0.00	0.00	0.77	0.00	0.95
10	5	0.98	0.00	0.98	0.98	0.01	0.98	0.98	0.00	0.24	0.98	0.00	0.98	0.21	0.00	0.00	0.66	0.00	0.97
10	6	1.00	0.00	1.00	1.00	0.00	1.00	1.00	0.00	0.53	1.00	0.00	1.00	0.73	0.00	0.00	0.95	0.00	0.97

KS test - Kolmogorov-Smirnov test, C - closeness, B - betweenness, D - degree

Table A19. Erdös-Rényi Power Based on Non-parametric Tests with Random Degrade

		p=1/7						p=1/10						p=1/20					
		KS Test			Sign Test			KS Test			Sign Test			KS Test			Sign Test		
k	m	C	B	D	C	B	D	C	B	D	C	B	D	C	B	D	C	B	D
5	2	0.00	0.00	0.00	0.00	0.00	0.01	0.00	0.00	0.00	0.00	0.00	0.01	0.00	0.00	0.00	0.00	0.00	0.01
5	3	0.00	0.00	0.00	0.00	0.00	0.00	0.00	0.00	0.00	0.00	0.00	0.00	0.00	0.00	0.00	0.00	0.00	0.00
5	4	0.00	0.00	0.00	0.00	0.00	0.00	0.00	0.00	0.00	0.00	0.00	0.00	0.00	0.00	0.00	0.00	0.00	0.00
5	5	0.00	0.00	0.00	0.00	0.00	0.00	0.00	0.00	0.00	0.00	0.00	0.00	0.00	0.00	0.00	0.00	0.00	0.00
5	6	0.00	0.00	0.00	0.00	0.00	0.00	0.00	0.00	0.00	0.00	0.00	0.00	0.00	0.00	0.00	0.00	0.00	0.00
6	2	0.00	0.00	0.00	0.01	0.00	0.01	0.00	0.00	0.00	0.01	0.00	0.01	0.00	0.00	0.00	0.00	0.00	0.01
6	3	0.00	0.00	0.00	0.04	0.00	0.01	0.00	0.00	0.00	0.04	0.00	0.01	0.00	0.00	0.00	0.00	0.00	0.01
6	4	0.00	0.00	0.00	0.09	0.00	0.00	0.00	0.00	0.00	0.10	0.00	0.00	0.00	0.00	0.00	0.00	0.00	0.00
6	5	0.01	0.00	0.00	0.12	0.00	0.00	0.01	0.00	0.00	0.13	0.00	0.00	0.00	0.00	0.00	0.00	0.00	0.00
6	6	0.26	0.00	0.00	0.37	0.00	0.00	0.27	0.00	0.00	0.37	0.00	0.00	0.00	0.00	0.00	0.00	0.00	0.00
7	2	0.01	0.00	0.00	0.12	0.00	0.03	0.00	0.00	0.00	0.03	0.00	0.01	0.00	0.00	0.00	0.00	0.00	0.01
7	3	0.10	0.00	0.00	0.40	0.00	0.05	0.00	0.00	0.00	0.12	0.00	0.02	0.00	0.00	0.00	0.00	0.00	0.01
7	4	0.42	0.00	0.00	0.77	0.00	0.04	0.06	0.00	0.00	0.36	0.00	0.02	0.00	0.00	0.00	0.02	0.00	0.01
7	5	0.64	0.00	0.00	0.86	0.00	0.05	0.08	0.00	0.00	0.47	0.00	0.01	0.00	0.00	0.00	0.03	0.00	0.00
7	6	0.72	0.00	0.00	0.89	0.00	0.05	0.11	0.00	0.00	0.46	0.00	0.01	0.00	0.00	0.00	0.04	0.00	0.00
8	2	0.12	0.00	0.00	0.25	0.00	0.11	0.02	0.00	0.00	0.13	0.00	0.07	0.00	0.00	0.00	0.00	0.00	0.02
8	3	0.67	0.00	0.00	0.80	0.00	0.29	0.25	0.00	0.00	0.59	0.00	0.16	0.00	0.00	0.00	0.02	0.00	0.04
8	4	0.96	0.00	0.00	0.97	0.00	0.34	0.70	0.00	0.00	0.87	0.00	0.17	0.00	0.00	0.00	0.07	0.00	0.03
8	5	1.00	0.00	0.00	1.00	0.00	0.37	0.99	0.00	0.00	0.99	0.00	0.17	0.01	0.00	0.00	0.28	0.00	0.03
8	6	1.00	0.00	0.00	1.00	0.00	0.39	1.00	0.00	0.00	1.00	0.00	0.17	0.03	0.00	0.00	0.37	0.00	0.02
9	2	0.19	0.00	0.00	0.24	0.00	0.22	0.08	0.00	0.00	0.22	0.00	0.20	0.00	0.00	0.00	0.04	0.00	0.12
9	3	0.80	0.00	0.00	0.80	0.00	0.65	0.73	0.00	0.00	0.81	0.00	0.51	0.02	0.00	0.00	0.30	0.00	0.24
9	4	0.96	0.00	0.00	0.96	0.00	0.79	0.97	0.00	0.00	0.97	0.00	0.57	0.11	0.00	0.00	0.62	0.00	0.23
9	5	0.99	0.00	0.00	0.99	0.00	0.84	1.00	0.00	0.00	1.00	0.00	0.59	0.46	0.00	0.00	0.86	0.00	0.21
9	6	1.00	0.00	0.00	1.00	0.00	0.86	1.00	0.00	0.00	1.00	0.00	0.60	0.98	0.00	0.00	1.00	0.00	0.19
10	2	0.09	0.00	0.00	0.10	0.00	0.27	0.12	0.00	0.00	0.16	0.00	0.32	0.01	0.00	0.00	0.11	0.00	0.35
10	3	0.63	0.00	0.00	0.63	0.00	0.73	0.74	0.00	0.00	0.74	0.00	0.79	0.25	0.00	0.00	0.66	0.00	0.69
10	4	0.92	0.00	0.00	0.92	0.00	0.93	0.95	0.00	0.00	0.95	0.00	0.92	0.92	0.00	0.00	0.97	0.00	0.69
10	5	0.99	0.00	0.00	0.99	0.00	0.99	0.99	0.00	0.00	0.99	0.00	0.96	0.98	0.00	0.00	0.99	0.00	0.65
10	6	1.00	0.00	0.01	1.00	0.01	1.00	1.00	0.00	0.00	1.00	0.00	0.97	1.00	0.00	0.00	1.00	0.00	0.62

KS test - Kolmogorov-Smirnov test, C - closeness, B - betweenness, D - degree

Table A20. Barabási-Albert Power Based on Non-parametric Tests with Low Degrade

		p=1/7						p=1/10						p=1/20					
		KS Test			Sign Test			KS Test			Sign Test			KS Test			Sign Test		
k	m	C	B	D	C	B	D	C	B	D	C	B	D	C	B	D	C	B	D
5	2	0.35	0.00	0.00	0.57	0.00	0.08	0.03	0.00	0.00	0.23	0.00	0.08	0.00	0.00	0.00	0.00	0.00	0.08
5	3	0.07	0.00	0.00	0.36	0.00	0.00	0.01	0.00	0.00	0.25	0.00	0.00	0.00	0.00	0.00	0.00	0.00	0.00
5	4	0.04	0.00	0.00	0.33	0.00	0.00	0.01	0.00	0.00	0.14	0.00	0.00	0.00	0.00	0.00	0.00	0.00	0.00
5	5	0.08	0.00	0.00	0.32	0.00	0.00	0.01	0.00	0.00	0.10	0.00	0.00	0.00	0.00	0.00	0.00	0.00	0.00
5	6	0.25	0.00	0.00	0.43	0.00	0.00	0.10	0.00	0.00	0.18	0.00	0.00	0.00	0.00	0.00	0.00	0.00	0.00
6	2	0.83	0.00	0.00	0.89	0.00	0.06	0.28	0.00	0.00	0.52	0.00	0.06	0.00	0.00	0.00	0.04	0.00	0.06
6	3	0.84	0.00	0.00	0.95	0.00	0.01	0.34	0.00	0.00	0.73	0.00	0.00	0.00	0.00	0.00	0.13	0.00	0.00
6	4	0.61	0.00	0.00	0.89	0.00	0.02	0.21	0.00	0.00	0.46	0.00	0.02	0.01	0.00	0.00	0.08	0.00	0.01
6	5	0.49	0.00	0.00	0.82	0.00	0.00	0.07	0.00	0.00	0.28	0.00	0.00	0.00	0.00	0.00	0.03	0.00	0.00
6	6	0.59	0.00	0.00	0.80	0.00	0.00	0.14	0.00	0.00	0.36	0.00	0.00	0.00	0.00	0.00	0.05	0.00	0.00
7	2	1.00	0.00	0.00	1.00	0.00	0.05	0.92	0.00	0.00	0.93	0.00	0.06	0.03	0.00	0.00	0.19	0.00	0.07
7	3	1.00	0.00	0.00	1.00	0.00	0.05	0.93	0.00	0.00	0.97	0.00	0.05	0.02	0.00	0.00	0.36	0.00	0.03
7	4	1.00	0.00	0.00	1.00	0.00	0.18	0.88	0.00	0.00	0.99	0.00	0.17	0.05	0.00	0.00	0.29	0.00	0.16
7	5	1.00	0.00	0.00	1.00	0.00	0.00	0.79	0.00	0.00	0.95	0.00	0.00	0.00	0.00	0.00	0.06	0.00	0.00
7	6	0.99	0.00	0.00	1.00	0.00	0.00	0.59	0.00	0.00	0.84	0.00	0.00	0.01	0.00	0.00	0.11	0.00	0.00
8	2	1.00	0.00	0.00	1.00	0.00	0.25	1.00	0.00	0.00	1.00	0.00	0.32	0.26	0.00	0.00	0.68	0.00	0.40
8	3	1.00	0.00	0.00	1.00	0.00	0.21	1.00	0.00	0.00	1.00	0.00	0.17	0.22	0.00	0.00	0.70	0.00	0.13
8	4	1.00	0.00	0.00	1.00	0.00	0.35	1.00	0.00	0.00	1.00	0.00	0.35	0.35	0.00	0.00	0.84	0.00	0.35
8	5	1.00	0.00	0.00	1.00	0.00	0.00	1.00	0.00	0.00	1.00	0.00	0.00	0.36	0.00	0.00	0.90	0.00	0.00
8	6	1.00	0.00	0.00	1.00	0.00	0.07	1.00	0.00	0.00	1.00	0.00	0.06	0.24	0.00	0.00	0.65	0.00	0.05
9	2	1.00	0.00	0.00	1.00	0.00	0.78	1.00	0.00	0.00	1.00	0.00	0.85	0.99	0.00	0.00	1.00	0.00	0.91
9	3	1.00	0.00	0.00	1.00	0.00	0.57	1.00	0.00	0.00	1.00	0.00	0.48	0.97	0.00	0.00	0.99	0.00	0.39
9	4	1.00	0.00	0.00	1.00	0.00	0.78	1.00	0.00	0.00	1.00	0.00	0.80	0.96	0.00	0.00	0.99	0.00	0.82
9	5	1.00	0.00	0.00	1.00	0.00	0.00	1.00	0.00	0.00	1.00	0.00	0.00	0.99	0.00	0.00	1.00	0.00	0.00
9	6	1.00	0.00	0.00	1.00	0.00	0.58	1.00	0.00	0.00	1.00	0.00	0.57	0.99	0.00	0.00	1.00	0.00	0.55
10	2	1.00	0.00	0.00	1.00	0.00	1.00	1.00	0.00	0.00	1.00	0.00	1.00	1.00	0.00	0.00	1.00	0.00	1.00
10	3	1.00	0.00	0.00	1.00	0.00	0.94	1.00	0.00	0.00	1.00	0.00	0.89	1.00	0.00	0.00	1.00	0.00	0.82
10	4	1.00	0.00	0.00	1.00	0.00	0.96	1.00	0.00	0.00	1.00	0.00	0.96	1.00	0.00	0.00	1.00	0.00	0.96
10	5	1.00	0.00	0.00	1.00	0.00	0.00	1.00	0.00	0.00	1.00	0.00	0.00	1.00	0.00	0.00	1.00	0.00	0.00
10	6	1.00	0.00	0.00	1.00	0.00	0.97	1.00	0.00	0.00	1.00	0.00	0.97	1.00	0.00	0.00	1.00	0.00	0.96

KS test - Kolmogorov-Smirnov test, C - closeness, B - betweenness, D - degree

Table A21. Barabási-Albert Power Based on Non-parametric Tests with Medium Degrade

		p=1/7						p=1/10						p=1/20					
		KS Test			Sign Test			KS Test			Sign Test			KS Test			Sign Test		
k	m	C	B	D	C	B	D	C	B	D	C	B	D	C	B	D	C	B	D
5	2	0.54	0.00	0.00	0.68	0.00	0.08	0.33	0.00	0.00	0.54	0.00	0.08	0.02	0.00	0.00	0.15	0.00	0.08
5	3	0.15	0.00	0.00	0.36	0.00	0.00	0.03	0.00	0.00	0.18	0.00	0.00	0.00	0.00	0.00	0.01	0.00	0.00
5	4	0.04	0.00	0.00	0.20	0.00	0.00	0.00	0.00	0.00	0.10	0.00	0.00	0.00	0.00	0.00	0.00	0.00	0.00
5	5	0.02	0.00	0.00	0.14	0.00	0.00	0.01	0.00	0.00	0.05	0.00	0.00	0.00	0.00	0.00	0.00	0.00	0.00
5	6	0.08	0.00	0.00	0.18	0.00	0.00	0.02	0.00	0.00	0.04	0.00	0.00	0.00	0.00	0.00	0.00	0.00	0.00
6	2	0.86	0.00	0.00	0.88	0.00	0.07	0.75	0.00	0.00	0.77	0.00	0.06	0.05	0.00	0.00	0.25	0.00	0.06
6	3	0.55	0.00	0.00	0.80	0.00	0.00	0.22	0.00	0.00	0.48	0.00	0.00	0.01	0.00	0.00	0.07	0.00	0.00
6	4	0.44	0.00	0.00	0.74	0.00	0.00	0.12	0.00	0.00	0.37	0.00	0.00	0.00	0.00	0.00	0.06	0.00	0.01
6	5	0.24	0.00	0.00	0.60	0.00	0.00	0.04	0.00	0.00	0.20	0.00	0.00	0.00	0.00	0.00	0.02	0.00	0.00
6	6	0.15	0.00	0.00	0.40	0.00	0.00	0.02	0.00	0.00	0.12	0.00	0.00	0.00	0.00	0.00	0.01	0.00	0.00
7	2	0.93	0.00	0.00	0.95	0.00	0.10	0.93	0.00	0.00	0.94	0.00	0.10	0.32	0.00	0.00	0.60	0.00	0.09
7	3	0.96	0.00	0.00	0.98	0.00	0.00	0.54	0.00	0.00	0.84	0.00	0.00	0.03	0.00	0.00	0.18	0.00	0.01
7	4	0.98	0.00	0.00	1.00	0.00	0.03	0.72	0.00	0.00	0.94	0.00	0.06	0.02	0.00	0.00	0.24	0.00	0.10
7	5	0.95	0.00	0.00	0.99	0.00	0.00	0.55	0.00	0.00	0.86	0.00	0.00	0.00	0.00	0.00	0.06	0.00	0.00
7	6	0.71	0.00	0.00	0.89	0.00	0.00	0.24	0.00	0.00	0.55	0.00	0.00	0.00	0.00	0.00	0.02	0.00	0.00
8	2	0.94	0.00	0.00	0.94	0.00	0.46	0.97	0.00	0.00	0.97	0.00	0.47	0.95	0.00	0.00	0.96	0.00	0.48
8	3	1.00	0.00	0.00	1.00	0.00	0.00	0.98	0.00	0.00	0.99	0.00	0.01	0.08	0.00	0.00	0.39	0.00	0.03
8	4	1.00	0.00	0.00	1.00	0.00	0.35	1.00	0.00	0.00	1.00	0.00	0.38	0.22	0.00	0.00	0.73	0.00	0.37
8	5	1.00	0.00	0.00	1.00	0.00	0.00	1.00	0.00	0.00	1.00	0.00	0.00	0.19	0.00	0.00	0.76	0.00	0.00
8	6	1.00	0.00	0.00	1.00	0.00	0.02	0.93	0.00	0.00	0.99	0.00	0.01	0.07	0.00	0.00	0.40	0.00	0.02
9	2	0.88	0.00	0.00	0.88	0.00	0.94	0.94	0.00	0.00	0.94	0.00	0.95	0.98	0.00	0.00	0.98	0.00	0.95
9	3	0.99	0.00	0.00	0.99	0.00	0.00	1.00	0.00	0.00	1.00	0.00	0.01	0.43	0.00	0.00	0.84	0.00	0.09
9	4	1.00	0.00	0.00	1.00	0.00	0.92	1.00	0.00	0.00	1.00	0.00	0.90	0.83	0.00	0.00	0.97	0.00	0.88
9	5	1.00	0.00	0.00	1.00	0.00	0.00	1.00	0.00	0.00	1.00	0.00	0.00	0.93	0.00	0.00	1.00	0.00	0.00
9	6	1.00	0.00	0.00	1.00	0.00	0.20	1.00	0.00	0.00	1.00	0.00	0.25	0.72	0.00	0.00	0.98	0.00	0.40
10	2	0.78	0.00	0.00	0.78	0.03	1.00	0.88	0.00	0.00	0.88	0.00	1.00	0.97	0.00	0.00	0.97	0.00	1.00
10	3	0.98	0.00	0.00	0.98	0.01	0.02	0.99	0.00	0.00	0.99	0.00	0.04	1.00	0.00	0.00	1.00	0.00	0.27
10	4	1.00	0.00	0.00	1.00	0.00	0.96	1.00	0.00	0.00	1.00	0.00	0.96	1.00	0.00	0.00	1.00	0.00	0.96
10	5	1.00	0.00	0.00	1.00	0.00	0.01	1.00	0.00	0.00	1.00	0.00	0.00	1.00	0.00	0.00	1.00	0.00	0.00
10	6	1.00	0.00	0.00	1.00	0.00	0.55	1.00	0.00	0.00	1.00	0.00	0.78	1.00	0.00	0.00	1.00	0.00	0.92

KS test - Kolmogorov-Smirnov test, C - closeness, B - betweenness, D - degree

Table A22. Barabási-Albert Power Based on Non-parametric Tests with High Degree Degrade

		p=1/7						p=1/10						p=1/20					
		KS Test			Sign Test			KS Test			Sign Test			KS Test			Sign Test		
k	m	C	B	D	C	B	D	C	B	D	C	B	D	C	B	D	C	B	D
5	2	0.05	0.00	0.00	0.09	0.01	0.07	0.01	0.00	0.00	0.01	0.00	0.08	0.00	0.00	0.00	0.00	0.00	0.08
5	3	0.01	0.00	0.00	0.03	0.00	0.01	0.00	0.00	0.00	0.00	0.00	0.00	0.00	0.00	0.00	0.00	0.00	0.00
5	4	0.00	0.00	0.00	0.02	0.00	0.00	0.00	0.00	0.00	0.00	0.00	0.00	0.00	0.00	0.00	0.00	0.00	0.00
5	5	0.00	0.00	0.00	0.02	0.00	0.00	0.00	0.00	0.00	0.00	0.00	0.00	0.00	0.00	0.00	0.00	0.00	0.00
5	6	0.03	0.00	0.00	0.14	0.00	0.00	0.00	0.00	0.00	0.00	0.00	0.00	0.00	0.00	0.00	0.00	0.00	0.00
6	2	0.10	0.00	0.00	0.14	0.02	0.21	0.06	0.00	0.00	0.10	0.01	0.11	0.00	0.00	0.00	0.00	0.00	0.06
6	3	0.03	0.00	0.00	0.08	0.01	0.03	0.01	0.00	0.00	0.04	0.00	0.01	0.00	0.00	0.00	0.00	0.00	0.00
6	4	0.01	0.00	0.00	0.05	0.00	0.03	0.00	0.00	0.00	0.02	0.00	0.00	0.00	0.00	0.00	0.00	0.00	0.01
6	5	0.00	0.00	0.00	0.03	0.00	0.01	0.00	0.00	0.00	0.01	0.00	0.00	0.00	0.00	0.00	0.00	0.00	0.00
6	6	0.00	0.00	0.00	0.05	0.00	0.01	0.00	0.00	0.00	0.01	0.00	0.00	0.00	0.00	0.00	0.00	0.00	0.00
7	2	0.14	0.01	0.00	0.18	0.03	0.57	0.11	0.01	0.00	0.17	0.03	0.49	0.05	0.00	0.00	0.08	0.01	0.24
7	3	0.11	0.01	0.01	0.20	0.03	0.02	0.06	0.01	0.00	0.13	0.01	0.01	0.02	0.00	0.00	0.04	0.00	0.01
7	4	0.05	0.00	0.01	0.22	0.03	0.39	0.02	0.00	0.00	0.10	0.01	0.16	0.00	0.00	0.00	0.01	0.00	0.07
7	5	0.03	0.00	0.01	0.20	0.02	0.08	0.00	0.00	0.00	0.07	0.01	0.02	0.00	0.00	0.00	0.01	0.00	0.00
7	6	0.02	0.00	0.01	0.16	0.02	0.19	0.00	0.00	0.00	0.04	0.00	0.04	0.00	0.00	0.00	0.00	0.00	0.00
8	2	0.13	0.02	0.01	0.15	0.03	0.70	0.15	0.02	0.00	0.19	0.03	0.82	0.08	0.01	0.00	0.13	0.02	0.81
8	3	0.22	0.05	0.14	0.32	0.08	0.08	0.13	0.03	0.01	0.23	0.04	0.01	0.05	0.01	0.00	0.10	0.01	0.01
8	4	0.21	0.04	0.18	0.36	0.08	0.66	0.09	0.02	0.01	0.25	0.04	0.63	0.02	0.00	0.00	0.07	0.01	0.58
8	5	0.29	0.03	0.19	0.53	0.07	0.48	0.11	0.01	0.01	0.38	0.03	0.12	0.00	0.00	0.00	0.05	0.00	0.00
8	6	0.33	0.02	0.20	0.58	0.06	0.40	0.10	0.01	0.01	0.39	0.03	0.31	0.00	0.00	0.00	0.03	0.00	0.08
9	2	0.07	0.05	0.05	0.07	0.01	0.96	0.13	0.02	0.01	0.15	0.03	0.97	0.12	0.01	0.00	0.18	0.03	0.99
9	3	0.33	0.10	0.70	0.38	0.15	0.33	0.21	0.06	0.15	0.31	0.09	0.04	0.09	0.02	0.00	0.16	0.03	0.01
9	4	0.35	0.13	0.85	0.44	0.19	0.68	0.19	0.06	0.20	0.34	0.10	0.77	0.06	0.01	0.00	0.14	0.02	0.94
9	5	0.47	0.12	0.89	0.54	0.20	0.96	0.29	0.05	0.22	0.46	0.10	0.59	0.03	0.01	0.00	0.18	0.02	0.05
9	6	0.67	0.10	0.92	0.77	0.19	0.35	0.51	0.04	0.26	0.69	0.09	0.22	0.03	0.00	0.00	0.34	0.02	0.20
10	2	0.01	0.01	0.01	0.01	0.00	1.00	0.07	0.05	0.05	0.07	0.01	1.00	0.15	0.02	0.00	0.20	0.03	1.00
10	3	0.44	0.19	0.74	0.42	0.22	0.76	0.34	0.09	0.76	0.41	0.16	0.16	0.15	0.03	0.01	0.23	0.06	0.02
10	4	0.45	0.23	0.98	0.52	0.33	0.68	0.30	0.12	0.88	0.42	0.18	0.93	0.10	0.03	0.01	0.21	0.05	0.96
10	5	0.54	0.28	1.00	0.53	0.39	1.00	0.36	0.13	0.90	0.46	0.21	0.97	0.09	0.03	0.01	0.24	0.06	0.28
10	6	0.77	0.28	1.00	0.67	0.40	0.54	0.60	0.13	0.94	0.63	0.22	0.10	0.17	0.02	0.01	0.45	0.05	0.17

KS test - Kolmogorov-Smirnov test, C - closeness, B - betweenness, D - degree

Table A23. Barabási-Albert Power Based on Non-parametric Tests with Random Degrade

		p=1/7						p=1/10						p=1/20					
		KS Test			Sign Test			KS Test			Sign Test			KS Test			Sign Test		
k	m	C	B	D	C	B	D	C	B	D	C	B	D	C	B	D	C	B	D
5	2	0.00	0.00	0.00	0.00	0.00	0.08	0.00	0.00	0.00	0.00	0.00	0.08	0.00	0.00	0.00	0.00	0.00	0.08
5	3	0.00	0.00	0.00	0.00	0.00	0.00	0.00	0.00	0.00	0.00	0.00	0.00	0.00	0.00	0.00	0.00	0.00	0.00
5	4	0.00	0.00	0.00	0.00	0.00	0.00	0.00	0.00	0.00	0.00	0.00	0.00	0.00	0.00	0.00	0.00	0.00	0.00
5	5	0.00	0.00	0.00	0.00	0.00	0.00	0.00	0.00	0.00	0.00	0.00	0.00	0.00	0.00	0.00	0.00	0.00	0.00
5	6	0.00	0.00	0.00	0.00	0.00	0.00	0.00	0.00	0.00	0.00	0.00	0.00	0.00	0.00	0.00	0.00	0.00	0.00
6	2	0.02	0.00	0.00	0.05	0.00	0.07	0.02	0.00	0.00	0.05	0.00	0.07	0.00	0.00	0.00	0.00	0.00	0.06
6	3	0.00	0.00	0.00	0.09	0.00	0.00	0.00	0.00	0.00	0.09	0.00	0.00	0.00	0.00	0.00	0.00	0.00	0.00
6	4	0.01	0.00	0.00	0.11	0.00	0.01	0.01	0.00	0.00	0.11	0.00	0.01	0.00	0.00	0.00	0.00	0.00	0.01
6	5	0.00	0.00	0.00	0.10	0.00	0.00	0.00	0.00	0.00	0.10	0.00	0.00	0.00	0.00	0.00	0.00	0.00	0.00
6	6	0.01	0.00	0.00	0.10	0.00	0.00	0.01	0.00	0.00	0.10	0.00	0.00	0.00	0.00	0.00	0.00	0.00	0.00
7	2	0.04	0.00	0.00	0.22	0.01	0.22	0.02	0.00	0.00	0.07	0.00	0.17	0.01	0.00	0.00	0.02	0.00	0.13
7	3	0.14	0.00	0.00	0.53	0.00	0.01	0.01	0.00	0.00	0.20	0.00	0.01	0.00	0.00	0.00	0.01	0.00	0.02
7	4	0.37	0.00	0.00	0.76	0.00	0.09	0.04	0.00	0.00	0.40	0.00	0.09	0.00	0.00	0.00	0.02	0.00	0.11
7	5	0.42	0.00	0.00	0.78	0.00	0.00	0.03	0.00	0.00	0.41	0.00	0.00	0.00	0.00	0.00	0.02	0.00	0.00
7	6	0.46	0.00	0.00	0.76	0.00	0.01	0.03	0.00	0.00	0.35	0.00	0.00	0.00	0.00	0.00	0.01	0.00	0.00
8	2	0.29	0.00	0.00	0.50	0.01	0.74	0.05	0.00	0.00	0.28	0.01	0.69	0.01	0.00	0.00	0.02	0.00	0.58
8	3	0.64	0.00	0.00	0.77	0.00	0.01	0.22	0.00	0.00	0.57	0.00	0.02	0.01	0.00	0.00	0.02	0.00	0.06
8	4	0.86	0.00	0.00	0.92	0.00	0.54	0.63	0.00	0.00	0.83	0.00	0.50	0.00	0.00	0.00	0.08	0.00	0.42
8	5	0.95	0.00	0.00	0.98	0.00	0.01	0.84	0.00	0.00	0.93	0.00	0.00	0.00	0.00	0.00	0.20	0.00	0.00
8	6	0.97	0.00	0.00	0.99	0.00	0.11	0.86	0.00	0.00	0.95	0.00	0.07	0.00	0.00	0.00	0.18	0.00	0.03
9	2	0.57	0.01	0.00	0.68	0.01	0.99	0.27	0.01	0.00	0.59	0.01	0.99	0.02	0.00	0.00	0.09	0.00	0.98
9	3	0.84	0.01	0.00	0.87	0.01	0.03	0.62	0.00	0.00	0.77	0.01	0.06	0.01	0.00	0.00	0.15	0.00	0.14
9	4	0.92	0.00	0.00	0.93	0.01	0.93	0.82	0.00	0.00	0.88	0.00	0.93	0.02	0.00	0.00	0.41	0.00	0.90
9	5	0.98	0.00	0.00	0.99	0.00	0.05	0.94	0.00	0.00	0.96	0.00	0.02	0.29	0.00	0.00	0.79	0.00	0.00
9	6	1.00	0.00	0.00	1.00	0.00	0.21	0.99	0.00	0.00	0.99	0.00	0.24	0.66	0.00	0.00	0.90	0.00	0.35
10	2	0.61	0.01	0.00	0.65	0.01	1.00	0.59	0.01	0.00	0.71	0.01	1.00	0.03	0.00	0.00	0.40	0.01	1.00
10	3	0.92	0.01	0.01	0.93	0.01	0.06	0.84	0.00	0.00	0.88	0.01	0.15	0.05	0.00	0.00	0.55	0.01	0.39
10	4	0.97	0.00	0.01	0.97	0.01	0.96	0.90	0.00	0.00	0.92	0.01	0.96	0.18	0.00	0.00	0.67	0.00	0.96
10	5	0.99	0.00	0.02	0.99	0.01	0.22	0.95	0.00	0.00	0.96	0.01	0.07	0.60	0.00	0.00	0.86	0.00	0.01
10	6	1.00	0.00	0.03	1.00	0.01	0.21	0.99	0.00	0.00	1.00	0.00	0.46	0.89	0.00	0.00	0.94	0.00	0.79

KS test - Kolmogorov-Smirnov test, C - closeness, B - betweenness, D - degree

Table A24. Watts-Strogratz Power Based on Non-parametric Tests with Low Degrade

		p=1/7						p=1/10						p=1/20					
		KS Test			Sign Test			KS Test			Sign Test			KS Test			Sign Test		
k	m	C	B	D	C	B	D	C	B	D	C	B	D	C	B	D	C	B	D
5	2	0.10	0.00	0.00	0.26	0.00	0.00	0.02	0.00	0.00	0.11	0.00	0.01	0.00	0.00	0.00	0.00	0.00	0.01
5	3	0.12	0.00	0.00	0.39	0.00	0.00	0.01	0.00	0.00	0.14	0.00	0.00	0.00	0.00	0.00	0.00	0.00	0.00
5	4	0.40	0.00	0.00	0.41	0.00	0.00	0.12	0.00	0.00	0.12	0.00	0.00	0.00	0.00	0.00	0.00	0.00	0.00
5	5	0.39	0.00	0.00	0.61	0.00	0.00	0.12	0.00	0.00	0.19	0.00	0.00	0.00	0.00	0.00	0.00	0.00	0.00
5	6	0.40	0.00	0.00	0.93	0.00	0.01	0.11	0.00	0.00	0.28	0.00	0.00	0.00	0.00	0.00	0.00	0.00	0.00
6	2	0.49	0.00	0.00	0.65	0.00	0.00	0.08	0.00	0.00	0.30	0.00	0.00	0.00	0.00	0.00	0.03	0.00	0.00
6	3	0.60	0.00	0.00	0.78	0.00	0.01	0.12	0.00	0.00	0.27	0.00	0.01	0.00	0.00	0.00	0.03	0.00	0.01
6	4	0.71	0.00	0.00	0.89	0.00	0.00	0.11	0.00	0.00	0.38	0.00	0.00	0.00	0.00	0.00	0.03	0.00	0.00
6	5	0.83	0.00	0.00	0.91	0.00	0.00	0.22	0.00	0.00	0.48	0.00	0.00	0.01	0.00	0.00	0.05	0.00	0.00
6	6	0.93	0.00	0.00	0.94	0.00	0.01	0.70	0.00	0.00	0.74	0.00	0.00	0.11	0.00	0.00	0.13	0.00	0.00
7	2	0.75	0.00	0.00	0.83	0.00	0.00	0.60	0.00	0.00	0.70	0.00	0.00	0.00	0.00	0.00	0.14	0.00	0.00
7	3	0.98	0.00	0.00	0.98	0.00	0.00	0.60	0.00	0.00	0.87	0.00	0.00	0.01	0.00	0.00	0.06	0.00	0.00
7	4	1.00	0.00	0.00	1.00	0.00	0.01	0.97	0.00	0.00	0.99	0.00	0.00	0.02	0.00	0.00	0.15	0.00	0.00
7	5	1.00	0.00	0.00	1.00	0.00	0.01	0.91	0.00	0.00	0.98	0.00	0.00	0.07	0.00	0.00	0.28	0.00	0.00
7	6	1.00	0.00	0.00	1.00	0.00	0.02	0.84	0.00	0.00	0.96	0.00	0.01	0.11	0.00	0.00	0.31	0.00	0.00
8	2	0.72	0.00	0.00	0.72	0.00	0.01	0.76	0.00	0.00	0.79	0.00	0.01	0.27	0.00	0.00	0.59	0.00	0.00
8	3	0.97	0.00	0.00	0.97	0.00	0.01	0.98	0.00	0.00	0.98	0.00	0.01	0.11	0.00	0.00	0.64	0.00	0.00
8	4	0.99	0.00	0.00	0.99	0.00	0.03	1.00	0.00	0.00	1.00	0.00	0.01	0.54	0.00	0.00	0.93	0.00	0.01
8	5	1.00	0.00	0.00	1.00	0.01	0.08	1.00	0.00	0.00	1.00	0.00	0.03	0.91	0.00	0.00	0.97	0.00	0.01
8	6	1.00	0.00	0.00	1.00	0.02	0.12	1.00	0.00	0.00	1.00	0.00	0.04	0.68	0.00	0.00	0.92	0.00	0.01
9	2	0.49	0.00	0.00	0.49	0.00	0.03	0.60	0.00	0.00	0.60	0.00	0.03	0.64	0.00	0.00	0.75	0.00	0.02
9	3	0.94	0.00	0.00	0.94	0.00	0.05	0.96	0.00	0.00	0.96	0.00	0.04	0.96	0.00	0.00	0.98	0.00	0.02
9	4	0.99	0.00	0.00	0.99	0.02	0.17	0.99	0.00	0.00	0.99	0.00	0.09	1.00	0.00	0.00	1.00	0.00	0.03
9	5	1.00	0.00	0.00	1.00	0.07	0.35	1.00	0.00	0.00	1.00	0.00	0.16	1.00	0.00	0.00	1.00	0.00	0.04
9	6	1.00	0.00	0.00	1.00	0.07	0.36	1.00	0.00	0.00	1.00	0.00	0.18	1.00	0.00	0.00	1.00	0.00	0.04
10	2	0.21	0.00	0.00	0.21	0.01	0.12	0.33	0.00	0.00	0.33	0.00	0.12	0.57	0.00	0.00	0.57	0.00	0.12
10	3	0.88	0.00	0.00	0.88	0.03	0.25	0.92	0.00	0.00	0.91	0.00	0.20	0.96	0.00	0.00	0.96	0.00	0.14
10	4	0.98	0.00	0.00	0.98	0.18	0.59	0.98	0.00	0.00	0.98	0.01	0.38	0.99	0.00	0.00	0.99	0.00	0.17
10	5	1.00	0.00	0.00	1.00	0.40	0.85	0.98	0.00	0.00	1.00	0.04	0.59	1.00	0.00	0.00	1.00	0.00	0.22
10	6	1.00	0.00	0.00	1.00	0.30	0.70	1.00	0.00	0.00	1.00	0.03	0.48	1.00	0.00	0.00	1.00	0.00	0.18

KS test - Kolmogorov-Smirnov test, C - closeness, B - betweenness, D - degree

Table A25. Watts-Strogratz Power Based on Non-parametric Tests with Medium Degrade

		p=1/7						p=1/10						p=1/20					
		KS Test			Sign Test			KS Test			Sign Test			KS Test			Sign Test		
k	m	C	B	D	C	B	D	C	B	D	C	B	D	C	B	D	C	B	D
5	2	0.06	0.00	0.00	0.16	0.00	0.01	0.01	0.00	0.00	0.04	0.00	0.01	0.00	0.00	0.00	0.00	0.00	0.01
5	3	0.15	0.00	0.00	0.32	0.00	0.01	0.01	0.00	0.00	0.09	0.00	0.00	0.00	0.00	0.00	0.00	0.00	0.00
5	4	0.35	0.00	0.00	0.33	0.00	0.02	0.14	0.00	0.00	0.12	0.00	0.01	0.00	0.00	0.00	0.00	0.00	0.00
5	5	0.28	0.00	0.00	0.49	0.00	0.03	0.14	0.00	0.00	0.34	0.00	0.01	0.00	0.00	0.00	0.00	0.00	0.00
5	6	0.24	0.00	0.00	0.78	0.00	0.04	0.16	0.00	0.00	0.59	0.00	0.01	0.00	0.00	0.00	0.00	0.00	0.00
6	2	0.18	0.00	0.00	0.28	0.00	0.01	0.03	0.00	0.00	0.13	0.00	0.00	0.00	0.00	0.00	0.00	0.00	0.00
6	3	0.60	0.00	0.00	0.69	0.00	0.03	0.17	0.00	0.00	0.34	0.00	0.01	0.00	0.00	0.00	0.03	0.00	0.00
6	4	0.66	0.00	0.00	0.79	0.00	0.04	0.18	0.00	0.00	0.48	0.00	0.01	0.00	0.00	0.00	0.09	0.00	0.00
6	5	0.66	0.00	0.00	0.81	0.00	0.04	0.29	0.00	0.00	0.51	0.00	0.01	0.01	0.00	0.00	0.10	0.00	0.00
6	6	0.92	0.00	0.00	0.91	0.00	0.06	0.58	0.00	0.00	0.62	0.00	0.01	0.21	0.00	0.00	0.22	0.00	0.00
7	2	0.36	0.00	0.00	0.42	0.00	0.05	0.20	0.00	0.00	0.32	0.00	0.02	0.00	0.00	0.00	0.05	0.00	0.00
7	3	0.89	0.00	0.00	0.91	0.00	0.14	0.62	0.00	0.00	0.76	0.00	0.04	0.01	0.00	0.00	0.14	0.00	0.01
7	4	0.99	0.00	0.00	0.99	0.00	0.18	0.84	0.00	0.00	0.93	0.00	0.04	0.09	0.00	0.00	0.38	0.00	0.01
7	5	0.99	0.00	0.00	0.99	0.00	0.20	0.87	0.00	0.00	0.93	0.00	0.05	0.08	0.00	0.00	0.33	0.00	0.01
7	6	0.98	0.00	0.00	0.99	0.00	0.21	0.81	0.00	0.00	0.89	0.00	0.05	0.07	0.00	0.00	0.20	0.00	0.01
8	2	0.38	0.00	0.00	0.43	0.00	0.16	0.32	0.00	0.00	0.41	0.00	0.09	0.04	0.00	0.00	0.20	0.00	0.03
8	3	0.91	0.00	0.00	0.91	0.00	0.53	0.92	0.00	0.00	0.93	0.00	0.23	0.26	0.00	0.00	0.62	0.00	0.04
8	4	0.99	0.00	0.00	0.99	0.00	0.68	0.99	0.00	0.00	0.99	0.00	0.29	0.43	0.00	0.00	0.72	0.00	0.04
8	5	1.00	0.00	0.00	1.00	0.00	0.70	1.00	0.00	0.00	1.00	0.00	0.31	0.65	0.00	0.00	0.90	0.00	0.04
8	6	1.00	0.00	0.00	1.00	0.01	0.67	1.00	0.00	0.00	1.00	0.00	0.30	0.72	0.00	0.00	0.89	0.00	0.03
9	2	0.25	0.00	0.00	0.25	0.00	0.20	0.31	0.00	0.00	0.35	0.00	0.20	0.28	0.00	0.00	0.34	0.00	0.11
9	3	0.81	0.00	0.01	0.81	0.00	0.80	0.87	0.00	0.00	0.87	0.00	0.69	0.89	0.00	0.00	0.92	0.00	0.22
9	4	0.98	0.00	0.02	0.98	0.01	0.97	0.99	0.00	0.00	0.99	0.00	0.85	0.97	0.00	0.00	0.99	0.00	0.23
9	5	1.00	0.00	0.03	1.00	0.01	0.99	1.00	0.00	0.00	1.00	0.00	0.84	0.99	0.00	0.00	1.00	0.00	0.23
9	6	1.00	0.00	0.03	1.00	0.02	0.98	1.00	0.00	0.00	1.00	0.00	0.81	1.00	0.00	0.00	1.00	0.00	0.20
10	2	0.06	0.00	0.00	0.06	0.00	0.15	0.15	0.00	0.00	0.15	0.00	0.22	0.21	0.00	0.00	0.29	0.00	0.28
10	3	0.66	0.00	0.16	0.66	0.02	0.69	0.76	0.00	0.00	0.76	0.00	0.78	0.88	0.00	0.00	0.88	0.00	0.68
10	4	0.95	0.01	0.49	0.95	0.06	0.96	0.97	0.00	0.00	0.97	0.00	0.97	0.99	0.00	0.00	0.99	0.00	0.79
10	5	0.99	0.01	0.59	0.99	0.09	0.99	1.00	0.00	0.01	1.00	0.01	1.00	1.00	0.00	0.00	1.00	0.00	0.75
10	6	1.00	0.00	0.64	1.00	0.09	1.00	1.00	0.00	0.01	1.00	0.01	1.00	1.00	0.00	0.00	1.00	0.00	0.69

KS test - Kolmogorov-Smirnov test, C - closeness, B - betweenness, D - degree

Table A26. Watts-Strogratz Power Based on Non-parametric Tests with High Degrade

		p=1/7						p=1/10						p=1/20					
		KS Test			Sign Test			KS Test			Sign Test			KS Test			Sign Test		
k	m	C	B	D	C	B	D	C	B	D	C	B	D	C	B	D	C	B	D
5	2	0.00	0.00	0.00	0.01	0.00	0.01	0.00	0.00	0.00	0.00	0.00	0.01	0.00	0.00	0.00	0.00	0.00	0.01
5	3	0.01	0.00	0.00	0.04	0.00	0.02	0.00	0.00	0.00	0.02	0.00	0.01	0.00	0.00	0.00	0.00	0.00	0.00
5	4	0.11	0.00	0.00	0.08	0.00	0.04	0.04	0.00	0.00	0.02	0.00	0.01	0.00	0.00	0.00	0.00	0.00	0.00
5	5	0.10	0.00	0.00	0.35	0.00	0.05	0.04	0.00	0.00	0.09	0.00	0.01	0.00	0.00	0.00	0.00	0.00	0.00
5	6	0.11	0.00	0.00	0.69	0.00	0.07	0.04	0.00	0.00	0.20	0.00	0.02	0.00	0.00	0.00	0.00	0.00	0.00
6	2	0.00	0.00	0.00	0.02	0.00	0.19	0.00	0.00	0.00	0.01	0.00	0.04	0.00	0.00	0.00	0.00	0.00	0.00
6	3	0.05	0.00	0.00	0.10	0.00	0.18	0.01	0.00	0.00	0.03	0.00	0.03	0.00	0.00	0.00	0.00	0.00	0.01
6	4	0.05	0.00	0.00	0.21	0.00	0.16	0.01	0.00	0.00	0.06	0.00	0.02	0.00	0.00	0.00	0.01	0.00	0.00
6	5	0.09	0.00	0.00	0.37	0.00	0.16	0.01	0.00	0.00	0.08	0.00	0.02	0.00	0.00	0.00	0.01	0.00	0.00
6	6	0.71	0.00	0.00	0.74	0.00	0.19	0.28	0.00	0.00	0.35	0.00	0.02	0.02	0.00	0.00	0.03	0.00	0.00
7	2	0.01	0.00	0.00	0.04	0.00	0.46	0.00	0.00	0.00	0.02	0.00	0.26	0.00	0.00	0.00	0.00	0.00	0.03
7	3	0.05	0.00	0.00	0.11	0.00	0.57	0.01	0.00	0.00	0.05	0.00	0.22	0.00	0.00	0.00	0.00	0.00	0.02
7	4	0.42	0.00	0.00	0.71	0.00	0.69	0.06	0.00	0.00	0.38	0.00	0.24	0.00	0.00	0.00	0.01	0.00	0.01
7	5	0.82	0.00	0.00	0.92	0.00	0.77	0.28	0.00	0.00	0.64	0.00	0.28	0.00	0.00	0.00	0.03	0.00	0.01
7	6	0.76	0.00	0.01	0.90	0.00	0.75	0.35	0.00	0.00	0.61	0.00	0.28	0.00	0.00	0.00	0.04	0.00	0.01
8	2	0.03	0.00	0.02	0.09	0.00	0.33	0.01	0.00	0.00	0.05	0.00	0.43	0.00	0.00	0.00	0.01	0.00	0.17
8	3	0.05	0.00	0.03	0.15	0.00	0.89	0.02	0.00	0.00	0.07	0.00	0.68	0.00	0.00	0.00	0.01	0.00	0.12
8	4	0.78	0.00	0.02	0.88	0.00	0.98	0.22	0.00	0.00	0.57	0.00	0.83	0.00	0.00	0.00	0.05	0.00	0.16
8	5	1.00	0.00	0.13	1.00	0.00	1.00	0.98	0.00	0.00	0.99	0.00	0.91	0.10	0.00	0.00	0.53	0.00	0.16
8	6	1.00	0.00	0.30	1.00	0.00	0.99	1.00	0.00	0.00	1.00	0.00	0.87	0.27	0.00	0.00	0.61	0.00	0.13
9	2	0.05	0.00	0.06	0.07	0.00	0.11	0.03	0.00	0.01	0.08	0.00	0.22	0.00	0.00	0.00	0.03	0.00	0.41
9	3	0.04	0.00	0.12	0.12	0.00	0.81	0.01	0.00	0.00	0.06	0.00	0.88	0.00	0.00	0.00	0.00	0.00	0.54
9	4	0.97	0.00	0.80	0.97	0.00	0.97	0.87	0.00	0.00	0.95	0.00	0.98	0.01	0.00	0.00	0.30	0.00	0.64
9	5	1.00	0.00	0.97	1.00	0.00	1.00	1.00	0.00	0.08	1.00	0.00	1.00	0.45	0.00	0.00	0.79	0.00	0.73
9	6	1.00	0.00	0.79	1.00	0.01	1.00	1.00	0.00	0.24	1.00	0.00	1.00	0.91	0.00	0.00	0.98	0.00	0.66
10	2	0.01	0.00	0.01	0.01	0.00	0.10	0.03	0.00	0.03	0.03	0.00	0.13	0.01	0.00	0.00	0.05	0.00	0.29
10	3	0.05	0.00	0.66	0.15	0.00	0.69	0.01	0.00	0.05	0.09	0.00	0.78	0.00	0.00	0.00	0.01	0.00	0.87
10	4	0.94	0.00	0.94	0.94	0.01	0.94	0.96	0.00	0.78	0.96	0.00	0.96	0.62	0.00	0.00	0.90	0.00	0.98
10	5	0.99	0.00	0.99	0.99	0.05	0.99	0.99	0.00	0.99	0.99	0.01	1.00	0.99	0.00	0.00	1.00	0.00	0.99
10	6	1.00	0.00	1.00	1.00	0.04	1.00	1.00	0.00	0.72	1.00	0.01	1.00	0.92	0.00	0.00	0.99	0.00	0.97

KS test - Kolmogorov-Smirnov test, C - closeness, B - betweenness, D - degree

Table A27. Watts-Strogratz Power Based on Non-parametric Tests with Random Degrade

		p=1/7						p=1/10						p=1/20					
		KS Test			Sign Test			KS Test			Sign Test			KS Test			Sign Test		
k	m	C	B	D	C	B	D	C	B	D	C	B	D	C	B	D	C	B	D
5	2	0.00	0.00	0.00	0.00	0.00	0.01	0.00	0.00	0.00	0.00	0.00	0.01	0.00	0.00	0.00	0.00	0.00	0.01
5	3	0.00	0.00	0.00	0.00	0.00	0.00	0.00	0.00	0.00	0.00	0.00	0.00	0.00	0.00	0.00	0.00	0.00	0.00
5	4	0.00	0.00	0.00	0.00	0.00	0.00	0.00	0.00	0.00	0.00	0.00	0.00	0.00	0.00	0.00	0.00	0.00	0.00
5	5	0.00	0.00	0.00	0.00	0.00	0.00	0.00	0.00	0.00	0.00	0.00	0.00	0.00	0.00	0.00	0.00	0.00	0.00
5	6	0.00	0.00	0.00	0.00	0.00	0.00	0.00	0.00	0.00	0.00	0.00	0.00	0.00	0.00	0.00	0.00	0.00	0.00
6	2	0.00	0.00	0.00	0.02	0.00	0.00	0.00	0.00	0.00	0.02	0.00	0.00	0.00	0.00	0.00	0.00	0.00	0.00
6	3	0.00	0.00	0.00	0.06	0.00	0.00	0.00	0.00	0.00	0.06	0.00	0.01	0.00	0.00	0.00	0.00	0.00	0.01
6	4	0.01	0.00	0.00	0.14	0.00	0.00	0.01	0.00	0.00	0.13	0.00	0.01	0.00	0.00	0.00	0.00	0.00	0.00
6	5	0.02	0.00	0.00	0.16	0.00	0.00	0.02	0.00	0.00	0.16	0.00	0.00	0.00	0.00	0.00	0.00	0.00	0.00
6	6	0.38	0.00	0.00	0.44	0.00	0.01	0.38	0.00	0.00	0.44	0.00	0.01	0.00	0.00	0.00	0.00	0.00	0.00
7	2	0.02	0.00	0.00	0.14	0.00	0.03	0.00	0.00	0.00	0.04	0.00	0.01	0.00	0.00	0.00	0.00	0.00	0.00
7	3	0.17	0.00	0.00	0.50	0.00	0.04	0.01	0.00	0.00	0.17	0.00	0.01	0.00	0.00	0.00	0.01	0.00	0.00
7	4	0.61	0.00	0.00	0.86	0.00	0.05	0.13	0.00	0.00	0.48	0.00	0.02	0.00	0.00	0.00	0.04	0.00	0.01
7	5	0.82	0.00	0.00	0.93	0.00	0.06	0.16	0.00	0.00	0.62	0.00	0.02	0.00	0.00	0.00	0.06	0.00	0.00
7	6	0.87	0.00	0.00	0.95	0.00	0.07	0.21	0.00	0.00	0.59	0.00	0.02	0.00	0.00	0.00	0.07	0.00	0.00
8	2	0.16	0.00	0.00	0.32	0.00	0.14	0.03	0.00	0.00	0.19	0.00	0.07	0.00	0.00	0.00	0.01	0.00	0.01
8	3	0.83	0.00	0.00	0.90	0.00	0.28	0.42	0.00	0.00	0.71	0.00	0.13	0.00	0.00	0.00	0.04	0.00	0.02
8	4	0.99	0.00	0.00	0.99	0.00	0.34	0.85	0.00	0.00	0.94	0.00	0.15	0.00	0.00	0.00	0.11	0.00	0.02
8	5	1.00	0.00	0.00	1.00	0.00	0.40	1.00	0.00	0.00	1.00	0.00	0.17	0.04	0.00	0.00	0.43	0.00	0.02
8	6	1.00	0.00	0.00	1.00	0.00	0.45	1.00	0.00	0.00	1.00	0.00	0.19	0.10	0.00	0.00	0.57	0.00	0.02
9	2	0.27	0.00	0.00	0.34	0.00	0.29	0.14	0.00	0.00	0.29	0.00	0.22	0.00	0.00	0.00	0.06	0.00	0.09
9	3	0.90	0.00	0.00	0.90	0.00	0.70	0.86	0.00	0.00	0.91	0.00	0.48	0.05	0.00	0.00	0.41	0.00	0.15
9	4	0.99	0.00	0.00	0.99	0.00	0.81	0.99	0.00	0.00	0.99	0.00	0.54	0.30	0.00	0.00	0.79	0.00	0.15
9	5	1.00	0.00	0.00	1.00	0.00	0.86	1.00	0.00	0.00	1.00	0.00	0.57	0.71	0.00	0.00	0.93	0.00	0.15
9	6	1.00	0.00	0.00	1.00	0.00	0.90	1.00	0.00	0.00	1.00	0.00	0.61	1.00	0.00	0.00	1.00	0.00	0.14
10	2	0.18	0.00	0.00	0.19	0.00	0.27	0.21	0.00	0.00	0.27	0.00	0.34	0.01	0.00	0.00	0.15	0.00	0.32
10	3	0.80	0.00	0.00	0.80	0.00	0.82	0.86	0.00	0.00	0.86	0.00	0.82	0.47	0.00	0.00	0.82	0.00	0.55
10	4	0.97	0.00	0.00	0.97	0.00	0.97	0.98	0.00	0.00	0.98	0.00	0.93	0.98	0.00	0.00	0.99	0.00	0.55
10	5	1.00	0.00	0.01	1.00	0.01	1.00	1.00	0.00	0.00	1.00	0.00	0.96	1.00	0.00	0.00	1.00	0.00	0.53
10	6	1.00	0.00	0.05	1.00	0.02	1.00	1.00	0.00	0.00	1.00	0.00	0.97	1.00	0.00	0.00	1.00	0.00	0.52

KS test - Kolmogorov-Smirnov test, C - closeness, B - betweenness, D - degree

Table A28. Power to Detect degrade High School Network for Day 1 at p = 1/3

	closeness	betweenness	degree	Node % Removed
Kolmogorov-Smirnov test				
Low	1.00	0.00	0.00	0.1033
Med	0.00	0.00	0.00	0.0413
High	0.00	0.00	0.00	0.1074
Random	0.81	0.00	0.00	0.1000
Sign test				
Low	1.00	0.00	0.00	0.10
Med	0.30	0.00	0.00	0.04
High	0.10	0.00	0.40	0.11
Random	1.00	0.00	0.00	0.10

Table A29. Power to Detect degrade High School Network for Day 2 at p = 1/3

	closeness	betweenness	degree	Node % Removed
Kolmogorov-Smirnov test				
Low	1.00	0.00	0.00	0.1033
Med	0.32	0.00	0.00	0.0413
High	0.00	0.00	0.00	0.1074
Random	0.70	0.00	0.00	0.1000
Sign test				
Low	1.00	0.00	0.00	0.10
Med	0.00	0.00	0.00	0.04
High	0.01	0.00	0.00	0.11
Random	0.17	0.00	0.00	0.10

Table A30. Power to Detect degrade High School Network for Day 3 at p = 1/3

	closeness	betweenness	degree	Node % Removed
Kolmogorov-Smirnov test				
Low	1.00	0.00	0.00	0.1033
Med	0.00	0.00	0.00	0.0413
High	0.04	0.00	0.02	0.1074
Random	0.94	0.00	0.00	0.1000
Sign test				
Low	1.00	0.00	0.00	0.10
Med	0.00	0.00	0.00	0.04
High	0.04	0.00	1.00	0.11
Random	0.63	0.00	0.01	0.10

Table A31. Power to Detect degrade High School Network for Day 4 at p = 1/3

	closeness	betweenness	degree	Node % Removed
Kolmogorov-Smirnov test				
Low	1.00	0.00	0.00	0.1033
Med	0.08	0.00	0.00	0.0413
High	0.34	0.00	0.21	0.1074
Random	0.90	0.00	0.00	0.1000
Sign test				
Low	1.00	0.00	0.00	0.10
Med	0.47	0.00	0.00	0.04
High	0.69	0.01	0.92	0.11
Random	0.98	0.00	0.00	0.10

Appendix B. Appendix B: Theoretical Derivations for the Exact Variance and Covariance of Sample L-moments

Appendix B has derivations for the exact variance and covariance equations. It begins by calculating various equations needed to solve the general variance and covariance for L-moments. In addition, the general equations for any Pareto are derived as well.

Expansion, Special Cases of Variance Equations

$$var(b_k, b_1) = \Theta_{kl}$$

$$\Theta_{ij} = \Theta_{ji} = (i+1)(j+1)\sum_{s=0}^{i} b_{ij}^{(s)}(n-j-1)^{(s)}/n^{(i+1)} \tag{79}$$

$$var(b_k, b_l) = \frac{1}{n^{(k+1)}}\sum_{s=0}^{k}(n-l-1)^{(s)}A_{k,l}^{s} \text{ Elamir Equation 19}$$

where $n^{(k+1)}$ and $(n-l-1)^{(s)}$ are of the form $n^{(r)} = n(n-1)...(n-r+1)$

Expansion of $var(b_k, b_l)$ in terms of $A^{(s)}_{k,l}$

$$
\begin{aligned}
var(b_0, b_0) =& \frac{1}{n} A^0_{0,0} \\
var(b_0, b_1) =& \frac{1}{n} A^0_{0,1} \\
var(b_1, b_1) =& \frac{1}{n(n-1)} [A^0_{1,1} + (n-2) A^1_{1,1}] \\
var(b_0, b_2) =& \frac{1}{n} A^0_{0,2} \\
var(b_1, b_2) =& \frac{1}{n(n-1)} [A^0_{1,2} + (n-3) A^1_{1,2}] \\
var(b_2, b_2) =& \frac{1}{n(n-1)(n-2)} [A^0_{2,2} + (n-3) A^1_{2,2} + (n-3)(n-4) A^2_{2,2}] \\
var(b_0, b_3) =& \frac{1}{n} A^0_{0,3} \\
var(b_1, b_3) =& \frac{1}{n(n-1)} [A^0_{1,3} + (n-4) A^1_{1,3}] \\
var(b_2, b_3) =& \frac{1}{n(n-1)(n-2)} [A^0_{2,3} + (n-4) A^1_{2,3} + (n-4)(n-5) A^2_{2,3}] \\
var(b_3, b_3) =& \frac{1}{n(n-1)...(n-3)} [A^0_{3,3} + (n-4) A^1_{3,3} + (n-4)(n-5) A^2_{3,3} + (n-4)(n-5)(n-6) A^3_{3,3}]
\end{aligned}
$$

Special Cases for $A^{(s)}_{kl}$.

$$
\begin{aligned}
\text{when } k = l\text{: } A^{(s)}_{kk} =& \frac{k!k!E[Y^2_{s+k+1;s+k+1}]}{(k-s)!s!s!(s+k+1)} + \\
& \frac{k!k!(k+1)^{(k+1-s)}}{(k+1-s)!} \sum_{r=0}^{s-1} (-1)^r \frac{E[Y_{k+1:k+2+r} Y_{k+2:k+2+r}]}{(k+2+r)!(s-1-r)!} - \\
& \frac{k!k!(k+1)^{(k+1-s)}}{(k+1-s)!} \sum_{r=0}^{k} (-1)^r \frac{E[Y_{s:s+1+r} Y_{s+1:s+1+r}]}{(k-r)!(s+1+r)!} + \\
& \frac{k!k!E[Y_{k+1:k+1}](E[Y_{s:s}] - E[Y_{k+1:k+1}])}{(k+1-s)!s!s!}
\end{aligned}
$$

$$\text{when } s=0\text{: } A_{kl}^{(s)} = \frac{l!E[Y_{l+1;l+1}^2]}{(l-k)!(l+1)} + \frac{k!l!(k+1)^{(k+1)}}{(k+1)!}\sum_{r=0}^{k}(-1)^r\frac{E[Y_{l-k:l-k+1+r}Y_{l-k+1:l-k+1+r}]}{(k-r)!(l-k+1+r)!} + \frac{k!l!E[Y_{k+1:k+1}](E[Y_{l-k:l-k}]-E[Y_{l+1:l+1}])}{(k+1)!(l-k)!}$$

$$\text{when } s,k=0\text{: } A_{0l}^{(0)} = \frac{E[Y_{l+1;l+1}^2]}{(l+1)} + \frac{E[Y_{l:l+1}Y_{l+1:l+1}]}{(l+1)} + E[Y_{1:1}](E[Y_{l:l}]-E[Y_{l+1:l+1}])$$

$$\text{when } k=l, s=0\text{: } A_{kk}^{(0)} = \frac{k!E[Y_{k+1;k+1}^2]-E[Y_{k+1:k+1}]^2}{(k+1)} = \frac{k!}{k+1}Var[Y]$$

Expansion of $A^{(s)}_{(k,l)}$ in terms of expectations and joint expectations

$$
\begin{aligned}
A^0_{0,0} =& E[Y^2_{1:1}] - E[Y_{1:1}]^2 \\
A^0_{0,1} =& \frac{1}{2}E[Y^2_{2:2}] - \frac{1}{2}E[Y_{1:2}Y_{2:2}] + E[Y_{1:1}](E[Y_{1:1}] - E[Y_{2:2}]) \\
A^0_{0,2} =& \frac{1}{3}E[Y^2_{3:3}] - \frac{1}{3}E[Y_{2:3}Y_{3:3}] + E[Y_{1:1}](E[Y_{2:2}] - E[Y_{3:3}]) \\
A^0_{0,3} =& \frac{1}{4}E[Y^2_{4:4}] - \frac{1}{4}E[Y_{3:4}Y_{4:4}] + E[Y_{1:1}](E[Y_{3:3}] - E[Y_{4:4}]) \\
A^0_{1,1} =& \frac{1}{2}E[Y^2_{2:2}] - \frac{1}{2}E[Y_{2:2}]^2 \\
A^0_{1,2} =& \frac{2}{3}E[Y^2_{3:3}] - E[Y_{1:2}Y_{2:2}] + \frac{1}{3}E[Y_{1:3}Y_{2:3}] + E[Y_{2:2}](E[Y_{1:1}] - E[Y_{3:3}]) \\
A^0_{1,3} =& \frac{3}{4}E[Y^2_{4:4}] - E[Y_{2:3}Y_{3:3}] + \frac{1}{4}E[Y_{2:4}Y_{3:4}] + \frac{3}{2}E[Y_{2:2}](E[Y_{2:2}] - E[Y_{4:4}]) \\
A^0_{2,2} =& \frac{2}{3}E[Y^2_{3:3}] - \frac{2}{3}E[Y_{3:3}]^2 \\
A^0_{2,3} =& \frac{3}{2}E[Y^2_{4:4}] - 3E[Y_{1:2}Y_{2:2}] + 2E[Y_{1:3}Y_{2:3}] - \frac{1}{2}E[Y_{1:4}Y_{2:4}] + 2E[Y_{3:3}](E[Y_{1:1}] - E[Y_{4:4}]) \\
A^0_{3,3} =& \frac{3}{2}E[Y^2_{4:4}] - \frac{3}{2}E[Y_{4:4}]^2 \\
A^1_{1,1} =& \frac{1}{3}E[Y^2_{3:3}] + \frac{1}{3}E[Y_{2:3}Y_{3:3}] - E[Y_{1:2}Y_{2:2}] + \frac{1}{3}E[Y_{1:3}Y_{2:3}] + E[Y_{2:2}](E[Y_{1:1}] - E[Y_{2:2}])] \\
A^1_{1,2} =& \frac{1}{4}E[Y^2_{4:4}] + \frac{1}{4}[Y_{3:4}Y_{4:4}] - \frac{2}{3}E[Y_{2:3}Y_{3:3}] + \frac{1}{6}E[Y_{2:4}Y_{3:4}] + E[Y_{2:2}](E[Y_{2:2}] - E[Y_{3:3}]) \\
A^1_{1,3} =& \frac{1}{5}E[Y^2_{5:5}] + \frac{1}{5}[Y_{4:5}Y_{5:5}] - \frac{1}{2}E[Y_{3:4}Y_{4:4}] + \frac{1}{10}E[Y_{3:5}Y_{4:5}] + E[Y_{2:2}](E[Y_{3:3}] - E[Y_{4:4}]) \\
A^1_{2,2} =& E[Y^2_{4:4}] + \frac{1}{2}E[Y_{3:4}Y_{4:4}] - 3E[Y_{1:2}Y_{2:2}] + 2E[Y_{1:3}Y_{2:3}] - \frac{1}{2}E[Y_{1:4}Y_{2:4}] + 2E[Y_{3:3}](E[Y_{1:1}] - E[Y_{3:3}]) \\
A^1_{2,3} =& \frac{6}{5}E[Y^2_{5:5}] + \frac{3}{5}E[Y_{4:5}Y_{5:5}] - 3E[Y_{2:3}Y_{3:3}] + \frac{3}{2}E[Y_{2:4}Y_{3:4}] - \frac{3}{10}E[Y_{2:5}Y_{3:5}] + 3E[Y_{3:3}](E[Y_{2:2}] - E[Y_{4:4}]) \\
A^1_{3,3} =& \frac{18}{5}E[Y^2_{5:5}] + \frac{6}{5}E[Y_{4:5}Y_{5:5}] - 12E[Y_{1:2}Y_{2:2}] + 12E[Y_{1:3}Y_{2:3}] - 6E[Y_{1:4}Y_{2:4}] + \frac{6}{5}E[Y_{1:5}Y_{2:5}]] \\
& + 6E[Y_{4:4}](E[Y_{1:1}] - E[Y_{4:4}]) \\
A^2_{2,2} =& \frac{1}{5}E[Y^2_{5:5}] + \frac{1}{2}E[Y_{3:4}Y_{4:4}] - \frac{1}{10}E[Y_{3:5}Y_{4:5}] - E[Y_{2:3}Y_{3:3}] + \frac{1}{2}E[Y_{2:4}Y_{3:4}] - \frac{1}{10}E[Y_{2:5}Y_{3:5}] \\
& + E[Y_{3:3}](E[Y_{2:2}] - E[Y_{3:3}]) \\
A^2_{2,3} =& \frac{1}{6}E[Y^2_{6:6}] + \frac{2}{5}E[Y_{4:5}Y_{5:5}] - \frac{1}{15}E[Y_{4:6}Y_{5:6}] - \frac{3}{4}E[Y_{3:4}Y_{4:4}] + \frac{3}{10}E[Y_{3:5}Y_{4:5}] - \frac{1}{20}E[Y_{3:6}Y_{4:6}] \\
& + E[Y_{3:3}](E[Y_{3:3}] - E[Y_{4:4}])
\end{aligned}
$$

$$
\begin{aligned}
A^2_{3,3} =& \frac{3}{2}E[Y^2_{6:6}] + \frac{9}{5}E[Y_{4:5}Y_{5:5}] - \frac{3}{10}E[Y_{4:6}Y_{5:6}] - 6E[Y_{2:3}Y_{3:3}] + \frac{9}{2}E[Y_{2:4}Y_{3:4}] - \frac{9}{5}E[Y_{2:5}Y_{3:5}] \\
& + \frac{3}{10}E[Y_{2:6}Y_{3:6}] + \frac{9}{2}[Y_{4:4}](E[Y_{2:2}] - E[Y_{4:4}]) \\
A^3_{3,3} =& \frac{1}{7}E[Y^2_{7:7}] + \frac{3}{5}E[Y_{4:5}Y_{5:5}] - \frac{1}{5}E[Y_{4:6}Y_{5:6}] + \frac{1}{35}E[Y_{4:7}Y_{5:7}] - E[Y_{3:4}Y_{4:4}] + \frac{3}{5}E[Y_{3:5}Y_{4:5}] \\
& - \frac{1}{5}E[Y_{3:6}Y_{4:6}] + \frac{1}{35}E[Y_{3:7}Y_{4:7}] + [Y_{4:4}](E[Y_{3:3}] - E[Y_{4:4}])
\end{aligned}
$$

Derivation of Exact Variance for L-moments

1st L-moment.

$$\begin{aligned} var(l_1) =& \Theta_{00} \\ =& var(b_0, b_0) \\ =& \frac{1}{n} A^{(0)}_{0,0} \end{aligned}$$

$$var(l_1) = \frac{1}{n}\left[E[Y^2_{1:1}] - E[Y_{1:1}]^2\right] \tag{80}$$

2nd L-moment.

$$\begin{aligned} var(l_2) =& 4\Theta_{11} - 4\Theta_{01} + \Theta_{00} \\ =& var(b_1, b_1) - 4var(b_0, b_1) + var(b_0, b_0) \\ =& \frac{4}{n(n-1)}\left[A^0_{1,1} + (n-2)A^1_{1,1}\right] - \frac{4}{n}A^0_{0,1} + \frac{1}{n}A^0_{0,0} \end{aligned}$$

$$
\begin{aligned}
=&4\left[\frac{1}{2}(E[Y_{2:2}^2]-E[Y_{2:2}]^2)\right]\\
&+4(n-2)\left[\frac{1}{3}E[Y_{3:3}^2]+\frac{1}{3}[Y_{2:3}Y_{3:3}]-E[Y_{1:2}Y_{2:2}]+\frac{1}{3}E[Y_{1:3}Y_{2:3}]+E[Y_{2:2}](E[Y_{1:1}]-E[Y_{2:2}])\right]\\
&-4(n-1)\left[\frac{1}{2}E[Y_{2:2}^2]-\frac{1}{2}E[Y_{1:2}Y_{2:2}]+E[Y_{1:1}](E[Y_{1:1}]-E[Y_{2:2}])\right]\\
&+(n-1)\Big[E[Y_{1:1}^2]-E[Y_{1:1}]^2\Big]
\end{aligned}
$$

$$
\begin{aligned}
var(l_2)=\Big[&\frac{4(n-2)}{3}\left[E(Y_{3:3}^2)+E(Y_{1:3}Y_{2:3})+E(Y_{2:3}Y_{3:3})\right]-2(n-3)E(Y_{1:2}Y_{2:2})\\
&-2(n-2)E(Y_{2:2}^2)+(n-1)E(Y_{1:1}^2)-2(2n-3)E(Y_{2:2})^2\\
&+4(2n-3)E(Y_{2:2})E(Y_{1:1})-5(n-1)E(Y_{1:1})^2\Big]/n(n-1)
\end{aligned}
\tag{81}
$$

3rd L-moment.

$$
\begin{aligned}
&var(l_3)\\
=&36\Theta_{22}-72\Theta_{12}+36\Theta_{11}+12\Theta_{02}-12\Theta_{01}+\Theta_{00}\\
=&36var(b_2,b_2)-72var(b_1,b_2)+36var(b_1,b_1)+12var(b_0,b_2)-12var(b_0,b_1)+var(b_0,b_0)\\
=&\frac{36}{n(n-1)(n-2)}[A_{2,2}^0+(n-3)A_{2,2}^1+(n-3)(n-4)A_{2,2}^2]-\frac{72}{n(n-1)}[A_{1,2}^0+(n-3)A_{1,2}^1]\\
&+\frac{36}{n(n-1)}[A_{1,1}^0+(n-2)A_{1,1}^1]+\frac{12}{n}A_{0,2}^0-\frac{12}{n}A_{0,1}^0+\frac{1}{n}A_{0,0}^0
\end{aligned}
$$

Placing them all under the common divisor of n(n-1)(n-2) yields the following linear

combination of order statistics:

$$
\begin{aligned}
=&36\left[\frac{2}{3}E[Y_{3:3}^2]-\frac{2}{3}E[Y_{3:3}]^2\right]\\
&+36(n-3)\Big[E[Y_{4:4}^2]+\frac{1}{2}[Y_{3:4}Y_{4:4}]-3E[Y_{1:2}Y_{2:2}]+2E[Y_{1:3}Y_{2:3}]-\frac{1}{2}E[Y_{1:4}Y_{2:4}]\\
&+2E[Y_{3:3}](E[Y_{1:1}]-E[Y_{3:3}])\Big]\\
&+36(n-3)(n-4)\Big[\frac{1}{5}E[Y_{5:5}^2]+\frac{1}{2}E[Y_{3:4}Y_{4:4}]-\frac{1}{10}E[Y_{3:5}Y_{4:5}]-E[Y_{2:3}Y_{3:3}]+\frac{1}{2}E[Y_{2:4}Y_{3:4}]\\
&-\frac{1}{10}E[Y_{2:5}Y_{3:5}]+E[Y_{3:3}](E[Y_{2:2}]-E[Y_{3:3}])\Big]\\
&-72(n-2)\left[\frac{2}{3}E[Y_{3:3}^2]-E[Y_{1:2}Y_{2:2}]+\frac{1}{3}E[Y_{1:3}Y_{2:3}]+E[Y_{2:2}](E[Y_{1:1}]-E[Y_{3:3}])\right]\\
&-72(n-2)(n-3)\left[\frac{1}{4}E[Y_{4:4}^2]+\frac{1}{4}[Y_{3:4}Y_{4:4}]-\frac{2}{3}E[Y_{2:3}Y_{3:3}]+\frac{1}{6}E[Y_{2:4}Y_{3:4}]+E[Y_{2:2}](E[Y_{2:2}]-E[Y_{3:3}])\right]\\
&+36(n-2)\left[\frac{1}{2}E[Y_{2:2}^2]-\frac{1}{2}E[Y_{2:2}]^2\right]\\
&+36(n-2)^2\left[\frac{1}{3}E[Y_{3:3}^2]+\frac{1}{3}E[Y_{2:3}Y_{3:3}]-E[Y_{1:2}Y_{2:2}]+\frac{1}{3}E[Y_{1:3}Y_{2:3}]+E[Y_{2:2}](E[Y_{1:1}]-E[Y_{2:2}])\right]\\
&+12(n-1)(n-2)\left[\frac{1}{3}E[Y_{3:3}^2]-\frac{1}{3}E[Y_{2:3}Y_{3:3}]+E[Y_{1:1}](E[Y_{2:2}]-E[Y_{3:3}])\right]\\
&-12(n-1)(n-2)\left[\frac{1}{2}E[Y_{2:2}^2]-\frac{1}{2}E[Y_{1:2}Y_{2:2}]+E[Y_{1:1}](E[Y_{1:1}]-E[Y_{2:2}])\right]\\
&+(n-1)(n-2)\Big[E[Y_{1:1}^2]-E[Y_{1:1}]^2\Big]
\end{aligned}
$$

Combining order statistics gives and taking the greatest common factor out as

well leads the the following:

$$
\begin{aligned}
&var(l_3) = \\
&\Big[36/10(n^2-7n+12)\left[2E[Y^2_{5:5}] - E[Y_{3:5}Y_{4:5}] - E[Y_{2:5}Y_{3:5}]\right] + 4(4n^2-27n+44)E[Y^2_{3:3}] \\
&+ 12(-3n^2+15n-20)E[Y_{3:3}]^2 + 18(-n^2+7n-12)E[Y^2_{4:4}] + 18(-n^2+3)\left[E[Y_{3:4}Y_{4:4}] + E[Y_{1:4}Y_{2:4}]\right] \\
&+ 6(-5n^2+15n+8)E[Y_{1:2}Y_{2:2}] + 12(n^2-10)E[Y_{1:3}Y_{2:3}] + 4(5n^2-6n-26)E[Y_{2:3}Y_{3:3}] \\
&+ 6(n^2-11n+24)E[Y_{2:4}Y_{3:4}] + 36(3n^2-15n+20)E[Y_{3:3}]E[Y_{2:2}] + 12(5n^2-24n+28)E[Y_{2:2}]E[Y_{1:1}] \\
&+ 54(-2n^2+9n-10)E[Y_{2:2}]^2 + 6(-n^2+6n-8)E[Y^2_{2:2}] + 12(-n^2+9n-20)E[Y_{1:1}]E[Y_{3:3}] \\
&+ 13(-n^2+3n-2)E[Y_{1:1}]^2 + (n^2-3n+2)E[Y^2_{1:1}]\Big]/n(n-1)(n-2)
\end{aligned}
\tag{82}
$$

4th L-moment.

$$
\begin{aligned}
&var(l_4) \\
=&\Theta_{00} - 24\Theta_{01} + 60\Theta_{02} - 40\Theta_{03} + 144\Theta_{11} - 720\Theta_{12} + 480\Theta_{13} + 900\Theta_{22} - 1200\Theta_{23} + 400\Theta_{33} \\
=&-24var(b_0,b_1) + 60var(b_0,b_2) - 40var(b_0,b_3) + 144var(b_1,b_1) - 720var(b_1,b_2) \\
&+ 480var(b_1,b_3) + 900var(b_2,b_2) - 1200var(b_2,b_3) + 400var(b_3,b_3) \\
=&\frac{1}{n}A^0_{0,0} - \frac{24}{n}A^0_{0,1} + \frac{60}{n}A^0_{0,2} - \frac{40}{n}A^0_{0,3} + \frac{144}{n(n-1)}[A^0_{1,1} + (n-2)A^1_{1,1}] - \frac{720}{n(n-1)}[A^0_{1,2} + (n-3)A^1_{1,2}] \\
&+ \frac{480}{n(n-1)}[A^0_{1,3} + (n-4)A^1_{1,3}] + \frac{900}{n(n-1)(n-2)}[A^0_{2,2} + (n-3)A^1_{2,2} + (n-3)(n-4)A^2_{2,2}] \\
&- \frac{1200}{n(n-1)(n-2)}[A^0_{2,3} + (n-4)A^1_{2,3} + (n-4)(n-5)A^2_{2,3}] \\
&+ \frac{400}{n(n-1)...(n-3)}[A^0_{3,3} + (n-4)A^1_{3,3} + (n-4)(n-5)A^2_{3,3} + (n-4)(n-5)(n-6)A^3_{3,3}]
\end{aligned}
$$

Placing them all under the common divisor of n(n-1)(n-2)(n-3) yields the following

linear combination of order statistics:

$$
\begin{aligned}
=&(n-1)(n-2)(n-3)\Big[E[Y_{1:1}^2]-E[Y_{1:1}]^2\Big] \\
&-24(n-1)(n-2)(n-3)\left[\frac{1}{2}E[Y_{2:2}^2]-\frac{1}{2}E[Y_{1:2}Y_{2:2}]+E[Y_{1:1}](E[Y_{1:1}]-E[Y_{2:2}])\right] \\
&+60(n-1)(n-2)(n-3)\left[\frac{1}{3}E[Y_{3:3}^2]-\frac{1}{3}E[Y_{2:3}Y_{3:3}]+E[Y_{1:1}](E[Y_{2:2}]-E[Y_{3:3}])\right] \\
&-40(n-1)(n-2)(n-3)\left[\frac{1}{4}E[Y_{4:4}^2]-\frac{1}{4}E[Y_{3:4}Y_{4:4}]+E[Y_{1:1}](E[Y_{3:3}]-E[Y_{4:4}])\right] \\
&+144(n-2)(n-3)\left[\frac{1}{2}E[Y_{2:2}^2]-\frac{1}{2}E[Y_{2:2}]^2\right] \\
&+144(n-2)^2(n-3)\Big[\frac{1}{3}E[Y_{3:3}^2]+\frac{1}{3}E[Y_{2:3}Y_{3:3}]-E[Y_{1:2}Y_{2:2}]+\frac{1}{3}E[Y_{1:3}Y_{2:3}] \\
&+E[Y_{2:2}](E[Y_{1:1}]-E[Y_{2:2}])\Big]
\end{aligned}
$$

$$
\begin{aligned}
&- 720(n-2)(n-3)\left[\frac{2}{3}E[Y_{3:3}^2] - E[Y_{1:2}Y_{2:2}] + \frac{1}{3}E[Y_{1:3}Y_{2:3}] + E[Y_{2:2}](E[Y_{1:1}] - E[Y_{3:3}])\right] \\
&- 720(n-2)(n-3)^2\left[\frac{1}{4}E[Y_{4:4}^2] + \frac{1}{4}[Y_{3:4}Y_{4:4}] - \frac{2}{3}E[Y_{2:3}Y_{3:3}] + \frac{1}{6}E[Y_{2:4}Y_{3:4}] + E[Y_{2:2}](E[Y_{2:2}] - E[Y_{3:3}])\right] \\
&+ 480(n-2)(n-3)\left[\frac{3}{4}E[Y_{4:4}^2] - E[Y_{2:3}Y_{3:3}] + \frac{1}{4}E[Y_{2:4}Y_{3:4}] + \frac{3}{2}E[Y_{2:2}](E[Y_{2:2}] - E[Y_{4:4}])\right] \\
&+ 480(n-2)(n-3)(n-4)\Big[\frac{1}{5}E[Y_{5:5}^2] + \frac{1}{5}[Y_{4:5}Y_{5:5}] - \frac{1}{2}E[Y_{3:4}Y_{4:4}] + \frac{1}{10}E[Y_{3:5}Y_{4:5}] \\
&+ E[Y_{2:2}](E[Y_{3:3}] - E[Y_{4:4}])\Big] \\
&+ 900(n-3)\left[\frac{2}{3}E[Y_{3:3}^2] - \frac{2}{3}E[Y_{3:3}]^2\right] \\
&+ 900(n-3)^2\Big[E[Y_{4:4}^2] + \frac{1}{2}E[Y_{3:4}Y_{4:4}] - 3E[Y_{1:2}Y_{2:2}] + 2E[Y_{1:3}Y_{2:3}] - \frac{1}{2}E[Y_{1:4}Y_{2:4}] \\
&+ 2E[Y_{3:3}](E[Y_{1:1}] - E[Y_{3:3}])\Big] \\
&+ 900(n-3)^2(n-4)\Big[\frac{1}{5}E[Y_{5:5}^2] + \frac{1}{2}E[Y_{3:4}Y_{4:4}] - \frac{1}{10}E[Y_{3:5}Y_{4:5}] - E[Y_{2:3}Y_{3:3}] + \frac{1}{2}E[Y_{2:4}Y_{3:4}] \\
&- \frac{1}{10}E[Y_{2:5}Y_{3:5}] + E[Y_{3:3}](E[Y_{2:2}] - E[Y_{3:3}])\Big] \\
&- 1200(n-3)\left[\frac{3}{2}E[Y_{4:4}^2] - 3E[Y_{1:2}Y_{2:2}] + 2E[Y_{1:3}Y_{2:3}] - \frac{1}{2}E[Y_{1:4}Y_{2:4}] + 2E[Y_{3:3}](E[Y_{1:1}] - E[Y_{4:4}])\right] \\
&- 1200(n-3)(n-4)\Big[\frac{6}{5}E[Y_{5:5}^2] + \frac{3}{5}E[Y_{4:5}Y_{5:5}] - 3E[Y_{2:3}Y_{3:3}] + \frac{3}{2}E[Y_{2:4}Y_{3:4}] - \frac{3}{10}E[Y_{2:5}Y_{3:5}] \\
&+ 3E[Y_{3:3}](E[Y_{2:2}] - E[Y_{4:4}])\Big] \\
&- 1200(n-3)(n-4)(n-5)\Big[\frac{1}{6}E[Y_{6:6}^2] + \frac{2}{5}E[Y_{4:5}Y_{5:5}] - \frac{1}{15}E[Y_{4:6}Y_{5:6}] - \frac{3}{4}E[Y_{3:4}Y_{4:4}] + \frac{3}{10}E[Y_{3:5}Y_{4:5}] \\
&- \frac{1}{20}E[Y_{3:6}Y_{4:6}] + E[Y_{3:3}](E[Y_{3:3}] - E[Y_{4:4}])\Big] \\
&+ 400\left[\frac{3}{2}E[Y_{4:4}^2] - \frac{3}{2}E[Y_{4:4}]^2\right] \\
&+ 400(n-4)\Big[\frac{18}{5}E[Y_{5:5}^2] + \frac{6}{5}E[Y_{4:5}Y_{5:5}] - 12E[Y_{1:2}Y_{2:2}] + 12E[Y_{1:3}Y_{2:3}] - 6E[Y_{1:4}Y_{2:4}] + \frac{6}{5}E[Y_{1:5}Y_{2:5}] \\
&+ 6E[Y_{4:4}](E[Y_{1:1}] - E[Y_{4:4}])\Big] \\
&+ 400(n-4)(n-5)\Big[\frac{3}{2}E[Y_{6:6}^2] + \frac{9}{5}E[Y_{4:5}Y_{5:5}] - \frac{3}{10}E[Y_{4:6}Y_{5:6}] - 6E[Y_{2:3}Y_{3:3}] + \frac{9}{2}E[Y_{2:4}Y_{3:4}] \\
&- \frac{9}{5}E[Y_{2:5}Y_{3:5}] + \frac{3}{10}E[Y_{2:6}Y_{3:6}] + \frac{9}{2}[Y_{4:4}](E[Y_{2:2}] - E[Y_{4:4}])\Big] \\
&+ 400(n-4)(n-5)(n-6)\Big[\frac{1}{7}E[Y_{7:7}^2] + \frac{3}{5}E[Y_{4:5}Y_{5:5}] - \frac{1}{5}E[Y_{4:6}Y_{5:6}] + \frac{1}{35}E[Y_{4:7}Y_{5:7}] - E[Y_{3:4}Y_{4:4}] \\
&+ \frac{3}{5}E[Y_{3:5}Y_{4:5}] - \frac{1}{5}E[Y_{3:6}Y_{4:6}] + \frac{1}{35}E[Y_{3:7}Y_{4:7}] + [Y_{4:4}](E[Y_{3:3}] - E[Y_{4:4}])\Big]
\end{aligned}
$$

Combining order statistics and factoring out the greatest common factor gives us the following linear combination for the variance of the 4th l-moment.

$$
\begin{aligned}
&var(l_4) = \\
&\Big[400/35(n^3-15n^2+74n-120)\left[[5E[Y_{7:7}^2]+E[Y_{3:7}Y_{4:7}]+E[Y_{4:7}Y_{5:7}]\right] \\
&+(n^3-6n^2+11n-6)\left[E[Y_{1:1}^2]-25E[Y_{1:1}]^2\right]+12(-n^3+12n^2-41n+42)E[Y_{2:2}^2] \\
&+4(17n^3-234n^2+997n-1344)E[Y_{3:3}^2]+10(-19n^3+276n^2-1289n+1956)E[Y_{4:4}^2] \\
&+12(23n^3-342n^2+1663n-2652)E[Y_{5:5}^2]+200(-n^3+15n^2-74n+120)E[Y_{6:6}^2] \\
&+72(-12n^3+103n^2-287n+258)E[Y_{2:2}]^2+300(-7n^3+72n^2-253n+300)E[Y_{3:3}]^2 \\
&+200(-2n^3+21n^2-79n+105)E[Y_{4:4}]^2+12(-11n^3-87n^2+769n-827)E[Y_{1:2}Y_{2:2}] \\
&+8(-49n^3+708n^2-2534n+1953)E[Y_{2:3}Y_{3:3}]+30(18n^3-177n^2+498n-307)E[Y_{3:4}Y_{4:4}] \\
&+24(2n^3+51n^2-268n+91)E[Y_{1:3}Y_{2:3}]+30(11n^3-114n^2+271n+36)E[Y_{2:4}Y_{3:4}] \\
&+150(-3n^2+6n+25)E[Y_{1:4}Y_{2:4}]+48(-3n^3+27n^2-68n+32)E[Y_{4:5}Y_{5:5}] \\
&+18(-9n^3+66n^2-49n-284)E[Y_{3:5}Y_{4:5}]+90(-n^3+6n^2+11n-76)E[Y_{2:5}Y_{3:5}] \\
&+480(n-4)E[Y_{1:5}Y_{2:5}]+120(n^2-9n+20)\left[E[Y_{4:6}Y_{5:6}]+E[Y_{2:6}Y_{3:6}]\right] \\
&+20(-n^3+24n^2-155n+300)E[Y_{3:6}Y_{4:6}]+12(19n^3-186n^2+59n-546)E[Y_{1:1}]E[Y_{2:2}] \\
&+100(-n^3+24n^2-143n+240)E[Y_{1:1}]E[Y_{3:3}]+40(n^3-6n^2+71n-246)E[Y_{1:1}]E[Y_{4:4}] \\
&+60(35n^3-366n^2+1315n-1596)E[Y_{2:2}]E[Y_{3:3}]+120(-4n^3+45n^2-209n+360)E[Y_{2:2}]E[Y_{4:4}] \\
&+800(2n^3-21n^2+79n-105)E[Y_{3:3}]E[Y_{4:4}]\Big]/n(n)(n-1)(n-2)
\end{aligned}
\tag{83}
$$

Derivation of Exact Covariance for L-moments

Covariance l_1, l_2.

$$\begin{aligned} cov(l_1, l_2) =& 2\Theta_{01} - \Theta_{00} \\ =& 2var(b_0, b_1) - var(b_0, b_0) \\ =& \frac{2}{n} A^0_{0,1} - \frac{1}{n} A^0_{0,0} \end{aligned}$$

$$\begin{aligned} =& \frac{2}{n}\left[\frac{1}{2}E[Y^2_{2:2}] - \frac{1}{2}E[Y_{1:2}Y_{2:2}] + E[Y_{1:1}](E[Y_{1:1}] - E[Y_{2:2}])\right] \\ & - \frac{1}{n}\Big[E[Y^2_{1:1}] - E[Y_{1:1}]^2\Big] \end{aligned}$$

$$\begin{aligned} & cov(l_1, l_2) \\ =& \Big[E[Y^2_{2:2}] - E[Y_{1:2}Y_{2:2}] + 3E[Y_{1:1}]^2 - 2E[Y_{1:1}]E[Y_{2:2}] - E[Y^2_{1:1}]\Big]/n \end{aligned} \tag{84}$$

Covariance l_1, l_3.

$$\begin{aligned} cov(l_1, l_3) =& 6\Theta_{02} - 6\Theta_{01} + \Theta_{00} \\ =& 6var(b_0, b_2) - 6var(b_0, b_1) + var(b_0, b_0) \\ =& \frac{6}{n} A^0_{0,2} - \frac{6}{n} A^0_{0,1} + \frac{1}{n} A^0_{0,0} \end{aligned}$$

$$\begin{aligned} =& \frac{6}{n} \left[\frac{1}{3} E[Y^2_{3:3}] - \frac{1}{3} E[Y_{2:3} Y_{3:3}] + E[Y_{1:1}](E[Y_{2:2}] - E[Y_{3:3}]) \right] \\ & - \frac{6}{n} \left[\frac{1}{2} E[Y^2_{2:2}] - \frac{1}{2} E[Y_{1:2} Y_{2:2}] + E[Y_{1:1}](E[Y_{1:1}] - E[Y_{2:2}]) \right] \\ & + \frac{1}{n} \Big[E[Y^2_{1:1}] - E[Y_{1:1}]^2 \Big] \end{aligned}$$

$$\begin{aligned} & cov(l_1, l_3) \\ =& \big[2E[Y^2_{3:3}] - 2E[Y_{2:3} Y_{3:3}] + 12E[Y_{1:1}]E[Y_{2:2}] - 6E[Y_{1:1}]E[Y_{3:3}] - 3E[Y^2_{2:2}] + 3E[Y_{1:2} Y_{2:2}] \\ & - 7E[Y_{1:1}]^2 + E[Y^2_{1:1}] \big] / n \end{aligned} \tag{85}$$

Covariance l_1, l_4.

$$
\begin{aligned}
cov(l_1, l_4) =& 20\Theta_{03} - 30\Theta_{02} + 12\Theta_{01} - \Theta_{00} \\
=& 20var(b_0, b_3) - 30var(b_0, b_2) + 12var(b_0, b_1) - var(b_0, b_0) \\
=& \frac{20}{n} A^0_{0,3} - \frac{30}{n} A^0_{0,2} + \frac{12}{n} A^0_{0,1} - \frac{1}{n} A^0_{0,0}
\end{aligned}
$$

$$
\begin{aligned}
=& \frac{20}{n} \left[\frac{1}{4} E[Y^2_{4:4}] - \frac{1}{4} E[Y_{3:4} Y_{4:4}] + E[Y_{1:1}](E[Y_{3:3}] - E[Y_{4:4}]) \right] \\
& - \frac{30}{n} \left[\frac{1}{3} E[Y^2_{3:3}] - \frac{1}{3} E[Y_{2:3} Y_{3:3}] + E[Y_{1:1}](E[Y_{2:2}] - E[Y_{3:3}]) \right] \\
& + \frac{12}{n} \left[\frac{1}{2} E[Y^2_{2:2}] - \frac{1}{2} E[Y_{1:2} Y_{2:2}] + E[Y_{1:1}](E[Y_{1:1}] - E[Y_{2:2}]) \right] \\
& - \frac{1}{n} \Big[E[Y^2_{1:1}] - E[Y_{1:1}]^2 \Big]
\end{aligned}
$$

$$
\begin{aligned}
& cov(l_1, l_4) \\
=& \big[5E[Y^2_{4:4}] - 5E[Y_{3:4} Y_{4:4}] + 50E[Y_{1:1}]E[Y_{3:3}] - 20E[Y_{1:1}]E[Y_{4:4}] - 10E[Y^2_{3:3}] - 10E[Y_{2:3} Y_{3:3}] \\
& - 42E[Y_{1:1}]E[Y_{2:2}] + 30E[Y_{1:1}]E[Y_{3:3}] + 6E[Y^2_{2:2}] - 6E[Y_{1:2} Y_{2:2}] + 13E[Y_{1:1}]^2 - E[Y_{1:1}]^2 \Big] / n
\end{aligned} \tag{86}
$$

Covariance l_2, l_3.

$$
\begin{aligned}
&cov(l_2, l_3) \\
&\quad =8\Theta_{01} - 6\Theta_{02} - 12\Theta_{11} + 12\Theta_{12} - \Theta_{00} \\
&\quad =8var(b_0b_1) - 6var(b_0b_2) - 12var(b_1b_1) + 12var(b_1b_2) - var(b_0b_0) \\
&\quad =\frac{8}{n}A^0_{0,1} - \frac{6}{n}A^0_{0,2} - \frac{12}{n(n-1)}\left[A^0_{1,1} + (n-2)A^1_{1,1}\right] + \frac{12}{n(n-1)}\left[A^0_{1,2} + (n-3)A^1_{1,2}\right] \\
&\qquad - \frac{1}{n}A^0_{0,0} \\
&\quad =8(n-1)A^0_{0,1} - 6(n-1)A^0_{0,2} - 12\left[A^0_{1,1} + (n-2)A^1_{1,1}\right] + 12\left[A^0_{1,2} + (n-3)A^1_{1,2}\right] \\
&\qquad - (n-1)A^0_{0,0}
\end{aligned}
$$

$$
\begin{aligned}
=&8(n-1)\left[\frac{1}{2}E[Y^2_{2:2}] - \frac{1}{2}E[Y_{1:2}Y_{2:2}] + E[Y_{1:1}](E[Y_{1:1}] - E[Y_{2:2}])\right] \\
&- 6(n-1)\left[\frac{1}{3}E[Y^2_{3:3}] - \frac{1}{3}E[Y_{2:3}Y_{3:3}] + E[Y_{1:1}](E[Y_{2:2}] - E[Y_{3:3}])\right] \\
&- 12\left[\frac{1}{2}E[Y^2_{2:2}] - \frac{1}{2}E[Y_{2:2}]^2\right] \\
&- 12(n-2)\left[\frac{1}{3}E[Y^2_{3:3}] + \frac{1}{3}E[Y_{2:3}Y_{3:3}] - E[Y_{1:2}Y_{2:2}] + \frac{1}{3}E[Y_{1:3}Y_{2:3}] + E[Y_{2:2}](E[Y_{1:1}] - E[Y_{2:2}])\right] \\
&+ 12\left[\frac{2}{3}E[Y^2_{3:3}] - E[Y_{1:2}Y_{2:2}] + \frac{1}{3}E[Y_{1:3}Y_{2:3}] + E[Y_{2:2}](E[Y_{1:1}] - E[Y_{3:3}])\right] \\
&+ 12(n-3)\left[\frac{1}{4}E[Y^2_{4:4}] + \frac{1}{4}[Y_{3:4}Y_{4:4}] - \frac{2}{3}E[Y_{2:3}Y_{3:3}] + \frac{1}{6}E[Y_{2:4}Y_{3:4}] + E[Y_{2:2}](E[Y_{2:2}] - E[Y_{3:3}])\right] \\
&- (n-1)\Big[E[Y^2_{1:1}] - E[Y_{1:1}]^2\Big]
\end{aligned}
$$

$$
\begin{aligned}
&cov(l_2 l_3) \\
=&\Big[(n-3)\left[3E[Y_{4:4}^2]-6E[Y_{3:3}^2]+3E[Y_{3:4}Y_{4:4}]+2E[Y_{2:4}Y_{3:4}]-10E[Y_{2:3}Y_{3:3}]-4E[Y_{1:3}Y_{2:3}]\right] \\
&+(n-1)\left[9E[Y_{1:1}]^2-E[Y_{1:1}^2]+6E[Y_{1:1}]E[Y_{3:3}]\right]+2(2n-5)E[Y_{2:2}^2]+6(4n-9)E[Y_{2:2}]^2 \\
&+8(n-4)E[Y_{1:2}Y_{2:2}]-2(13n-25)E[Y_{1:1}]E[Y_{2:2}]-12(n-2)E[Y_{2:2}]E[Y_{3:3}]\Big]/n(n-1)
\end{aligned} \tag{87}
$$

Covariance l_2, l_4.

$$
\begin{aligned}
&cov(l_2, l_4) \\
=&-14\Theta_{01}+30\Theta_{02}-20\Theta_{03}+24\Theta_{11}-60\Theta_{12}+40\Theta_{13}+\Theta_{00} \\
=&-14var(b_0b_1)+30var(b_0b_2)-20var(b_0b_3)+24var(b_1b_1)-60var(b_1b_2)+40var(b_1b_3) \\
&+var(b_0b_0) \\
=&\frac{-14}{n}A_{0,1}^0+\frac{30}{n}A_{0,2}^0-\frac{20}{n}A_{0,3}^0+\frac{24}{n(n-1)}\left[A_{1,1}^0+(n-2)A_{1,1}^1\right]-\frac{60}{n(n-1)}\left[A_{1,2}^0+(n-3)A_{1,2}^1\right] \\
&-\frac{40}{n(n-1)}\left[A_{1,3}^0+(n-4)A_{1,3}^1\right]+\frac{1}{n}A_{0,0}^0 \\
=&-14(n-1)A_{0,1}^0+30(n-1)A_{0,2}^0-20(n-1)A_{0,3}^0+24\left[A_{1,1}^0+(n-2)A_{1,1}^1\right] \\
&-60\left[A_{1,2}^0+(n-3)A_{1,2}^1\right]+40\left[A_{1,3}^0+(n-4)A_{1,3}^1\right]+(n-1)A_{0,0}^0
\end{aligned}
$$

$$
\begin{aligned}
=& -14(n-1)\left[\frac{1}{2}E[Y_{2:2}^2]-\frac{1}{2}E[Y_{1:2}Y_{2:2}]+E[Y_{1:1}](E[Y_{1:1}]-E[Y_{2:2}])\right]\\
&+30(n-1)\left[\frac{1}{3}E[Y_{3:3}^2]-\frac{1}{3}E[Y_{2:3}Y_{3:3}]+E[Y_{1:1}](E[Y_{2:2}]-E[Y_{3:3}])\right]\\
&-20(n-1)\left[\frac{1}{4}E[Y_{4:4}^2]-\frac{1}{4}E[Y_{3:4}Y_{4:4}]+E[Y_{1:1}](E[Y_{3:3}]-E[Y_{4:4}])\right]\\
&+24\left[\frac{1}{2}E[Y_{2:2}^2]-\frac{1}{2}E[Y_{2:2}]^2\right]\\
&+24(n-2)\left[\frac{1}{3}E[Y_{3:3}^2]+\frac{1}{3}E[Y_{2:3}Y_{3:3}]-E[Y_{1:2}Y_{2:2}]+\frac{1}{3}E[Y_{1:3}Y_{2:3}]+E[Y_{2:2}](E[Y_{1:1}]-E[Y_{2:2}])\right]\\
&-60\left[\frac{2}{3}E[Y_{3:3}^2]-E[Y_{1:2}Y_{2:2}]+\frac{1}{3}E[Y_{1:3}Y_{2:3}]+E[Y_{2:2}](E[Y_{1:1}]-E[Y_{3:3}])\right]\\
&-60(n-3)\left[\frac{1}{4}E[Y_{4:4}^2]+\frac{1}{4}[Y_{3:4}Y_{4:4}]-\frac{2}{3}E[Y_{2:3}Y_{3:3}]+\frac{1}{6}E[Y_{2:4}Y_{3:4}]+E[Y_{2:2}](E[Y_{2:2}]-E[Y_{3:3}])\right]\\
&+40\left[\frac{3}{4}E[Y_{4:4}^2]-E[Y_{2:3}Y_{3:3}]+\frac{1}{4}E[Y_{2:4}Y_{3:4}]+\frac{3}{2}E[Y_{2:2}](E[Y_{2:2}]-E[Y_{4:4}])\right]\\
&+40(n-4)\left[\frac{1}{5}E[Y_{5:5}^2]+\frac{1}{5}[Y_{4:5}Y_{5:5}]-\frac{1}{2}E[Y_{3:4}Y_{4:4}]+\frac{1}{10}E[Y_{3:5}Y_{4:5}]+E[Y_{2:2}](E[Y_{3:3}]-E[Y_{4:4}])\right]\\
&+(n-1)\Big[E[Y_{1:1}^2]-E[Y_{1:1}]^2\Big]
\end{aligned}
$$

$$
\begin{aligned}
&cov(l_2,l_4)\\
=&\Big[(n-1)\left[E[Y_{1:1}^2]-15E[Y_{1:1}]^2-10E[Y_{1:1}](E[Y_{3:3}]-2E[Y_{4:4}])\right]\\
&+(n-4)\left[8E[Y_{5:5}^2]-20E[Y_{4:4}^2]-30E[Y_{3:4}Y_{4:4}]-10E[Y_{2:4}Y_{3:4}]+8E[Y_{4:5}Y_{5:5}]+4E[Y_{3:5}Y_{4:5}]\right]\\
&+(-7n+19)E[Y_{2:2}^2]+6(3n-11)E[Y_{3:3}^2]-4(21n-69)E[Y_{2:2}]^2-(17n+101)E[Y_{1:2}Y_{2:2}]\\
&+2(19n-83)E[Y_{2:3}Y_{3:3}]+4(2n-9)E[Y_{1:3}Y_{2:3}]+4(17n-38)E[Y_{1:1}]E[Y_{2:2}]\\
&+20(5n-14)E[Y_{2:2}]E[Y_{3:3}]-20(2n-5)E[Y_{2:2}]E[Y_{4:4}]\Big]/n(n-1)
\end{aligned}
\tag{88}
$$

Covariance l_3, l_4.

$$
\begin{aligned}
&cov(l_3, l_4) \\
=&120\Theta_{23} - 180\Theta_{22} - 120\Theta_{13} + 252\Theta_{12} - 72\Theta_{11} + 20\Theta_{03} - 36\Theta_{02} + 18\Theta_{01} - \Theta_{00} \\
=&120var(b_2, b_3) - 180var(b_2, b_2) - 120var(b_1, b_3) + 252var(b_1, b_2) \\
&- 72var(b_1, b_1) + 20var(b_0, b_3) - 36var(b_0, b_2) + 18var(b_0, b_1) - var(b_0, b_0) \\
=&\frac{120}{n(n-1)(n-2)}[A^0_{2,3} + (n-4)A^1_{2,3} + (n-4)(n-5)A^2_{2,3}] \\
&- \frac{180}{n(n-1)(n-2)}[A^0_{2,2} + (n-3)A^1_{2,2} + (n-3)(n-4)A^2_{2,2}] - \frac{120}{n(n-1)}[A^0_{1,3} + (n-4)A^1_{1,3}] \\
&+ \frac{252}{n(n-1)}[A^0_{1,2} + (n-3)A^1_{1,2}] - \frac{72}{n(n-1)}[A^0_{1,1} + (n-2)A^1_{1,1}] + \frac{20}{n}A^0_{0,3} - \frac{36}{n}A^0_{0,2} \\
&+ \frac{18}{n}A^0_{0,1} - \frac{1}{n}A^0_{0,0}
\end{aligned}
$$

$$
\begin{aligned}
=&120(n-3)\Big[\frac{3}{2}E[Y^2_{4:4}] - 3E[Y_{1:2}Y_{2:2}] + 2E[Y_{1:3}Y_{2:3}] - \frac{1}{2}E[Y_{1:4}Y_{2:4}] + 2E[Y_{3:3}](E[Y_{1:1}] - E[Y_{4:4}])\Big] \\
&120(n-3)(n-4)\Big[\frac{6}{5}E[Y^2_{5:5}] + \frac{3}{5}E[Y_{4:5}Y_{5:5}] - 3E[Y_{2:3}Y_{3:3}] + \frac{3}{2}E[Y_{2:4}Y_{3:4}] - \frac{3}{10}E[Y_{2:5}Y_{3:5}] \\
&+ 3E[Y_{3:3}](E[Y_{2:2}] - E[Y_{4:4}])\Big] \\
&120(n-3)(n-4)(n-5)\Big[\frac{1}{6}E[Y^2_{6:6}] + \frac{2}{5}E[Y_{4:5}Y_{5:5}] - \frac{1}{15}E[Y_{4:6}Y_{5:6}] - \frac{3}{4}E[Y_{3:4}Y_{4:4}] + \frac{3}{10}E[Y_{3:5}Y_{4:5}] \\
&- \frac{1}{20}E[Y_{3:6}Y_{4:6}] + E[Y_{3:3}](E[Y_{3:3}] - E[Y_{4:4}])\Big] \\
&- 180(n-3)\Big[\frac{2}{3}E[Y^2_{3:3}] - \frac{2}{3}E[Y_{3:3}]^2\Big] \\
&- 180(n-3)^2\Big[E[Y^2_{4:4}] + \frac{1}{2}E[Y_{3:4}Y_{4:4}] - 3E[Y_{1:2}Y_{2:2}] + 2E[Y_{1:3}Y_{2:3}] - \frac{1}{2}E[Y_{1:4}Y_{2:4}] \\
&+ 2E[Y_{3:3}](E[Y_{1:1}] - E[Y_{3:3}])\Big] \\
&- 180(n-3)^2(n-4)\Big[\frac{1}{5}E[Y^2_{5:5}] + \frac{1}{2}E[Y_{3:4}Y_{4:4}] - \frac{1}{10}E[Y_{3:5}Y_{4:5}] - E[Y_{2:3}Y_{3:3}] + \frac{1}{2}E[Y_{2:4}Y_{3:4}] \\
&- \frac{1}{10}E[Y_{2:5}Y_{3:5}] + E[Y_{3:3}](E[Y_{2:2}] - E[Y_{3:3}])\Big]
\end{aligned}
$$

$$
\begin{aligned}
&- 120(n-2)(n-3)\Big[\frac{3}{4}E[Y_{4:4}^2] - E[Y_{2:3}Y_{3:3}] + \frac{1}{4}E[Y_{2:4}Y_{3:4}] + \frac{3}{2}E[Y_{2:2}](E[Y_{2:2}] - E[Y_{4:4}])\Big] \\
&- 120(n-2)(n-3)(n-4)\Big[\frac{1}{5}E[Y_{5:5}^2] + \frac{1}{5}[Y_{4:5}Y_{5:5}] - \frac{1}{2}E[Y_{3:4}Y_{4:4}] + \frac{1}{10}E[Y_{3:5}Y_{4:5}] \\
&+ E[Y_{2:2}](E[Y_{3:3}] - E[Y_{4:4}])\Big] \\
&+ 252(n-2)(n-3)\Big[\frac{2}{3}E[Y_{3:3}^2] - E[Y_{1:2}Y_{2:2}] + \frac{1}{3}E[Y_{1:3}Y_{2:3}] + E[Y_{2:2}](E[Y_{1:1}] - E[Y_{3:3}])\Big] \\
&+ 252(n-2)(n-3)^2\Big[\frac{1}{4}E[Y_{4:4}^2] + \frac{1}{4}[Y_{3:4}Y_{4:4}] - \frac{2}{3}E[Y_{2:3}Y_{3:3}] + \frac{1}{6}E[Y_{2:4}Y_{3:4}] + E[Y_{2:2}](E[Y_{2:2}] - E[Y_{3:3}])\Big] \\
&- 72(n-2)(n-3)\Big[\frac{1}{2}E[Y_{2:2}^2] - \frac{1}{2}E[Y_{2:2}]^2\Big] \\
&- 72(n-2)^2(n-3)\Big[\frac{1}{3}E[Y_{3:3}^2] + \frac{1}{3}E[Y_{2:3}Y_{3:3}] - E[Y_{1:2}Y_{2:2}] + \frac{1}{3}E[Y_{1:3}Y_{2:3}] + E[Y_{2:2}](E[Y_{1:1}] - E[Y_{2:2}])\Big] \\
&+ 20(n-1)(n-2)(n-3)\Big[\frac{1}{4}E[Y_{4:4}^2] - \frac{1}{4}E[Y_{3:4}Y_{4:4}] + E[Y_{1:1}](E[Y_{3:3}] - E[Y_{4:4}]) \\
&- 36(n-1)(n-2)(n-3)\Big[\frac{1}{3}E[Y_{3:3}^2] - \frac{1}{3}E[Y_{2:3}Y_{3:3}] + E[Y_{1:1}](E[Y_{2:2}] - E[Y_{3:3}])\Big] \\
&+ 18(n-1)(n-2)(n-3)\Big[\frac{1}{2}E[Y_{2:2}^2] - \frac{1}{2}E[Y_{1:2}Y_{2:2}] + E[Y_{1:1}](E[Y_{1:1}] - E[Y_{2:2}])\Big] \\
&- (n-1)(n-2)(n-3)\Big[E[Y_{1:1}^2] - E[Y_{1:1}]^2\Big]
\end{aligned}
$$

$$
\begin{aligned}
&cov(l_3, l_4) = \\
&\Big[(n^3 - 12n^2 + 47n - 60)\big[20E[Y_{6:6}^2] - 8E[Y_{4:6}Y_{5:6}] - 6E[Y_{3:6}Y_{4:6}] + 24E[Y_{4:5}Y_{5:5}] + 42E[Y_{3:5}Y_{4:5}] \\
&+ 18E[Y_{2:5}Y_{3:5}] - 60E[Y_{5:5}^2]\big] + (n^3 - 6n^2 + 11n - 6)\left[-E[Y_{1:1}^2] + 19E[Y_{1:1}]^2 - 20E[Y_{1:1}]E[Y_{4:4}]\right] \\
&+ 9(n^3 - 10n^2 + 31n - 30)E[Y_{2:2}^2] + 12(-3n^3 + 34n^2 - 123n + 144)E[Y_{3:3}^2] \\
&+ 4(17n^3 - 201n^2 + 772n - 966)E[Y_{4:4}^2] + 36(9n^3 - 74n^2 + 199n - 174)E[Y_{2:2}]^2 \\
&+ 60(5n^3 - 48n^2 + 159n - 180)E[Y_{3:3}]^2 + 9(7n^3 - 18n^2 - 143n + 402)E[Y_{1:2}Y_{2:2}] \\
&+ 120(-5n^2 + 34n - 57)E[Y_{2:3}Y_{3:3}] + 2(-31n^3 + 438n^2 - 1916n + 2643)E[Y_{3:4}Y_{4:4}] \\
&+ 12(-2n^3 - 9n^2 + 133n - 264)E[Y_{1:3}Y_{2:3}] + 6(-8n^3 + 119n^2 - 533n + 744)E[Y_{2:4}Y_{3:4}] \\
&+ 30(3n^2 - 20n + 33)E[Y_{1:4}Y_{2:4}] + 18(-7n^3 + 60n^2 - 167n + 150)E[Y_{1:1}]E[Y_{2:2}] \\
&+ 8(7n^3 - 87n^2 + 377n - 537)E[Y_{1:1}]E[Y_{3:3}] + 12(-46n^3 + 417n^2 - 1301n + 1392)E[Y_{2:2}]E[Y_{3:3}] \\
&+ 60(2n^3 - 15n^2 + 37n - 30)E[Y_{2:2}]E[Y_{4:4}] + 120(-n^3 + 9n^2 - 28n + 30)E[Y_{3:3}]E[Y_{4:4}]\Big] \\
&/n(n)(n-1)(n-2)
\end{aligned}
\tag{89}
$$

Additional Algebraic steps for higher order variances and covariances.

3rd L-moment.

$E[Y^2_{1:1}] = (n-1)(n-2) = \mathbf{n^2 - 3n + 3}$

$E[Y^2_{2:2}] = 18(n-2) - 6(n-1)(n-2) = \mathbf{-6n^2 + 36n - 48}$

$E[Y^2_{3:3}] = 24 - 48(n-2) + 12(n-2)^2 + 4(n-1)(n-2) = \mathbf{16n^2 - 108 + 176}$

$E[Y^2_{4:4}] = 36(n-3) - 18(n-2)(n-3) = \mathbf{-18n^2 + 126n - 216}$

$E[Y^2_{5:5}] = 36/5(n-3)(n-4) = \mathbf{36/5(n^2 - 7n + 12)}$

$E[Y_{1:1}]^2 = -12(n-1)(n-2) - (n-1)(n-2) = \mathbf{-13n^2 + 39n - 26}$

$E[Y_{2:2}]^2 = -72(n-2)(n-3) - 36(n-2)^2 - 18(n-2) = \mathbf{-108n^2 + 486n - 540}$

$E[Y_{3:3}]^2 = -24 - 72(n-3) - 36(n-3)(n-4) = \mathbf{-36n^2 + 180n - 240}$

$E[Y_{1:2}Y_{2:2}] = -108(n-3)+72(n-2)+6(n-1)(n-2)-36(n-2)^2 = \mathbf{-30n^2 + 90n + 48}$

$E[Y_{1:3}Y_{2:3}] = 72(n-3) - 24(n-2) + 12(n-2)^2 = \mathbf{12n^2 - 120}$

$E[Y_{1:4}Y_{2:4}] = -18(n-3) = \mathbf{-18n + 54}$

$E[Y_{2:3}Y_{3:3}] = -36(n-3)(n-4) + 48(n-2)(n-3) - 4(n-1)(n-2) + 12(n-2)^2 =$
$\mathbf{20n^2 - 24n - 104}$

$E[Y_{2:4}Y_{3:4}] = 18(n-3)(n-4) - 12(n-2)(n-3) = \mathbf{6n^2 - 66n + 144}$

$E[Y_{2:5}Y_{3:5}] = -36/10(n-3)(n-4) = \mathbf{-36/10(n^2 - 7n + 12)}$

$E[Y_{3:4}Y_{4:4}] = 18(n-3) + 18(n-3)(n-4) - 18(n-2)(n-3) = \mathbf{-18n + 54}$

$E[Y_{3:5}Y_{4:5}] = -36/10(n-3)(n-4) = \mathbf{-36/10(n^2 - 7n + 12)}$

$E[Y_{1:1}]E[Y_{2:2}] = -72(n-2) + 36(n-2)^2 + 12(n-1)(n-2) + 12(n-1)(n-2) =$
$\mathbf{60n^2 - 288 + 336}$

$E[Y_{1:1}]E[Y_{3:3}] = 72(n-3) - 12(n-1)(n-2) = \mathbf{-12n^2 + 108n - 240}$

$E[Y_{2:2}]E[Y_{3:3}] = 36(n-3)(n-4)+72(n-2)+72(n-2)(n-3) = \mathbf{108n^2 - 540n + 720}$

4th L-moment.

$E[Y^2_{1:1}] = (n-1)(n-2)(n-3) = \mathbf{n^3 - 6n^2 + 11n - 6}$

$E[Y^2_{2:2}] = -12(n-1)(n-2)(n-3)+72(n-2)(n-3) = \mathbf{-12n^3 + 144n^2 - 492n + 504}$

$E[Y^2_{3:3}] = 20(n-1)(n-2)(n-3)+48(n-2)^2(n-3)-480(n-2)(n-3)+600(n-3) =$

$\mathbf{68n^3 - 936n^2 + 3988n - 5376}$

$E[Y^2_{4:4}] = -10(n-1)(n-2)(n-3) - 180(n-2)(n-3)^2 + 360(n-2)(n-3) + 900(n-$

$3)^2 - 1800(n-3) + 600 = \mathbf{-190n^3 + 2760n^2 - 12890n + 19560}$

$E[Y^2_{5:5}] = 96(n-2)(n-3)(n-4)+180(n-3)^2(n-4)-1440(n-3)(n-4)+1440(n-4) =$

$\mathbf{276n^3 - 4104n^2 + 19956n - 31824}$

$E[Y^2_{6:6}] = -200(n-3)(n-4)(n-5)+600(n-4)(n-5) = \mathbf{-200n^3 + 3000n^2 - 14800n + 24000}$

$E[Y^2_{7:7}] = 400/7(n-4)(n-5)(n-6) = \mathbf{400/7(n^3 - 15n^2 + 74n - 120)}$

$E[Y_{1:1}]^2 = -24(n-1)(n-2)(n-3)-(n-1)(n-2)(n-3) = \mathbf{-25n^3 + 150n^2 - 275n + 150}$

$E[Y_{2:2}]^2 = -144(n-2)^2(n-3)-720(n-2)(n-3)^2+720(n-2)(n-3)-72(n-2)(n-3) =$

$\mathbf{-864n^3 + 7416n^2 - 20664n + 18576}$

$E[Y_{3:3}]^2 = -600(n-3)-1800(n-3)^2-900(n-3)^2(n-4)-1200(n-3)(n-4)(n-5) =$

$\mathbf{-2100n^3 + 21600n^2 - 75900n + 90000}$

$E[Y_{4:4}]^2 = -600 - 2400(n-4) - 1800(n-4)(n-5) - 400(n-4)(n-5)(n-6) =$

$\mathbf{-400n^3 + 4200n^2 - 15800n + 21000}$

$E[Y_{1:2}Y_{2:2}] = 12(n-1)(n-2)(n-3) - 144(n-2)^2(n-3) + 720(n-2)(n-3) -$

$2700(n-3)^2 + 3600(n-3) - 4800(n-4) = \mathbf{-132n^3 - 1044n^2 + 9228n - 9924}$

$E[Y_{2:3}Y_{3:3}] = 3600(n-3)(n-4)-20(n-1)(n-2)(n-3)+48(n-2)^2(n-3)+480(n-$

$2)(n-3)^2 - 480(n-2)(n-3) - 2400*(n-3)*(n-4) - 900*(n-3)^2*(n-4) =$

$\mathbf{-392n^3 + 5664n^2 - 20272n + 15624}$

$E[Y_{3:4}Y_{4:4}] = 10(n-1)(n-2)(n-3) - 240(n-2)(n-3)(n-4) + 450(n-3)^2 + 450(n-3)^2(n-4) + 900(n-3)(n-4)(n-5) - 400(n-4)(n-5)(n-6) - 180(n-2)(n-3)^2 = \mathbf{540n^3 - 5310n^2 + 14940n - 9210}$

$E[Y_{1:3}Y_{2:3}] = 48(n-2)^2(n-3) - 240(n-2)(n-3) + 1800(n-3)^2 - 2400(n-3) + 4800(n-4) = \mathbf{48n^3 + 1224n^2 - 6432n + 2184}$

$E[Y_{2:4}Y_{3:4}] = -120(n-2)(n-3)^2 + 120(n-2)(n-3) - 1800(n-3)(n-4) + 1800(n-4)(n-5) + 450(n-3)^2(n-4) = \mathbf{330n^3 - 3420n^2 + 8130n + 1080}$

$E[Y_{1:4}Y_{2:4}] = -450(n-3)^2 + 600(n-3) - 2400(n-4) = \mathbf{-450n^2 + 900n + 3750}$

$E[Y_{4:5}Y_{5:5}] = 96(n-2)(n-3)(n-4) - 720(n-3)(n-4) - 480(n-3)(n-4)(n-5) + 480(n-4) + 720(n-4)(n-5) + 240(n-4)(n-5)(n-6) = \mathbf{-144n^3 + 1296n^2 - 3264n + 1536}$

$E[Y_{3:5}Y_{4:5}] = 48(n-2)(n-3)(n-4) - 90(n-3)^2(n-4) - 360(n-3)(n-4)(n-5) + 240(n-4)(n-5)(n-6) = \mathbf{-162n^3 + 1188n^2 - 882n - 5112}$

$E[Y_{2:5}Y_{3:5}] = -90(n-3)^2(n-4) + 360(n-3)(n-4) - 720(n-4)(n-5) = \mathbf{-90n^3 + 540n^2 + 990n - 6840}$

$E[Y_{1:5}Y_{2:5}] = 480(n-4) = \mathbf{480n - 1920}$

$E[Y_{4:6}Y_{5:6}] = -120(n-4)(n-5) - 80(n-4)(n-5)(n-6) + 80(n-3)(n-4)(n-5) = \mathbf{120n^2 - 1080n + 2400}$

$E[Y_{3:6}Y_{4:6}] = 60(n-3)(n-4)(n-5) - 80(n-4)(n-5)(n-6) = \mathbf{-20n^3 + 480n^2 - 3100n + 6000}$

$E[Y_{2:6}Y_{3:6}] = 120(n-4)(n-5) = \mathbf{120(n^2 - 9n + 20)}$

$E[Y_{3:7}Y_{4:7}] = 400/35(n-4)(n-5)(n-6) = \mathbf{400/35(n^3 - 15n^2 + 74n - 120)}$

$E[Y_{4:7}Y_{5:7}] = 400/35(n-4)(n-5)(n-6) = \mathbf{400/35(n^3 - 15n^2 + 74n - 120)}$

$E[Y_{1:1}]E[Y_{2:2}] = 60(n-1)(n-2)(n-3) + 24(n-1)(n-2)(n-3) + 144(n-2)^2(n-3) - 720(n-2)(n-3) = \mathbf{228n^3 - 2232n^2 + 6828n - 6552}$

$E[Y_{1:1}]E[Y_{3:3}] = -60(n-1)(n-2)(n-3) + 1800(n-3)^2 - 2400(n-3) - 40(n-1)(n-2)(n-3) = \mathbf{-100n^3 + 2400n^2 - 14300n + 24000}$

$E[Y_{1:1}]E[Y_{4:4}] = 40(n-1)(n-2)(n-3)+2400(n-4) = \mathbf{40n^3 - 240n^2 + 2840n - 9840}$

$E[Y_{2:2}]E[Y_{3:3}] = 720(n-2)(n-3)^2 + 480(n-2)(n-3)(n-4) + 900(n-3)^2(n-4) - 3600(n-3)(n-4) + 720(n-2)(n-3) = \mathbf{2100n^3 - 21960n^2 + 78900n - 95760}$

$E[Y_{2:2}]E[Y_{4:4}] = -720(n-2)(n-3) - 480(n-2)(n-3)(n-4) + 1800(n-4)(n-5) = \mathbf{-480n^3 + 5400n^2 - 25080n + 43200}$

$E[Y_{3:3}]E[Y_{4:4}] = +3600(n-3)(n-4) + 1200(n-3)(n-4)(n-5) + 400(n-4)(n-5)(n-6) + 2400(n-3) = \mathbf{1600n^3 - 16800n^2 + 63200n - 84000}$

Covariance l_2 and l_3.

$$E[Y_{1:1}^2] = -(n-1) = -(\mathbf{n-1})$$

$$E[Y_{2:2}^2] = 4(n-1) - 6 = \mathbf{2}(\mathbf{2n-5})$$

$$E[Y_{3:3}^2] = -4(n-2) - 2(n-1) + 8 = -\mathbf{6}(\mathbf{n-3})$$

$$E[Y_{4:4}^2] = 3(n-3) = \mathbf{3}(\mathbf{n-3})$$

$$E[Y_{1:1}]^2 = (n-1) + 8(n-1) = \mathbf{9}(\mathbf{n-1})$$

$$E[Y_{2:2}]^2 = 6 + 12(n-2) + 12(n-3) = \mathbf{6}(\mathbf{4n-9})$$

$$E[Y_{1:2}Y_{2:2}] = -4(n-1) + 12(n-2) - 12 = \mathbf{8}(\mathbf{n-4})$$

$$E[Y_{2:3}Y_{3:3}] = -4(n-2) + 2(n-1) - 8(n-3) = -\mathbf{10}(\mathbf{n-3})$$

$$E[Y_{1:3}Y_{2:3}] = -4(n-2) + 4 = -\mathbf{4}(\mathbf{n-3})$$

$$E[Y_{3:4}Y_{4:4}] = 3(n-3) = \mathbf{3}(\mathbf{n-3})$$

$$E[Y_{2:4}Y_{3:4}] = 2(n-3) = \mathbf{2}(\mathbf{n-3})$$

$$E[Y_{1:1}]E[Y_{2:2}] = -8(n-1) - 6(n-1) - 12(n-2) + 12 = -\mathbf{2}(\mathbf{13n-25})$$

$$E[Y_{2:2}]E[Y_{3:3}] = -12 - 12(n-3) = -\mathbf{12}(\mathbf{n-2})$$

$$E[Y_{1:1}]E[Y_{3:3}] = 6(n-1) = \mathbf{6}(\mathbf{n-1})$$

Covariance l_2 and l_4.

$$
\begin{aligned}
E[Y_{1:1}^2] =& (n-1) = (\mathbf{n-1}) \\
E[Y_{2:2}^2] =& -7(n-1)+12 = \mathbf{-7n+19} \\
E[Y_{3:3}^2] =& 8(n-2)+10(n-1)-40 = \mathbf{6(3n-11)} \\
E[Y_{4:4}^2] =& -15(n-3)+30-5(n-1) = \mathbf{-20(n-4)} \\
E[Y_{5:5}^2] =& 8(n-4) = \mathbf{8(n-4)}
\end{aligned}
$$

$$
\begin{aligned}
E[Y_{1:1}]^2 =& -(n-1)-14(n-1) = \mathbf{-15(n-1)} \\
E[Y_{2:2}]^2 =& -12-24(n-2)-60(n-3)+60 = \mathbf{-4(21n-69)}
\end{aligned}
$$

$$
\begin{aligned}
E[Y_{1:2}Y_{2:2}] =& 7(n-1)-24(n-2)+60 = \mathbf{-17n+101} \\
E[Y_{2:3}Y_{3:3}] =& 8(n-2)+40(n-3)-10(n-1)-40 = \mathbf{2(19n-83)} \\
E[Y_{1:3}Y_{2:3}] =& 8(n-2)-20 = \mathbf{4(2n-9)} \\
E[Y_{3:4}Y_{4:4}] =& 5(n-1)-15(n-3)-20(n-4) = \mathbf{-30(n-4)} \\
E[Y_{2:4}Y_{3:4}] =& -10(n-3)+10 = \mathbf{-10(n-4)} \\
E[Y_{4:5}Y_{5:5}] =& 8(n-4) = \mathbf{8(n-4)} \\
E[Y_{3:5}Y_{4:5}] =& 4(n-4) = \mathbf{4(n-4)}
\end{aligned}
$$

$$
\begin{aligned}
E[Y_{1:1}]E[Y_{2:2}] =& 14(n-1)+30(n-1)+24(n-2)-60 = \mathbf{4(17n-38)} \\
E[Y_{1:1}]E[Y_{3:3}] =& -20(n-1)-30(n-1) = \mathbf{-10(n-1)} \\
E[Y_{1:1}]E[Y_{4:4}] =& 20(n-1) = \mathbf{20(n-1)} \\
E[Y_{2:2}]E[Y_{3:3}] =& 60+60(n-3)+40(n-4) = \mathbf{20(5n-14)} \\
E[Y_{2:2}]E[Y_{4:4}] =& -60-40(n-4) = \mathbf{-20(2n-5)}
\end{aligned}
$$

Covariance l_3 and l_4.

$E[Y_{1:1}^2] = -(n-1)(n-2)(n-3) = \mathbf{-n^3 + 6n^2 - 11n + 6}$

$E[Y_{2:2}^2] = 9(n-1)(n-2)(n-3) - 36(n-2)(n-3) = \mathbf{9n^3 - 90n^2 + 279n - 270}$

$E[Y_{3:3}^2] = -12(n-1)(n-2)(n-3) - 24(n-2)^2(n-3) + 168(n-2)(n-3) - 120(n-3) = \mathbf{-36n^3 + 408n^2 - 1476n + 1728}$

$E[Y_{4:4}^2] = 5(n-1)(n-2)(n-3) + 63(n-2)(n-3)^3 - 90(n-2)(n-3) - 180(n-3)^2 + 180(n-3) = \mathbf{68n^3 - 804n^2 + 3088n - 3864}$

$E[Y_{5:5}^2] = -24(n-2)(n-3)(n-4) - 36(n-3)^2(n-4) + 144(n-3)(n-4) = \mathbf{-60n^3 + 720n^2 - 2820n + 3600}$

$E[Y_{6:6}^2] = 20(n-3)(n-4)(n-5) = \mathbf{20(n^3 - 12n^2 + 47n - 60)}$

$E[Y_{1:1}]^2 = (n-1)(n-2)(n-3) + 18(n-1)(n-2)(n-3) = \mathbf{19n^3 - 114n^2 + 209n - 114}$

$E[Y_{2:2}]^2 = 36(n-2)(n-3) + 72(n-2)^2(n-3) + 252(n-2)(n-3)^2 - 180(n-2)(n-3) = \mathbf{324n^3 - 2664n^2 + 7164n - 6264}$

$E[Y_{3:3}]^2 = 180(n-3)^2(n-4) + 360(n-3)^2 + 120(n-3) + 120(n-3)(n-4)(n-5) = \mathbf{300n^3 - 2880n^2 + 9540n - 10800}$

$E[Y_{1:2}Y_{2:2}] = -360(n-3) + 540(n-3)^2 - 252(n-2)(n-3) + 72(n-2)^2(n-3) - 9(n-1)(n-2)(n-3) = \mathbf{63n^3 - 162n^2 - 1287n + 3618}$

$E[Y_{2:3}Y_{3:3}] = -360(n-3)(n-4) + 180(n-3)^2(n-4) + 120(n-2)(n-3) - 168(n-2)(n-3)^2 - 24(n-2)^2(n-3) + 12(n-1)(n-2)(n-3) = \mathbf{-600n^2 + 4080n - 6840}$

$E[Y_{3:4}Y_{4:4}] = -90(n-3)(n-4)(n-5) - 90(n-3)^2 - 90(n-3)^2(n-4) + 60(n-2)(n-3)(n-4) + 63(n-2)(n-3)^2 - 5(n-1)(n-2)(n-3) = \mathbf{-62n^3 + 876n^2 - 3832n + 5286}$

$E[Y_{1:3}Y_{2:3}] = 240(n-3) - 360(n-3)^2 + 84(n-2)(n-3) - 24(n-2)^2(n-3) = \mathbf{-24n^3 - 108n^2 + 1596n - 3168}$

$E[Y_{2:4}Y_{3:4}] = 180(n-3)(n-4) - 90(n-3)^2(n-4) - 30(n-2)(n-3) + 42(n-2)(n-3)^2 =$

$\mathbf{-48n^3 + 714n^2 - 3198n + 4464}$

$E[Y_{1:4}Y_{2:4}] = -60(n-3) + 90(n-3)^2 = \mathbf{90n^2 - 600n + 990}$

$E[Y_{4:5}Y_{5:5}] = 72(n-3)(n-4) + 48(n-3)(n-4)(n-5) - 24(n-2)(n-3)(n-4) =$

$\mathbf{24n^3 - 288n^2 + 1128n - 1440}$

$E[Y_{3:5}Y_{4:5}] = 18(n-3)^2(n-4) + 36(n-3)(n-4)(n-5) - 12(n-2)(n-3)(n-4) =$

$\mathbf{42n^3 - 504n^2 + 1974n - 2520}$

$E[Y_{2:5}Y_{3:5}] = -36(n-3)(n-4) + 18(n-3)^2(n-4) = \mathbf{18n^3 - 216n^2 + 846n - 1080}$

$E[Y_{4:6}Y_{5:6}] = -8(n-3)(n-4)(n-5) = \mathbf{-8(n^3 - 12n^2 + 47n - 60)}$

$E[Y_{3:6}Y_{4:6}] = -6(n-3)(n-4)(n-5) = \mathbf{-6(n^3 - 12n^2 + 47n - 60)}$

$E[Y_{1:1}]E[Y_{2:2}] = 252(n-2)(n-3) - 72(n-2)^2(n-3) - 36(n-1)(n-2)(n-3) -$

$18(n-1)(n-2)(n-3) = \mathbf{-126n^3 + 1080n^2 - 3006n + 2700}$

$E[Y_{1:1}]E[Y_{3:3}] = 240(n-3) - 360(n-2)^2 + 20(n-1)(n-2)(n-3) + 36(n-1)(n-$

$2)(n-3) = \mathbf{56n^3 - 696n^2 + 3016n - 4296}$

$E[Y_{1:1}]E[Y_{4:4}] = -20(n-1)(n-2)(n-3) = \mathbf{-20(-n^3 + 6n^2 - 11n + 6)}$

$E[Y_{2:2}]E[Y_{3:3}] = 360(n-3)(n-4) - 180(n-3)^2(n-4) - 120(n-2)(n-3)(n-4) -$

$252(n-2)(n-3) - 252(n-2)(n-3)^2 = \mathbf{-552n^3 + 5004n^2 - 15612n + 16704}$

$E[Y_{2:2}]E[Y_{4:4}] = 180(n-2)(n-3) + 120(n-2)(n-3)(n-4) = \mathbf{120n^3 - 900n^2 + 2220n - 1800}$

$E[Y_{3:3}]E[Y_{4:4}] = -240(n-3) - 360(n-3)(n-4) - 120(n-3)(n-4)(n-5) =$

$\mathbf{-120n^3 + 1080n^2 - 3360n + 3600}$

Derivation of Exact Variance for Pareto(a, v)

Explicit Form for specific expectations and joint expectations of order statistics from Pareto Distribution.

$$E(Z^1_{1,1}) = \frac{a\Gamma(1-1/v)}{\Gamma(2-1/v)} = \frac{av}{(v-1)}$$
$$E(Z^1_{2,2}) = \frac{2a\Gamma(1-1/v)}{\Gamma(3-1/v)} = \frac{2av^2}{(2v-1)(v-1)}$$
$$E(Z^1_{3,3}) = \frac{6a\Gamma(1-1/v)}{\Gamma(4-1/v)} = \frac{6av^3}{(3v-1)(2v-1)(v-1)}$$
$$E(Z^1_{4,4}) = \frac{24a\Gamma(1-1/v)}{\Gamma(5-1/v)} = \frac{24av^4}{(4v-1)(3v-1)(2v-1)(v-1)}$$
$$E(Z^1_{5,5}) = \frac{120a\Gamma(1-1/v)}{\Gamma(6-1/v)} = \frac{120av^5}{(5v-1)(4v-1)(3v-1)(2v-1)(v-1)}$$

$$E(Z^2_{1,1}) = \frac{a^2\Gamma(1-2/v)}{\Gamma(2-2/v)} = \frac{a^2v}{(v-2)}$$
$$E(Z^2_{2,2}) = \frac{2a^2\Gamma(1-2/v)}{\Gamma(3-2/v)} = \frac{2a^2v^2}{(2v-2)(v-2)}$$
$$E(Z^2_{3,3}) = \frac{6a^2\Gamma(1-2/v)}{\Gamma(4-2/v)} = \frac{6a^2v^3}{(3v-2)(2v-2)(v-2)}$$
$$E(Z^2_{4,4}) = \frac{24a^2\Gamma(1-2/v)}{\Gamma(5-2/v)} = \frac{24a^2v^4}{(4v-2)(3v-2)(2v-2)(v-2)}$$
$$E(Z^2_{5,5}) = \frac{120a^2\Gamma(1-2/v)}{\Gamma(6-2/v)} = \frac{120a^2v^5}{(5v-2)(4v-2)(3v-2)(2v-2)(v-2)}$$
$$E(Z^2_{6,6}) = \frac{720a^2\Gamma(1-2/v)}{\Gamma(7-2/v)} = \frac{720a^2v^6}{(6v-2)(5v-2)(4v-2)(3v-2)(2v-2)(v-2)}$$
$$E(Z^2_{7,7}) = \frac{5040a^2\Gamma(1-2/v)}{\Gamma(8-2/v)} = \frac{5040a^2v^7}{(7v-2)(6v-2)(5v-2)(4v-2)(3v-2)(2v-2)(v-2)}$$

$$E[Z^1_{1,2}Z^1_{2,2}] = 2a^2\frac{\Gamma(2-2/v)}{\Gamma(3-2/v)}\frac{\Gamma(1-1/v)}{\Gamma(2-1/v)} = \frac{2a^2v^2}{(2v-2)(v-1)}$$

$$E[Z^1_{2,3}Z^1_{3,3}] = 6a^2\frac{\Gamma(2-2/v)}{\Gamma(4-2/v)}\frac{\Gamma(1-1/v)}{\Gamma(2-1/v)} = \frac{6a^2v^3}{(3v-2)(2v-2)(v-1)}$$

$$E[Z^1_{3,4}Z^1_{4,4}] = 24a^2\frac{\Gamma(2-2/v)}{\Gamma(5-2/v)}\frac{\Gamma(1-1/v)}{\Gamma(2-1/v)} = \frac{24a^2v^4}{(4v-2)(3v-2)(2v-2)(v-1)}$$

$$E[Z^1_{1,3}Z^1_{2,3}] = 6a^2\frac{\Gamma(3-2/v)}{\Gamma(4-2/v)}\frac{\Gamma(2-1/v)}{\Gamma(3-1/v)} = \frac{6a^2v^2}{(3v-2)(2v-1)}$$

$$E[Z^1_{2,4}Z^1_{3,4}] = 24a^2\frac{\Gamma(3-2/v)}{\Gamma(5-2/v)}\frac{\Gamma(2-1/v)}{\Gamma(3-1/v)} = \frac{24a^2v^3}{(4v-2)(3v-2)(2v-1)}$$

$$E[Z^1_{1,4}Z^1_{2,4}] = 12a^2\frac{\Gamma(4-2/v)}{\Gamma(5-2/v)}\frac{\Gamma(3-1/v)}{\Gamma(4-1/v)} = \frac{12a^2v^2}{(4v-2)(3v-1)}$$

$$E[Z^1_{4,5}Z^1_{5,5}] = 120a^2\frac{\Gamma(2-2/v)}{\Gamma(6-2/v)}\frac{\Gamma(1-1/v)}{\Gamma(2-1/v)} = \frac{120a^2v^5}{(2v-2)(3v-2)(4v-2)(5v-2)(v-1)}$$

$$E[Z^1_{3,5}Z^1_{4,5}] = 120a^2\frac{\Gamma(3-2/v)}{\Gamma(6-2/v)}\frac{\Gamma(2-1/v)}{\Gamma(3-1/v)} = \frac{120a^2v^4}{(3v-2)(4v-2)(5v-2)(2v-1)}$$

$$E[Z^1_{2,5}Z^1_{3,5}] = 60a^2\frac{\Gamma(4-2/v)}{\Gamma(6-2/v)}\frac{\Gamma(3-1/v)}{\Gamma(4-1/v)} = \frac{60a^2v^3}{(4v-2)(5v-2)(3v-1)}$$

$$E[Z^1_{1,5}Z^1_{2,5}] = 20a^2\frac{\Gamma(5-2/v)}{\Gamma(6-2/v)}\frac{\Gamma(4-1/v)}{\Gamma(5-1/v)} = \frac{20a^2v^2}{(5v-2)(4v-1)}$$

$$E[Z^1_{4,6}Z^1_{5,6}] = 720a^2\frac{\Gamma(3-2/v)}{\Gamma(7-2/v)}\frac{\Gamma(2-1/v)}{\Gamma(3-1/v)} = \frac{720a^2v^5}{(3v-2)(4v-2)(5v-2)(6v-2)(2v-1)}$$

$$E[Z^1_{3,6}Z^1_{4,6}] = 360a^2\frac{\Gamma(4-2/v)}{\Gamma(7-2/v)}\frac{\Gamma(3-1/v)}{\Gamma(4-1/v)} = \frac{360a^2v^4}{(4v-2)(5v-2)(6v-2)(3v-1)}$$

$$E[Z^1_{2,6}Z^1_{3,6}] = 120a^2\frac{\Gamma(5-2/v)}{\Gamma(7-2/v)}\frac{\Gamma(4-1/v)}{\Gamma(5-1/v)} = \frac{120a^2v^3}{(5v-2)(6v-2)(4v-1)}$$

$$E[Z^1_{3,7}Z^1_{4,7}] = 840a^2\frac{\Gamma(5-2/v)}{\Gamma(8-2/v)}\frac{\Gamma(4-1/v)}{\Gamma(5-1/v)} = \frac{840a^2v^4}{(5v-2)(6v-2)(7v-2)(4v-1)}$$

$$E[Z^1_{4,7}Z^1_{5,7}] = 2520a^2\frac{\Gamma(4-2/v)}{\Gamma(8-2/v)}\frac{\Gamma(3-1/v)}{\Gamma(4-1/v)} = \frac{2520a^2v^5}{(4v-2)(5v-2)(6v-2)(7v-2)(3v-1)}$$

Exact Variance for Pareto l_1.

$$
\begin{aligned}
var(l_1) =& \frac{1}{n}\left[\frac{a^2 v}{(v-2)} - [\frac{av}{(v-1)}]^2\right] \\
var(l_1) =& \frac{a^2 v}{n}\left[\frac{1}{(v-2)} - [\frac{v}{(v-1)^2}]\right]
\end{aligned}
$$

$$
var(l_1) = \frac{a^2 v}{n(v-1)^2(v-2)} \tag{90}
$$

Exact Variance for Pareto l_2.

$$
\begin{aligned}
&var(l_2) = \\
&\frac{4(n-2)}{3}\left[\frac{6a^2v^3}{(3v-2)(2v-2)(v-2)} + \frac{6a^2v^2}{(3v-2)(2v-1)} + \frac{6a^2v^3}{(3v-2)(2v-2)(v-1)}\right] \\
&+ 2(3-n)\frac{2a^2v^2}{(2v-2)(v-1)} \\
&+ 2(2-n)\frac{2a^2v^2}{(2v-2)(v-2)} \\
&+ (n-1)\frac{a^2v}{(v-2)} \\
&+ 2(3-2n)\left[\frac{2av^2}{(2v-1)(v-1)}\right]^2 \\
&+ 4(2n-3)\frac{2av^2}{(2v-1)(v-1)}\frac{av}{(v-1)} \\
&+ 5(1-1n)\left[\frac{av}{(v-1)}\right]^2
\end{aligned}
$$

$$var(l_2) =$$
$$\Big[\frac{8a^2v^2(n-2)[6v^3-16v^2+13v-4]}{(3v-2)(2v-2)(v-2)(2v-1)(v-1)}+\frac{4a^2v^2(3-n)}{(2v-2)(v-1)}+\frac{4a^2v^2(2-n)}{(2v-2)(v-2)}$$
$$+\frac{a^2v(n-1)}{(v-2)}+\frac{8a^2v^4(3-2n)}{(2v-1)^2(v-1)^2}+\frac{8a^2v^3(2n-3)}{(2v-1)(v-1)^2}+\frac{5a^2v^2(1-n)}{(v-1)^2}\Big]/(n(n-1)) \tag{91}$$

Exact Variance for Pareto l_3.

$$var(l_3) =$$
$$\frac{36(n^2-7n+12)}{10}\Big[2\frac{120a^2v^5}{(5v-2)(4v-2)(3v-2)(2v-2)(v-2)}-$$
$$\frac{120a^2v^4}{(3v-2)(4v-2)(5v-2)(2v-1)}-\frac{60a^2v^3}{(4v-2)(5v-2)(3v-1)}\Big]$$
$$+4(4n^2-27n+44)\frac{6a^2v^3}{(3v-2)(2v-2)(v-2)}$$
$$+12(-3n^2+15n-20)[\frac{6av^3}{(3v-1)(2v-1)(v-1)}]^2$$
$$+18(-n^2+7n-12)\frac{24a^2v^4}{(4v-2)(3v-2)(2v-2)(v-2)}$$
$$+18(-n+3)\left[\frac{24a^2v^4}{(4v-2)(3v-2)(2v-2)(v-1)}+\frac{12a^2v^2}{(4v-2)(3v-1)}\right]$$
$$+6(-5n^2+15n+8)\frac{2a^2v^2}{(2v-2)(v-1)}$$
$$+12(n^2-10)\frac{6a^2v^2}{(3v-2)(2v-1)}+$$
$$4(5n^2-6n-26)\frac{6a^2v^3}{(3v-2)(2v-2)(v-1)}$$

$$
\begin{aligned}
&+ 6(n^2-11n+24)\frac{24a^2v^3}{(4v-2)(3v-2)(2v-1)} \\
&+ 36(3n^2-15n+20)\frac{6av^3}{(3v-1)(2v-1)(v-1)}\frac{2av^2}{(2v-1)(v-1)} \\
&+ 12(5n^2-24n+28)\frac{2av^2}{(2v-1)(v-1)}\frac{av}{(v-1)} \\
&+ 54(-2n^2+9n-10)[\frac{2av^2}{(2v-1)(v-1)}]^2 \\
&+ 6(-n^2+6n-8)\frac{2a^2v^2}{(2v-2)(v-2)} \\
&+ 12(-n^2+9n-20)\frac{av}{(v-1)}\frac{6av^3}{(3v-1)(2v-1)(v-1)} \\
&+ 13(-n^2+3n-2)E[\frac{av}{(v-1)}]^2 \\
&+ (n^2-3n+2)\frac{a^2v}{(v-2)}
\end{aligned}
$$

Pareto $var(l_3) =$

$$
\begin{aligned}
&\frac{432a^2v^3(n^2-7n+12)[35v^3-51v^2+24v-4]}{(5v-2)(4v-2)(3v-2)(2v-2)(2v-1)(v-2)(3v-1)} + \frac{24a^2v^3(4n^2-27n+44)}{(3v-2)(2v-2)(v-2)} \\
&- \frac{432a^2v^6(3n^2-15n+20)}{(3v-1)^2(2v-1)^2(v-1)^2} + \frac{432a^2v^4(-n^2+7n-12)}{(4v-2)(3v-2)(2v-2)(v-2)} \\
&+ \frac{432a^2v^2(-n+3)[6v^3-9v^2+7v-2]}{(4v-2)(3v-2)(2v-2)(3v-1)(v-1)} + \frac{12a^2v^2(-5n^2+15n+8)}{(2v-2)(v-1)} \\
&+ \frac{72a^2v^2(n^2-10)}{(3v-2)(2v-1)} + \frac{24a^2v^3(5n^2-6n-26)}{(3v-2)(2v-2)(v-1)} + \frac{144a^2v^3(n^2-11n+24)}{(4v-2)(3v-2)(2v-1)} \\
&+ \frac{432a^2v^5(3n^2-15n+20)}{(3v-1)(2v-1)^2(v-1)^2} + \frac{24a^2v^3(5n^2-24n+28)}{(2v-1)(v-1)^2} + \frac{216a^2v^4(-2n^2+9n-10)}{(2v-1)^2(v-1)^2} \\
&+ \frac{12a^2v^2(-n^2+6n-8)}{(2v-2)(v-2)} + \frac{72a^2v^4(-n^2+9n-20)}{(3v-1)(2v-1)(v-1)^2} + \frac{a^2v(-n^2+3n-2)[12v^2-24v-1]}{(v-1)^2(v-2)}
\end{aligned}
$$

Exact Variance for Pareto l_4.

$$\frac{400(n^3-15n^2+74n-120)}{35}\Big[\frac{840a^2v^4}{(5v-2)(6v-2)(7v-2)(4v-1)}$$
$$+\frac{2520a^2v^5}{(4v-2)(5v-2)(6v-2)(7v-2)(3v-1)}$$
$$+5\frac{5040a^2v^7}{(7v-2)(6v-2)(5v-2)(4v-2)(3v-2)(2v-2)(v-2)}\Big]$$
$$+(n^3-6n^2+11n-6)\frac{a^2v}{(v-2)}$$
$$+12(-n^3+12n^2-41n+42)\frac{2a^2v^2}{(2v-2)(v-2)}$$
$$+4(17n^3-234n^2+997n-1344)\frac{6a^2v^3}{(3v-2)(2v-2)(v-2)}$$
$$+10(-19n^3+276n^2-1289n+1956)\frac{24a^2v^4}{(4v-2)(3v-2)(2v-2)(v-2)}$$
$$+12(23n^3-342n^2+1663n-2652)\frac{120a^2v^5}{(5v-2)(4v-2)(3v-2)(2v-2)(v-2)}$$
$$+200(-n^3+15n^2-74n+120)\frac{720a^2v^6}{(6v-2)(5v-2)(4v-2)(3v-2)(2v-2)(v-2)}$$
$$+25(-n^3+6n^2-11n+6)\Big[\frac{av}{(v-1)}\Big]^2$$
$$+72(-12n^3+103n^2-287n+258)\Big[\frac{2av^2}{(2v-1)(v-1)}\Big]^2$$
$$+300(-7n^3+72n^2-253n+300)\Big[\frac{6av^3}{(3v-1)(2v-1)(v-1)}\Big]^2$$
$$+200(-2n^3+21n^2-79n+105)\Big[\frac{24av^4}{(4v-1)(3v-1)(2v-1)(v-1)}\Big]^2$$
$$+12(-11n^3-87n^2+769n-827)\frac{2a^2v^2}{(2v-2)(v-1)}$$
$$+8(-49n^3+708n^2-2534n+1953)\frac{6a^2v^3}{(3v-2)(2v-2)(v-1)}$$
$$+30(18n^3-177n^2+498n-307)\frac{24a^2v^4}{(4v-2)(3v-2)(2v-2)(v-1)}$$
$$+24(2n^3+51n^2-268n+91)\frac{6a^2v^2}{(3v-2)(2v-1)}$$

$$
\begin{aligned}
&+ 30(11n^3 - 114n^2 + 271n + 36)\frac{24a^2v^3}{(4v-2)(3v-2)(2v-1)} \\
&+ 150(-3n^2 + 6n + 25)\frac{12a^2v^2}{(4v-2)(3v-1)} \\
&+ 48(-3n^3 + 27n^2 - 68n + 32)\frac{120a^2v^5}{(2v-2)(3v-2)(4v-2)(5v-2)(v-1)} \\
&+ 18(-9n^3 + 66n^2 - 49n - 284)\frac{120a^2v^4}{(3v-2)(4v-2)(5v-2)(2v-1)} \\
&+ 90(-n^3 + 6n^2 + 11n - 76)\frac{60a^2v^3}{(4v-2)(5v-2)(3v-1)} \\
&+ 480(n-4)\frac{20a^2v^2}{(5v-2)(4v-1)} \\
&+ 120(n^2 - 9n + 20)\frac{720a^2v^5}{(3v-2)(4v-2)(5v-2)(6v-2)(2v-1)} \\
&+ 20(-n^3 + 24n^2 - 155n + 300)\frac{360a^2v^4}{(4v-2)(5v-2)(6v-2)(3v-1)} \\
&+ (120(n^2 - 9n + 20)\frac{120a^2v^3}{(5v-2)(6v-2)(4v-1)} \\
&+ 12(19n^3 - 186n^2 + 569n - 546)\frac{av}{(v-1)}\frac{2av^2}{(2v-1)(v-1)} \\
&+ 100(-n^3 + 24n^2 - 143n + 240)\frac{av}{(v-1)}\frac{6av^3}{(3v-1)(2v-1)(v-1)} \\
&+ 40(n^3 - 6n^2 + 71n - 246)\frac{av}{(v-1)}\frac{24av^4}{(4v-1)(3v-1)(2v-1)(v-1)} \\
&+ 60(35n^3 - 366n^2 + 1315n - 1596)\frac{2av^2}{(2v-1)(v-1)}\frac{6av^3}{(3v-1)(2v-1)(v-1)} \\
&+ 120(-4n^3 + 45n^2 - 209n + 360)\frac{2av^2}{(2v-1)(v-1)}\frac{24av^4}{(4v-1)(3v-1)(2v-1)(v-1)} \\
&+ 800(2n^3 - 21n^2 + 79n - 105)\frac{6av^3}{(3v-1)(2v-1)(v-1)}\frac{24av^4}{(4v-1)(3v-1)(2v-1)(v-1)}
\end{aligned}
$$

Pareto $var(l_4) =$

$$\Big[\frac{384000a^2v^4(n^3-15n^2+74n-120)[126v^5-204v^4+226v^3-146v^2+38v-4]}{(7v-2)(6v-2)(5v-2)(4v-2)(3v-2)(2v-2)(v-2)(4v-1)(3v-1)}$$
$$+\frac{a^2v(n^3-6n^2+11n-6)[-24v^2+48v+1]}{(v-1)^2(v-2)}+\frac{24a^2v^2(-n^3+12n^2-41n+42)}{(2v-2)(v-2)}$$
$$+\frac{24a^2v^3(17n^3-234n^2+997n-1344)}{(3v-2)(2v-2)(v-2)}+\frac{240a^2v^4(-19n^3+276n^2-1289n+1956)}{(4v-2)(3v-2)(2v-2)(v-2)}$$
$$+\frac{1440a^2v^5(23n^3-342n^2+1663n-2652)}{(5v-2)(4v-2)(3v-2)(2v-2)(v-2)}+\frac{144000a^2v^6(-n^3+15n^2-74n+120)}{(6v-2)(5v-2)(4v-2)(3v-2)(2v-2)(v-2)}$$
$$+\frac{288a^2v^4(-12n^3+103n^2-287n+258)}{(2v-1)^2(v-1)^2}+\frac{10800a^2v^6(-7n^3+72n^2-253n+300)}{(3v-1)^2(2v-1)^2(v-1)^2}$$
$$+\frac{24a^2v^2(-11n^3-87n^2+769n-827)}{(2v-2)(v-1)}+\frac{48a^2v^3(-49n^3+708n^2-2534n+1953)}{(3v-2)(2v-2)(v-1)}$$
$$+\frac{720a^2v^4(18n^3-177n^2+498n-307)}{(4v-2)(3v-2)(2v-2)(v-1)}+\frac{144a^2v^2(2n^3+51n^2-268n+91)}{(3v-2)(2v-1)}$$
$$+\frac{720a^2v^3(11n^3-114n^2+271n+36)}{(4v-2)(3v-2)(2v-1)}+\frac{1800a^2v^2(-3n^2+6n+25)}{(4v-2)(3v-1)}$$
$$+\frac{5760a^2v^5(-3n^3+27n^2-68n+32)}{(2v-2)(3v-2)(4v-2)(5v-2)(v-1)}+\frac{2160a^2v^4(-9n^3+66n^2-49n-284)}{(3v-2)(4v-2)(5v-2)(2v-1)}$$
$$+\frac{5400a^2v^3(-n^3+6n^2+11n-76)}{(4v-2)(5v-2)(3v-1)}+\frac{9600a^2v^2(n-4)}{(5v-2)(4v-1)}$$
$$+\frac{7200a^2v^4(-n^3+24n^2-155n+300)}{(4v-2)(5v-2)(6v-2)(3v-1)}+\frac{14400a^2v^3(n^2-9n+20)[48v^3-46v^2+22v-4]}{(5v-2)(6v-2)(4v-1)}$$
$$+\frac{24a^2v^3(19n^3-186n^2+569n-546)}{(2v-1)(v-1)^2}+\frac{600a^2v^4(-n^3+24n^2-143n+240)}{(3v-1)(2v-1)(v-1)^2}$$
$$+\frac{960a^2v^5(n^3-6n^2+71n-246)}{(v-1)^2(4v-1)(3v-1)(2v-1)}+\frac{720a^2v^5(35n^3-366n^2+1315n-1596)}{(3v-1)(2v-1)^2(v-1)^2}$$
$$+\frac{5760a^2v^6(-4n^3+45n^2-209n+360)}{(4v-1)(3v-1)(2v-1)^2(v-1)^2}+\frac{115200a^2v^7(2n^3-21n^2+79n-105)}{(4v-1)^2(3v-1)(2v-1)^2(v-1)^2}\Big]$$

$$/n(n-1)(n-2)(n-3)$$

(92)

Appendix C. Appendix C: Math Lab and R Code for Generating Coefficients for the Four Joint Intervals Methods from Chapter 5

Appendix C has Math lab and R Code functions and scripts that are used in calculating the four Joint Method Intervals. The section begins with MathLab code for deriving the Exact Bootstrap estimators for L-moments. Then a script follows for deriving the cdf based on the Characteristic Generating Function. This Appendix concludes with R code for estimating the variance and covariance based either on the exact equations from Chapter 2, or the unbiased estimator of variance.

MatLab Functions: L-moments, Exact Bootstrap, and Characteristic Generating Function Estimates

```
function sum = datal2function(n)

    sum = zeros(1,n);

    for i = 2:(n-1)

        sum(i) = (nchoosek((i-1),1)-nchoosek((n-i),1));

    end

    sum(1) = -nchoosek((n-1),1);
    sum(n) = nchoosek((n-1),1);

    sum = 1/2*nchoosek(n,2)^(-1)*sum;
```

```
15 end

1  function sum = datal3function(n)
2
3      sum = zeros(1,n);
4
5      for i = 3:(n-2)
6
7          sum(i) = (nchoosek((i-1),2)-2*nchoosek((i-1),1)*
               nchoosek((n-i),1)+nchoosek((n-i),2));
8
9      end
10
11     sum(1) = nchoosek((n-1),2);
12     sum(2) = (-2*nchoosek((n-2),1)+nchoosek((n-2),2));
13     sum(n-1) = (nchoosek((n-2),2)-2*nchoosek((n-2),1));
14     sum(n) = nchoosek((n-1),2);
15
16     sum = 1/3*nchoosek(n,3)^(-1)*sum;
17
18 end

1  function sum = l4function(n)
2
3      sum = zeros(1,n);
4
5      for i = 4:(n-3)
```

```
6
7           sum(i) = (nchoosek((i-1),3)-3*nchoosek((i-1),2)*
                nchoosek((n-i),1)+3*nchoosek((i-1),1)*nchoosek((n-
                i),2)-nchoosek((n-i),3));
8
9       end
10
11      sum(1) = -nchoosek((n-1),3);
12      sum(2) = (3*nchoosek(1,1)*nchoosek((n-2),2)-nchoosek((n
            -2),3));
13      sum(3) = (-3*nchoosek(2,2)*nchoosek((n-3),1)+3*nchoosek
            (2,1)*nchoosek((n-3),2)-nchoosek((n-3),3));
14      sum(n-1) = (nchoosek((n-2),3)-3*nchoosek((n-2),2)*
            nchoosek(1,1));
15      sum(n-2) = (nchoosek((n-3),3)-3*nchoosek((n-3),2)*
            nchoosek(2,1)+3*nchoosek((n-3),1)*nchoosek(2,2));
16      sum(n) = nchoosek((n-1),3);
17
18      sum = 1/4*nchoosek(n,4)^(-1)*sum;
19
20  end


1
2   function MuRNk = MUrn2(data, WM, k)
3
4       n = length(data);
5       MuRNk = zeros(1,n);
```

```
6
7       for r = 1:n
8
9           muRN = 0;
10
11          for j = 1:n
12              muhat = WM(r,j)*data(j)^k;
13              muRN = muRN+muhat;
14          end
15          MuRNk(r) = muRN;
16      end
17
18  end
```

```
1       function Var = SigmaSq(data, WM, ExactbsMU)
2
3       n = length(data);
4       Var = zeros(1,n);
5
6       for r = 1:n
7
8           SumSigmaR = 0;
9
10          for j = 1:n
11
12              SigmaR = WM(r,j)*(data(j)-ExactbsMU(r))^2;
13              SumSigmaR = SumSigmaR+SigmaR;
```

```
14          end
15
16          Var(r) = SumSigmaR;
17
18      end
```

```
1   function [Wv, Vv, Iv, Jv] = CovMstructures(n)
2
3       ns = n*(n-1)/2;
4       Wv = zeros(ns);
5       Vv = zeros(ns, n);
6       Iv = zeros(1, ns);
7       Jv = zeros(1, ns);
8       row = 1;
9
10      for r = 1:n
11          r
12          for s = (r+1):n
13
14              Vv(row,1:n) = VjrsM(r,s,n);
15              Wv(row,1:ns) = WijrsM(r,s,n);
16              row = row+1;
17          end
18      end
19      row2 = 1;
20
21      for j = 2:n
```

```
22          for i = 1:(j-1)
23
24              Iv(row2) = i;
25              Jv(row2) = j;
26              row2 = row2+1;
27          end
28      end
29  end
```

```
1
2   function WM = WjrM(n)
3
4       WM = zeros(n);
5
6       for r = 1:n
7           for j = 1:n
8
9       y1 = j/n;
10      y2 = (j-1)/n;
11
12      fun = @(x) (x.^(r-1).*(1-x).^(n-r));
13
14      WM(r,j) = r*nchoosek(n,r)*(integral(fun, 0, y1)-integral(
            fun,0,y2));
15          end
16      end
17
```

```
18 end

1  function Vvector = VjrsM(r,s,n)
2
3      Vvector = zeros(1,n);
4
5      for j = 1:n
6
7          fun = @(x,y) (y.^(r-1).*(x-y).^(s-r-1).*(1-x).^(n-s))
               ;
8          Vvector(j) = (factorial(n)/(factorial(r-1)*factorial(
               s-r-1)*factorial(n-s)))*(integral2(fun,(j-1)/n,j/n
               ,(j-1)/n,@(x) x));
9
10     end
11
12 end

1  function Wvector = WijrsM(r,s,n)
2
3      Wvector = zeros(1,n*(n-1)/2);
4      count = 1;
5
6      for j = 2:n
7
8          for i = 1:(j-1)
9
```

```
10          fun = @(x,y) (y.^(r-1).*(x-y).^(s-r-1).*(1-x).^(n-s))
                ;
11          Wvector(count) = factorial(n)/(factorial(r-1)*
                factorial(s-r-1)*factorial(n-s))*(integral2(fun,(j
                -1)/n,j/n,(i-1)/n,i/n));
12
13          count = count+1;
14
15          end
16
17      end
18
19  end
```

```
1   function CovarM = CovM(data, MU, Var, Wv, Vv, Iv, Jv)
2
3       n = length(data);
4       CovarM = diag(Var);
5       row = 1;
6
7       J2v = 1:n;
8
9       for r = 1:n
10
11          for s = (r+1):n
12
13              CovarM(r,s) = sum(Wv(row,:).*(data(Iv)-MU(r)).*(
```

```
                    data(Jv)-MU(s)))+sum(Vv(row,:).*(data(J2v)-MU(
                    r)).*(data(J2v)-MU(s)));
14                  row = row + 1;
15              end
16          end
17  end

1
2   function C = Mcoeffs(data, Wv, Vv, Iv, Jv)
3
4       data = sort(data);
5       n = length(data);
6
7       % code to generate expected value / mu for each order
            statistic and value
8       % of k
9       WM1 = WjrM(n);
10      ExactbsMUk1 = MUrn2(data, WM1, 1);
11      ExactbsMUk2 = MUrn2(data, WM1, 2);
12      ExactbsMUk3 = MUrn2(data, WM1, 3);
13      ExactbsMUk4 = MUrn2(data, WM1, 4);
14
15      ExactbsVar = SigmaSq(data, WM1, ExactbsMUk1);
16      ExactbsCov = CovM(data, ExactbsMUk1, ExactbsVar, Wv, Vv,
            Iv, Jv);
17      ExactbsCov = triu(ExactbsCov)+triu(ExactbsCov,1)';
18
```

```
19      %csvwrite('ExactbsCov.txt', ExactbsCov);
20      %ExactbsCov = table2array(readtable('ExactbsCov.txt'));
21
22      k3 = 2*ExactbsMUk1.^3-3*ExactbsMUk1.*ExactbsMUk2+
            ExactbsMUk3;
23      k4 = -6*ExactbsMUk1.^4+12*ExactbsMUk1.^2.*ExactbsMUk2-3*
            ExactbsMUk2.^2-4*ExactbsMUk1.*ExactbsMUk3+ExactbsMUk4;
24
25      l2 = datal2function(n);
26      l3 = datal3function(n);
27      l4 = datal4function(n);
28
29      J = [l2; l3; l4];
30
31      coeff1 = l3*ExactbsMUk1';
32      coeff2 = l3*ExactbsCov*l3';
33      coeff3 = sum(l3.^3.*k3)/6;
34      coeff4 = sum(l3.^4.*k4)/24;
35      coeff5 = sum(l3.^3.*k3).*sum(l3.^3.*k3)/72;
36
37      coeff6 = l4*ExactbsMUk1';
38      coeff7 = l4*ExactbsCov*l4';
39      coeff8 = sum(l4.^3.*k3)/6;
40      coeff9 = sum(l4.^4.*k4)/24;
41      coeff10 = sum(l4.^3.*k3).*sum(l4.^3.*k3)/72;
42
```

```
43      covarM = J*ExactbsCov*J';
44      covarl2l3 = covarM(1,2);
45      covarl2l4 = covarM(1,3);
46      covarl3l4 = covarM(2,3);
47
48      varl2 = covarM(2,2);
49      l2estimate = l2*data';
50      l2bsestimate = l2*ExactbsMUk1';
51
52      C = [coeff1, coeff2, coeff3, coeff4, coeff5, coeff6,
            coeff7, coeff8, coeff9, coeff10, l2bsestimate,
            l2estimate, varl2, covarl2l3, covarl2l4, covarl3l4];
53      %csvwrite('C.txt', C);
54  end
```

MatLab Script: Numerical Inversion of Characteristic Generating Function based on Bootstrapped Estimates.

```
1  alpha = 0.05;
2
3  power = 0;
4  t3power = 0;
5  t4power = 0;
6
7  repetitions = 2000;
8  width = 0.50;
9  discretized = 2000;
```

```
10
11 % next 4 parameters depend on the parameteric assumption
       being tested
12 data = csvread('expCoeffsM150.txt');
13
14 %trueParameter = [0, 0.1226];          % normal
15 %trueParameter = [0, 0];                % uniform
16 trueParameter = [1/3, 1/6];           % exponential
17 %trueParameter = [0.1699, 0.1504];    % gumbel
18
19 %x1 = linspace(-1,1, discretized);       % determined by
       distribution based off l3
20 %x2 = linspace(-1,1, discretized);       % determined by
       distribution based off l4
21
22 x1 = linspace((trueParameter(1)-width),(trueParameter(1)+
       width), discretized);        % determined by distribution
       based off l3
23 x2 = linspace((trueParameter(2)-width),(trueParameter(2)+
       width), discretized);        % determined by distribution
       based off l4
24
25
26 for reps = 1:repetitions
27
28     realResults = zeros(1,length(x1));
```

```
29      C = data(reps,:);
30      l2 = C(11);      % C(11) is the bootstrapped estimate,
           while C(12) is the sample lmoment for r = 2
31
32      if mod(reps,200)==0
33          reps
34      end
35
36      for j = 1:length(x1)
37
38          y = x1(j);
39          f1 = @(t) (exp(1i*t*y).*(exp(-1i*t*C(1)-1/2*t.^2.*C
               (2)).*(1+(1i*t).^3.*C(3)+(1i*t).^4.*C(4)+(1i*t)
               .^6.*C(5)))-exp(-1i*t*y).*(exp(1i*t*C(1)-1/2*t
               .^2.*C(2)).*(1-(1i*t).^3.*C(3)+(1i*t).^4.*C(4)+(1i
               *t).^6.*C(5)))./(1i*t);
40          results = integral(f1, 0, Inf);
41
42          realResults(j) = 1/2+1/(2*pi)*real(results);
43
44      end
45
46      k1 = find(realResults > 0.0125);
47      k2 = find(realResults < 0.9875);
48
49      lb1 = x1(k1(1));
```

```
50      ub1 = x1(k2(end));
51
52      realResults2 = zeros(1,length(x2));
53
54      for j = 1:length(x2)
55
56          y = x2(j);
57          f2 = @(t) (exp(1i*t*y).*(exp(-1i*t*C(6)-1/2*t.^2.*C
                (7)).*(1+(1i*t).^3.*C(8)+(1i*t).^4.*C(9)+(1i*t)
                .^6.*C(10)))-exp(-1i*t*y).*(exp(1i*t*C(6)-1/2*t
                .^2.*C(7)).*(1-(1i*t).^3.*C(8)+(1i*t).^4.*C(9)+(1i
                *t).^6.*C(10)))./(1i*t);
58          results2 = integral(f2, 0, Inf);
59
60          realResults2(j) = 1/2+1/(2*pi)*real(results2);
61
62      end
63
64      k3 = find(realResults2 > 0.0125);
65      k4 = find(realResults2 < 0.9875);
66
67      lb2 = x2(k3(1));
68      ub2 = x2(k4(end));
69
70      % if statement returns 0 or 1
71      if lb1/l2 <= trueParameter(1) && ub1/l2 >= trueParameter
```

```
        (1)
72          t3coverage = 1;
73      else
74          t3coverage = 0;
75      end
76      t3power = t3power + t3coverage;
77
78      if lb2/l2 <= trueParameter(2) && ub2/l2 >= trueParameter
            (2)
79          t4coverage = 1;
80      else
81          t4coverage = 0;
82      end
83      t4power = t4power + t4coverage;
84
85      if t3coverage == 1 && t4coverage == 1
86          jointcoverage = 1;
87      else
88          jointcoverage = 0;
89          disp(reps)
90          break
91      end
92      power = power + jointcoverage;
93
94  end
```

Rstudio Function: Distribution Free Unbiased Variance Estimator for L-moments.

```
#function to calculate the unbaised estimator of variance
    from order statistics for the L-moments

UBE.lmom = function(RS){

  RS <- unlist(RS)
  rs.order <- RS[order(RS)]

  n <- length(rs.order)
  subsample <- combn(n,2)

  Omega2 <- matrix(0, nrow = 1, ncol = 10)
  colnames(Omega2) <- c("00","01","11","02","12","22","03","
      13","23","33")


  Omega1 <- matrix(0, nrow = 1, ncol = 10)
  colnames(Omega1) <- c("00","01","11","02","12","22","03","
      13","23","33")


  for (k in seq(1,choose(n,2),1)){

    i <- subsample[1,k]
```

```
22      j <- subsample[2,k]
23
24      pm <- rs.order[i]*rs.order[j]
25
26      o00 <- 2*pm
27      o01 <- (j+i-3)*pm
28      o11 <- ((i-1)*(j-3)+(i-1)*(j-3))*pm
29      o02 <- ((j-2)*(j-3)+(i-1)*(i-2))*pm
30      o12 <- ((i-1)*(j-3)*(j-4)+(i-1)*(i-2)*(j-4))*pm
31      o22 <- (2*(i-1)*(i-2)*(j-4)*(j-5))*pm
32      o03 <- ((j-2)*(j-3)*(j-4)+(i-1)*(i-2)*(i-3))*pm
33      o13 <- ((i-1)*(j-3)*(j-4)*(j-5)+(i-1)*(i-2)*(i-3)*(j-5))*
            pm
34      o23 <- ((i-1)*(i-2)*(j-4)*(j-5)*(j-6)+(i-1)*(i-2)*(i-3)*(
            j-5)*(j-6))*pm
35      o33 <- (2*(i-1)*(i-2)*(i-3)*(j-5)*(j-6)*(j-7))*pm
36
37      omega2 <- c(o00,o01,o11,o02,o12,o22,o03,o13,o23,o33)
38      Omega2 <- omega2 + Omega2
39    }
40
41    coeff2 <- c(1/(n*(n-1)), 1/(n*(n-1)*(n-2)), 1/(n*(n-1)*(n
        -2)*(n-3)), 1/(n*(n-1)*(n-2)*(n-3)), 1/(n*(n-1)*(n-2)*(n
        -3)*(n-4)), 1/(n*(n-1)*(n-2)*(n-3)*(n-4)*(n-5)), 1/(n*(n
        -1)*(n-2)*(n-3)*(n-4)), 1/(n*(n-1)*(n-2)*(n-3)*(n-4)*(n
        -5)), 1/(n*(n-1)*(n-2)*(n-3)*(n-4)*(n-5)*(n-6)), 1/(n*(n
```

```
    -1)*(n-2)*(n-3)*(n-4)*(n-5)*(n-6)*(n-7)))
42  Omega22 <- coeff2*Omega2
43  Omega22[is.nan(Omega22)] <- 0
44
45  for (i in seq(1,n,1)){
46    for (j in seq(1,n,1)){
47
48      pm <- rs.order[j]*rs.order[i]
49
50
51      o00 <- pm
52      o01 <- (j-1)*pm
53      o11 <- ((i-1)*(j-1))*pm
54      o02 <- ((j-1)*(j-2))*pm
55      o12 <- ((i-1)*(j-1)*(j-2))*pm
56      o22 <- ((i-1)*(i-2)*(j-1)*(j-2))*pm
57      o03 <- ((j-1)*(j-2)*(j-3))*pm
58      o13 <- ((i-1)*(j-1)*(j-2)*(j-3))*pm
59      o23 <- ((i-1)*(i-2)*(j-1)*(j-2)*(j-3))*pm
60      o33 <- ((i-1)*(i-2)*(i-3)*(j-1)*(j-2)*(j-3))*pm
61
62      omega1 <- c(o00,o01,o11,o02,o12,o22,o03,o13,o23,o33)
63      Omega1 <- omega1 + Omega1
64    }
65  }
66
```

```
67  coeff1 <- c(1/n^2, 1/(n^2*(n-1)), 1/((n*(n-1))^2), 1/(n^2*(
        n-1)*(n-2)), 1/(n^2*(n-1)^2*(n-2)), 1/((n*(n-1)*(n-2))
        ^2), 1/(n^2*(n-1)*(n-2)*(n-3)), 1/(n^2*(n-1)^2*(n-2)*(n
        -3)), 1/(n^2*(n-1)^2*(n-2)^2*(n-3)), 1/(n*(n-1)*(n-2)*(n
        -3))^2)
68  Omega11 <- coeff1*Omega1
69
70  Omega <- Omega11 - Omega22
71
72  hat.lmom1 <-  Omega[1]
73  hat.lmom2 <- (4*Omega[3]-4*Omega[2]+Omega[1])
74  hat.lmom3 <- (36*Omega[6]-72*Omega[5]+36*Omega[3]+12*Omega
        [4]-12*Omega[2]+Omega[1])
75  hat.lmom4 <- (Omega[1]-24*Omega[2]+60*Omega[4]-40*Omega
        [7]+144*Omega[3]-720*Omega[5]+480*Omega[8]+900*Omega
        [6]-1200*Omega[9]+400*Omega[10])
76  hat.lmom23 <- (8*Omega[2]-6*Omega[4]-12*Omega[3]+12*Omega
        [5]-Omega[1])
77  hat.lmom24 <- (-14*Omega[2]+30*Omega[4]-20*Omega[7]+24*
        Omega[3]-60*Omega[5]+40*Omega[8]+Omega[1])
78  hat.lmom34 <- (-Omega[1]+18*Omega[2]-36*Omega[4]+20*Omega
        [7]-72*Omega[3]+252*Omega[5]-120*Omega[8]-180*Omega
        [6]+120*Omega[9])
79
80  hat <- c(hat.lmom1, hat.lmom2, hat.lmom3, hat.lmom4, hat.
        lmom23, hat.lmom24, hat.lmom34)
```

```
81    return(hat)
82  }
```

Rstudio Function: Exact Variance/Covariance.

```
1  exactVariance <- function(name, sample){
2
3    if (name == "normal"){
4
5      norm.exactL1 <- sapply(sample, function(x) 1/x)
6      norm.exactL2 <- sapply(sample, function(x) (0.16275*x
           +0.037877)/(x*(x-1)))
7      norm.exactL3 <- sapply(sample, function(x) (0.05938*x
           ^2+0.04905*x+0.01037)/(x*(x-1)*(x-2)))
8      norm.exactL4 <- sapply(sample, function(x) (0.02829*x
           ^3+0.05650*x^2+0.05482*x+0.01214)/(x*(x-1)*(x-2)*(x-3)
           ))
9      norm.exact <- cbind(norm.exactL1, norm.exactL2, norm.
           exactL3, norm.exactL4)
10     return(norm.exact)
11
12   }
13
14   else if (name == "exponential"){
15
16     exponential.exactL1 <- sapply(sample, function(x) 1/x)
17     exponential.exactL2 <- sapply(sample, function(x) (2*x-1)
```

```
      /(6*x*(x-1)))
18    exponential.exactL3 <- sapply(sample, function(x) (4*x
      ^2-3*x-2)/(30*x*(x-1)*(x-2)))
19    exponential.exactL4 <- sapply(sample, function(x) (3*x
      ^3-3*x^2-2*x-3)/(42*x*(x-1)*(x-2)*(x-3)))
20    exp.exact <- cbind(exponential.exactL1, exponential.
      exactL2, exponential.exactL3, exponential.exactL4)
21    return(exp.exact)
22  }
23
24  else if (name == "uniform"){
25
26    uniform.exactL1 <- sapply(sample, function(x) 1/(12*x))
27    uniform.exactL2 <- sapply(sample, function(x) (0.00555*x
      +0.01666)/(x*(x-1)))
28    uniform.exactL3 <- sapply(sample, function(x) (0.00476*x
      ^2+0.02380)/(x*(x-1)*(x-2)))
29    uniform.exactL4 <- sapply(sample, function(x) (0.00158*x
      ^3+0.00476*x^2+0.01746*x+0.05238)/(x*(x-1)*(x-2)*(x-3)
      ))
30    uni.exact <- cbind(uniform.exactL1, uniform.exactL2,
      uniform.exactL3, uniform.exactL4)
31    return(uni.exact)
32  }
33
34
```

```
35  else if (name == "uniform2"){
36
37    uniform.exactL1 <- sapply(sample, function(x) 1/(x))
38    uniform.exactL2 <- sapply(sample, function(x) (x+3)/(15*x
        *(x-1)))
39    uniform.exactL3 <- sapply(sample, function(x) (2*x^2+10)/
        (35*x*(x-1)*(x-2)))
40    uniform.exactL4 <- sapply(sample, function(x) (2*x^3+6*x
        ^2+22*x+66)/(105*x*(x-1)*(x-2)*(x-3)))
41    uni.exact <- cbind(uniform.exactL1, uniform.exactL2,
        uniform.exactL3, uniform.exactL4)
42    return(uni.exact)
43  }
44
45  else if (name == "pareto"){
46
47    pareto.exactL1 <- sapply(sample, function(x) 1/x)
48    pareto.exactL2 <- sapply(sample, function(x) (0.57551*x
        -0.47755)/(x*(x-1)))
49    pareto.exactL3 <- sapply(sample, function(x) (0.35800*x
        ^2-0.81413*x+0.33226)/(x*(x-1)*(x-2)))
50    pareto.exactL4 <- sapply(sample, function(x) (0.25863*x
        ^3-1.14400*x^2+1.46285*x-0.56405)/(x*(x-1)*(x-2)*(x-3)
        ))
51    par.exact <- cbind(pareto.exactL1, pareto.exactL2, pareto
        .exactL3, pareto.exactL4)
```

```
52      return(par.exact)
53    }
54
55   else if (name == "gumbel"){
56
57      gumbel.exactL1 <- sapply(sample, function(x) (pi^2)/(6*x)
            )
58      gumbel.exactL2 <- sapply(sample, function(x) (0.38658*x
            +0.08913)/(x*(x-1)))
59      gumbel.exactL3 <- sapply(sample, function(x) (0.15395*x
            ^2+0.04810*x-0.02506)/(x*(x-1)*(x-2)))
60      gumbel.exactL4 <- sapply(sample, function(x) (0.08114*x
            ^3+0.02696*x^2-0.03536*x+0.02153)/(x*(x-1)*(x-2)*(x-3)
            ))
61      gum.exact <- cbind(gumbel.exactL1, gumbel.exactL2, gumbel
            .exactL3, gumbel.exactL4)
62      return(gum.exact)
63      }
64
65    else print("Distribution not found")
66
67 }
68
69 exactCovariance <- function(name, sample){
70
71    if (name == "normal"){
```

```
72
73      norm.exact.l213 <- sapply(sample, function(x) 0)
74      norm.exact.l214 <- sapply(sample, function(x) (0.01080*x
            +0.00022)/(x*(x-1)))
75      norm.exact.l314 <- sapply(sample, function(x) 0)
76
77      return(c(norm.exact.l213, norm.exact.l214, norm.exact.
            l314))
78
79    }
80
81    else if (name == "exponential"){
82
83      exp.exact.l213 <- sapply(sample, function(x) (x)/(6*x*(x
            -1)))
84      exp.exact.l214 <- sapply(sample, function(x) (x)/(12*x*(x
            -1)))
85      exp.exact.l314 <- sapply(sample, function(x) (x)/(12*x*(x
            -1)*(x-2)))
86
87      return(c(exp.exact.l213, exp.exact.l214, exp.exact.l314))
88    }
89
90    else if (name == "uniform"){
91
92      uni.exact.l213 <- sapply(sample, function(x) 0)
```

```
93      uni.exact.l2l4 <- sapply(sample, function(x) (-0.00238*x
            -0.00714)/(x*(x-1)))
94      uni.exact.l3l4 <- sapply(sample, function(x) 0)
95
96      return(c(uni.exact.l2l3, uni.exact.l2l4, uni.exact.l3l4))
97    }
98
99    else if (name == "pareto"){
100
101
102     par.exact.l2l3 <- sapply(sample, function(x) (0.42486*x
            -0.29128)/(x*(x-1)))
103     par.exact.l2l4 <- sapply(sample, function(x) (0.32566*x
            -0.21286)/(x*(x-1)))
104     par.exact.l3l4 <- sapply(sample, function(x) (0.29330*x
            ^2-0.59656*x+0.24659)/(x*(x-1)*(x-2)))
105
106     return(c(par.exact.l2l3, par.exact.l2l4, par.exact.l3l4))
107   }
108
109   else if (name == "gumbel"){
110
111     gum.exact.l2l3 <- sapply(sample, function(x) (0.15699*x
            +0.00008)/(x*(x-1)))
112     gum.exact.l2l4 <- sapply(sample, function(x) (0.07942*x
            -0.00575)/(x*(x-1)))
```

```
113       gum.exact.l314 <- sapply(sample, function(x) (0.07927*x
              ^2-0.00298*x+0.00048)/(x*(x-1)*(x-2)))
114
115       return(c(gum.exact.l213, gum.exact.l214, gum.exact.l314))
116     }
117
118     else print("Distribution not found")
119
120
121 }
```

Bibliography

1. The DBLP Computer Science Bibliography.

2. Mohammad Ahsanullah and Valery Nevzorov. *Records via Probability Theory*. Altanic Press.

3. A. L. Barabási, Réka Albert, and Hawoong Jeong. Mean-field theory for scale-free random networks. *Physica A: Statistical Mechanics and its Applications*, 272(1):173–187, 1999.

4. George Casella and Roger L. Berger. *Statistical Inference*. 2002.

5. D. Conte, P. Foggia, C. Sansone, and M. Vento. Thirty Years of Graph Matching in Pattern Recognition. *International Journal of Pattern Recognition and Artificial Intelligence*, 18(03):265–298, 2004.

6. Matthew Denny. Social Network Analysis. *Institute for Social Science Research*, 10(September):1–20, 2014.

7. F. Downton. Linear estimates with polynomial coefficients. *Biometrika*, 53(1-2):129–141, 1966.

8. Elsayed A.H. Elamir and Allan H. Seheult. Exact variance structure of sample L-moments. *Journal of Statistical Planning and Inference*, 124(2):337–359, 2004.

9. P Erdös and a Rényi. On random graphs. *Publicationes Mathematicae*, 6:290–297, 1959.

10. J. Fournet and A Barrat. Contact pattern among high school students, 2014.

11. Csardi Gabor. igraphdata: A collection of Network Data Sets for the 'igraph' package. 2015.

12. D. Gfeller. *Simplifying complex networks: from a clustering to a coarse graining strategy*. PhD thesis, 2007.

13. Nathaniel B. Guttman. On the Sensitivity of Sample L Moments to Sample Size, 1993.

14. Joshua D. Guzman, Richard F. Deckro, Matthew J. Robbins, James F. Morris, and Nicholas A. Ballester. An analytical comparison of social network measures. *IEEE Transactions on Computational Social Systems*, 1(1):35–45, 2014.

15. F. Hausdorff. Summationsmethoden und Momentfolgen I. *Mathematicsche Zeitschrift*, 9:74–109, 1921.

16. Myles Hollander, Douglas A. Wolfe, and Eric Chicken. *Nonparametric Statistical Methods*. 2014.

17. J R M Hosking. Estiamtion of generalized extreme-value distributions via probability weighted moments, 1985.

18. J R M Hosking. L-moments: analysis and estimation of distributions using linear combinations of order statistics, 1990.

19. J. R.M. Hosking. Some theory and practical uses of trimmed L-moments. *Journal of Statistical Planning and Inference*, 137(9):3024–3039, 2007.

20. J. S. Huang. A note on Order Statistics from Pareto Distribution, 1975.

21. Alan D. Hutson and Michael D. Ernst. The exact bootstrap mean and variance of an L-estimator. *Journal of the Royal Statistical Society. Series B: Statistical Methodology*, 62(1):89–94, 2000.

22. Ning Jin, Calvin Young, and Wei Wang. Graph classification based on pattern co-occurrence. *Proceeding of the 18th ACM conference on Information and knowledge management - CIKM '09*, page 573, 2009.

23. Hyunsoo Kim and Hee Yong Youn. Prompt Detection of Changepoint in the. pages 1125–1129, 2005.

24. Michael H. Kutner, Christopher J. Nachtshemim, John Neter, and William Li. *Applied Linear Satistical Models*. 2013.

25. Da Lamothe. Watch Perdix, the secretive Pentagon program dropping tiny drones from jets, 2018.

26. Ping Li, Jie Zhang, and Michael Small. Emergence of scaling and assortative mixing through altruism. *Physica A: Statistical Mechanics and its Applications*, 390(11):2192–2197, 2011.

27. Lorenzo Livi and Antonello Rizzi. The graph matching problem. *Pattern Analysis and Applications*, 16(3):253–283, 2013.

28. Owen Macindoe and Whitman Richards. Graph Comparison Using Fine Structure Analysis. *2010 IEEE Second International Conference on Social Computing*, pages 193–200, 2010.

29. H. C. Manjunatha and R. Mohanasundaram. BRNADS: Big data real-time node anomaly detection in social networks. *Proceedings of the 2nd International Conference on Inventive Systems and Control, ICISC 2018*, (Icisc):929–932, 2018.

30. Fairul Mohd-zaid, Christine M Schubert Kabban, and Richard F Deckro. A Test on the L-moments of the Degree Distribution of a Barabasi-Albert Network for Detecting Nodal and Edge Degradation. *Journal of Complex Networks*, pages 1–29, 2016.

31. H. D.K. Moonesinghe, Hamed Valizadegan, Samah Fodeh, and Pang Ning Tan. A probabilistic substructure-based approach for graph classification. *Proceedings - International Conference on Tools with Artificial Intelligence, ICTAI*, 1:346–349, 2007.

32. James F. Morris, Jerome W. O'Neal, and Richard F. Deckro. A random graph generation algorithm for the analysis of social networks. *The Journal of Defense Modeling and Simulation: Applications, Methodology, Technology*, 11(3):265–276, 2014.

33. M E J Newman. *Networks, An Introduction*. Oxford, 1st editio edition, 2010.

34. NH Perez, SC Menendez, and Luis Seco. A theoretical comparison between moments and L-moments. pages 1–23, 2003.

35. A. Sankarasubramanian and K. Srinivasan. Investigation and comparison of sampling properties of L-moments and conventional moments. *Journal of Hydrology*, 218(1-2):13–34, 1999.

36. E. Serin and S. Balcisoy. Entropy Based Sensitivity Analysis and Visualization of Social Networks. *2012 IEEE/ACM International Conference on Advances in Social Networks Analysis and Mining*, pages 1099–1104, 2012.

37. D. Teichroew. Tables of expected values of order statistics and products of order statistics for samples of size twenty and less from the normal distribution. *Annals of Mathematical Statistics*, 26:410–426, 1954.

38. Dongliang Wang and Alan D. Hutson. Joint confidence region estimation of L-moment ratios with an extension to right censored data. *Journal of Applied Statistics*, 40(2):368–379, 2013.

39. D J Watts and S H Strogatz. Collective dynamics of 'small-world' networks. *Nature*, 393(6684):440–2, 1998.

REPORT DOCUMENTATION PAGE

Form Approved
OMB No. 0704–0188

1. REPORT DATE *(DD–MM–YYYY)*	2. REPORT TYPE	3. DATES COVERED *(From — To)*
09–02–2019	Dissertation	Sept 2016 — Aug 2019

4. TITLE AND SUBTITLE

STATISTICAL L-MOMENT AND L-MOMENT RATIO ESTIMATION AND THEIR APPLICABILITY IN NETWORK ANALYSIS

5a. CONTRACT NUMBER

5b. GRANT NUMBER

5c. PROGRAM ELEMENT NUMBER

6. AUTHOR(S)

Timothy S. Anderson

5d. PROJECT NUMBER

5e. TASK NUMBER

5f. WORK UNIT NUMBER

7. PERFORMING ORGANIZATION NAME(S) AND ADDRESS(ES)

Air Force Institute of Technology
Graduate School of Engineering and Management (AFIT/EN)
2950 Hobson Way
WPAFB OH 45433-7765

8. PERFORMING ORGANIZATION REPORT NUMBER

AFIT-ENC-DS-19-S-001

9. SPONSORING / MONITORING AGENCY NAME(S) AND ADDRESS(ES)

711th Human Performance Wing, Machine Learning Section
2255 H Street, Bldg 248
WPAFB OH 45433-7022
DSN 785-8808
Email: fairul.mohd-zaid@us.af.mil

10. SPONSOR/MONITOR'S ACRONYM(S)

711 HPW/RHCML

11. SPONSOR/MONITOR'S REPORT NUMBER(S)

12. DISTRIBUTION / AVAILABILITY STATEMENT

DISTRIBUTION STATEMENT A:
APPROVED FOR PUBLIC RELEASE; DISTRIBUTION UNLIMITED.

13. SUPPLEMENTARY NOTES

14. ABSTRACT This research centers on finding the statistical moments, network measures, and statistical tests that are most sensitive to various node degradation for the Barabási-Albert, Erdös-Rényi, and Watts-Strogratz network models. Thirty-five different graph structures were simulated for each of the random graph generation algorithms, and sensitivity analysis was undertaken on three different network measures: degree, betweenness, and closeness. In an effort to find the statistical moments that are the most sensitive to degradation within each network, four traditional moments: mean, variance, skewness, and kurtosis as well as three non-traditional moments: L-variance, L-skewness, and L-kurtosis were examined. Each of these moments were examined across 18 degrade settings to highlight which moments were able to detect node degradation the quickest. Closeness was the most sensitive network measure, and the mean was the most sensitive moment across all scenarios. The results showed L-moments and L-moment ratios were less sensitive than traditional moments. Subsequently sample size guidance and confidence interval estimation for univariate and joint L-moments were derived across many common statistical distributions for future research with L-moments.

15. SUBJECT TERMS

L-moments, L-moment ratios, Sample Size, Confidence Intervals, Estimations, Networks, Change Detection

16. SECURITY CLASSIFICATION OF:			17. LIMITATION OF ABSTRACT	18. NUMBER OF PAGES	19a. NAME OF RESPONSIBLE PERSON
a. REPORT	b. ABSTRACT	c. THIS PAGE			Dr. Christine M. Schubert Kabban, AFIT/ENC
U	U	U	U	259	19b. TELEPHONE NUMBER *(include area code)* (937)-255-3636, x4549